ZONGULDAK BÜLENT ECEVİT UNIVERSITY

GRADUATE SCHOOL OF NATURAL AND APPLIED SCIENCES

CONVENTIONAL NOMA AND THE INTERPLAYS WITH COOPERATIVE COMMUNICATION AND SPATIAL MODULATION: PERFORMANCE EVALUATION AND ANALYSIS UNDER IMPERFECT SIC

DEPARTMENT OF ELECTRICAL AND ELECTRONICS ENGINEERING

DOCTOR OF PHILOSOPHY THESIS

FERDİ KARA

JULY 2019

ZONGULDAK BÜLENT ECEVİT UNIVERSITY
GRADUATE SCHOOL OF NATURAL AND APPLIED SCIENCES

CONVENTIONAL NOMA AND THE INTERPLAYS WITH COOPERATIVE COMMUNICATION AND SPATIAL MODULATION: PERFORMANCE EVALUATION AND ANALYSIS UNDER IMPERFECT SIC

DEPARTMENT OF ELECTRICAL AND ELECTRONICS ENGINEERING

DOCTOR OF PHILOSOPHY THESIS

Ferdi KARA

ADVISOR: Assist. Prof. Hakan KAYA

ZONGULDAK
July 2019

APPROVAL OF THE THESIS:

The thesis entitled "Conventional NOMA and The Interplays with Cooperative Communication and Spatial Modulation: Performance Evaluation and Analysis under Imperfect SIC" and submitted by Ferdi KARA has been examined and accepted by the jury as a Doctor of Philosophy thesis in Department of Electrical and Electronics Engineering Graduate School of Natural and Applied Sciences, Zonguldak Bülent Ecevit University. 25/07/2019

Advisor: Assist. Prof. Hakan KAYA
Zonguldak Bülent Ecevit University, Faculty of Engineering, Department of Electrical and Electronics Engineering

Member: Assist. Prof. Tuğba Özge ONUR
Zonguldak Bülent Ecevit University, Faculty of Engineering, Department of Electrical and Electronics Engineering

Member: Assist. Prof. Okan ERKAYMAZ
Zonguldak Bülent Ecevit University, Faculty of Engineering, Department of Computer Engineering

Member: Assist. Prof. Selman KULAÇ
Duzce University, Faculty of Engineering, Department of Electrical and Electronics Engineering

Member: Assist. Prof. Serdar ÖZYURT
Ankara Yıldırım Beyazıt University, Faculty of Engineering and Natural Sciences, Department of Electrical and Electronics Engineering

Approved by the Graduate School of Natural and Applied Sciences.   ..../..../2019

Prof. Ahmet ÖZARSLAN
Director

ii

"With this thesis it is declared that all the information in this thesis is obtained and presented according to academic rules and ethical principles. Also as required by academic rules and ethical principles all works that are not result of this study are cited properly."

Ferdi KARA

ABSTRACT

Doctor of Philosophy Thesis

CONVENTIONAL NOMA AND THE INTERPLAYS WITH COOPERATIVE COMMUNICATION AND SPATIAL MODULATION: PERFORMANCE EVALUATION AND ANALYSIS UNDER IMPERFECT SIC

Ferdi KARA

Zonguldak Bülent Ecevit University
Graduate School of Natural and Applied Sciences
Department of Electrical and Electronic Engineering

Thesis Advisor: Assist. Prof. Hakan KAYA
July 2019, 177 pages

In recent years, exponential increase in connected devices (i.e., smart-phones, tablets, watches etc.) to the internet and with the introduce of the Internet of Things (IoT), future radio networks (FRN) are keen to serve massive users in dense networks which is called as Massive Machine Type Communication (mMTC) -one of the three major concepts of 5G and beyond-. Non-orthogonal Multiple Access (NOMA) is seen a strong candidate for mMTC in FRN due to its high spectral efficiency and ability to support massive connections. In NOMA, users are assigned into same resource block to increase spectral efficiency and the most attracted scheme is power domain (PD)-NOMA where users share the same resource block with different power allocation coefficients. The interference mitigation in PD-NOMA is held by successive interference canceler (SIC). Due to its potential for 5G and beyond, NOMA has attracted tremendous attention from researchers where NOMA is widely investigated mostly in terms of achievable rate and outage probability. However, in those work mostly perfect SIC is assumed

ABSTRACT (continued)

at the receivers which is not that reasonable assumption considering the fading channels. In addition, whereas numerous efforts have been devoted to investigating NOMA in terms of capacity and outage, one of the most important key performance indicators (KPIs): bit/symbol error rate (BER/SER) has not been regarded. These two major concerns about NOMA have initially motivated us to do this PhD research. This work aims to investigate three KPIs (capacity, outage and BER) of NOMA with imperfect SIC. Then, the same analysis is done for the interplays of NOMA with cooperative communication and spatial modulation (SM).

Firstly, conventional NOMA (downlink and uplink) networks is analyzed under imperfect SIC and exact closed-from expressions for ergodic capacity (EC), outage probability (OP) and bit error probability (BEP) are derived over fading channels. All derived expressions are validated via computer simulations.

The interplay between NOMA and cooperative communication is one of the most attracted NOMA related topics in the literature. This interplay is divided into three concepts: 1) cooperative-NOMA (C-NOMA) where strong NOMA users act as relays for weaker users to improve reliability of them. 2) relay-assisted/aided-NOMA where dedicated relays help source serving to NOMA users. 3) NOMA based cooperative relaying system (CRS) where NOMA is applied for different symbol of the destination to improve the inefficiency of device-to-device cooperative communication. All three concepts have been analysed in terms of the same performance metrics (i.e., EC, OP, BEP) under imperfect SIC and have been validated via Monte Carlo simulations. Then, threshold-based selective cooperative NOMA (TBS-C-NOMA) have been proposed to eliminate the effect of error propagation in C-NOMA and it is proved that TBS-C-NOMA outperforms C-NOMA and achieves full diversity order.

In order to neutralize the decay in BER of conventional NOMA networks, the spatial multiple access (SMA) and Space Shift Keying (SSK)-NOMA have been introduced as alternatives to two users and multiple users multiple-input-multiple-output (MIMO)-NOMA networks. Closed form expressions of EC, OP and BEP have been derived for both systems and the derived expressions have been validated via computer simulations.

ABSTRACT (continued)

Then, a comprehensive evaluation of NOMA involved systems is presented by extensive simulations. It is proved that NOMA outperforms orthogonal multiple access (OMA) techniques in terms of EC and OP. However, due to the inter-user interference (IUI), NOMA cannot compete with OMA networks. Thus, the trade-off between capacity and reliability of NOMA networks is emphasized and it is revealed that NOMA design should be handled considering the target reliability of networks. In addition, the performance improvement of the proposed TBS-C-NOMA scheme are presented compared to C-NOMA schemes. Furthermore, based on the extensive simulation results, it is proved that the proposed SMA and SSK-NOMA systems outperform their NOMA counterparts in terms of all three performance metrics (i.e,, EC, OP and BER). Moreover, the effect of power allocation on the performances of NOMA involved systems are investigated and the optimum power allocation in terms of three KPIs is discussed.

Finally, all results are discussed and the thesis is concluded with the opportunities, challenges and the insights for future researches.

Keywords: Non-orthogonal multiple access, Imperfect SIC, Error analysis, Outage analysis, Capacity analysis, Cooperative communication, Spatial modulation, Space shift keying

Science Code: 608.04.04, 608.04.05

ÖZET

Doktora Tezi

GELENEKSEL DİK OLMAYAN ÇOKLU ERİŞİM (NOMA) VE NOMA'NIN İŞBİRLİKLİ İLETİŞİM VE UZAYSAL MODULASYONLA BİRLİKTE UYGULANMASI: HATALI ARDIŞIK GİRİŞİM ENGELLEYİCİ (SIC) ALTINDA PERFORMANS DEĞERLENDİRMESİ VE ANALİZİ

Ferdi KARA

Zonguldak Bülent Ecevit Üniversitesi
Fen Bilimleri Enstitüsü
Elektrik-Elektronik Mühendisliği Anabilim Dalı

Tez Danışmanı: Dr. Öğr. Üyesi Hakan KAYA
Temmuz 2019, 177 sayfa

Son yıllardaki akıllı-telefon, tablet ve akıllı saat gibi internete bağlı cihaz sayısındaki üstel artış ve Nesnelerin İnterneti (Internet of Things -IoT) kavramının da gelişmesiyle birlikte, yeni nesil telsiz ağların yoğun hücrelerden (dense networks) oluşması ve kitlesel iletişimi (massive connection) desteklemesi gerektiği kaçınılmaz olmuştur. Kitlesel makine tipi iletişim (massive Machine Type Communication -mMTC) olarak adlandırılan bu konsept 5G ve sonrası olarak bilinen yeni nesil telsiz ağların üç ana konseptinden biri olarak görülmektedir. Dik olmayan çoklu erişim (Non-orthogonal Multiple Access -NOMA), yüksek spektral verimlilik sağlaması ve kitlesel iletişime olanak sağlaması nedeniyle mMTC için en önemli adaylardan biri konumundadır. NOMA'da kullanıcılar aynı kaynak bloklarına (resource block) atanarak spektral verimliliğin arttırılması amaçlanmaktadır. En fazla ilgi çeken NOMA konsepti olan güç eksenli (power domain -PD) NOMA'da, kullanıcılar aynı kaynak bloklarını farklı güç

ÖZET (devam ediyor)

paylaşım katsayıları ile paylaşırlar. PD-NOMA'da ki kullanıcılar arası girişim, ardışık girişim giderici (successive interference canceler -SIC) kullanılarak giderilir. NOMA'nın 5G ve sonrası ağları için önemli bir potansiyele sahiptir ve bu nedenle araştırmacıların oldukça fazla ilgisini çekmektedir. NOMA erişilebilir kapasite ve kesinti olasılığı açısından fazlasıyla araştırılmıştır/incelenmiştir. Fakat, bu çalışmalarda çoğunlukla, alıcıların hatasız SIC uyguladığı varsayılmıştır. Bu varsayım sönümlemeli kanallar göz önüne alındığında gerçekçi bir varsayım olmaktan çıkmaktadır. Bununla birlikte, NOMA erişilebilir kapasite ve kesinti olasılığı açısından fazlasıyla incelenmesine rağmen, bir diğer önemli kriter olan bit/sembol hata oranı göz ardı edilmiştir. NOMA hakkındaki bu endişeler bu tez çalışmasının ana motivasyon kaynağı olmuştur. Bu çalışmada, NOMA için hatalı SIC varlığında erişilebilir hız, kesinti olasılığı ve bit hata olasılığı açısından analizlerinin yapılması amaçlanmıştır. NOMA'nın bir diğer avantajı da diğer fiziksel seviye teknikleri ile beraber kullanılabilmesidir. Bu nedenle, aynı analizler, NOMA ile işbirlikli iletişimin ve uzaysal modülasyonun birlikte kullanıldığı durumlar için de genişletilmiştir.

Tez çalışmasında ilk olarak geleneksel NOMA ağları (aşağı yönlü ve yukarı yönlü) hatalı SIC varlığında incelenmiştir. Üç önemli performans kriteri olan, erişilebilir hız, kesinti olasılığı ve bit hata olasılığı için tam ifadeler kapalı formda türetilmiştir. Elde edilen tüm analitik sonuçlar bilgisayar benzetimleri ile doğrulanmıştır.

NOMA ve işbirlikli iletişimin beraber kullanıldığı ağlar araştırmacılar tarafından en fazla ilgi çeken konulardan biri olmuştur. Bu etkileşim üç ana konsepte incelenmektedir: 1) Daha iyi kanal kalitesine sahip NOMA kullanıcılarının daha kötü kanal kalitesine sahip kullanıcılar için röle olarak görev yaptığı, İşbirlikli-NOMA konsepti. 2) Ortamda bulunan rölelerin NOMA kullanıcılarıyla olan iletişime yardımcı olduğu, Röle-destekli/yardımlı-NOMA konsepti. 3) Geleneksel işbirlikli iletişimdeki spektral verimsizliğinin önüne geçmek için kullanılan, NOMA-destekli işbirlikli iletişim sistemleri (cooperative relaying systems -CRS) konsepti. Her üç konsept de hatalı SIC varlığında tüm performans kriterli açısından incelenmiştir ve sonuçlar bilgisayar benzetimleri ile doğrulanmıştır. İşbirlikli-NOMA sistemlerindeki hata yayılımının etkisini ortadan kaldırmak için, Eşik değer tabanlı seçmeli işbirlikli-NOMA

ÖZET (devam ediyor)

(Threshold-base selective cooperative-NOMA – TBS-C-NOMA) sistemi önerilmiş ve önerilen TBS-C-NOMA'nın işbirlikli-NOMA'ya üstünlük sağladığı kanıtlanmıştır. TBS-C-NOMA tam çeşitleme derecesi sağlamaktadır.

Geleneksel NOMA ağlarının BHO başarımdaki kaybın önüne geçmek için, uzaysal çoklu erişim (Spatial Multiple Access (SMA)) ve Uzay kaydırmalı Anahtarlama (Space Shift Keying SSK)-NOMA yapıları sırasıyla iki kullanıcılı ve çok kullanıcılı NOMA ağlarına alternatif olarak önerilmiştir. Önerilen her iki yöntem için de erişilebilir kapasite, kesinti olasılığı ve bit hata olasılığı ifadeleri kapalı-formda türetilmiştir. Sonuçlar bilgisayar benzetimleri ile doğrulanmıştır.

Daha sonra, NOMA'nın kullanıldığı sitemler için detaylı benzetimler sunularak kapsamlı bir performans değerlendirmesi verilmiştir. NOMA erişilebilir kapasite ve kesinti başarımı açısından dikgen çoklu erişim tekniklerine (Orthogonal Multiple Access -OMA) üstünlük göstermesine rağmen kullanıcılar arası girişim sebebiyle bit hata başarımı açısından OMA kadar iyi performans gösterememektedir. Farklı performans kriterleri arasındaki bu ödünleşime (trade-off) dikkat çekilerek, NOMA sistemlerinin hedef güvenirlilik (target reliability) kriteri göz önünde bulundurularak tasarlanması gerektiği ortaya konmuştur. Sunulan detaylı benzetim sonuçları doğrultusunda, önerilen TBS-C-NOMA'nın C-NOMA'ya, SMA ve SSK-NOMA'nın da geleneksel NOMA sistemlerine üstünlük sağladığı gösterilmiştir. Bu bölümde son olarak, farklı performans kriterleri göz önüne alınarak, en iyi güç paylaşımının nasıl olması gerektiği tartışılmıştır.

Son olarak, elde edilen tüm sonuçlar değerlendirilerek, tez gelecek çalışmalar hakkındaki görüşler, olası çalışma alanları ve zorluklar sunularak sonlandırılmıştır.

Anahtar Kelimeler: Dik olmayan çoklu erişim, Hatalı SIC, Hata analizi, Kesinti analizi, Kapasite analizi, İşbirlikli iletişim, Uzaysal modülasyon, Uzay kaydırmalı anahtarlama

Bilim Kodu: 608.04.04, 608.04.05

ACKNOWLEDGMENTS

DEDICATION

to my dear wife, Çağla and to my lovely daughter, Eylül Mavi

TABLE OF CONTENTS

LIST OF FIGURES

LIST OF TABLES

LIST OF SYMBOLS AND ABBREVIATIONS

SYMBOLS

σ_λ^2 : Average channel power (variance) of the link λ

x_i : Base-band complex modulated symbol of i

α_i : Power allocation coefficient at the source/base-station for i

y_i : Received base-band signal at i

w_i : Additive white Gaussian noise at i

h_λ : Flat fading complex channel coefficient of the link λ

P_s : Transmit power of source/base-station

M_i : Modulation order/level of i for M-ary modulation

ρ_s : Transmit signal-to-noise ratio (SNR) of source/base-station

β : Imperfect successive interference canceler (SIC) factor

R_i : Achievable (Shannon) rate of i

C_i : Ergodic capacity of i

γ_λ : Norm square of the fading coefficient h_λ

$P_i(out)$: Outage probability of i

$\acute{R}_i$: Target rate of i

F_{γ_λ} : Cumulative distribution function of γ_λ

$P_i(e)$: Bit error probability of i

ε : Energies of the superposition-coded (SC) symbols

p_{γ_λ} : Probability density function of γ_λ

P_i : Transmit power of user i

ρ_i : Transmit SNR of user i

ζ : Constellation points of superimposed symbols in uplink

ϱ_i : Power allocation coefficient at the relay for i

N_t : Number of transmit antennas

N_r : Number of receive antennas

L : Number of users in a resource block

δ_i : Number of required complex operations for the detection i

$\mathcal{O}$: Number of required detections

ABBREVIATIONS

3GPP   **:** 3rd Generation Partnership Project

5G   **:** 3th Generation

ABEP   **:** Average Bit Error Probability

AF   **:** Amplify-Forward

AWGN   **:** Additive White Gaussian Noise

BEP   **:** Bit Error Probability

BER   **:** Bit Error Rate

BPCU   **:** Bit Per Channel Usage

bps   **:** Bit Per Second

BPSK   **:** Binary Phase Shift Keying

BS   **:** Base Station

CDMA   **:** Code Division Multiple Access

CDF   **:** Cumulative Distribution Function

CD-NOMA   **:** Code Domain Non-Orthogonal Multiple Access

C-NOMA   **:** Cooperative Non-Orthogonal Multiple Access

CoMP   **:** Coordinated Multipoint

CQI   **:** Channel Quality Index

CR   **:** Cognitive Radio

CRS   **:** Cooperative Relaying Systems

CSI   **:** Channel State Information

DF   **:** Decode-Forward

DRN   **:** Diamond Relaying Network

e2e   **:** End-to-End

eMBC   **:** Enhanced Mobile Broadband Communication

EC   **:** Ergodic Capacity

FD   **:** Full Duplex

FDMA   **:** Frequency Division Multiple Access

FRN   **:** Future Radio Network

HD   **:** Half Duplex

HetNet   **:** Heterogeneous Network

KPI   **:** Key Performance Indicator

LTE   **:** Long Term Evolution

IDMA   **:** Interleave Division Multiple Access

IM   **:** Index Modulation

IoT   **:** Internet of Things

IUI   **:** Inter-User-Interference

MBM   **:** Media Based Modulation

MEC   **:** Mobile Edge Computing

MIMO   **:** Multiple-Input-Multiple-Output

ML   **:** Maximum Likelihood

mMTC   **:** Massive Machine Type Communication

mmWC   **:** Millimeter-Wave Communication

MPA   **:** Message Passing Algorithm

MRC   **:** Maximum Ratio Combining

MUD   **:** Multi-User Detection

NOMA   **:** Non-Orthogonal Multiple Access

OFDMA   **:** Orthogonal Frequency Multiple Access

OMA   **:** Orthogonal Multiple Access

OP   **:** Outage Probability

QAM   **:** Quadrature-Amplitude Modulation

QoS   **:** Quality of Service

QPSK   **:** Quadrature Phase Shift Keying

PDF   **:** Probability Density Function

PDMA   **:** Pattern Division Multiple Access

PD-NOMA   **:** Power Domain Non-Orthogonal Multiple Access

SC   **:** Superposition Coding

SCMA   **:** Sparse Code Multiple Access

LIST OF SYMBOLS AND ABBREVIATIONS (continued)

SIC	:	Successive Interference Canceler
SIMO	:	Single-Input-Multiple-Output
SINR	:	Signal-to-Interference plus Noise Ratio
SNR	:	Signal-to-Noise Ratio
SM	:	Spatial Modulation
SMA	:	Spatial Multiple Access
SSK	:	Space Shift Keying
TBS	:	Threshold-based Selective
TDMA	:	Time Division Multiple Access
UE	:	User Equipment
uRLLC	:	Ultra-Reliable Low Latency Communication
VBLAST	:	Vertical-Bell Laboratories Layered Space-Time
VLC	:	Visible Light Communication

CHAPTER 1

INTRODUCTION

Wireless communication technologies have been improved for five decades. This evolution of the communications has been driven by the users'/customers'/clients' requirements and by the development of technology. Every big step of wireless technologies has been named as new generation (i.e., 1G, 2G, 3G and 4G) and multiple access (MA) techniques have been cornerstones for this evolution. Frequency Division Multiple Access (FDMA) had been implemented for voice communication in 1G. Then, with the increase of users, a hybrid multiple access including both Time Division Multiple Access (TDMA) and FDMA was used for voice and data communication in 2G. After then, applications such as internet using and video calling on mobile devices required relatively higher data rate and it has been succeeded by Code Division Multiple Access (CDMA) in 3G. In addition to increase in required data rate, the receiver complexity in CDMA have made the Orthogonal Frequency Division Multiple Access (OFDMA) for downlink and Single Carrier FDMA (SC-FDMA) to take the role in 4G called as Long Term Evolution (LTE). However, new generations (i.e. 5G and beyond) need a major paradigm shift unlike previous four generations of cellular networks. It is beyond improving data rate or increasing number of served users [1]. With the 5G, wireless technologies step into new era which may be called as Wireless 2.0. According to visual network index (VNI) report [2], driven largely by smart-phones, tablets and video streaming, the amount of IP data by wireless networks will be higher than 80 exabytes per month by 2022. It was only about 10 exabytes in 2017. Only this pace of growth can prove us what 5G will be. In addition to this extreme data rate, since it is now beyond personal communication, the demands for 5G and beyond vary according to serving applications/vertical sectors such as Internet of things (IoT), tactile internet, health-care applications, etc. [3]. The major requirements for 5G [4] are given as follow:

- very high data rate (100 times higher than LTE)

- ultra low latency (below 1ms)

- ultra wide coverage (almost %100)

- ultra high mobility

- supporting massive connection (ultra dense networks -1000 times higher than LTE).

Although it is our duty as engineers to meet all demands, it is not possible to meet them in all once. In addition, critical requirements depend on the vertical sectors of future radio networks (FRN). For example, very high data rate is required for video streaming on mobile communications whereas ultra dense networks are demanded by IoT. On the other hand, ultra low latency is crucial for health care applications such as remote surgeon. In addition to ultra low latency, ultra wide coverage is also essential in vehicular communication for autonomous vehicles. Thus, according to above requirements, 5G and beyond networks are categorized in three main concepts [5, 6] as:

- enhanced Mobile Broadband Communication (eMBBC)

- ultra Reliable Low Latency Communication (uRLLC)

- massive Machine Type Communication (mMTC).

In the standardization process, it has been mostly focused on eMBBC as the first phase of 5G [7] which can be considered as an evolved LTE and it is based on flexible OFDMA. To cover concepts above, a new waveform design is essential for the next phases of 5G and beyond. However, to the best of researchers'/engineers' knowledge, it is not possible to serve in all these concepts with a single waveform, hence it is expected to be heterogeneous networks (HetNet) where different waveforms are combined in harmony to meet different requirements according to users' demands. A few of candidate physical layer techniques are as follow [1, 3]: millimeter-wave communication (mmWC), massive-multiple-input-multiple-output (massive MIMO), index modulation (IM), visible light communication (VLC), cognitive radio (CR), non-orthogonal multiple access (NOMA), etc. In this PhD dissertation, it is focused on NOMA which is one of the strongest candidates for mMTC

due to its high spectral efficiency and ability to support massive connections and it has been already taken place in 3GPP standards for mMTC [8, 9].

1.1 LITERATURE OVERVIEW

In the previous four generations of cellular network, users/devices are served on orthogonal resource blocks (i.e, time, frequency, code) to avoid inter-user-interference (IUI). Hence, all used multiple access techniques are called as orthogonal multiple access techniques (OMA)[1]. However, the number of users in a cell is limited by the number of orthogonal blocks in OMA. Thus, OMA schemes cannot compete with the growth in the number of connected devices in such application IoT. To resolve this problem, NOMA has emerged as a potential multiple access scheme for future wireless networks [10]. NOMA concept is based on allowing multiple users to be served on same resource blocks. NOMA schemes can be handled in two main categories: power domain-NOMA (PD-NOMA) and code domain-NOMA (CD-NOMA). In PD-NOMA, multiple users are allocated on the same resource block with different power allocation coefficients. This intentionally created IUI is eliminated at receivers by successive interference canceler (SIC) [11]. On the other hand, in CD-NOMA, users are allocated on same time/frequency blocks with different codes (low density non-orthogonal codes as differs from CDMA). In CD-NOMA, receivers implement message passing algorithm (MPA) to detect own data. Sparse code multiple access (SCMA) is the most attracted version of CD-NOMA [12]. In addition, by combining these two main NOMA schemes, a few more NOMA schemes have been also proposed, such as pattern division multiple access (PDMA) [13] and interleave-division multiple access (IDMA) [14]. In this PhD dissertation, the performances of PD-NOMA schemes are investigated. The other NOMA schemes are out of the scope of this work, thus NOMA is used for PD-NOMA in the following of this work.

Although its application for FRN has emerged to resolve the bottleneck in supporting massive connection [15, 16], SIC and MPA in NOMA have been well-known techniques in terms of information theoretic perspective for decades [17, 18]. NOMA was firstly proposed for FRN in [19], and its superiority to OMA schemes in terms of achievable

---

[1]Although CDMA serves on same time and frequency blocks, the used codes (Walsh-Hadamard) are orthogonal in CDMA.

rate was proved. Then, NOMA has attracted great attention from both industry and academia [20–22]. NOMA has been investigated in terms of different key performance indicators (KPIs) such as outage probability, secrecy sum-rate, mutual information, etc. and it has been compared to OMA counterparts. In addition, NOMA is based on such very simple principle as superposition coding (SC) at transmitter and SIC at receivers, and its implementation into other physical layer techniques can be easily succeeded. Thus, the interplays between NOMA and other physical layer techniques, such as cooperative communication [23, 24], MIMO systems [25], mmWC [26, 27], CR [28] and VLC [29] have also taken recent attention. Furthermore, besides mMTC, NOMA has a huge potential for mobile edge computing (MEC) [30] and NOMA in MEC has been analyzed widely.

In this subsection, NOMA have been introduced and a general literature overview about its applications for FRN and the interplays between other techniques have been provided. The detailed literature researches will be provided in related sections in the following chapters.

1.2 CONTRIBUTIONS

The main contributions of the thesis are summarized as follow:

- As firstly, conventional NOMA networks (i.e., downlink and uplink) are analyzed under imperfect SIC and closed form expressions are derived for ergodic capacity/sum-rate, outage probability (OP) and bit error probability (BEP) of networks. The trade-off between achievable rate and data reliability in NOMA networks is raised and the user fairness is discussed in terms of all performance metrics. In addition, extensive simulations for downlink and uplink NOMA are presented to compare them related OMA networks. Then power allocation is discussed under various constraints (i.e., capacity maximization, outage minimization and error minimization) in downlink NOMA. Based on simulations, it is revealed that it is not possible to provide an optimum power allocation in terms of all users. Hence, power allocation can be only handled by considering users' QoS demands -which performance metric is crucial according to used application-.

- The interplay between NOMA and cooperative communication is investigated in

terms of all aspects.

– Closed-form expressions are derived for BEP in cooperative-NOMA (C-NOMA). It is proved that error performance of C-NOMA is highly affected by error propagation from intra-cell user to cell-edge user which occurs due to erroneous detection in SIC and C-NOMA cannot provide diversity order. In order to resolve this, Threshold-based selective C-NOMA (TBS-C-NOMA) is proposed and optimum threshold for TBS-C-NOMA is derived which minimizes end-to-end (e2e) error performance of TBS-C-NOMA. By introducing optimum threshold, TBS-C-NOMA outperforms significantly C-NOMA and full diversity order is achieved.

– Error performance of relay-aided/assisted NOMA (RA-NOMA) networks is investigated and closed-form BEP expressions are derived. Then, the user fairness is raised in RA-NOMA and a new model for RA-NOMA which is called reversed RA-NOMA is investigated. Based on extensive simulations, it is presented that reversed RA-NOMA can provide improved user fairness in some situations.

– Error performance in NOMA-based cooperative relaying systems (CRS) is investigated and closed-form BEP expressions are derived. It is presented that NOMA-CRS has worse error performance although it provides gain in achievable rate compared to conventional CRS. NOMA-based diamond relaying network (DRN) is also analyzed as a subset of NOMA-CRS and the same discussions/results have been revealed.

The optimum power allocation is further discussed for all three concepts in terms of EC, OP and BEP for various conditions. Likewise in conventional NOMA networks, it is very complex to obtain an optimum power allocation scheme.

• In order to resolve the decay in error performance of NOMA networks, Spatial Multiple Access (SMA) and Space Shift Keying (SSK)-NOMA are proposed as alternatives to two users and multiple users NOMA networks, respectively.

– Closed-form expressions of EC, OP and BEP are derived for SMA and all derived expressions are validated via simulations. Based on simulations, SMA

outperforms NOMA in terms of all KPIs (EC, OP and BEP). In addition, SMA has the same error performance with OMA networks. Thus, it is proved that SMA provides higher spectral efficiency than NOMA without any performance decay. In addition to its superiority to NOMA in terms of error performance, SMA provides the same spectral efficiency with NOMA by $\sim 6dB$ less energy consumption which is very promising for the green communication concept in 5G. Furthermore, SMA requires less receiver complexity than NOMA.

– Optimum detectors are provided for SSK-NOMA. Then, SSK-NOMA is analyzed in terms of EC, OP and BEP. Closed-form expressions are derived for EC and OP. In addition, closed-form BEP expressions are derived when the number of users in a resource block is equal to $L = 3$. Nevertheless, a union bound of BEP is provided for arbitrary number of users in a resource block. All these analysis also provide insights for conventional single-input-multiple-output (SIMO) NOMA networks which have not been also regarded in the literature, yet, to the best of our knowledge. Based on extensive simulations, SSK-NOMA outperforms NOMA in terms of all three performance metrics (i.e., EC, OP and BEP) and this is provided by an affordable complexity cost in cell-edge user. All other users in SSK-NOMA have less complexity than those in NOMA. Unlike almost all previous researches of NOMA, SSK-NOMA allows serving more than two users in a resource block without encountering a decay in any performance metrics compared to NOMA. This is very promising to increase the number of served users in such applications as IoT for mMTC.

1.3 LIST OF PUBLISHED, SUBMITTED AND IN PREPARATION MANUSCRIPTS

1.3.1 Journal Papers - Published and Accepted

- **Kara, F.** and Kaya, H. "BER performances of downlink and uplink NOMA in the presence of SIC errors over fading channels". *IET Communications*, 12 (15), 1834-44, sep. 2018

- **Kara, F.** and Kaya, H. "On the error performance of Cooperative-NOMA with statistical CSIT", *IEEE Communications Letters*, 23 (1), 128-31, jan. 2019

- **Kara, F.** and Kaya, H. "Performance analysis of SSK-NOMA", *IEEE Transactions on Vehicular Technology, Early Access*, jul. 2019

- **Kara, F.** and Kaya, H. "Threshold-based Selective Cooperative-NOMA", *IEEE Communications Letters*, 23 (7), 1263-1266, jul. 2019

- **Kara, F.** and Kaya, H. "The error performance analysis of the decode-forward relay-aided-NOMA systems and a power allocation scheme for user fairness (in Turkish)", *Journal of the Faculty of Engineering and Architecture of Gazi University, in Press*

- **Kara, F.** and Kaya, H. "Non-Orthogonal Multiple Access (NOMA): Solution to massive connectivity and high spectral efficiency for Future Radio Access (FRA) networks (in Turkish)", *Karaelmas Science and Engineering Journal*, 9 (1), 152-165, jul. 2019

- **Kara, F.** and Kaya, H. "Error analysis of Cooperative-Non-Orthogonal Multiple Access (NOMA) over Nakagami-m fading channels (in Turkish)",*Karaelmas Science and Engineering Journal*, 9 (1), 130-141, jul. 2019

1.3.2 Conference Papers - Published

- **Kara F.** and Kaya H., "Spatial Multiple Access (SMA): Enhancing performances of MIMO-NOMA systems", *42nd Int. Conf. on Telecomm. and Sig. Process. (TSP)*, jul. 2019, Budapest, Hungary

- Emir, A., **Kara, F.** and Kaya, H. "Deep Learning-based Joint Symbol Detection for NOMA (in Turkish)", *27th Signal Processing and Communications Applications Conference (SIU)*, apr. 2019, Sivas, Turkey

- **Kara, F.** and Kaya, H. "Derivation of the closed-form BER expressions for DL-NOMA over Nakagami-m fading channels (in Turkish)", *26th Signal Processing and Communications Applications Conference (SIU)*, may. 2019, İzmir, Turkey

7

1.3.3 Papers - Submitted or in Preparation

- **Kara, F.** and Kaya, H. "Error Probability Analysis of NOMA-based Diamond Relaying Networks", *IEEE Transactions on Vehicular Technology, submitted at: 15 June 2019*

- **Kara, F.** and Kaya, H. "On the Achievable Rate and Outage Probability of Threshold-Based Selective Cooperative-NOMA", *in preparation*

- **Kara, F.** and Kaya, H. "On the Performance of NOMA involved systems under imperfect SIC: A comparative study and the trade-off between achievable rate and data reliability",*in preparation*

- **Kara, F.** and Kaya, H. "The interplay between NOMA an Cooperative communication: A comprehensive analysis under imperfect SIC", *in preparation*

- **Kara, F.** and Kaya, H. "Error analysis of NOMA-based Cooperative relaying systems and Machine learning-aided optimum power allocation under various constraints", *in preparation*

- Emir, A., **Kara, F.** and Kaya, H. "Model-Driven Deep Learning Aided Joint Symbol Detection and Threshold Selection for Threshold-based Selective Cooperative-NOMA", *in preparation*

1.3.4 Conference Papers - On Other Research Topics

- Çakar, E., Emir, A., **Kara, F.** and Kaya, H. "Maximization of Error Performance of Device-to-Device (D2D) Cooperative Communication Systems with Deep Learning Aided-Optimum Threshold (in Turkish)", *International Congress on Human-Computer Interaction, Optimization and Robotic Applications (HORA)*, jul. 2019, Nevşehir, Turkey

- Çakar, E., **Kara, F.** and Kaya, H. "Error Analysis of Threshold Based Three-hop Device to Device (D2D) Communication Systems (in Turkish)", *27th Signal Processing and Communications Applications Conference (SIU)*, apr. 2019, Sivas, Turkey

- Şanlı E., **Kara F.** and Kaya H., "Effect of the error propagation on the error performance of cooperative communications with the best relay selection schemes (in Turkish)", *26th Signal Processing and Communications Applications Conference (SIU)*, may. 2019, İzmir, Turkey

- **Kara F.**, Kaya H. , Erkaymaz O., and Öztürk E. "Prediction of the optimal threshold value in DF relay selection schemes based on artificial neural networks", *International Symposium on INnovations in Intelligent SysTems and Applications (IN-ISTA)*, jun. 2016, Sinaia, Romania

1.4 ORGANIZATION

The remainder of this work is as follows:

In Chapter 2, NOMA systems are introduced for downlink and uplink communication and the basic concepts of NOMA at transmitter(s) and receiver(s) are defined. Then, the analytical expressions of ergodic capacity (EC), outage probability (OP) and bit error probability (BEP) are derived in closed-forms for two-user networks. All derived expressions are validated via computer simulations.

In Chapter 3, the interplay between NOMA and cooperative communication is handled in three aspects as: Cooperative-NOMA (C-NOMA), NOMA-based cooperative relaying systems (NOMA-CRS) and relay-aided NOMA networks (RA-NOMA). EC, OP and BEP are derived in closed-forms and validated via Monte Carlo simulations. Based on simulations, performance evaluation of all three concepts are provided and the chapter is concluded with chapter remarks.

In Chapter 4, Spatial Multiple Access (SMA) are introduced as an alternative to conventional two-user NOMA networks and SSK-NOMA is proposed to enhance performance of MIMO-NOMA networks. The same KPIs are also derived for SMA and SSK-NOMA and they are validated by simulations.

In chapter 5, extensive simulations are presented to evaluate the performances of NOMA

involved systems and to compare them with OMA counterparts. Then, the effect of power allocation coefficient on the performances of NOMA systems is investigated and the optimum threshold is discussed for different constraints such as EC, OP, BER and user fairness.

In Chapter 6, all results are discussed and a comprehensive evaluation of NOMA and of NOMA involved systems are provided in terms of all aspects. This PhD dissertation is concluding by presenting opportunities, challenges and future directions of NOMA systems.

1.4.1 Notation

Table 1.1: Common used functions

Name of Function	Symbol	Definition
Marcum-Q Function	$Q(.)$	$Q\left(z\right)=\frac{1}{\sqrt{2\pi}}\int\limits_{z}^{\infty}e^{-t^{2}/2}dt$
Error Function	$erf(.)$	$erf\left(z\right)=\frac{2}{\sqrt{\pi}}\int\limits_{0}^{z}e^{-t^{2}}dt$
Complementary Error Function	$erfc(.)$	$erfc\left(z\right)=1-erf\left(z\right)$
Exponential Integral Function	$Ei(.)$	$Ei\left(z\right)=-\int\limits_{-z}^{\infty}\frac{e^{-t}}{t}dt$
Gamma (Factorial) Function	$\Gamma(.)$	$\Gamma\left(z\right)=\int\limits_{0}^{\infty}t^{z-1}e^{-t}dt \quad Rez>0$

In the rest of this thesis, used notations are defined as follow:

The bold uppercase and lowercase letters denote the matrices and the vectors, respectively. We use $(.)^{T}$ for transpose, $(.)^{H}$ for conjugate transpose and $\|.\|_{F}$ for the Frobenius form of a matrix/vector. We use $|.|$ for the absolute value of a scalar/vector and $\binom{.}{.}$ for the binomial coefficient. $\hat{}$ denotes the estimated symbol or index. $Re\{\}$ is the real component of a complex symbol or vector. The superscripts $(.)^{I}$ and $(.)^{Q}$ denote the in-phase and quadrature companent of a variable, respectively. $P(A)$ denotes the probability of the event A whereas $P(A|_{B})$ and and $P(A|_{B\cap C})$ are the probability of the event A under the conditions that B or both B and C have already occurred, respectively. $CN(\mu,\sigma)$

is a complex Gaussian distribution which has independent real and imaginary random variables with the μ mean and the $\frac{\sigma}{2}$ variance. Moreover, most common functions are presented in Table 1.1.

CHAPTER 2

CONVENTIONAL NOMA NETWORKS

2.1 RELATED WORKS AND MOTIVATION

As mentioned in the previous chapter, NOMA was actually a well-known technique in terms of information theoretic perspective which is actually based on multiple-user detection (MUD) schemes. However, after the authors in [19] proposed NOMA for future wireless networks and proved that its system level sum-rate outperforms OMA [31], it has started to take numerous attention from both industry and academia.

The cornerstone researches of NOMA for conventional networks (downlink and uplink) as a multiple access technique are summarized as follow. The outage performance of NOMA networks has been analyzed in [32] where the users are randomly deployed in a disc and users are assumed to be ordered with instantaneous channel conditions. Then, since the user ordering by channel conditions is considered in NOMA, the user fairness has been raised in [33], and the impact of user paring has been investigated to improve user fairness in NOMA [34]. Then, to emphasize the effect of channel ordering, NOMA has been investigated with partial channel information [35] and then channel ordering with limited feedback signaling has been proposed in [36]. System-level performance has been investigated for MIMO-NOMA applications in [37] and then a general framework has been drawn in for MIMO-NOMA applications [38, 39]. Then, the ergodic rate has been analyzed for MIMO-NOMA [40] and compared to MIMO-OMA counterpart to emphasize its superiority in terms of achievable rate [41, 42]. Small-packet design MIMO is proposed in [43] for IoT applications. The multi-carrier (MC)-NOMA has been introduced in [44] and optimal power allocation for MC-NOMA is investigated in [45]. MIMO-NOMA applications are extended for antenna selection [46] and quasi-degradation [47].

The power allocation has dominant effect on the performance of NOMA systems. Thus,

a great deal of literature has been devoted to investigate optimum power allocation under different constraints such as max-min rate [48–51], sum-rate [52–55] and outage [56–59]. Besides power allocation algorithms, other optimization problems in NOMA such as power minimization, user grouping/clustering, sum rate, sub-carrier allocation for MC-NOMA and resource allocation have been also analyzed widely [60–66]. In addition, performance of downlink NOMA networks have been also analyzed from different perspectives such as physical layer security [67, 68] or secrecy sum rate [69–72].

On the other hand, uplink-NOMA studies are very limited compared to downlink NOMA [73, 74]. Nevertheless, the studies focus on the same performance analysis aspects with downlink NOMA such as ergodic rate [75], outage probability [76, 77]. User fairness has been raised also in uplink NOMA and proportional fairness (PF)-based scheduling algorithm is proposed [78]. For MIMO-NOMA in uplink, a precoding scheme is proposed to minimize the power consumption [79]. Raising attention to the complexity of uplink NOMA, a suboptimal scheme based on user pairing for uplink NOMA has been proposed in [80] and from the same perspective, new receiver designs have been proposed to reduce complexity [81, 82].

Despite enormous efforts on NOMA, the aforementioned studies mostly assume perfect SIC at the receivers side to eliminate interferences of other users. However, this is not a reasonable assumption for wireless communications due to the channel effects. In addition, at the time of writing this thesis, NOMA studies were mostly devoted to analyze such metrics ergodic rate and outage probability whereas error performance (bit/symbol error rate -BER/SER) which is one of the important KPIs had not been regarded, yet. To the best of our knowledge, only simulation results of BER were provided in [83] for donwlink NOMA and the BER expressions were derived for uplink NOMA over additive white Gaussian noise (AWGN) channels [84] which does not include effects of channel fading. Thus, downlink and uplink NOMA schemes are analyzed under imperfect SIC case in this chapter. The analytical expressions are derived for ergodic capacity and outage probability in the following of this chapter and bit error probability (BEP) expressions are derived in closed-forms for both downlink and uplink schemes [85, 86].
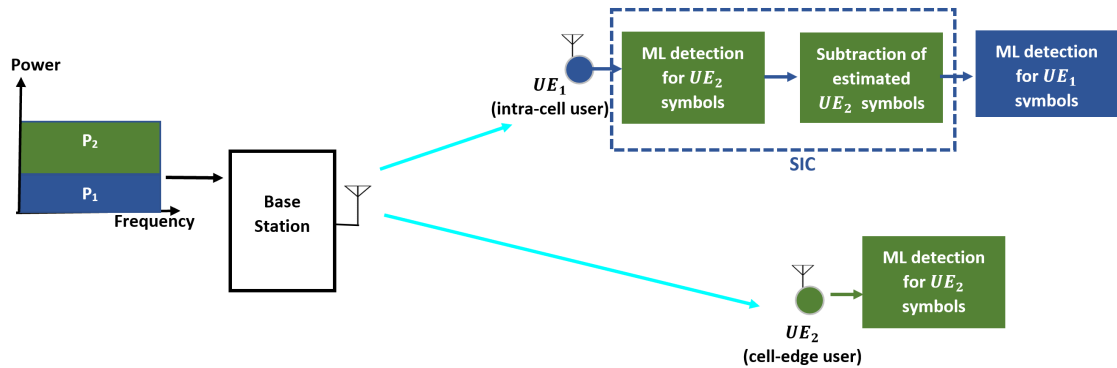
Figure 2.1: The illustration of downlink-NOMA

2.2 DOWNLINK NOMA NETWORKS

2.2.1 System Model

A downlink network is considered where a base station (BS) and two user equipments[1] (i.e., UE_1 and UE_2) are located. Users are denoted as near user (intra-cell user) and far user (cell-edge user) according to their large scale fading coefficients which are dominated by their distances to the BS. As shown in Figure 2.1, all nodes are assumed to be equipped with single antenna. The fading channel coefficient between each node follows $CN(0, \sigma_\lambda^2)$ i.e., $\lambda = s1, s2$. $\sigma_\lambda^2 = \mu d_\lambda^{-\tau}$ is defined where μ and τ are propagation constant and path-loss exponent, respectively. d_λ is the distance between related nodes -from source (BS) to UE_1 and UE_2-. It is assumed that $d_{s1} < d_{s2}$ so that $\sigma_{s1}^2 > \sigma_{s2}^2$, thus UE_1 and UE_2 denote the near user and far user[2], respectively. The BS implements superposition-coding (SC) for the base-band symbols of users and transmits them on the same resource block [19]. The total received symbols by users are given as

$$y_\lambda = \sqrt{P_s} h_\lambda x_{sc} + w_\lambda, \ \lambda = s1, s2, \tag{2.1}$$

---

[1]Although NOMA has ability to serve more than two users, the advantage of NOMA becomes trivial when the number of users becomes more. Hence, almost all studies in the literature assume that only two users in a resource block are served. In addition, in the 3GPP standards, it is also assumed to be two users [7–9].

[2]The near user and far user are determined according to their large-scale fading coefficients unlike instantaneous channel fading coefficients (i.e., h_λ) which is mostly assumed in the literature. However, ordering channels according to their instantaneous fading coefficients requires perfect channel state information at the transmitter (CSIT) and this may cost overload of feedback signaling and may neutralize the advantage of NOMA. In addition, it is not practical for physical implementation [87].

where P_s is the transmit power of BS and h_λ is the channel coefficient between BS and users. w_λ is the additive white Gaussian noise (AWGN) at each users' receiver. w_λ follows $CN(0, N_0)$. x_{sc} is the superposition-coded signal at BS and is defined as

$$x_{sc} = \sqrt{\alpha_1}x_1 + \sqrt{\alpha_2}x_2, \tag{2.2}$$

where x_1 and x_2 denote the base-band symbols -modulated by M_i-ary, $i = 1, 2$ modulation order/level- of UE_1 and UE_2, respectively. α_1 and α_2 are the power allocation coefficients for users. Since the UE_2 has worse channel condition, it is given as $\alpha_2 > \alpha_1$ and $\alpha_1 + \alpha_2 = 1$.

Based on received signals, the users detect their base-band signals. Since the symbols of UE_2 have been allocated with higher power coefficient, UE_2 detects own symbols by pretending symbols of UE_1 as noise. The detection is held by Maximum-Likelihood (ML) detector likewise in conventional modulation schemes as

$$\hat{x}_2 = \underset{m}{\arg\min} \left| y_{s2} - \sqrt{\alpha_2 P_s}h_{s2}x_{2,m} \right|^2, \quad m = 1, 2, ..M_2, \tag{2.3}$$

where $\hat{x}_2$ is the estimated/detected symbols of UE_2, and $x_{2,m}$ denotes each constellation point for M_2-ary modulation.

On the other hand, UE_1 should implement successive interference canceler (SIC) in order to detect own symbols. Thus, UE_1 firstly detects symbols of UE_2 by ML detector such in (2.3) and then, it subtracts regeneration of detected symbols of UE_2 from total received signals. Finally, it detects own symbols by implementing ML detector as

$$\hat{x}_1 = \underset{m}{\arg\min} \left| y'_{s1} - \sqrt{\alpha_1 P_s}h_{s1}x_{1,m} \right|^2, \quad m = 1, 2, ..M_1, \tag{2.4}$$

where

$$y'_{s1} = y_{s1} - \sqrt{\alpha_2 P_s}h_{s1}\hat{x}_2. \tag{2.5}$$

2.2.2 Performance Analysis

2.2.2.1 Ergodic Sum Rate Analysis

NOMA has been proposed to increase spectral efficiency of the system and to serve multiple users on the same resource block compared to OMA schemes. Thus, in this subsection,

achievable rate is analyzed for the system model given in the previous subsection. Achievable rate analysis is presented in terms of information theoretic perspective and it is given according to theoretical Shannon capacity limit [88] likewise in all NOMA researches.

As given in the previous subsection, UE_2 detects own symbol by only ML detector by assuming that the other user's symbols as noise. Thus, the signal-to-interference plus noise ratio (SINR) at UE_2 is given as [19]

$$SINR_2 = \frac{\alpha_2 \rho_s |h_{s2}|^2}{\alpha_1 \rho_s |h_{s2}|^2 + 1}, \tag{2.6}$$

where $\rho_s = P_s/N_0$ is the transmit signal-to-noise ratio (SNR). On the other hand, UE_1 implements SIC to detect own symbols. After SIC, the SINR at the UE_1 is given as

$$SINR_1 = \frac{\alpha_1 \rho_s |h_{s1}|^2}{\beta \alpha_2 \rho_s |h_{s1}|^2 + 1}. \tag{2.7}$$

It is hereby noteworthy that the imperfect SIC case is taken into account and the β denotes it. $\beta = 0$ shows the perfect SIC and it means that the effect of UE_2 symbols is completely eliminated and $\beta = 1$ is the worst case that the effect of UE_2 symbols remains as transmitted (SIC is not succeeded at all).

According to given SINRs at users, the achievable rates of users are given as

$$\begin{aligned} R_1 &= \log_2\left(1 + SINR_1\right), \\ R_2 &= \log_2\left(1 + SINR_2\right). \end{aligned} \tag{2.8}$$

Ergodic capacity of each user is obtained by averaging the achievable rates over instantaneous channel coefficients as [32]

$$\begin{aligned} C_1 &= \int_0^\infty \log_2\left(1 + SINR_1\right) p_{\gamma_{s1}}(\gamma_{s1}) d\gamma_{s1}, \\ C_2 &= \int_0^\infty \log_2\left(1 + SINR_2\right) p_{\gamma_{s2}}(\gamma_{s2}) d\gamma_{s2}. \end{aligned} \tag{2.9}$$

where $\gamma_\lambda \triangleq |h_\lambda|^2$ and $p_{\gamma_\lambda}(\gamma_\lambda)$ is the probability density function (PDF) of γ_λ. With some

algebraic manipulations, ergodic capacities are given as

$$C_1 = \int\limits_0^\infty \log_2\left(1 + (\alpha_1 + \beta\alpha_2)\rho_s\gamma_{s1}\right)p_{\gamma_{s1}}(\gamma_{s1})d\gamma_{s1} - \int\limits_0^\infty \log_2\left(1 + \beta\alpha_2\rho_s\gamma_{s1}\right)p_{\gamma_{s1}}(\gamma_{s1})d\gamma_{s1},$$

$$C_2 = \int\limits_0^\infty \log_2\left(1 + \rho_s\gamma_{s2}\right)p_{\gamma_{s2}}(\gamma_{s2})d\gamma_{s2} - \int\limits_0^\infty \log_2\left(1 + \alpha_1\rho_s\gamma_{s2}\right)p_{\gamma_{s1}}(\gamma_{s2})d\gamma_{s2}.$$

$$(2.10)$$

Since γ_λ follows exponential distribution, with the aid of [89, eq.(4.337.2)], after some algebraic manipulations, ergodic capacities are derived in the closed-form as follow

$$
\begin{aligned}
C_1 = \log_2 e \left[exp\left(\frac{1}{\beta\alpha_2\rho_s\sigma_{s1}^2}\right) Ei\left(-\frac{1}{\beta\alpha_2\rho_s\sigma_{s1}^2}\right) \right. \\
\left. -exp\left(\frac{1}{(\alpha_1 + \beta\alpha_2)\rho_s\sigma_{s1}^2}\right) Ei\left(-\frac{1}{(\alpha_1 + \beta\alpha_2)\rho_s\sigma_{s1}^2}\right) \right],
\end{aligned}
$$

$$(2.11)$$

and

$$C_2 = \log_2 e \left[exp\left(\frac{1}{\alpha_1\rho_s\sigma_{s2}^2}\right) Ei\left(-\frac{1}{\alpha_1\rho_s\sigma_{s2}^2}\right) - exp\left(\frac{1}{\rho_s\sigma_{s2}^2}\right) Ei\left(-\frac{1}{\rho_s\sigma_{s2}^2}\right) \right], \quad (2.12)$$

where $Ei(.)$ [89, eq.(8.21)] is the exponential integral function.

Finally, ergodic sum rate of downlink NOMA is obtained as

$$C_{sum} = C_1 + C_2. \tag{2.13}$$

2.2.2.2 Outage Probability Analysis

The outage event occurs when the achievable rate of users is below the Quality of Service (QoS) requirements of the users. Thus, the outage probability (OP) of users is given as [32]

$$
\begin{aligned}
P_1(out) &= P(R_1 < \acute{R}_1), \\
P_2(out) &= P(R_2 < \acute{R}_2),
\end{aligned}
$$

$$(2.14)$$

where $\acute{R}_1$ and $\acute{R}_2$ denote the target rates of users. By substituting (2.8) into (2.14), OP of users can be easily determined as

$$
\begin{aligned}
P_1(out) &= P(SINR_1 < \phi_1) \\
P_2(out) &= P(SINR_2 < \phi_2)
\end{aligned}
$$

$$(2.15)$$

where $\phi_i = 2^{\acute{R}_i} - 1$. With some algebraic manipulations, OP is given as

$$P_1(out) = F_{\gamma_{s1}}(\psi_1),$$
$$P_2(out) = F_{\gamma_{s2}}(\psi_2),$$
(2.16)

where $F_{\gamma_\lambda}(.)$ is the CDF of γ_λ. By substituting (2.6) into (2.15), it can be easily obtained that

$$\psi_1 = \frac{\phi_1}{\rho_s (\alpha_1 - \beta\alpha_2\phi_1)},$$
$$\psi_2 = \frac{\phi_2}{\rho_s (\alpha_2 - \alpha_1\phi_2)}.$$
(2.17)

However, outage event for UE_1 also occurs when the target rate of UE_2 (i.e., $\acute{R}_2$) is not achieved by SIC. Thus, taking steps for outage of UE_2 at UE_1, it is derived that

$$P_{1\to2}(out) = F_{\gamma_{s1}}(\psi_2).$$
(2.18)

Recalling γ_λ follows exponential distribution, OP of UE_1 is obtained by applying union probability of events as

$$P_1(out) = F_{\gamma_{s1}}(\psi_1) + F_{\gamma_{s1}}(\psi_2) - F_{\gamma_{s1}}(\psi_1)F_{\gamma_{s1}}(\psi_2)$$
$$= (1 - exp(-\psi_1/\sigma_{s1}^2)) + (1 - exp(-\psi_2/\sigma_{s1}^2)) - (1 - exp(-\psi_1/\sigma_{s1}^2))(1 - exp(-\psi_2/\sigma_{s1}^2)),$$
(2.19)

and the OP of UE_2

$$P_2(out) = 1 - exp(-\psi_2/\sigma_{s2}^2).$$
(2.20)

It is hereby noted that, the condition $\alpha_2 \geq \alpha_1\phi_2$ for UE_2 should be accomplished, otherwise UE_2 always remains in outage. Likewise, the conditions $\alpha_2 \geq \alpha_1\phi_2$ and $\alpha_1 \geq \beta\alpha_2\phi_1$ should be accomplished for UE_1 to be reached out.

2.2.2.3 Bit Error Probability (BEP) Analysis

Since BS implements SC, error performance of NOMA networks is highly dependent to chosen digital modulation constellations. In this analysis, it is assumed that Quadrature

19
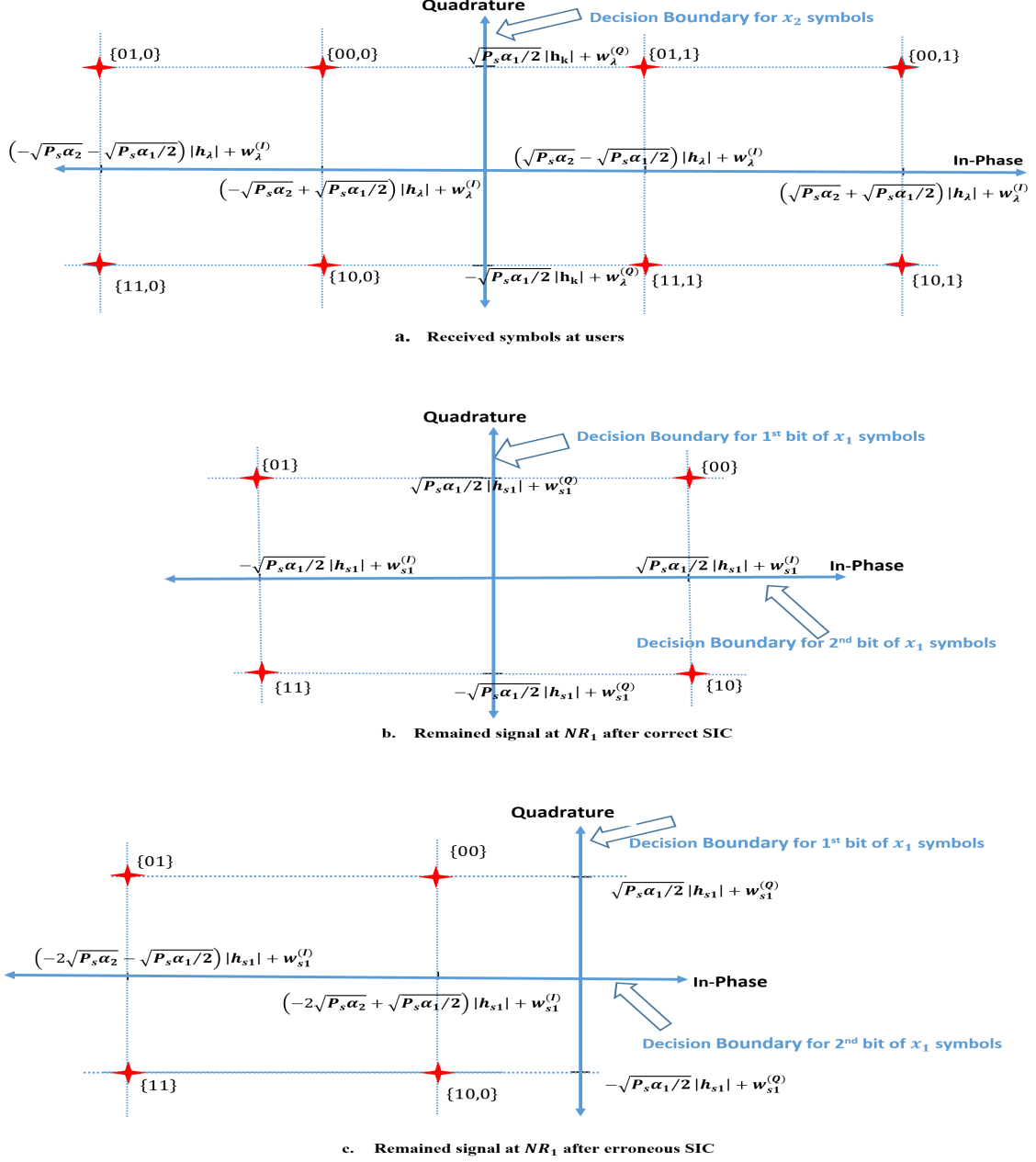
Figure 2.2: Received superposition coded symbols at the users

Phase Shift Keying (QPSK) and Binary Phase Shift Keying (BPSK)[3] are used for UE_1 and UE_2, respectively. This assumption is reasonable since the modulation levels are chosen adaptively in wireless communications according to channel quality index (CQI) where users with better channel conditions are served with higher modulation level constellations. With the chosen modulation constellations, the received signals at users are

---

[3]The analysis can be easily extended for different modulation pairs by considering chosen constellations.

presented in Figure 2.2.a[4] where the binary bit representations for two users are given in the form of $\{i_{1,2}i_{1,1}, i_2\}$. Firstly, the error performance of UE_2 is analyzed since it directly detects its own symbols from total received signal by pretending x_1 symbols as noise. Considering the ML decision boundary for BPSK modulated x_2 symbols, UE_2 detects its own symbols according to the case whether in-phase component of received signal is higher than or lower and equal to zero (i.e., $y_{s2}^{(I)} < 0$ or $y_{s2}^{(I)} \geq 0$). From Figure 2.2.a, one can easily see that the received signals have different energy levels according to which x_1 and x_2 symbols are transmitted. Hence, assuming all priori probabilities for x_1 and x_2 symbols are equal, the conditional BEP for UE_2 can be formulated as

$$
\begin{aligned}
P_2\left(e|_{h_{s2}}\right) = \frac{1}{4} &\left[P\left(w_{s2}^{(I)} \geq \sqrt{\varepsilon_A} |h_{s2}| \right) + P\left(w_{s2}^{(I)} \geq \sqrt{\varepsilon_B} |h_{s2}| \right) \right. \\
&\left. + P\left(w_{s2}^{(I)} < -\sqrt{\varepsilon_A} |h_{s2}| \right) + P\left(w_{s2}^{(I)} < -\sqrt{\varepsilon_B} |h_{s2}| \right) \right],
\end{aligned}
\tag{2.21}
$$

where $\varepsilon_A \triangleq \left(\sqrt{\alpha_2 P_s} + \sqrt{\alpha_1 P_s/2} \right)^2$ and $\varepsilon_B \triangleq \left(\sqrt{\alpha_2 P_s} - \sqrt{\alpha_1 P_s/2} \right)^2$ are defined. Considering each dimension (i.e., in-phase and quadrature) of noise has zero mean and $N_0/2$ variance, with some algebraic manipulations, we obtain the conditional BEP for UE_2 as

$$
P_2\left(e|_{h_{s2}}\right) = \frac{1}{2} \left[Q\left(\sqrt{\frac{2\varepsilon_A \gamma_{s2}}{N_0}} \right) + Q\left(\sqrt{\frac{2\varepsilon_B \gamma_{s2}}{N_0}} \right) \right],
\tag{2.22}
$$

The average bit error probability (ABEP) is obtained by averaging conditional BEP over instantaneous γ_{s2} as $P_2\left(e\right) = \int_0^\infty P_2\left(e|_{h_{s2}}\right) p_{\gamma_{s2}}(\gamma_{s2}) d\gamma_{s2}$. For exponential distribution, with the aid of [90, eq. (5.6)], the ABEP of UE_2 is derived as

$$
P_2\left(e\right) = \frac{1}{4} \left[2 - \sqrt{\frac{\varepsilon_A \sigma_{s2}^2}{N_0 + \varepsilon_A \sigma_{s2}^2}} - \sqrt{\frac{\varepsilon_B \sigma_{s2}^2}{N_0 + \varepsilon_B \sigma_{s2}^2}} \right].
\tag{2.23}
$$

On the other hand, in order to derive BEP of UE_1, the cases whether the symbols of UE_2 are estimated correctly or not should be considered since the SIC is implemented by subtracting this estimated symbol from total received signal at UE_1. After the SIC process, remained signals at UE_1 are given in Figure 2.2.b and Figure 2.2.c for the correct SIC and erroneous SIC, respectively. For simplicity, we present erroneous SIC case where $x_2 = +1$ (i.e., binary 1) is sent and estimated as $\hat{x}_2 = -1$ (i.e., binary 0). The provided analysis will be same vice versa. It is firstly assumed that correct SIC is succeeded. In this case, only x_1 symbols with channel coefficient and noise remain after SIC process.

---

[4]For simplicity, the effects of channel coefficients and noise are not represented

Nevertheless, it here should be noted that this is a conditional event on correct detection of x_2 symbols at UE_1. The correct detection of x_2 symbols at UE_1 can be easily obtained by adopting (2.21) for correct detection and by changing channel coefficient with h_{s1}. Considering this correct detection condition and the decision rule for QPSK which is shown in Figure 2, BEP for x_1 symbols, under the condition that x_2 symbols are detected correctly, is obtained as

$$P_1\left(e|_{h_{s1}\cap correct_{x_2}}\right) = \frac{1}{2}\left[\frac{1}{2}P\left(w_{s1}^{(I)} < \sqrt{\varepsilon_A}\,|h_{s1}|\right) \times \left\{P\left(w_{s1}^{(I)} \geq \sqrt{\varepsilon_C}\,|h_{s1}|\Big|w_{s1}^{(I)} < \sqrt{\varepsilon_A}\,|h_{s1}|\right)\right.\right.$$
$$+ P\left(w_{s1}^{(Q)} \geq \sqrt{\varepsilon_C}\,|h_{s1}|\right)\bigg\} + \frac{1}{2}P\left(w_{s1}^{(I)} < \sqrt{\varepsilon_B}\,|h_{s1}|\right)$$
$$\times \left\{P\left(w_{s1}^{(I)} < -\sqrt{\varepsilon_C}\,|h_{s1}|\Big|w_{s1}^{(I)} < \sqrt{\varepsilon_B}\,|h_{s1}|\right) + P\left(w_{s1}^{(Q)} \geq \sqrt{\varepsilon_C}\,|h_{s1}|\right)\right\}\bigg],$$
$$(2.24)$$

where $\varepsilon_C \triangleq \alpha_1 P_s$ and the first $^1\!/_2$ coefficient denotes the averaging error in each binary bit. $^1\!/_2 P\left(w_{s1}^{(I)} < \sqrt{\varepsilon_A}\,|h_{s1}|\right)$ and $^1\!/_2 P\left(w_{s1}^{(I)} < \sqrt{\varepsilon_B}\,|h_{s1}|\right)$ denote the priori probability for correct detecting of x_2 symbols at UE_1. Conditional probabilities denote the erroneous detections of the first bit of x_1 symbols. The error in second bits of x_1 symbols is not dependent to the detection of x_2 symbols since they are affected by different components of noise (i.e., quadrature and in-phase). Thus, the error probabilities for second bit are given unconditionally. Recalling the conditional probability $P(X \mid Y) = {}^{P(X \cap Y)}/_{P(Y)}$ [91], the BEP for x_1 symbols under the condition x_1 symbols are detected correctly, is obtained as

$$P_1\left(e|_{h_{s1}\cap correct_{x_2}}\right) = \frac{1}{4}\left[P\left(w_{s1}^{(I)} < \sqrt{\varepsilon_A}\,|h_{s1}|\right) \times P\left(w_{s1}^{(Q)} \geq \sqrt{\varepsilon_C}\,|h_{s1}|\right)\right.$$
$$+ P\left(\sqrt{\varepsilon_C}\,|h_{s1}| \leq w_{s1}^{(I)} < \sqrt{\varepsilon_A}\,|h_{s1}|\right) + P\left(w_{s1}^{(I)} < \sqrt{\varepsilon_B}\,|h_{s1}|\right) \quad (2.25)$$
$$\times P\left(w_{s1}^{(Q)} \geq \sqrt{\varepsilon_C}\,|h_{s1}|\right) + P\left(w_{s1}^{(I)} < -\sqrt{\varepsilon_C}\,|h_{s1}|\right)\bigg].$$

Then, after some algebraic manipulations, it is derived as

$$P_1\left(e|_{h_{s1}\cap correct_{x_2}}\right) =$$
$$\frac{1}{4}\left[Q\left(\sqrt{\frac{2\varepsilon_C\gamma_{s1}}{N_0}}\right) \times \left\{4 - Q\left(\sqrt{\frac{2\varepsilon_A\gamma_{s1}}{N_0}}\right) - Q\left(\sqrt{\frac{2\varepsilon_B\gamma_{s1}}{N_0}}\right)\right\} - Q\left(\sqrt{\frac{2\varepsilon_A\gamma_{s1}}{N_0}}\right)\right].$$
$$(2.26)$$

In the second case, it is assumed that x_2 symbols are detected erroneously and subtracted

from total received signal at UE_1. Likewise previous case, by adopting (2.21) and considering decision rule for QPSK symbols, under the condition x_2 symbols are detected erroneously, conditional BEP is given as

$$P_1\left(e|_{h_{s1}\cap error_{x_2}}\right) = \frac{1}{2}\left[\frac{1}{2}P\left(w_{s1}^{(I)} \geq \sqrt{\varepsilon_A}\,|h_{s1}|\right) \times \left\{P\left(w_{s1}^{(I)} \geq \sqrt{\varepsilon_D}\,|h_{s1}|\Big|w_{s1}^{(I)} \geq \sqrt{\varepsilon_A}\,|h_{s1}|\right)\right.\right.$$
$$+ P\left(w_{s1}^{(Q)} \geq \sqrt{\varepsilon_C}\,|h_{s1}|\right)\Big\} + \frac{1}{2}P\left(w_{s1}^{(I)} \geq \sqrt{\varepsilon_B}\,|h_{s1}|\right)$$
$$\times \left\{P\left(w_{s1}^{(I)} < \sqrt{\varepsilon_E}\,|h_{s1}|\Big|w_{s1}^{(I)} \geq \sqrt{\varepsilon_B}\,|h_{s1}|\right) + P\left(w_{s1}^{(Q)} \geq \sqrt{\varepsilon_C}\,|h_{s1}|\right)\right\}\Big],$$
$$(2.27)$$

where $\varepsilon_D \triangleq \left(2\sqrt{\alpha_2 P_s} + \sqrt{\alpha_1 P_s/2}\right)^2$ and $\varepsilon_E \triangleq \left(2\sqrt{\alpha_2 P_s} - \sqrt{\alpha_1 P_s/2}\right)^2$ are defined and by modifying conditional probabilities, it is obtained as

$$P_1\left(e|_{h_{s1}\cap error_{x_2}}\right) = \frac{1}{4}\left[P\left(w_{s1}^{(I)} \geq \sqrt{\varepsilon_A}\,|h_{s1}|\right) \times P\left(w_{s1}^{(Q)} \geq \sqrt{\varepsilon_C}\,|h_{s1}|\right)\right.$$
$$+ P\left(w_{s1}^{(I)} \geq \sqrt{\varepsilon_D}\,|h_{s1}|\right) + P\left(w_{s1}^{(I)} \geq \sqrt{\varepsilon_B}\,|h_{s1}|\right) \qquad (2.28)$$
$$\times P\left(w_{s1}^{(Q)} \geq \sqrt{\varepsilon_C}\,|h_{s1}|\right) + P\left(\sqrt{\varepsilon_B}\,|h_{s1}| \leq w_{s1}^{(I)} < \sqrt{\varepsilon_E}\,|h_{s1}|\right)\Big].$$

Then, under the condition x_2 symbols are detected erroneously, the conditional BEP for x_1 symbols is derived as

$$P_1\left(e|_{h_{s1}\cap error_{x_2}}\right) = \frac{1}{4}\left[Q\left(\sqrt{\frac{2\varepsilon_C\gamma_{s1}}{N_0}}\right) \times \left\{Q\left(\sqrt{\frac{2\varepsilon_A\gamma_{s1}}{N_0}}\right) + Q\left(\sqrt{\frac{2\varepsilon_B\gamma_{s1}}{N_0}}\right)\right\}\right.$$
$$+ Q\left(\sqrt{\frac{2\varepsilon_B\gamma_{s1}}{N_0}}\right) + Q\left(\sqrt{\frac{2\varepsilon_D\gamma_{s1}}{N_0}}\right) - Q\left(\sqrt{\frac{2\varepsilon_E\gamma_{s1}}{N_0}}\right)\Big]. \qquad (2.29)$$

In order to total conditional BEP of x_1, two cases (2.26) and (2.29) are summed, and it is derived as

$$P_1\left(e|_{h_{s1}}\right) = Q\left(\sqrt{\frac{2\varepsilon_C\gamma_{s1}}{N_0}}\right)$$
$$+ \frac{1}{4}\left[-Q\left(\sqrt{\frac{2\varepsilon_A\gamma_{s1}}{N_0}}\right) + Q\left(\sqrt{\frac{2\varepsilon_B\gamma_{s1}}{N_0}}\right) + Q\left(\sqrt{\frac{2\varepsilon_D\gamma_{s1}}{N_0}}\right) - Q\left(\sqrt{\frac{2\varepsilon_E\gamma_{s1}}{N_0}}\right)\right]. \qquad (2.30)$$

The ABEP of x_1 symbols is obtained by averaging over instantaneous γ_{s1} and it is derived as

$$P_1\left(e\right) = \frac{1}{2}\left[1 - \sqrt{\frac{\varepsilon_C\sigma_{s1}^2}{N_0 + \varepsilon_C\sigma_{s1}^2}}\right.$$
$$+ \frac{1}{4}\left\{\sqrt{\frac{\varepsilon_A\sigma_{s1}^2}{N_0 + \varepsilon_A\sigma_{s1}^2}} - \sqrt{\frac{\varepsilon_B\sigma_{s1}^2}{N_0 + \varepsilon_B\sigma_{s1}^2}} - \sqrt{\frac{\varepsilon_D\sigma_{s1}^2}{N_0 + \varepsilon_D\sigma_{s1}^2}} + \sqrt{\frac{\varepsilon_E\sigma_{s1}^2}{N_0 + \varepsilon_E\sigma_{s1}^2}}\right\}\right]. \qquad (2.31)$$
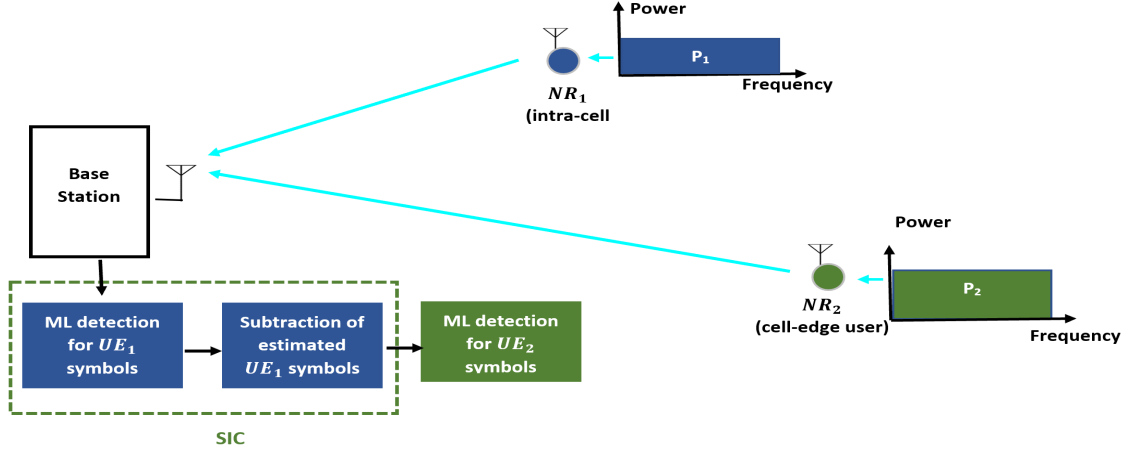
Figure 2.3: The illustration of uplink-NOMA

2.3 UPLINK NOMA NETWORKS

2.3.1 System Model

Likewise downlink, an uplink communication is considered where a BS and two users are located (i.e., UE_1, UE_2). All nodes are assumed to have single antenna and channel fading between nodes follows $CN(0, \sigma_\lambda^2)$ i.e., $\lambda = s1, s2$. $\sigma_{s1}^2 > \sigma_{s2}^2$ is assumed, thus UE_1 and UE_2 denote the near user and far user. Considered system model is given in Figure 2.3. According to CQI of users, the symbols of UE_1 and UE_2 are modulated by QPSK and BPSK, respectively. The users transmit their intended symbols on the same resource block and the received signal by BS is given as

$$y = \sqrt{P_1}h_{s1}x_1 + \sqrt{P_2}h_{s2}x_2 + w, \tag{2.32}$$

where P_i, h_{si}, and x_i, $i = 1, 2$ denote transmit power of user, channel fading coefficient between user and BS and the base-band complex modulated symbol of related user, respectively. w is the AWGN and follows $CN(0, N_0)$.

Based on received signal, BS detects users' symbols by implementing SIC. Since the channel quality of UE_1 is higher, its symbols are expected to be received by higher energy. Thus, BS detects symbols of UE_1 with ML detector by pretending symbols of UE_2 as noise. The detection is given as

$$\hat{x}_1 = \operatorname*{argmin}_{m} \left| y - \sqrt{P_1}h_{s1}x_{1,m} \right|^2, \quad m = 1, 2, ..M_1, \tag{2.33}$$

where $\hat{x}_1$ is the estimated/detected symbols of UE_1, M_1 is the modulation order/level for the symbols of UE_1 and $x_{1,m}$ denotes each point in M_1-ary modulation constellation. After detecting of x_1 symbols, BS implements SIC to detect x_2 symbols as

$$\hat{x}_2 = \operatorname*{argmin}_m \left| y' - \sqrt{P_2} h_{s2} x_{2,m} \right|^2, \quad m = 1, 2, ..M_2, \tag{2.34}$$

where

$$y' = y - \sqrt{P_2} h_{s1} \hat{x}_1. \tag{2.35}$$

2.3.2 Performance Analysis

2.3.2.1 Ergodic Sum Rate Analysis

As in the downlink NOMA, achievable rates of users are analyzed in terms of Shannon limit and ergodic capacity for uplink NOMA is provided in this subsection. In order to calculate Shannon limit, the SINR for each users' symbols should be firstly defined. Since BS firstly detects symbols of UE_1 by pretending x_2 symbols as noise, the SINR for UE_1 is given as [74]

$$SINR_1 = \frac{\rho_1 |h_{s1}|^2}{\rho_2 |h_{s2}|^2 + 1}, \tag{2.36}$$

where $\rho_1 = {P_1}/{N_0}$ and $\rho_2 = {P_2}/{N_0}$ denote transmit SNR for each user. After SIC at BS, the SINR for UE_2 is defined as

$$SINR_2 = \frac{\rho_2 |h_{s2}|^2}{\beta \rho_1 |h_{s1}|^2 + 1}, \tag{2.37}$$

where β denotes the effect of imperfect SIC just as in downlink NOMA.

According to given SINRs at BS, the achievable rates of users are given as

$$
\begin{aligned}
R_1 &= \log_2 \left(1 + SINR_1 \right), \\
R_2 &= \log_2 \left(1 + SINR_2 \right),
\end{aligned}
\tag{2.38}
$$

and with some algebraic manipulations, the achievable rates of users are determined as [76]

$$
\begin{aligned}
R_1 &= \log_2 \left(1 + \rho_1 \gamma_{s1} + \rho_2 \gamma_{s2} \right) - \log_2 \left(1 + \rho_2 \gamma_{s2} \right), \\
R_2 &= \log_2 \left(1 + \rho_2 \gamma_{s2} + \beta \rho_1 \gamma_{s1} \right) - \log_2 \left(1 + \beta \rho_1 \gamma_{s1} \right),
\end{aligned}
\tag{2.39}
$$

In order to derive ergodic rates, as firstly $\Psi_1 \triangleq \rho_1\gamma_{s1} + \rho_2\gamma_{s2}$ and $\Psi_2 \triangleq \rho_2\gamma_{s2} + \beta\rho_1\gamma_{s1}$ are defined where $\gamma_{s1} \triangleq |h_{s1}|^2$ and $\gamma_{s2} \triangleq |h_{s2}|^2$. Then, the ergodic capacities are obtained by

$$
\begin{aligned}
C_1 &= \int_0^\infty \log_2\left(1 + \Psi_1\right)p_{\Psi_1}(\Psi_1)d\Psi_1 - \int_0^\infty \log_2\left(1 + \rho_2\gamma_{s2}\right)p_{\gamma_{s2}}(\gamma_{s2})d\gamma_{s2}, \\
C_2 &= \int_0^\infty \log_2\left(1 + \Psi_2\right)p_{\Psi_2}(\Psi_2)d\Psi_2 - \int_0^\infty \log_2\left(1 + \beta\rho_1\gamma_{s1}\right)p_{\gamma_{s1}}(\gamma_{s1})d\gamma_{s1},
\end{aligned}
\tag{2.40}
$$

where $p_{\Psi_i}(\Psi_i)$, $i = 1, 2$ is the PDF for Ψ_i. Since both γ_{s1} and γ_{s2} follow exponential distribution, the PDF Ψ_i is given as [91],

$$
\begin{aligned}
p_{\Psi_1}(t) &= \frac{\exp\left(-t/\rho_1\sigma_{s1}^2\right) - \exp\left(-t/\rho_2\sigma_{s2}^2\right)}{\rho_1\sigma_{s1}^2 - \rho_2\sigma_{s2}^2}, \quad t > 0, \\
p_{\Psi_2}(t) &= \frac{\exp\left(-t/\rho_2\sigma_{s2}^2\right) - \exp\left(-t/\beta\rho_1\sigma_{s1}^2\right)}{\rho_2\sigma_{s2}^2 - \beta\rho_1\sigma_{s1}^2}, \quad t > 0.
\end{aligned}
\tag{2.41}
$$

Substituting (2.41) into (2.40), and with the aid of [89, eq. (4.337.2)], ergodic capacity of each user is derived as

$$
\begin{aligned}
C_1 = \log_2 e &\left[\exp\left(\frac{1}{\rho_2\sigma_{s2}^2}\right) Ei\left(-\frac{1}{\rho_2\sigma_{s2}^2}\right)\left(1 + \frac{\rho_2\sigma_{s2}^2}{\rho_1\sigma_{s1}^2 - \rho_2\sigma_{s2}^2}\right) \right. \\
&\left. - \frac{\rho_1\sigma_{s1}^2 \exp\left(\frac{1}{\rho_1\sigma_{s1}^2}\right) Ei\left(-\frac{1}{\rho_1\sigma_{s1}^2}\right)}{\rho_1\sigma_{s1}^2 - \rho_2\sigma_{s2}^2} \right],
\end{aligned}
\tag{2.42}
$$

and

$$
\begin{aligned}
C_2 = \log_2 e &\left[\exp\left(\frac{1}{\beta\rho_1\sigma_{s1}^2}\right) Ei\left(-\frac{1}{\beta\rho_1\sigma_{s1}^2}\right)\left(1 + \frac{\beta\rho_1\sigma_{s1}^2}{\rho_2\sigma_{s2}^2 - \beta\rho_1\sigma_{s1}^2}\right) \right. \\
&\left. - \frac{\rho_2\sigma_{s2}^2 \exp\left(\frac{1}{\rho_2\sigma_{s2}^2}\right) Ei\left(-\frac{1}{\rho_2\sigma_{s2}^2}\right)}{\rho_2\sigma_{s2}^2 - \beta\rho_1\sigma_{s1}^2} \right].
\end{aligned}
\tag{2.43}
$$

Finally, ergodic sum rate of uplink NOMA is obtained as

$$
C_{sum} = C_1 + C_2.
\tag{2.44}
$$

2.3.2.2 Outage Probability Analysis

As in the downlink NOMA, OP is defined as the probability of achievable rates being below the target rates of users [77]. It is given as

$$
\begin{aligned}
P_1(out) &= P(R_1 < \acute{R}_1), \\
P_2(out) &= P(R_2 < \acute{R}_2),
\end{aligned}
\tag{2.45}
$$

where $\acute{R}_1$ and $\acute{R}_2$ denote the target rates of users. Substituting (2.38) into (2.45), it is determined as

$$P_1(out) = P(\frac{\rho_1 |h_{s1}|^2}{\rho_2 |h_{s2}|^2 + 1} < \phi_1),$$

$$P_2(out) = P(\frac{\rho_2 |h_{s2}|^2}{\beta\rho_1 |h_{s1}|^2 + 1} < \phi_2), \tag{2.46}$$

where $\phi_i = 2^{\acute{R}_i} - 1$. With some algebraic manipulations, OPs of users are obtained as

$$P_1(out) = P(\Psi_3 < \phi_1),$$

$$P_2(out) = P(\Psi_4 < \phi_2), \tag{2.47}$$

where $\Psi_3 \triangleq \rho_1\gamma_{s1} - \phi_1\rho_2\gamma_{s2}$ and $\Psi_4 \triangleq \rho_2\gamma_{s2} - \phi_2\beta\rho_1\gamma_{s1}$. The OPs of users turn out to be

$$P_1(out) = F_{\Psi_3}(\phi_1),$$

$$P_2(out) = F_{\Psi_4}(\phi_2), \tag{2.48}$$

where $F_{\Psi_3}(.)$ and $F_{\Psi_3}(.)$ are CDFs of Ψ_3 and Ψ_4, respectively. Since γ_{s1} and γ_{s2} are both exponentially distributed, the CDFs of Ψ_3 and Ψ_3 are derived by difference of scaled exponentially distributions. With the aid of [91], they are derived as

$$F_{\Psi_3}(t) = 1 - \frac{\rho_1\sigma_{s1}^2}{\rho_1\sigma_{s1}^2 + \phi_1\rho_2\sigma_{s2}^2} \exp\left(-\frac{t}{\rho_1\sigma_{s1}^2}\right), t \geq 0,$$

$$F_{\Psi_4}(t) = 1 - \frac{\rho_2\sigma_{s2}^2}{\rho_2\sigma_{s2}^2 + \phi_2\beta\rho_1\sigma_{s1}^2} \exp\left(-\frac{t}{\rho_2\sigma_{s2}^2}\right), t \geq 0. \tag{2.49}$$

OPs of users are derived as

$$P_1(out) = 1 - \frac{\rho_1\sigma_{s1}^2}{\rho_1\sigma_{s1}^2 + \phi_1\rho_2\sigma_{s2}^2} \exp\left(-\frac{\phi_1}{\rho_1\sigma_{s1}^2}\right),$$

$$P_2(out) = 1 - \frac{\rho_2\sigma_{s2}^2}{\rho_2\sigma_{s2}^2 + \phi_2\beta\rho_1\sigma_{s1}^2} \exp\left(-\frac{\phi_2}{\rho_2\sigma_{s2}^2}\right). \tag{2.50}$$

It is noteworthy that OPs of users are highly dependent to target rates and wrong target rates cause users to be always in outage. Hence, for UE_1, the condition $\rho_1\sigma_{s1}^2 \geq \phi_1\rho_2\sigma_{s2}^2$ should be accomplished. On the other hand, for UE_2, in addition to $\rho_2\sigma_{s2}^2 \geq \phi_2\beta\rho_1\sigma_{s1}^2$ condition, we note that UE_2 will be in outage if UE_1 is in outage (SIC can not be succeeded at all). Hence, the OP of UE_2 turns out to be

$$P_2(out) =$$

$$\left\{1 - \frac{\rho_2\sigma_{s2}^2}{\rho_2\sigma_{s2}^2 + \phi_2\beta\rho_1\sigma_{s1}^2} \exp\left(-\frac{\phi_2}{\rho_2\sigma_{s2}^2}\right)\right\} + \left\{1 - \frac{\rho_1\sigma_{s1}^2}{\rho_1\sigma_{s1}^2 + \phi_1\rho_2\sigma_{s2}^2} \exp\left(-\frac{\phi_1}{\rho_1\sigma_{s1}^2}\right)\right\}$$

$$- \left\{1 - \frac{\rho_2\sigma_{s2}^2}{\rho_2\sigma_{s2}^2 + \phi_2\beta\rho_1\sigma_{s1}^2} \exp\left(-\frac{\phi_2}{\rho_2\sigma_{s2}^2}\right)\right\}\left\{1 - \frac{\rho_1\sigma_{s1}^2}{\rho_1\sigma_{s1}^2 + \phi_1\rho_2\sigma_{s2}^2} \exp\left(-\frac{\phi_1}{\rho_1\sigma_{s1}^2}\right)\right\}.$$

2.3.2.3   Bit Error Probability (BEP) Analysis

In order to analyze BEP for uplink NOMA, received signal at BS on the same resource block should be considered. In case QPSK and BPSK are used as digital modulation constellations for UE_1 and UE_2 according to CQI, respectively, the total received signal constellation at BS is given in Figure 2.4.a. BS firstly implements ML detector to detect x_1 symbols by pretending x_2 symbols as noise. ML decision rule for QPSK modulated symbols is given as whether in-phase/quadrature component of received signals is higher than zero or lower and equal to zero (i.e., $y^{(I)} > 0$ or $y^{(I)} \leq 0$ and $y^{(Q)} > 0$ or $y^{(Q)} \leq 0$). Thus, the conditional BEP of x_1 symbols is given as

$$P_1\left(e|_{h_{s1} \cap h_{s2}}\right) = \frac{1}{2}\left[P\left(w^{(Q)} \geq \sqrt{P_1/2}\,|h_{s1}|\right) + \frac{1}{2}\left\{ P\left(w^{(I)} \geq \sqrt{P_1/2}\,|h_{s1}| + \sqrt{P_2}\,|h_{s2}|\right) \right.\right.$$
$$\left.\left. + P\left(w^{(I)} \geq \sqrt{P_1/2}\,|h_{s1}| - \sqrt{P_2}\,|h_{s2}|\right)\right\}\right],$$

(2.52)

where first $^1\!/_2$ coefficient denotes averaging error in each bit for total BEP. It is noteworthy that the decision on the first of x_1 symbols only depends on the h_{s1} since x_2 symbols has no effect on quadrature component of received signal. With some algebraic manipulations, conditional BEP for x_1 symbols is determined as

$$P_1\left(e|_{h_{s1} \cap h_{s2}}\right) = \frac{1}{2}\left[\frac{1}{2}\left\{ Q\left(\sqrt{2}\zeta_A\right) + Q\left(\sqrt{2}\zeta_B\right)\right\} + Q\left(\sqrt{2}\zeta_C\right)\right],$$ (2.53)

where $\zeta_A \triangleq \sqrt{\rho_1/2}\,|h_{s1}| + \sqrt{\rho_2}\,|h_{s2}|$, $\zeta_B \triangleq \sqrt{\rho_1/2}\,|h_{s1}| - \sqrt{\rho_2}\,|h_{s2}|$ and $\zeta_C \triangleq \sqrt{\rho_1/2}\,|h_{s1}|$ are defined. By averaging conditional BEP over instantaneous channel conditions, the average BEP of UE_1 is obtained as

$$P_1\left(e\right) = \frac{1}{2}\left[\frac{1}{2}\left\{\int_0^\infty Q\left(\sqrt{2}\zeta_A\right) p_{\zeta_A}(\zeta_A)d\zeta_A + \int_0^\infty Q\left(\sqrt{2}\zeta_B\right) p_{\zeta_B}(\zeta_B)d\zeta_B\right\}\right.$$
$$\left. + \int_0^\infty Q\left(\sqrt{2}\zeta_C\right) p_{\zeta_C}(\zeta_C)d\zeta_C\right],$$

(2.54)

where $p_{\zeta_i}(\zeta_i), i = A, B, C$ denotes PDF of ζ_i. One can easily see that ζ_C is a scaled Rayleigh distribution. However, PDFs should be defined for ζ_A and ζ_B which are sum and difference of two scaled Rayleigh distributions (channel fading), respectively.
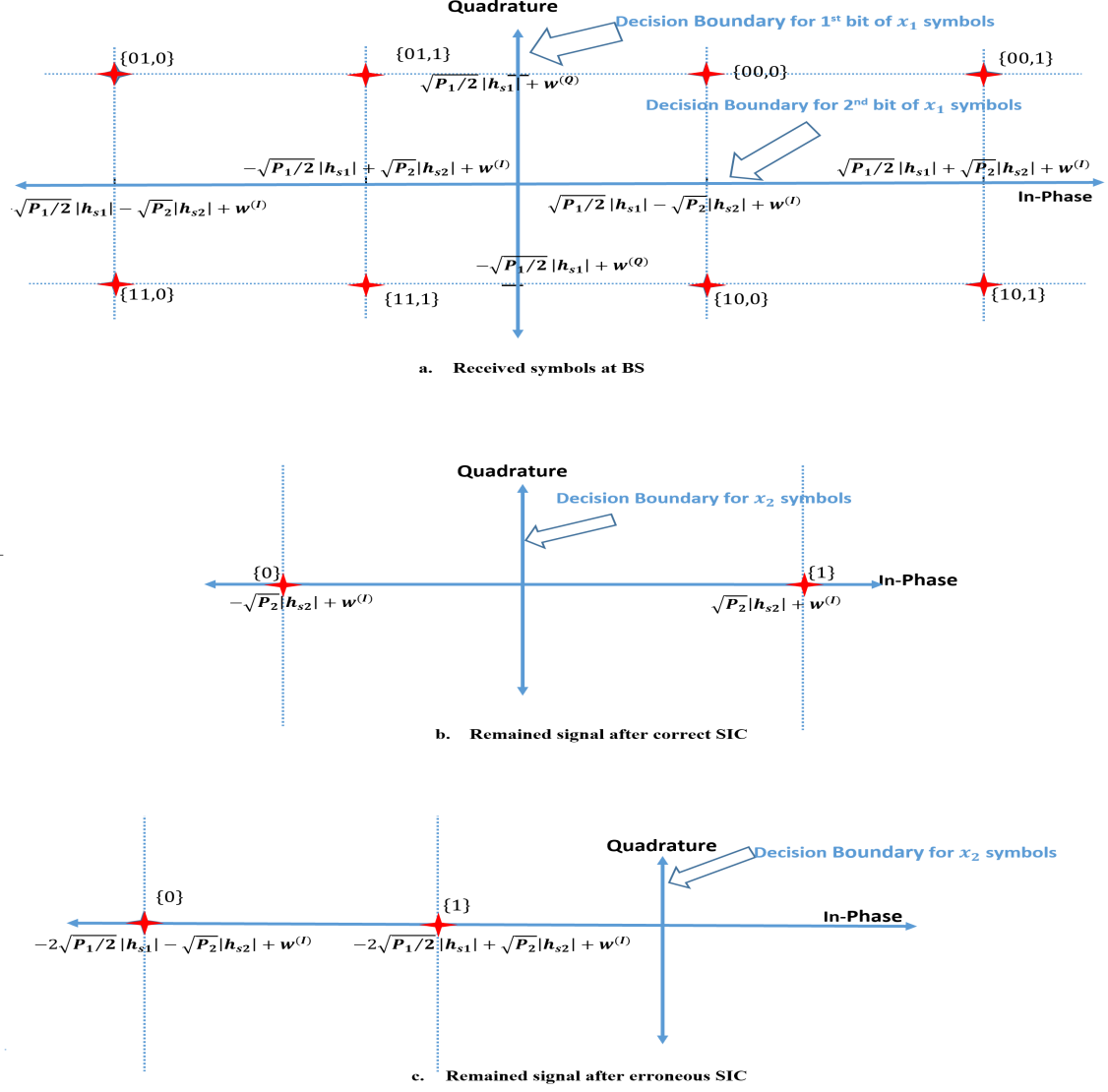
Figure 2.4: Received superimposed symbols of users at the BS

Let assume X and Y are two independent Rayleigh distributions with scale parameters σ_X andσ_Y. The PDFs for $Z = X + Y$ is given [92] as

$$
p_Z(z) =
$$

$$
\frac{\sigma_X^2 z}{(\sigma_X^2 + \sigma_Y^2)^2} exp\left(-\frac{z^2}{2\sigma_X^2}\right) + \frac{\sigma_Y^2 z}{(\sigma_X^2 + \sigma_Y^2)^2} exp\left(-\frac{z^2}{2\sigma_Y^2}\right) + \sqrt{\frac{\pi}{2}} \frac{\sigma_X \sigma_Y [z^2 - (\sigma_X^2 + \sigma_Y^2)]}{(\sigma_X^2 + \sigma_Y^2)^{\frac{5}{2}}}
$$

$$
\times exp\left(-\frac{z^2}{2(\sigma_X^2 + \sigma_Y^2)}\right) \left[erf\left(\frac{z\sigma_Y}{\sigma_X \sqrt{2(\sigma_X^2 + \sigma_Y^2)}}\right) + erf\left(\frac{z\sigma_X}{\sigma_Y \sqrt{2(\sigma_X^2 + \sigma_Y^2)}}\right)\right],
$$

$$(2.55)$$

where $erf(.)$ is the error function and $erf(x) = 2/\sqrt{\pi} \int_0^x e^{-t^2} dt$.

The PDF of $W = X - Y$ is given [85] as

$$p_W(w) = \begin{cases} \frac{4e^{-w^2/\sigma_X^2}}{\sigma_X^2 \sigma_Y^2} \left[\frac{\sqrt{\pi}erfc\left(\frac{w\left(1-\tau\sigma_X^2\right)}{\sqrt{\tau}\sigma_X^2}\right)\exp\left(\frac{w^2}{\tau\sigma_X^4}\right)}{2\tau^{\frac{3}{2}}\sigma_X^2}\left\{\frac{\tau\sigma_X^4+2w^2}{2\tau\sigma_X^2}-w^2\right\} - \frac{w\,exp\left(-w^2\left(\tau-\frac{2}{\sigma_X^2}\right)\right)}{2\tau^2\sigma_X^2} \right], & \\ & w < 0, \\ \frac{4e^{-w^2/\sigma_X^2}}{\sigma_X^2 \sigma_Y^2} \left[\frac{\sqrt{\pi}erfc\left(\frac{w}{\sqrt{\tau}\sigma_X^2}\right)\exp\left(\frac{w^2}{\tau\sigma_X^4}\right)}{2\tau^{\frac{3}{2}}\sigma_X^2}\left\{\frac{\tau\sigma_X^4+2w^2}{2\tau\sigma_X^2}-w^2\right\} + \frac{w}{2\tau}\left(1-\frac{1}{\tau\sigma_X^2}\right) \right], & w \geq 0. \end{cases}$$

(2.56)

where $erfc(x) = 1 - erf(x)$ and $\tau = (\sigma_X^2 + \sigma_Y^2)/(\sigma_X^2\sigma_Y^2)$.

Recalling that $\zeta_A \sim Z$ and $\zeta_B \sim W$ with $\sigma_X \triangleq \sigma_{s1}\sqrt{\rho_1/2}$ and $\sigma_Y \triangleq \sigma_{s2}\sqrt{\rho_2}$, and with the aid of [90, eq. (5.6)], average BEP of UE_1 symbols is derived as

$$P_1(e) = \frac{1}{4}\left[\int_0^\infty Q\left(\sqrt{2}\zeta_A\right)p_{\zeta_A}(\zeta_A)d\zeta_A + \int_0^\infty Q\left(\sqrt{2}\zeta_B\right)p_{\zeta_B}(\zeta_B)d\zeta_B + \left(1 - \sqrt{\frac{\rho_1\sigma_{s1}^2}{2+\rho_1\sigma_{s1}^2}}\right)\right].$$

(2.57)

In order to derive BEP of x_2 symbols in uplink NOMA, correct SIC or erroneous SIC cases should be considered likewise at UE_1 in downlink NOMA. It is firstly assumed that BS has detected x_1 symbols correctly and subtracted regenerated form of them from total received signal. The remained signal after correct SIC is given in Figure 2.4.b. Since the symbols of UE_2 are modulated by BPSK, the decision rule for ML decision after SIC is given as: the in-phase component of remained signal is higher than zero or lower and equal to zero (i.e., $y'^{(I)} > 0$ or $y'^{(I)} \leq 0$). Thus, neither the quadrature component of noise nor the decision for the first bits of x_1 symbols has a role on decision. Considering correct detection of the second bits of x_1 symbols, conditional BEP for x_2 symbols under correct SIC is defined as

$$\begin{aligned} P_2\left(e|_{correct_{x_1}\cap h_{s1}\cap h_{s2}}\right) = \frac{1}{2}\Big[&P\left(w^{(I)} < \sqrt{P_1/2}\,|h_{s1}| + \sqrt{P_2}\,|h_{s2}|\right) \\ &\times P\left(w^{(I)} \geq \sqrt{P_2}\,|h_{s2}|\Big|w^{(I)} < \sqrt{P_1/2}\,|h_{s1}| + \sqrt{P_2}\,|h_{s2}|\right) \\ &+ P\left(w^{(I)} < \sqrt{P_1/2}\,|h_{s1}| - \sqrt{P_2}\,|h_{s2}|\right) \\ &\times P\left(w^{(I)} < -\sqrt{P_2}\,|h_{s2}|\Big|w^{(I)} < \sqrt{P_1/2}\,|h_{s1}| - \sqrt{P_2}\,|h_{s2}|\right)\Big]. \end{aligned}$$

(2.58)

By applying conditional probabilities into (2.58) and after some algebraic manipulations, the conditional BEP of x_2 symbols under correct SIC is derived as

$$P_2\left(e|_{correct_{x_1} \cap h_{s1} \cap h_{s2}}\right) = Q\left(\sqrt{2}\zeta_D\right) - \frac{1}{2}Q\left(\sqrt{2}\zeta_A\right), \tag{2.59}$$

where $\zeta_D \triangleq \sqrt{\rho_2}\,|h_{s2}|$.

Then, it is assumed that x_1 symbols have been detected erroneously and subtracted from received signal. Remained signal after erroneous SIC is given in Figure 2.4.c. Considering the ML decision rule and the priori probability for erroneous detection of x_1 symbols, conditional BEP under erroneous SIC is obtained as

$$
\begin{aligned}
P_2\left(e|_{error_{x_1} \cap h_{s1} \cap h_{s2}}\right) = \frac{1}{2}\Bigg[& P\left(w^{(I)} \geq \sqrt{P_1/2}\,|h_{s1}| + \sqrt{P_2}\,|h_{s2}|\right) \\
\times & P\left(w^{(I)} \geq 2\sqrt{P_1/2}\,|h_{s1}| + \sqrt{P_2}\,|h_{s2}|\Big| w^{(I)} \geq \sqrt{P_1/2}\,|h_{s1}| + \sqrt{P_2}\,|h_{s2}|\right) \\
+ & P\left(w^{(I)} \geq \sqrt{P_1/2}\,|h_{s1}| - \sqrt{P_2}\,|h_{s2}|\right) \\
\times & P\left(w^{(I)} < 2\sqrt{P_1/2}\,|h_{s1}| - \sqrt{P_2}\,|h_{s2}|\Big| w^{(I)} \geq \sqrt{P_1/2}\,|h_{s1}| - \sqrt{P_2}\,|h_{s2}|\right) \Bigg].
\end{aligned}
\tag{2.60}
$$

By applying conditional probabilities and with some simplifications, conditional BEP is obtained as

$$P_2\left(e|_{error_{x_1} \cap h_{s1} \cap h_{s2}}\right) = \frac{1}{2}\left[Q\left(\sqrt{2}\zeta_B\right) + Q\left(\sqrt{2}\zeta_E\right) - Q\left(\sqrt{2}\zeta_F\right)\right], \tag{2.61}$$

where $\zeta_E \triangleq \sqrt{2\rho_1}\,|h_{s1}| + \sqrt{\rho_2}\,|h_{s2}|$, $\zeta_F \triangleq \sqrt{2\rho_1}\,|h_{s1}| - \sqrt{\rho_2}\,|h_{s2}|$. By summing two cases (i.e., correct SIC (2.59) and erroneous SIC (2.61)), total conditional BEP of UE_2 is derived as

$$P_2\left(e|_{h_{s1} \cap h_{s2}}\right) = Q\left(\sqrt{2}\zeta_D\right) + \frac{1}{2}\left[-Q\left(\sqrt{2}\zeta_A\right) + Q\left(\sqrt{2}\zeta_B\right) + Q\left(\sqrt{2}\zeta_E\right) - Q\left(\sqrt{2}\zeta_F\right)\right]. \tag{2.62}$$

Recalling $\zeta_E \sim Z$ and $\zeta_F \sim W$ with $\sigma_X \triangleq \sigma_{s1}\sqrt{2\rho_1}$ and $\sigma_Y \triangleq \sigma_{s2}\sqrt{\rho_2}$, average BEP for UE_1 is derived by averaging instantaneous channel conditions with the PDFs in (2.55) and (2.56) as

$$
\begin{aligned}
P_2\left(e\right) = \frac{1}{2}\Bigg[& \left(1 - \sqrt{\frac{\rho_2\sigma_{s2}^2}{1+\rho_2\sigma_{s2}^2}}\right) - \int\limits_0^\infty Q\left(\sqrt{2}\zeta_A\right) p_{\zeta_A}(\zeta_A)d\zeta_A \\
& + \int\limits_0^\infty Q\left(\sqrt{2}\zeta_B\right) p_{\zeta_B}(\zeta_B)d\zeta_B + \int\limits_0^\infty Q\left(\sqrt{2}\zeta_E\right) p_{\zeta_E}(\zeta_E)d\zeta_E - \int\limits_0^\infty Q\left(\sqrt{2}\zeta_F\right) p_{\zeta_F}(\zeta_F)d\zeta_F \Bigg].
\end{aligned}
\tag{2.63}
$$

2.3.2.3.1 Approximate BEP Analysis

Although exact analysis is provided for BEP of uplink NOMA, to the best of our knowledge, the average BEP expressions in (2.57) and (2.63) cannot be derived in closed-forms. The derived expressions are in single-integral forms and can be easily obtained by numerical tools such as MATLAB, MAPPLE and MATHEMATICA. Nevertheless, in this subsection, approximated average BEP for uplink NOMA is derived in closed-form.

Corollary 2.1. *Considering the values of $Q(.)$ function, one can easily see that $Q(\eta) >> Q(\xi)$ when $\xi >> \eta > 0$. Hence, $Q(\sqrt{2}\zeta_A)$ in (2.57) and (2.63), and $Q(\sqrt{2}\zeta_E)$ in (2.63) can be omitted since $\zeta_A >> \zeta_B$ and $\zeta_E >> \zeta_F$. Validation of this assumption/approximation is provided in Table 2.1. In Table 2.1, to validate these assumptions, exact expressions in (2.57) and (2.63) are calculated via numerical tools such as MATLAB, MAPPLE. The comparisons are provided between $\int_0^\infty Q\left(\sqrt{2\zeta_A}\right) p_{\zeta_A}(\zeta_A)d\zeta_A$ and $\int_0^\infty Q\left(\sqrt{2\zeta_B}\right) p_{\zeta_B}(\zeta_B)d\zeta_B$, and between $\int_0^\infty Q\left(\sqrt{2\zeta_E}\right) p_{\zeta_E}(\zeta_E)d\zeta_E$ and $\int_0^\infty Q\left(\sqrt{2\zeta_F}\right) p_{\zeta_F}(\zeta_F)d\zeta_F$ in Table 1.1. The comparison are given for two different scenarios. In Scenario I, $\sigma_{s1}^2 = \sigma_{s2}^2 = 0dB$ and $\rho_2 = \rho_1/3$ are assumed. In Scenario II, it is assumed that $\sigma_{s1}^2 = 10dB$, $\sigma_{s2}^2 = 0dB$ and $\rho_2 = \rho_1/2$.*

Table 2.1: Validation of Corollary 2.1

	Scheme I			Scheme II		
	$\rho_1 = P_1/N_0(dB)$			$\rho_1 = P_1/N_0(dB)$		
	10	20	30	10	20	30
$\int_0^\infty Q\left(\sqrt{2\zeta_A}\right) p_{\zeta_A}(\zeta_A)d\zeta_A$	.0029	3.1e-5	5.2e-8	2.2e-4	2.1e-6	1.9e-9
$\int_0^\infty Q\left(\sqrt{2\zeta_B}\right) p_{\zeta_B}(\zeta_B)d\zeta_B$	.4098	.4008	.3997	.0980	.0916	.0909
$\int_0^\infty Q\left(\sqrt{2\zeta_E}\right) p_{\zeta_E}(\zeta_E)d\zeta_E$	7.7e-4	6.0e-6	1.1e-10	5.4e-5	3.9e-7	2.6e-12
$\int_0^\infty Q\left(\sqrt{2\zeta_F}\right) p_{\zeta_F}(\zeta_F)d\zeta_F$	.1566	.1440	.1426	.0266	.0246	.0244

Lemma 2.1. *In case X and Y are Rayleigh distributed random variables and $W = X - Y$, it can be approximated as*

$$\int_0^\infty Q\left(W\right) p_W(w)dw \approx \frac{\sigma_Y^2}{\sigma_X^2 + \sigma_Y^2}. \qquad (2.64)$$

Proof. In order to prove, firstly ML decision rules for first bits in QPSK modulated symbols or symbols in BPSK (i.e., $y^{(I)} > 0$ or $y^{(I)} \leq 0$) are considered. Thus, without loss of generality, it is assumed that the in-phase component of received signal is $y^{(I)} = \sqrt{P_1/2}\,|h_{s1}| - \sqrt{P_2}\,|h_{s2}| + w$. In this case, BS makes a erroneous detection only if $y^{(I)} \leq 0$ and this is mostly dominated by $\sqrt{P_1/2}\,|h_{s1}|$ and $\sqrt{P_2}\,|h_{s2}|$ rather than the noise (i.e.,w). Erroneous detection occurs with high probability when $\sqrt{P_1/2}\,|h_{s1}| = \sqrt{P_2}\,|h_{s2}|$ even if the noise (w) is very low. Thus, the decision rule of erroneous detection can be re-defined as $\sqrt{P_1/2}\,|h_{s1}| - \sqrt{P_2}\,|h_{s2}| \leq 0$. Considering this, $\lambda \triangleq \sqrt{P_1/2}\,|h_{s1}|$ and $\mu \triangleq \sqrt{P_2}\,|h_{s2}|$ are defined and it is approximated as

$$\int_0^\infty Q\left(W\right) p_W(w)dw \approx \int_0^\infty \int_0^\mu p_\lambda\left(\lambda\right)d\lambda\; p_\mu\left(\mu\right)d\mu. \tag{2.65}$$

Then, by substituting Rayleigh PDFs into (2.65), it is obtained as

$$\int_0^\infty Q\left(W\right) p_W(w)dw \approx \int_0^\infty \int_0^\mu \frac{\mu}{\sigma_\mu^2} e^{-\frac{\mu^2}{\sigma_\mu^2}} \frac{\lambda}{\sigma_\lambda^2} e^{-\frac{\lambda^2}{\sigma_\lambda^2}} d\mu d\lambda. \tag{2.66}$$

After some algebraic manipulations, it is simplified as

$$\int_0^\infty Q\left(W\right) p_W(w)dw \approx \frac{\sigma_\mu^2}{\sigma_\mu^2 + \sigma_\lambda^2}. \tag{2.67}$$

The proof is completed. $\qquad\square$

With the aid of Corollary 2.1, BEP expressions of uplink NOMA given in (2.57) and (2.63) are approximated as

$$P_1\left(e\right) \approx \frac{1}{4}\left[\int_0^\infty Q\left(\sqrt{2}\zeta_B\right) p_{\zeta_B}(\zeta_B)d\zeta_B + \left(1 - \sqrt{\frac{\rho_1\sigma_{s1}^2}{2 + \rho_1\sigma_{s1}^2}}\right)\right], \tag{2.68}$$

and

$$P_2\left(e\right) = \frac{1}{2}\left[\left(1 - \sqrt{\frac{\rho_2\sigma_{s2}^2}{1 + \rho_2\sigma_{s2}^2}}\right) + \int_0^\infty Q\left(\sqrt{2}\zeta_B\right) p_{\zeta_B}(\zeta_B)d\zeta_B - \int_0^\infty Q\left(\sqrt{2}\zeta_F\right) p_{\zeta_F}(\zeta_F)d\zeta_F\right]. \tag{2.69}$$

Lastly, with the aid of Lemma 2.1, average BEP expressions for uplink NOMA are derived in closed-forms as

$$P_1\left(e\right) \approx \frac{1}{4}\left[\frac{2\rho_2\sigma_{s2}^2}{2\rho_2\sigma_{s2}^2 + \rho_1\sigma_{s1}^2} + \left(1 - \sqrt{\frac{\rho_1\sigma_{s1}^2}{2 + \rho_1\sigma_{s1}^2}}\right)\right], \tag{2.70}$$

and

$$P_2\left(e\right) = \frac{1}{2}\left[\left(1 - \sqrt{\frac{\rho_2\sigma_{s2}^2}{1 + \rho_2\sigma_{s2}^2}}\right) + \frac{2\rho_2\sigma_{s2}^2}{2\rho_2\sigma_{s2}^2 + \rho_1\sigma_{s1}^2} - \frac{\rho_2\sigma_{s2}^2}{\rho_2\sigma_{s2}^2 + 2\rho_1\sigma_{s1}^2}\right]. \tag{2.71}$$
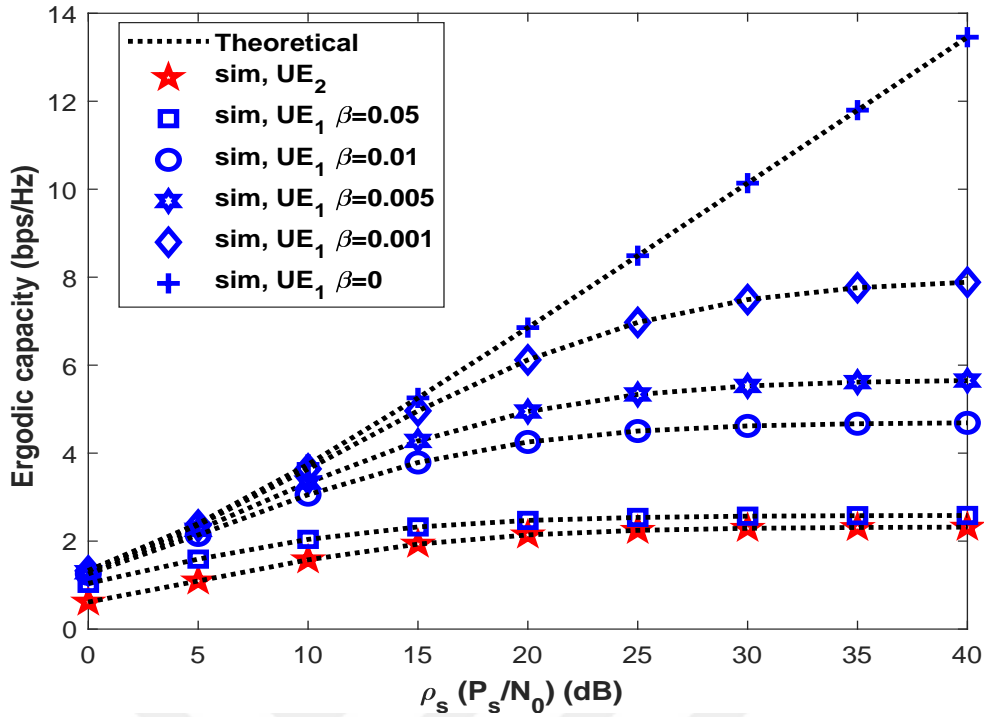
Figure 2.5: Ergodic capacity of users in downlink NOMA when $\alpha_1 = 0.2, \ \alpha_2 = 0.8$

2.4 NUMERICAL RESULTS

In this section, validations of the derived expressions (i.e., EC, OP and BEP) are provided for both downlink and uplink NOMA. In the figures through this section, unless otherwise stated, lines and markers denote theoretical curves and simulations results, respectively.

In donwlink NOMA, validations are presented when $\sigma_{s1}^2 = 10dB$ and $\sigma_{s2}^2 = 0dB$ for two different power allocation pairs. Extended simulations and detail comparisons with OMA and other NOMA schemes are provided in Chapter 5. Results for ECs of users are presented for $\alpha_1 = 0.2, \ \alpha_2 = 0.8$ and $\alpha_1 = 0.1, \ \alpha_2 = 0.9$ in Figure 2.5 and 2.6, respectively. The results are provided for $\beta = 0.05, 0.01, 0.005, 0.001, 0$ to emphasize the effect of imperfect SIC. As expected, when β increases, a decay in the EC of UE_1 occurs.

Then, OPs of users are provided in Figure 2.7 and 2.8 for the same channel conditions given in Figure 2.5 and Figure 2.6. Outage performances are provided for different target rates of users. As seen from figures, the imperfect SIC factor β has important role on
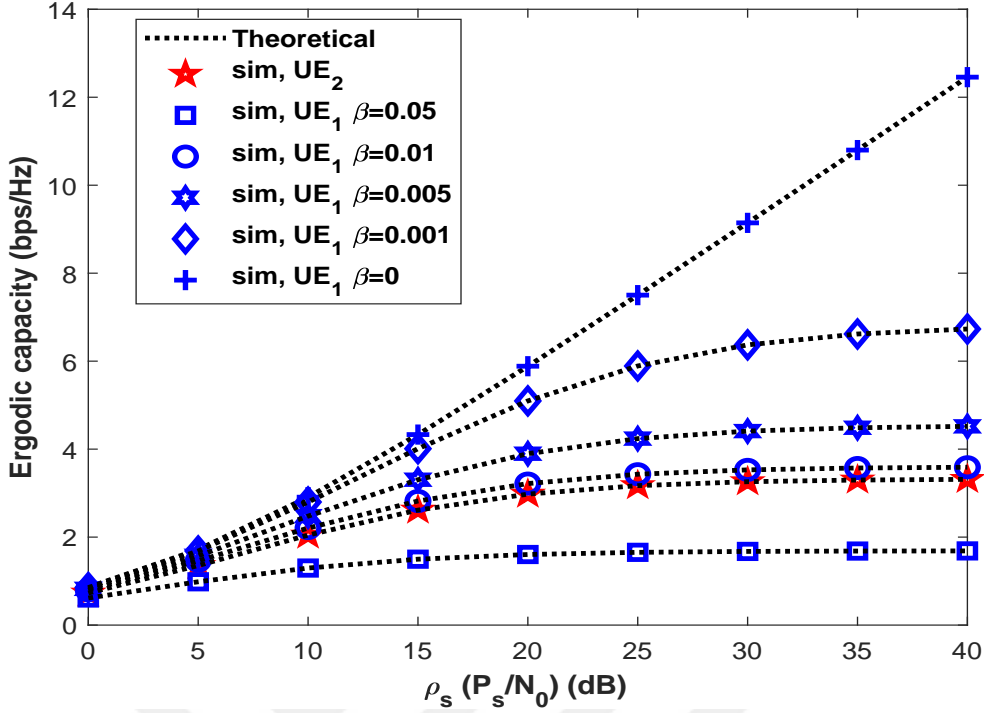
Figure 2.6: Ergodic capacity of users in downlink NOMA when $\alpha_1 = 0.1$, $\alpha_2 = 0.9$

outage as much as target rate. In particularly, one can easily see in Figure 2.8, if the SIC cannot be accomplished with good factor (i.e., higher β), UE_1 always remains in outage.

The validations of the derived BEPs for both users in downlink NOMA are presented in Figure 2.9 for the same channel conditions above and power allocation coefficients are chosen as $\alpha_1 = 0.2$, $\alpha_2 = 0.8$ and $\alpha_1 = 0.1$, $\alpha_2 = 0.9$. As it can be seen from results, power allocation coefficients have dominant effect on error performances of users and there is a trade-off between performances of users which will be discussed in detail in Chapter 5.

On the other hand, the validations in uplink NOMA are provided for two different power scenarios of users i.e., $P_2 = P_1/2$ and $P_2 = P_1/5$. $\sigma_{s1}^2 = 10dB$ and $\sigma_{s2}^2 = 0dB$ are assumed as in downlink NOMA. ECs of users are presented in Figure 2.10 and Figure 2.11 for various imperfect SIC factor (β).

Then, the validations of the derived OPs of users are provided for the same conditions in
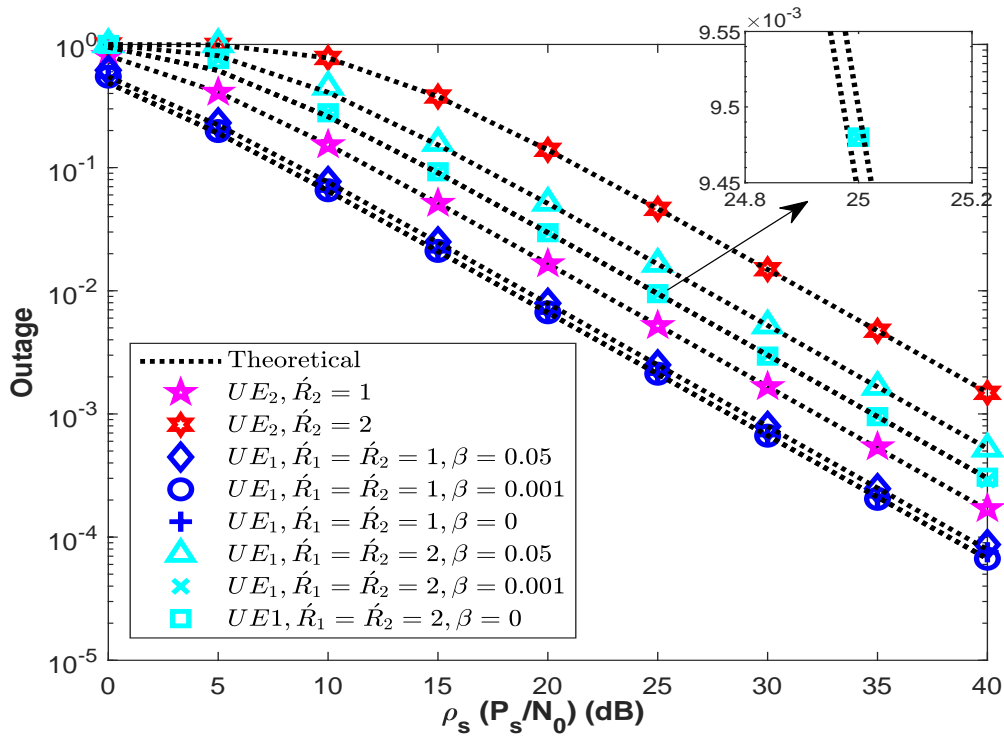
Figure 2.7: Outage performance of users in downlink NOMA when $\alpha_1 = 0.2,\ \alpha_2 = 0.8$
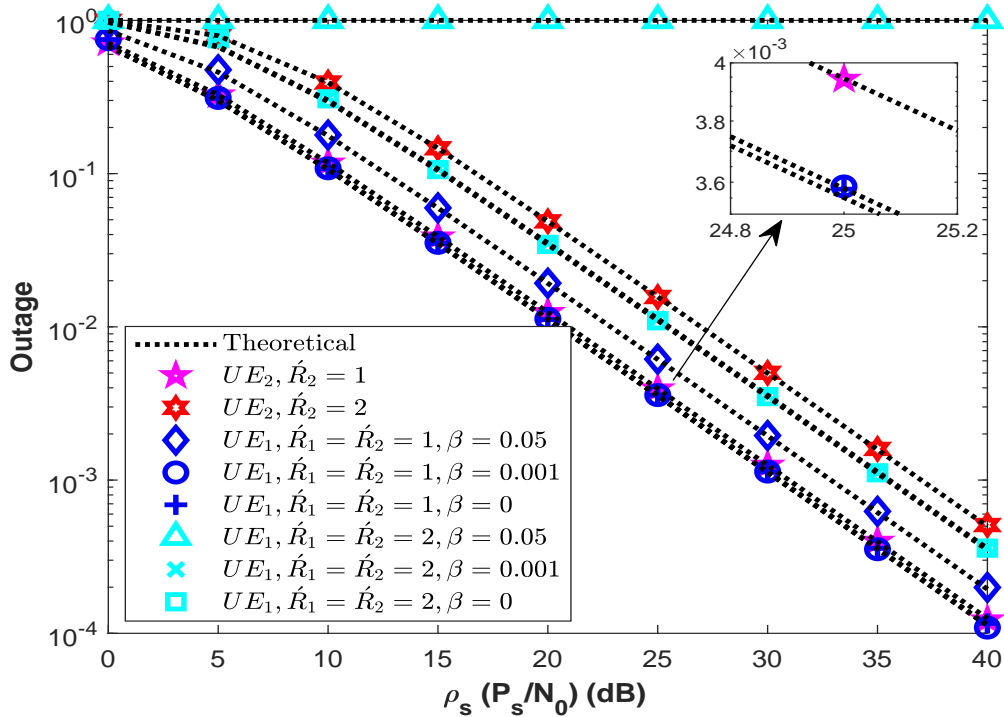
Figure 2.8: Outage performance of users in downlink NOMA when $\alpha_1 = 0.1,\ \alpha_2 = 0.9$
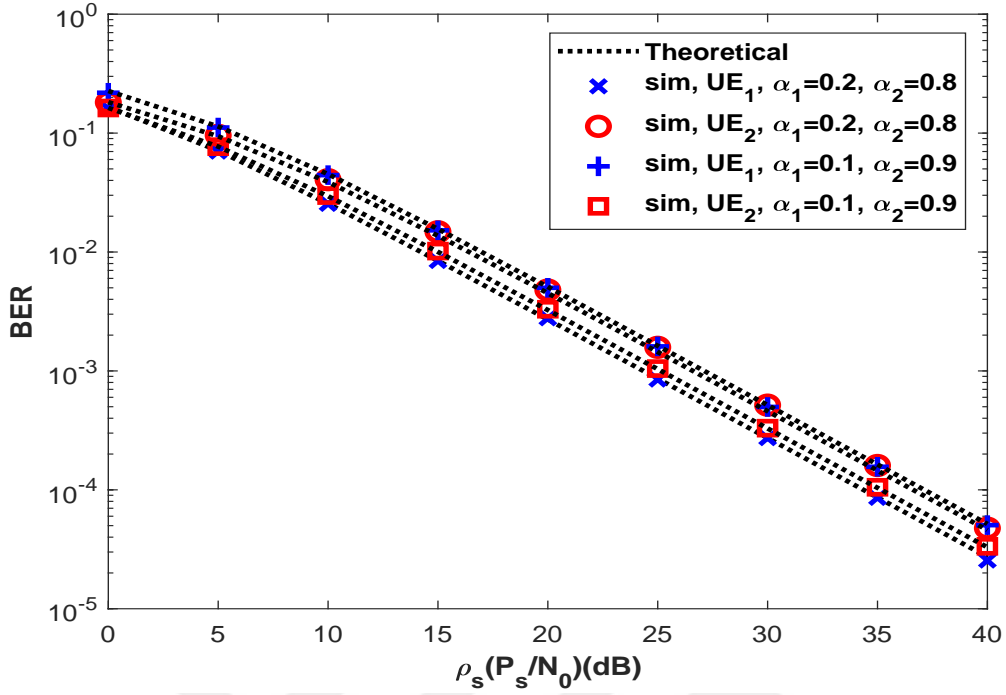
Figure 2.9: Error (BER) performances of users in downlink NOMA
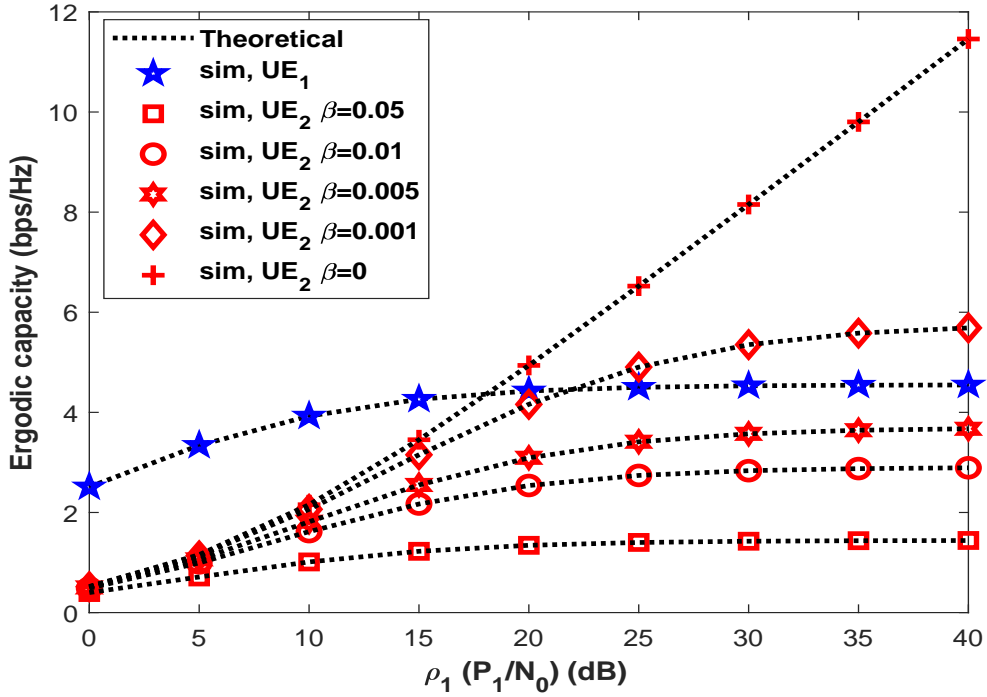
Figure 2.10: Ergodic capacity of users in uplink NOMA when $P_2 = {}^{P_1}/_2$
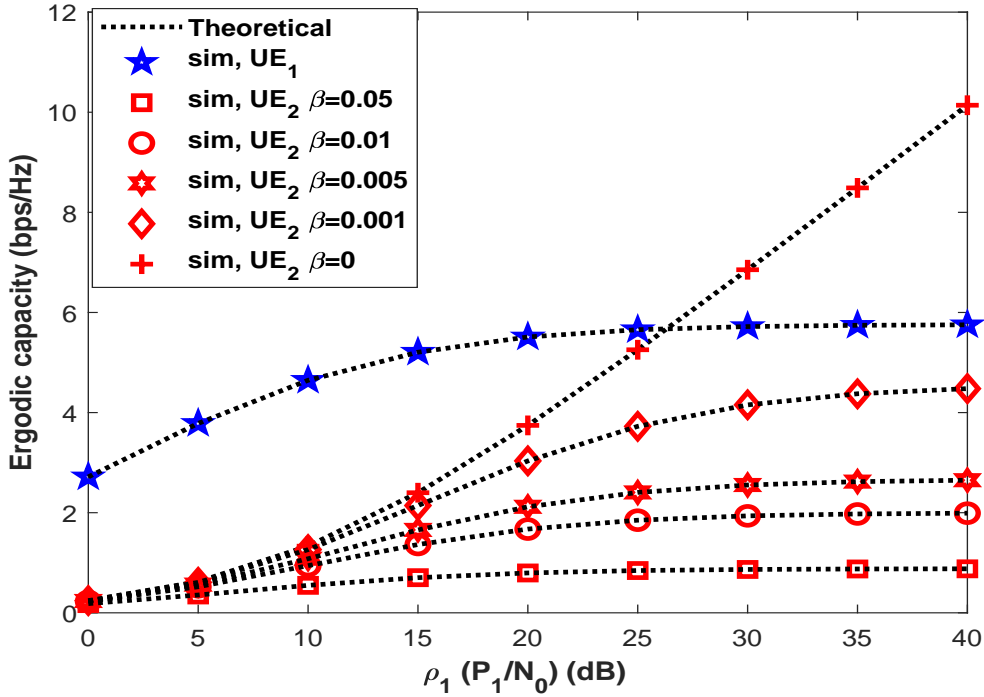
Figure 2.11: Ergodic capacity of users in uplink NOMA when $P_2 = {}^{P_1}/_5$

Figure 2.12 and Figure 2.13. One can easily see that increase in power for both users does not provide performance gain since IUI also increases. Thus, NOMA is more meaningful for uplink when the power of users differs significantly.

Lastly, the validations of derived BEPs of uplink NOMA are presented in Figure 2.14. The derived single-integral form exact BEP expressions match perfectly with simulations. In addition, provided closed-form approximated expressions match well with simulations. One can easily see that error performances of users in uplink NOMA are dominated by the power difference between users. Hence, UE_2 has better performance when $P_2 = {}^{P_1}/_2$ although it has less transmit power. This can be easily explained by SIC process as: if UE_2 has more power, it means that UE_1 encounters much more IUI and this causes much more detection errors for UE_1. These erroneous detections of UE_1 during SIC cause poor performance for UE_2 also. In order to emphasize this effect, we also provide error performance of uplink NOMA versus the transmit SNR of UE_2 in Figure 2.15 when UE_1 has fixed power. $\rho_1 = 20dB$ is assumed. As seen from the Figure 2.15, the increase in power of UE_2 firstly provides better performance for UE_2, however then, erroneous
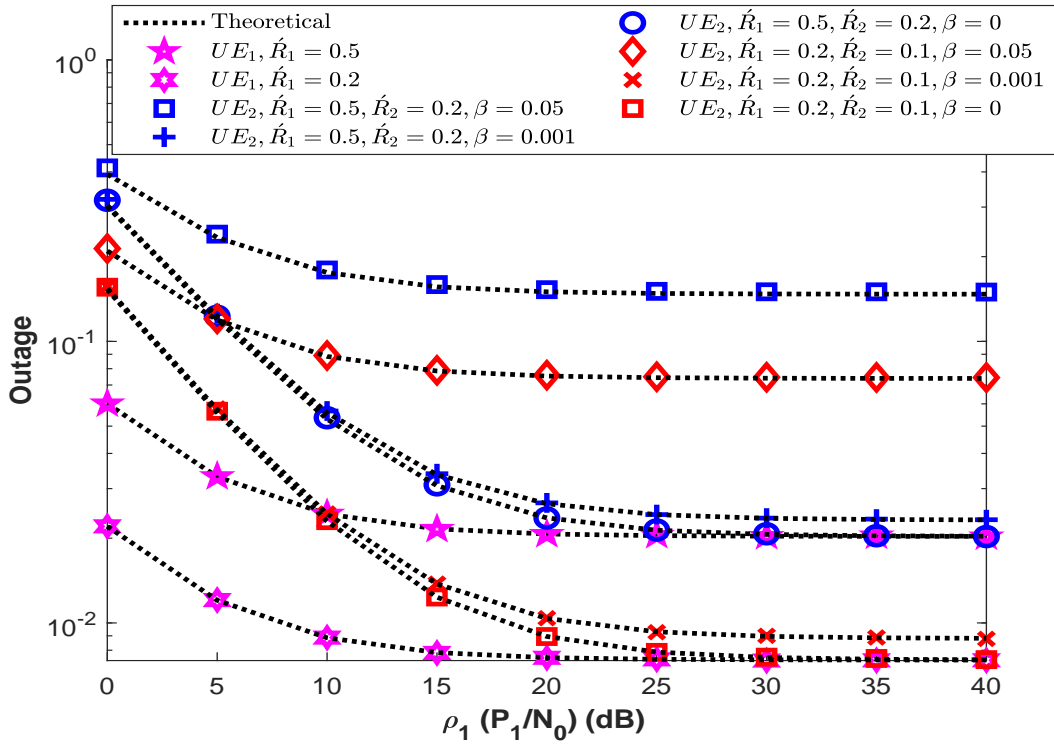
Figure 2.12: Outage performance of users in uplink NOMA when $P_2 = {}^{P_1}/_2$
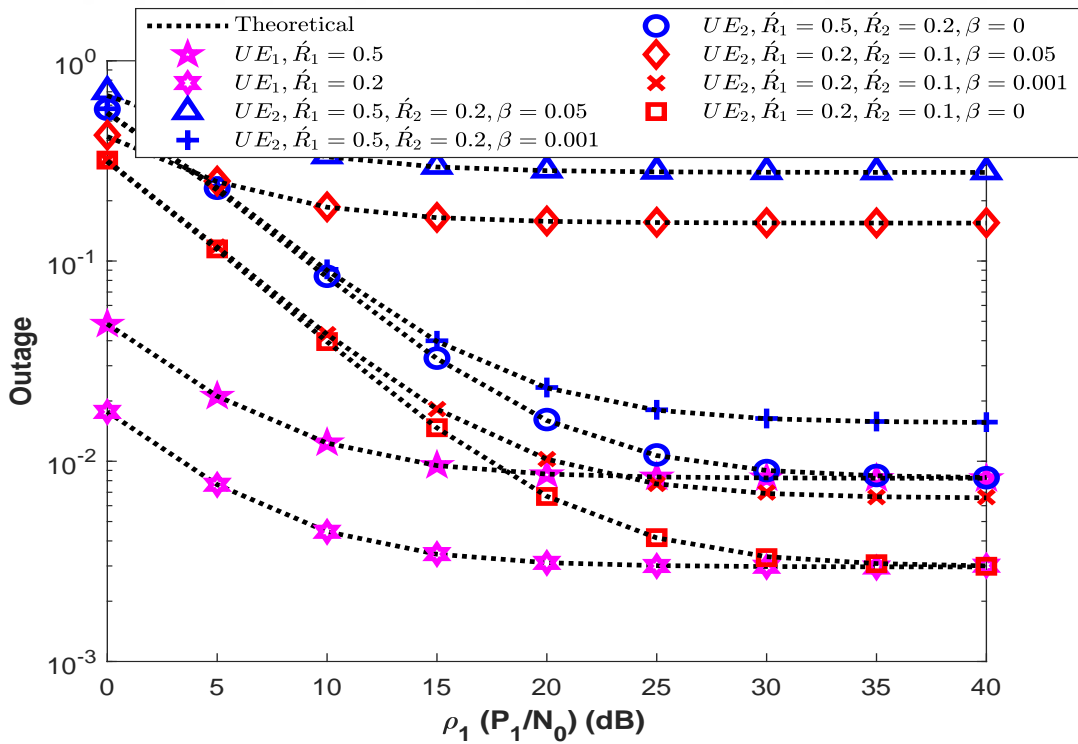
Figure 2.13: Outage performance of users in uplink NOMA when $P_2 = {}^{P_1}/_5$
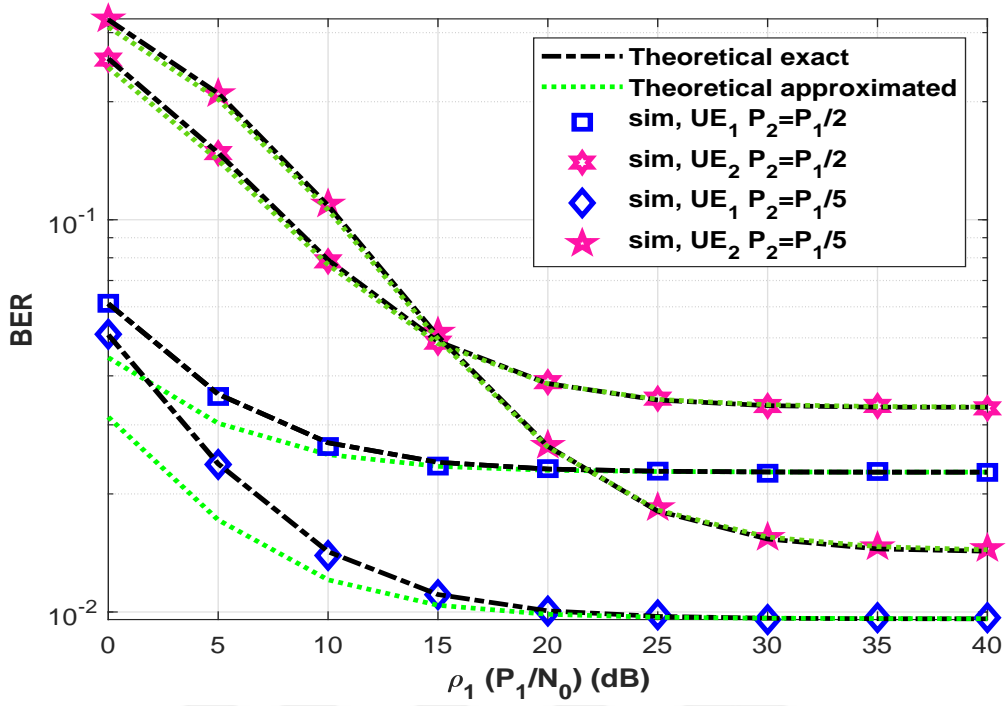
Figure 2.14: Error (BER) performances of users in uplink NOMA
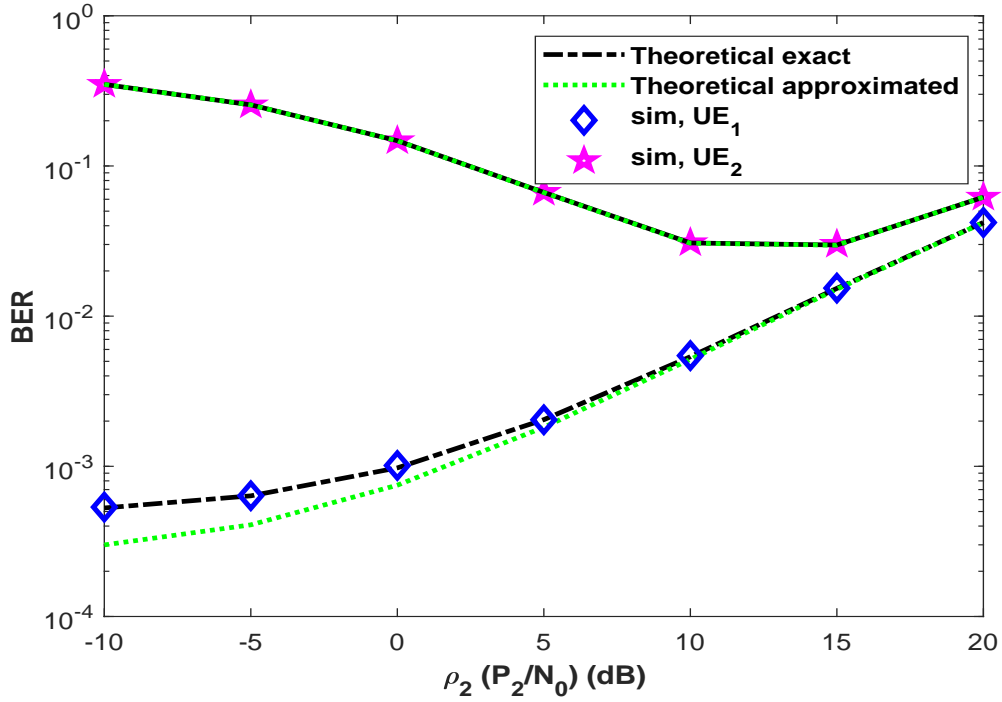
Figure 2.15: Error (BER) performances of users in uplink NOMA vs ρ_2

detections during SIC become dominant and the performance of UE_2 gets worse even if its power increases.

CHAPTER 3

INTERPLAY BETWEEN NOMA AND COOPERATIVE COMMUNICATION

3.1 BACKGROUND FOR COOPERATIVE COMMUNICATION

In wireless communications, the intended information (electromagnetic wave) is transmitted to destination from source via atmosphere (wireless channel) by antennas. The wireless channel conditions change randomly according to the effects such as reflection, diffraction and scattering of electromagnetic waves. These are categorized as path-loss, shadowing and fading in wireless communication models and have dominant effect on the system performances. To eliminate these effects, diversity is one of the applied techniques in wireless communications. Diversity is based on transmitting copies of the intended signal over independent/uncorrelated channels. Channels are guaranteed to be uncorrelated by sending/receiving signals with different frequency (frequency diversity), time (time diversity) and antennas (antenna/spatial diversity). Spatial diversity can be succeeded by placing more than one antenna with sufficient distances between each other according to used wavelength. However, placing multiple antennas on mobile devices cannot be possible due to the physical limitations. Hence, as named virtual-MIMO, cooperative communication has been proposed as a diversity technique [93, 94].

Unlike conventional point-to-point communications, in cooperative communications, devices named as relays not only transmit/receive their own signals but also help to transmit/receive signals of other devices. Relays can be dedicated devices or the other idle users in network. According to implemented operations at relays, cooperative communication is divided into two major concepts: amplify-forward (AF) and decode-forward (DF) [93]. In AF, relay forwards the received signal to the destination after amplifying whereas in DF, relay firstly decodes/demodulates the received signal and forwards it after re-coded/re-modulated. The illustration of AF and DF relaying is given in Figure 3.1.
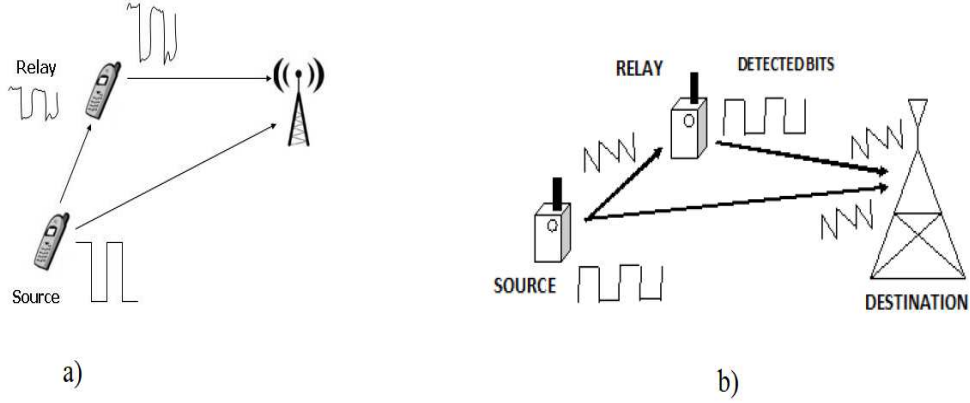
Figure 3.1: Representation of cooperative communication a) AF relaying b) DF relaying

On the other hand, according to used protocol of relays, relaying strategies are named as half-duplex (HD) and full-duplex (FD) relaying. In HD relaying [95], relay receives the signals transmitted by source in the first phase (time slot) of communication and then in the second phase forwards to the destination according to relaying mode (i.e., AF or DF). In FD relaying [96], relay receives the signals and forwards it after implementing AF or DF on the same phase of communication, thus total communication covers only one phase in FD relaying. However, FD relaying suffers from self-interference where transmitted signal is suppressed by the received signals from source.

In last two decades, numerous studies have been devoted to investigate performances of cooperative communication systems for both AF or DF relaying. In DF relaying schemes, in order to increase data reliability at relay, selective relaying schemes have been proposed where relay decides whether to forward or not received symbols according to received SNR [97, 98]. In both AF and DF relaying schemes, multiple relay situations and relay selection algorithms have been investigated [99–102]. Multi-hop cooperative relaying systems have also attracted attention from researchers and path selection algorithms have been investigated to maximize the performance of system [103, 104]. In multi-hop systems, required time slots increases when the number of hops increases in DF relaying, on the other hand, self-interferences of relay become dominant in FD relaying [105, 106]. Consequently, cooperative communication systems provide better error performance and diversity order. However, in HD relaying, overall capacity decreases since communication

covers more than one time slot and it is seen as the main drawback of HD cooperative communication systems [107].

3.2   RELATED WORKS AND MOTIVATION

Cooperative communication is to provide high mobility and high coverage, on the other hand, NOMA is proposed to increase spectral efficiency for future wireless networks. Thus, the interplay between these two physical layer techniques has become one of the most attracted topics. The interplay between NOMA and cooperative diversity/relaying is mainly categorized in three main aspects: 1) cooperative-NOMA, 2) relay-assisted/aided-NOMA and 3) NOMA-based cooperative relaying systems.

In NOMA schemes, users with the higher channel qualities (i.e., intra-cell users) have the priori knowledge for the symbols of the users with weaker channel conditions (i.e., cell-edge users) since SIC is implemented at the intra-cell users in order to detect their own symbols. Thus, intra-cell users can act as relays and forward the priori knowledge of cell-edge users obtained during SIC to the cell-edge users to improve reliability. This system model is called as cooperative-NOMA (C-NOMA). Achievable rate and outage performance of C-NOMA have been investigated in [108] where a short range-communication is considered like Bluetooth and it is proved that C-NOMA outperforms conventional NOMA networks. The authors in [109] derive closed form OP expressions for C-NOMA. C-NOMA with FD relaying is introduced in [110] and outage performance is analyzed. Then, achievable rate and outage performance are investigated in [111, 112], when hybrid HD/FD relaying strategies are implemented at intra-cell user. In order to improve cell-edge user performance in terms of ergodic rate and outage, two different strategies are proposed in [113] and [114] called as successive relaying and on/off relaying, respectively. C-NOMA is investigated for MIMO case in [115] and a sub-optimum algorithm is proposed under max-rate constraint. The impact of user pairing on maximum sum rate and minimum user rate is analyzed in [116]. Then, the trade-off for energy efficiency-delay is raised in [117] and various NOMA schemes with energy harvesting -simultaneous wireless and power transfer (SWIPT)- are investigated in [118–120]. To the best of our knowledge, all researches on C-NOMA investigate the performance and try to optimize in terms of achievable rate and outage. Thus, the error performance of C-NOMA has been

analyzed and closed-form expressions for BEP have been derived in [121,122]. It has been shown that imperfect SIC is dominated the error performance of C-NOMA and diversity order cannot be achieved. Then, threshold-based selective cooperative-NOMA (TBS-C-NOMA) has been proposed [123] to increase the data reliability of C-NOMA [108].

The relay-assisted-NOMA networks have been also analyzed widely. In these works, a AF or DF relay helps source/BS to transmit symbols to the user [124]. Hybrid DF/AF relaying strategies have been also investigated to improve outage performance of relay-assisted-NOMA [125]. Outage and sum-rate performance of relay-assisted-NOMA networks have been also analyzed whether a direct link between source and user exists [126] or not [127, 128]. Then, relay-assisted-NOMA networks have been analyzed in terms of achievable rate and outage performance under different conditions such as buffer aided-relaying [129, 130], partial CSIT [131] and imperfect CSI at receiver [132] when a single relay is located between source and users. In addition, relay selection schemes have been investigated when multiple relays are available [133–136]. Relay selection schemes are based on guaranteeing QoS of users and maximizing outage performance of users. Moreover, two-way relaying strategies where relay operates as a coordinated multi-point (CoMP), have been investigated in terms of achievable rate and outage performance [137–140]. Likewise in C-NOMA, at the time of writing, error performance analysis of relay-assisted-NOMA networks had not been regarded, yet. Thus, BEP has been derived for a DF relay-assisted-NOMA and a sub-optimum algorithm has been provided for power allocation at source and relay mutually [141].

NOMA-based cooperative relaying systems (NOMA-CRS) have been proposed to eliminate the spectral inefficiency of HD relaying [142] and it is proved that NOMA-CRS outperforms conventional CRS in terms of achievable rate over Rayleigh fading channels. Then, the analysis in [142] is extended for Rician fading channels [143]. In order to improve achievable rate of NOMA-CRS, an extended NOMA-CRS is proposed in [144] and the performance analysis is provided under imperfect CSI at receiver in terms of achievable rate and OP. Then, the authors in [145] consider an AF NOMA-CRS rather than previous studies and it is shown that further improvement in achievable rate is possible with proposed AF relaying and combining at destination. Moreover, the authors in [146]
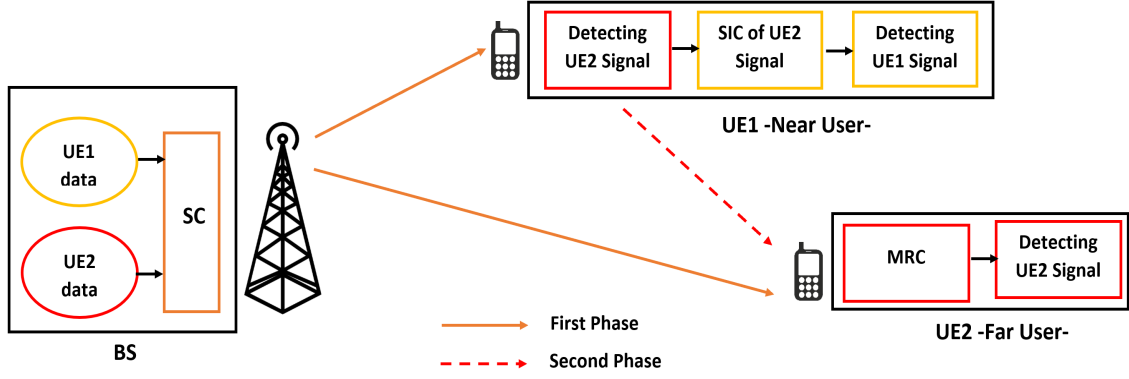
Figure 3.2: The illustration of C-NOMA

propose a NOMA based diamond relaying and analyze the achievable rate of proposed scheme when the direct link between source and destination is not available. Since there is no investigation for BEP analysis of NOMA-CRS, in the next subsections of this chapter, BEP analysis for both basic NOMA-CRS [142] and NOMA based diamond relaying (NOMA-DRN) [146] are provided in this thesis.

3.3 COOPERATIVE-NOMA

3.3.1 System Model

A downlink NOMA scheme is considered where a BS and two users (i.e. UE_1 and UE_2) are located. All nodes are equipped with single antenna. It is assumed that the statistical CSIT and full CSIR are available. The users are denoted as near (intra-cell) user and far (cell-edge) user according to their statistical CSIT. $\sigma_{s1}^2 > \sigma_{s2}^2$ is assumed where σ_{s1}^2 and σ_{s2}^2 are the average channel powers of users and denote the large-scale fading (pathloss) component driven by the distance between nodes. Thus, it is considered that UE_1 is the intra-cell user and UE_2 is the cell-edge user. In downlink NOMA schemes, UE_1 should implement SIC to detect its own symbols, and during this SIC process, it will have knowledge of UE_2 symbols. Hence, it is assumed that UE_1 also acts as decode-and-forward relay to improve reliability of UE_2. The system model is given in Figure 3.2. In the first phase, BS implements SC and transmits total symbols of users on the same resource block just as in downlink NOMA. The received signal by users in the first phase is given as

47

$$y_{sk} = \sqrt{P_s} x_{sc} h_{sk} + w_{sk}, \quad k = 1, 2, \tag{3.1}$$

where $\sqrt{P_s}$ is the transmit power of BS and $x_{sc} = \sqrt{\alpha_1} x_1 + \sqrt{\alpha_2} x_2$ is total SC symbol of users. h_{sk} is the channel fading coefficient between nodes and follows $CN(0, \sigma_{sk}^2)$ and w_{sk} is the AWGN at users which follows $CN(0, N_0)$. α_1, x_1 and α_2, x_2 pairs are power allocation coefficient and base-band modulated symbol of UE_1 and UE_2, respectively. Since UE_1 denotes the intra-cell user, UE_1 detects x_2 symbols firstly to implement SIC and to detect its own symbols. After detecting x_2 symbols, UE_1 forwards that detected symbols as a DF relay to the UE_2 in the second phase. The received signal by UE_2 in the second phase is given as

$$y_r = \sqrt{P_r} \hat{x}_2 h_r + w_r, \tag{3.2}$$

where P_r is the transmit power of UE_1 -relay-. $\hat{x}_2$ and h_r denote estimated x_2 symbols at UE_1 and the channel fading coefficient between users, respectively. h_r is the channel coefficient between users and follows $CN(0, \sigma_r^2)$. w_r is the AWGN at UE_2.

Then, UE_2 implements maximum-ratio-combining (MRC) for the received symbols in two phases. After MRC, UE_2 detects its own symbols with ML detector by pretending x_1 symbols received in the first phase as noise.

3.3.2 Performance Analysis

In this section, analytical analysis is provided to evaluate performance of cooperative-NOMA (C-NOMA). Provided analysis is only handled for UE_2 since the analysis for UE_1 is the same for downlink NOMA provided in the previous chapter.

3.3.2.1 Ergodic Capacity Analysis

Likewise conventional NOMA networks, in order to derive ergodic capacity, achievable Shannon rate should firstly be obtained for C-NOMA. Since MRC is applied at UE_2 after two phases, the SINR at UE_2 is given as[1]

$$SINR_{CN} = \frac{\alpha_2 \rho_s |h_{s2}|^2 + \rho_r |h_r|^2}{\alpha_1 \rho_s |h_{s2}|^2 + 1}, \tag{3.3}$$

---

[1]In equations, CN is used to refer the C-NOMA.

where $\rho_s = {P_s}/{N_0}$ and $\rho_r = {P_r}/{N_0}$ are the transmit SNR of BS and UE_1 -relay-, respectively. Thus, the achievable rate of C-NOMA is given as [108]

$$R_{CN} = \frac{1}{2} \log_2 \left(1 + \frac{\alpha_2 \rho_s |h_{s2}|^2 + \rho_r |h_r|^2}{\alpha_1 \rho_s |h_{s2}|^2 + 1} \right), \tag{3.4}$$

where $1/2$ coefficient exists since the total communication is completed in two phases[2]. After some algebraic manipulations and by averaging over instantaneous channel conditions, ergodic capacity of C-NOMA is given as

$$C_{CN} = \frac{1}{2}$$
$$\left[\int_0^\infty \int_0^\infty \log_2 (1 + \rho_s \gamma_{s2} + \rho_r \gamma_r) p_{\gamma_{s2}}(\gamma_{s2}) p_{\gamma_r}(\gamma_r) d\gamma_{s2} d\gamma_r - \int_0^\infty \log_2 (1 + \alpha_1 \rho_s \gamma_{s2}) p_{\gamma_{s2}}(\gamma_{s2}) d\gamma_{s2} \right], \tag{3.5}$$

where $\gamma_\lambda \triangleq |h_\lambda|^2$, $\lambda = s1, s2, r$ and $p_{\gamma_\lambda}(.)$ is the PDF of γ_λ. Likewise in uplink NOMA, $\Psi \triangleq \rho_s \gamma_{s2} + \rho_r \gamma_r$ is defined and, it turns out to be

$$C_{CN} = \frac{1}{2} \left[\int_0^\infty \log_2 (1 + \Psi) p_\Psi(\Psi) d\Psi - \int_0^\infty \log_2 (1 + \alpha_1 \rho_s \gamma_{s2}) p_{\gamma_{s2}}(\gamma_{s2}) d\gamma_{s2} \right]. \tag{3.6}$$

Then, by substituting exponential PDF for γ_{s2} and PDF of sum of two exponential distributions given in (2.49) for Ψ, with the aid of [89, eq. (4.337.2)], ergodic capacity of C-NOMA is derived as

$$C_{CN} = \frac{\log_2 e}{2} \left[\exp \left(\frac{1}{\alpha_1 \rho_s \sigma_{s2}^2} \right) Ei \left(-\frac{1}{\alpha_1 \rho_s \sigma_{s2}^2} \right) \right.$$
$$\left. + \frac{1}{\rho_r \sigma_r^2 - \rho_s \sigma_{s2}^2} \left\{ \rho_s \sigma_{s2}^2 \exp \left(\frac{1}{\rho_s \sigma_{s2}^2} \right) Ei \left(-\frac{1}{\rho_s \sigma_{s2}^2} \right) - \rho_r \sigma_r^2 \exp \left(\frac{1}{\rho_r \sigma_r^2} \right) Ei \left(-\frac{1}{\rho_r \sigma_r^2} \right) \right\} \right]. \tag{3.7}$$

3.3.2.2 Outage Probability Analysis

The outage event occurs when the achievable rate of C-NOMA is below the target rate and it is given as [108]

$$P_{CN}(out) = P(R_{CN} < \acute{R}_{CN}), \tag{3.8}$$

---

[2]C-NOMA is firstly proposed for short range communication and to provide better achievable rate than conventional NOMA, thus $1/2$ coefficient is neglected [108]. However, we think that completing total communication in only one phase is not reasonable for practical issues, hence we provide analysis for half-duplex mode.

and by substituting (3.4) into (3.8), it is obtained as

$$P_{CN}(out) = P\left(\frac{\alpha_2\rho_s\left|h_{s2}\right|^2 + \rho_r\left|h_r\right|^2}{\alpha_1\rho_s\left|h_{s2}\right|^2 + 1} < \phi_{CN}\right), \tag{3.9}$$

where $\phi_{CN} = 2^{2\acute{R}_{CN}} - 1$. With some simplifications, it turns out to be

$$P_{CN}(out) = F_{\Psi_{CN}}\left(\phi_{CN}\right), \tag{3.10}$$

where $\Psi_{CN} = \rho_s\left(\alpha_2 - \alpha_1\phi_{CN}\right)\gamma_{s2} + \rho_r\gamma_r$ and $F_{\Psi_{CN}}(.)$ CDF of Ψ_{CN}. By substituting CDF for sum of two exponential distributions into (3.10), OP of C-NOMA is derived as

$$P_{CN}(out) =$$
$$\frac{\rho_r\sigma_r^2\left(1 - \exp\left(-\frac{\phi_{CN}}{\rho_r\sigma_r^2}\right)\right) - \rho_s\left(\alpha_2 - \alpha_1\phi_{CN}\right)\sigma_{s2}^2\left(1 - \exp\left(-\frac{\phi_{CN}}{\rho_s(\alpha_2-\alpha_1\phi_{CN})\sigma_{s2}^2}\right)\right)}{\rho_r\sigma_r^2 - \rho_s\left(\alpha_2 - \alpha_1\phi_{CN}\right)\sigma_{s2}^2}. \tag{3.11}$$

3.3.2.3 Bit Error Probability (BEP) Analysis

The error performance of C-NOMA should be handled in two cases: whether the UE_1 detects x_2 symbols correctly and diversity is achieved for UE_2 or detects x_2 symbols erroneously and error propagation from UE_1 to UE_2 occurs. Thus, with the total probability law, the end-to-end (e2e) BEP of C-NOMA is given as

$$P_{CN}^{(e2e)}(e) = (1 - P_{SIC}(e)) \times P_{div}(e) + P_{SIC}(e) \times P_{prop}(e), \tag{3.12}$$

where $P_{SIC}(e)$ is the error probability of x_2 symbols during SIC at UE_1, $P_{div}(e)$ is the error probability after MRC when the UE_1 forwards correct detected symbols and diversity is achieved, and $P_{prop}(e)$ is the error probability after MRC when the UE_1 forwards erroneous detected symbols and error propagation occurs. In order to obtain e2e average BEP of C-NOMA given in (3.12), all these error probabilities should be derived.

Let firstly handling the error probability of SIC -error probability of x_2 symbols at UE_1-. Since UE_1 detects x_2 symbols by pretending own symbols as noise, one can easily see that $P_{SIC}(e)$ turns out to be BEP of conventional downlink NOMA provided in previous chapter. In 3GPP standards, various modulation constellations are considered for NOMA according to CQI of users [7–9]. Thus, the BEP of x_2 symbols at UE_1 is extended for various modulation pair modes of UE_1 and UE_2 as,

$$P_{SIC}(e|_{\gamma_{s1}}) = \sum_{i=1}^{N} \varsigma_i Q\left(\sqrt{2\nu_i\rho_s\gamma_{s1}}\right), \tag{3.13}$$

Table 3.1: Coefficients for error probability of x_2 symbols

mode	Constellations UE_1 UE_2	BEP Coefficients
1	BPSK BPSK	$N = 2, \quad \varsigma_i = 0.5, \quad i = 1, 2$ $\nu_i = \left(\sqrt{\alpha_2} \mp \sqrt{\alpha_1}\right)^2 i = 1, 2$
2	BPSK QPSK	$N = 3, \quad \varsigma_i = 0.25, \ i = 1, 2 \quad a_3 = 0.5$ $\nu_i = \begin{cases} \left(\sqrt{\frac{\alpha_2}{2}} \mp \sqrt{\alpha_1}\right)^2 & i = 1, 2 \\ \alpha_2/2 & i = 3 \end{cases}$
3	QPSK BPSK	$N = 2, \quad \varsigma_i = 0.5, \quad i = 1, 2$ $\nu_i = \left(\sqrt{\alpha_2} \mp \sqrt{\frac{\alpha_1}{2}}\right)^2 i = 1, 2$
4	QPSK QPSK	$N = 2, \quad \varsigma_i = 0.5, \quad i = 1, 2$ $\nu_i = \frac{1}{2}\left(\sqrt{\alpha_2} \mp \sqrt{\alpha_1}\right)^2 i = 1, 2$
5	16-QAM BPSK	$N = 4, \quad \varsigma_i = 0.25, \quad i = 1, 2, 3, 4$ $\nu_i = \begin{cases} \left(\sqrt{\alpha_2} \mp \sqrt{\frac{\alpha_1}{10}}\right)^2 & i = 1, 2 \\ \left(\sqrt{\alpha_2} \mp 3\sqrt{\frac{\alpha_1}{10}}\right)^2 & i = 3, 4 \end{cases}$
6	16-QAM QPSK	$N = 4, \quad \varsigma_i = 0.25, \quad i = 1, 2, 3, 4$ $\nu_i = \begin{cases} \left(\sqrt{\frac{\alpha_2}{2}} \mp \sqrt{\frac{\alpha_1}{10}}\right)^2 & i = 1, 2 \\ \left(\sqrt{\frac{\alpha_2}{2}} \mp 3\sqrt{\frac{\alpha_1}{10}}\right)^2 & i = 3, 4 \end{cases}$

where ν_i is defined according to total SC symbols and ς_i denotes the priori probability of ν_i to be occurred. Taking steps of derivation error probability of cell-edge user in down-link NOMA considering different modulation pairs. The coefficients are given in Table 3.1.

Then by averaging conditional BEP given in (3.13) over instantaneous γ_{s1}, average BEP

for x_2 symbols at UE_1 is obtained as

$$P_{SIC}(e) = \sum_{i=1}^{N} \frac{\varsigma_i}{2} \left(1 - \sqrt{\frac{\nu_i \rho_s \sigma_{s1}^2}{1 + \nu_i \rho_s \sigma_{s1}^2}} \right). \tag{3.14}$$

In order to obtain BEP for diversity communication, total received signal after MRC should be considered. Since the MRC is applied, the total received signal is given as

$$y_{CN} = h_{s2}^* y_{s2} + h_r^* y_r. \tag{3.15}$$

Thus, by using (3.13) and with the aid of [90, pp. 320 and 3121], the conditional BEP of diversity communication is given as

$$P_{div}(e|_{\gamma_{s2}, \gamma_r}) = \sum_{i=1}^{N} \varsigma_i Q \left(\sqrt{2 \left(\nu_i \rho_s \gamma_{s2} + \rho_r \gamma_r \right)} \right). \tag{3.16}$$

The average BEP of diversity communication is derived by using average BEP of 2-branch MRC for Rayleigh fading channels [147, pp. 846 and 847] as

$$P_{div}(e) = \sum_{i=1}^{N} \frac{\varsigma_i}{2} \left[1 - \frac{1}{\nu_i \rho_s \sigma_{s2}^2 - \rho_r \sigma_r^2} \left(\nu_i \rho_s \sigma_{s2}^2 \sqrt{\frac{\nu_i \rho_s \sigma_{s2}^2}{1 + \nu_i \rho_s \sigma_{s2}^2}} - \rho_r \sigma_r^2 \sqrt{\frac{\rho_r \sigma_r^2}{1 + \rho_r \sigma_r^2}} \right) \right]. \tag{3.17}$$

In order to derive P_{prop}, without loss of generality, it is assumed that BPSK is used for both UE_1 and UE_2 and $x_2 = +1$ is transmitted by BS, then this assumption will be relaxed. In case error propagation, UE_1 -relay- detects it as $x_2 = -1$ and forwards to UE_2. After MRC at UE_2, the received signal is given as [97]

$$\begin{aligned}
y_2 &= h_{s2}^* \, y_{s2} + h_r^* \, y_r \\
&= \sqrt{P_s} \left(\alpha_2 \mp \alpha_1 \right) |h_{s2}|^2 - \sqrt{P_r} \, |h_{sr}|^2 + \tilde{w},
\end{aligned} \tag{3.18}$$

where $\tilde{w}$ is effective noise term and it has $E[\tilde{w}] = 0$ mean and $E[\tilde{w}^2] = {}^{N_0}\!/_2 \left(\sigma_{s2}^2 + \sigma_r^2 \right)$ variance. Considering the ML decision rule for BPSK, conditional BEP under error propagation is derived as

$$\begin{aligned}
P_{prop}(e|_{\gamma_{s2}, \gamma_r}) &= P \left(\tilde{w} > \sqrt{P_s} \left(\alpha_2 \mp \alpha_1 \right) \gamma_{s2} - \sqrt{P_r} \gamma_r \right) \\
&= Q \left(\frac{\sqrt{P_s} \left(\alpha_2 \mp \alpha_1 \right) \gamma_{s2} - \sqrt{P_r} \gamma_r}{\sqrt{sfrac N_0 2 \left(\sigma_{s2}^2 + \sigma_r^2 \right)}} \right),
\end{aligned} \tag{3.19}$$

With the aid of Lemma 2.1, it is approximated as

$$P_{prop}(e) \approx \frac{\rho_r \sigma_r^2}{\rho_r \sigma_r^2 + \rho_s \sigma_{s2}^2}. \tag{3.20}$$

The assumption of BPSK is relaxed for M-ary constellations by considering the coefficients given in Table 3.1 and with the aid of [121] as

$$P_{prop}(e) \approx \sum_{i=1}^{N} \varsigma_i \frac{c_{j,M} \rho_r \sigma_r^2}{c_{j,M} \rho_r \sigma_r^2 + \nu_i \rho_s \sigma_{s2}^2}, \tag{3.21}$$

where $c_{j,M}$ is given for M-ary constellations as [97, appendix B]

$$c_{j,M} \triangleq \begin{cases} \frac{\sin(\pi(2j-1)/M)}{\sin(\pi/M)} & j = 1, 2, \ldots, M/2 \\ -\frac{\sin(\pi(2j+1)/M)}{\sin(\pi/M)} & j = M/2 + 1, \ldots, M - 1. \end{cases} \tag{3.22}$$

Lastly, substituting (3.14), (3.17) and (3.21) into (3.12), e2e average BEP of C-NOMA is derived in closed-form as

$$\begin{aligned} P_{CN}^{(e2e)}(e) = \sum_{i=1}^{N} \varsigma_i &\left[\frac{1}{4} \left(-1 + \sqrt{\frac{\nu_i \rho_s \sigma_{s1}^2}{1 + \nu_i \rho_s \sigma_{s1}^2}} \right) \times \right. \\ &\left\{ 1 - \frac{1}{\nu_i \rho_s \sigma_{s2}^2 - \rho_r \sigma_r^2} \left(\nu_i \rho_s \sigma_{s2}^2 \sqrt{\frac{\nu_i \rho_s \sigma_{s2}^2}{1 + \nu_i \rho_s \sigma_{s2}^2}} - \rho_r \sigma_r^2 \sqrt{\frac{\rho_r \sigma_r^2}{1 + \rho_r \sigma_r^2}} \right) \right\} \\ &\left. + \frac{1}{2} \left(1 - \sqrt{\frac{\nu_i \rho_s \sigma_{s1}^2}{1 + \nu_i \rho_s \sigma_{s1}^2}} \right) \times \frac{c_{j,M} \rho_r \sigma_r^2}{c_{j,M} \rho_r \sigma_r^2 + \nu_i \rho_s \sigma_{s2}^2} \right]. \end{aligned} \tag{3.23}$$

3.3.3 Threshold-based Selective Cooperative-NOMA

Cooperative-NOMA networks suffer from error propagation from UE_1 to UE_2 and this error propagation causes significant decay in e2e error performance of C-NOMA networks. Thus, diversity order cannot be achieved at UE_2 although it receives two copies of signal from independent paths/links which will be shown by simulations in the numerical results section of this chapter. Hence, in order to resolve this problem, Threshold-based Selective Cooperative-NOMA (TBS-C-NOMA) is proposed to increase reliability in the second phase of C-NOMA and to minimize the error propagation. TBS-C-NOMA is based on introducing a condition on UE_1 -relay- and UE_1 decides whether to forward or not the symbols of UE_2 in the second phase of C-NOMA according to this condition. UE_1 forwards estimated x_2 symbols in the second phase if the condition is succeeded otherwise UE_2 remains idle in the second phase of communication. In TBS-C-NOMA, the first
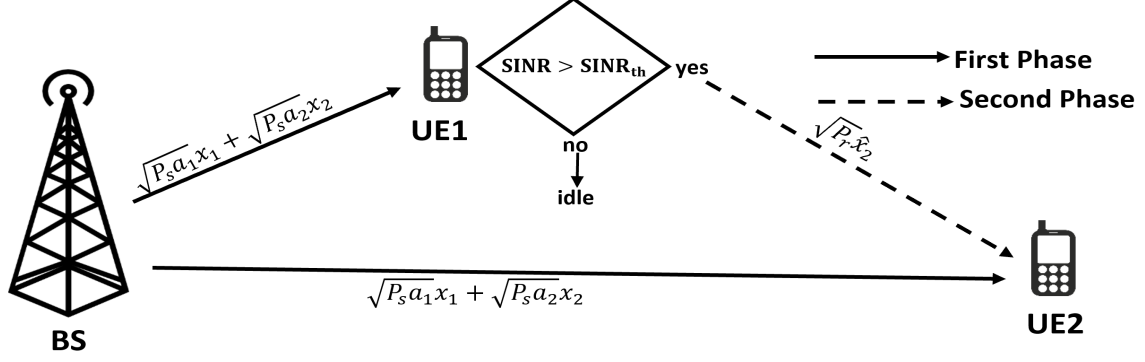
Figure 3.3: The illustration of TBS-C-NOMA

phase of communication is the same with conventional C-NOMA and the received signal by users is given in (3.1). However, the second phase of communication is modified and the received signal by UE_2 in the second phase is given as

$$y_r = \begin{cases} 0, & SINR_2^{(1)} < SINR_{th}, \\ \sqrt{P_r} h_r \hat{x}_2 + w_r, & SINR_2^{(1)} \geq SINR_{th}, \end{cases} \tag{3.24}$$

where $SINR_2^{(1)}$ denotes the SINR for x_2 symbols at UE_1 -SINR before SIC process at UE_1 to detect x_2 symbols firstly- and it is given as

$$SINR_2^{(1)} = \frac{\rho_s \alpha_2 |h_{s1}|^2}{\rho_s \alpha_1 |h_{s1}|^2 + 1}, \tag{3.25}$$

and $SINR_{th}$ is the pre-determined threshold value at UE_1 to evaluate whether the detection of x_2 symbols is reliable or not.

Then, UE_2 implement MRC to combine signals in two phases likewise conventional C-NOMA. The illustration of TBS-C-NOMA is given in Figure 3.3.

3.3.3.1 Performance Analysis

In this subsection, analysis of C-NOMA given in the Section 3.3.2 is extended for TBS-C-NOMA.

3.3.3.1.1 Ergodic Capacity Analysis

Achievable rate of TBS-C-NOMA should be handled in two cases which are UE_1 -relay-forwards x_2 symbols and cooperative diversity is accomplished or UE_1 -relay- remains in

silence and only the direct link between BS and UE_2 remains. Thus, the achievable rate for TBS-C-NOMA is defined as[3]

$$R_{TBS} = \begin{cases} \frac{1}{2}\log_2\left(1 + SINR_2\right), & SINR_2^{(1)} < SINR_{th}, \\ \frac{1}{2}\log_2\left(1 + SINR_{CN}\right), & SINR_2^{(1)} \geq SINR_{th}, \end{cases} \tag{3.26}$$

where $1/2$ coefficient exists since each phase of communication is assumed to cover half of total time unlike short range communication in [108]. $SINR_2$ and $SINR_{CN}$ are the SINR at UE_2 for direct link and the SINR for cooperative diversity which are given in (2.6) and (3.3), respectively. In order to derive ergodic capacity, eq. (3.26) should be averaged over instantaneous SINRs by considering the condition $SINR_2^{(1)} \geq SINR_{th}$ is succeeded or not.

By substituting (2.6) and (3.3) into (3.26), with some simplifications, ergodic capacity is derived as

$$\begin{aligned} C_{TBS} = \frac{1}{2}\Bigg[&P\left(SINR_2^{(1)} < SINR_{th}\right) \times \\ &\left\{\int_0^\infty \log_2\left(1 + \rho_s\gamma_{s2}\right)p_{\gamma_{s2}}(\gamma_{s2})d\gamma_{s2} - \int_0^\infty \log_2\left(1 + \alpha_1\rho_s\gamma_{s2}\right)p_{\gamma_{s1}}(\gamma_{s2})d\gamma_{s2}\right\} \\ &+ P\left(SINR_2^{(1)} \geq SINR_{th}\right) \times \\ &\left\{\int_0^\infty \log_2\left(1 + \Psi\right)p_\Psi(\Psi)d\Psi - \int_0^\infty \log_2\left(1 + \alpha_1\rho_s\gamma_{s2}\right)p_{\gamma_{s2}}(\gamma_{s2})d\gamma_{s2}\right\}\Bigg], \end{aligned} \tag{3.27}$$

where $\Psi \triangleq \rho_s\gamma_{s2} + \rho_r\gamma_r$ is defined likewise in C-NOMA.

The probability for cooperative diversity to be achieved (.e., $SINR_2^{(1)} \geq SINR_{th}$) is derived as

$$\begin{aligned} P_{dec} &= P\left(SINR \geq SINR_{th}\right) \\ &= P\left(\frac{\rho_s\alpha_2\left|h_{s1}\right|^2}{\rho_s\alpha_1\left|h_{s1}\right|^2 + 1} \geq SINR_{th}\right) \\ &= P\left(\rho_s\gamma_{s1} \geq \phi_{th}\right), \end{aligned} \tag{3.28}$$

where $\phi_{th} = \frac{SINR_{th}}{\alpha_2 - \alpha_1 SINR_{th}}$ is defined. By substituting CDF of γ_{s1}, it is derived as

$$P_{dec} = \exp\left(-\frac{\phi_{th}}{\rho_s\sigma_{s1}^2}\right). \tag{3.29}$$

---

[3]In equations, TBS is used to refer the TBS-C-NOMA.

It is worth to note that $\alpha_2 > \alpha_1 SINR_{th}$ should be succeeded otherwise UE_1 always remains idle in the second phase of communication.

Then substituting (3.29) into (3.27) and with the aid of [89, eq. (4.337.2)], EC of TBS-C-NOMA is derived as

$$
\begin{aligned}
C_{TBS} = \frac{\log_2 e}{2} & \left[\left(1 - \exp\left(-\frac{\phi_{th}}{\rho_s \sigma_{s1}^2} \right) \right) \left\{ -\exp\left(\frac{1}{\alpha_1 \rho_s \sigma_{s2}^2} \right) Ei\left(-\frac{1}{\alpha_1 \rho_s \sigma_{s2}^2} \right) \right\} \right. \\
& + exp\left(\frac{1}{\rho_s \sigma_{s2}^2} \right) Ei\left(-\frac{1}{\rho_s \sigma_{s2}^2} \right) \\
& + \frac{\exp\left(-\frac{\phi_{th}}{\rho_s \sigma_{s1}^2} \right)}{\rho_s \sigma_{s2}^2 - \rho_r \sigma_r^2} \left\{ \rho_s \sigma_{s2}^2 \exp\left(\frac{1}{\rho_s \sigma_{s2}^2} \right) Ei\left(-\frac{1}{\rho_s \sigma_{s2}^2} \right) - \rho_r \sigma_r^2 \exp\left(\frac{1}{\rho_r \sigma_r^2} \right) Ei\left(-\frac{1}{\rho_r \sigma_r^2} \right) \right\} \bigg].
\end{aligned}
$$

$$(3.30)$$

3.3.3.1.2 Outage Probability Analysis

The outage event for TBS-C-NOMA occurs when the achievable rate of TBS-C-NOMA cannot meet QoS requirement (target data rate) likewise all NOMA involved systems. Thus, OP of TBS-CNOMA is given as

$$
P_{TBS}(out) = P(R_{TBS} < \acute{R}_{TBS}), \tag{3.31}
$$

where $\acute{R}_{TBS}$ is the target rate for TBS-C-NOMA. Substituting (3.26) into (3.31), it turns out to be

$$
P_{TBS}(out) = \begin{cases} P\left(\frac{\rho_s \alpha_2 |h_{s2}|^2}{\rho_s \alpha_1 |h_{s2}|^2 + 1} < \phi_{TBS} \right), & SINR_2^{(1)} < SINR_{th}, \\ P\left(\frac{\alpha_2 \rho_s |h_{s2}|^2 + \rho_r |h_r|^2}{\alpha_1 \rho_s |h_{s2}|^2 + 1} < \phi_{TBS} \right), & SINR_2^{(1)} \geq SINR_{th}, \end{cases} \tag{3.32}
$$

where $\phi_{TBS} = 2^{\acute{R}_{TBS}} - 1$ is defined. Considering the probability for the $SINR_2^{(1)}$ being above threshold and with some simplifications, OP is obtained as

$$
P_{TBS}(out) = (1 - P_{dec}) P\left(\gamma_{s2} < \psi_2 \right) + P_{dec} P\left(\Psi_{CN} < \phi_{TBS} \right), \tag{3.33}
$$

where $\psi_2 = \frac{\phi_2}{\rho(\alpha_2 - \alpha_1 \phi_{TBS})}$ and $\Psi_{TBS} = \rho_s \left(\alpha_2 - \alpha_1 \phi_{TBS} \right) \gamma_{s2} + \rho_r \gamma_r$ are given likewise in the downlink NOMA and C-NOMA, respectively. Thus, substituting (2.20), (3.11) and

(3.29) into (3.33), OP of TBS-C-NOMA is derived as

$$
P_{TBS}(out) = \left(1 - \exp\left(-\frac{\phi_{th}}{\rho_s \sigma_{s1}^2}\right)\right)\left(1 - exp(-\psi_2/\sigma_{s2}^2)\right) + \exp\left(-\frac{\phi_{th}}{\rho_s \sigma_{s1}^2}\right)
$$

$$
\times \left\{ \frac{\rho_r \sigma_r^2 \left(1 - \exp\left(-\frac{\phi_{TBS}}{\rho_r \sigma_r^2}\right)\right) - \rho_s \left(\alpha_2 - \alpha_1 \phi_{TBS}\right)\sigma_{s2}^2 \left(1 - \exp\left(-\frac{\phi_{TBS}}{\rho_s(\alpha_2 - \alpha_1 \phi_{TBS})\sigma_{s2}^2}\right)\right)}{\rho_r \sigma_r^2 - \rho_s \left(\alpha_2 - \alpha_1 \phi_{TBS}\right)\sigma_{s2}^2} \right\},
$$

$$(3.34)$$

3.3.3.1.3 Bit Error Probability (BEP) Analysis

The BEP of C-NOMA is modified by considering the introduced condition for TBS-C-NOMA. Thus, the e2e average BEP for TBS-C-NOMA is obtained as

$$
P_{TBS}^{(e2e)}(e) = (1 - P_{dec}) \times P_{direct}(e) + P_{dec} \times \left\{ P_{div}(e) \times \left(1 - P_{SIC}^{(th)}(e)\right) + P_{SIC}^{(th)}(e) \times P_{(prop)}(e) \right\},
$$

$$(3.35)$$

where P_{dec} is the probability for the event where SINR of x_2 symbols at UE_1 is above threshold and it is derived in the previous subsections (3.29). $P_{direct}(e)$ denotes the BEP when the UE_1 is idle in the second phase and only direct transmission between BS and UE_2 remains. Thus, it is BEP of conventional downlink NOMA. $P_{div}(e)$ and $P_{(prop)}$ denote the BEP at UE_2 after MRC whether the UE_1 forwards correct detected symbols and diversity is achieved or erroneous detected symbols and error propagation occurs, respectively. They have been derived for C-NOMA in the previous subsection as (3.17) and (3.21), respectively. $P_{SIC}^{(th)}(e)$ is the BEP for x_2 symbols at UE_1 even if the SINR of x_2 symbols at UE_1 above threshold and it should be derived to obtain e2e BEP of TBS-C-NOMA.

Firstly, $P_{direct}(e)$ is derived for different modulation pairs given in Table 3.1. One can easily see that $P_{direct}(e)$ is the similar to $P_{SIC}(e)$ of C-NOMA given in (3.14) since they both denote the BEP of x_2 symbols when only one path exists and ML detector is implemented by pretending x_1 symbols as noise. Thus, $P_{direct}(e)$ can be easily obtained by changing channel conditions in $P_{SIC}(e)$ of C-NOMA (3.14) and it is derived as

$$
P_{direct}(e) = \sum_{i=1}^{N} \frac{\varsigma_i}{2} \left(1 - \sqrt{\frac{\nu_i \rho_s \sigma_{s2}^2}{1 + \nu_i \rho_s \sigma_{s1}^2}}\right).
$$

$$(3.36)$$

In order to derive $P_{SIC}^{(th)}(e)$, with the aid of (3.13), the BEP for x_2 symbols for arbitrary fading channel is defined as

$$P(e|_\gamma) = \sum_{i=1}^{N} \varsigma_i Q\left(\sqrt{2\nu_i \rho_s \gamma}\right), \tag{3.37}$$

where $\gamma \triangleq |h|^2$ denotes the arbitrary channel condition. It is noteworthy that this BEP is for the error event when the $SINR_2^{(1)} \geq SINR_{th}$. Thus, to obtain average BEP, conditional BEP is averaged by recalling the SINR of x_2 symbols at UE_1 is above the threshold

$$P_{SIC}^{(th)}(e|_{\gamma_{s1}}) = \sum_{i=1}^{N} \varsigma_i \int_{\phi_{th}/\rho_s}^{\infty} Q\left(\sqrt{2\nu_i \rho_s \gamma_{s1}}\right) p_{\gamma_{s1}}(\gamma_{s1}) d\gamma_{s1}, \tag{3.38}$$

then $u(\gamma) \triangleq \int p_{\gamma_{s1}}(\gamma_{s1}) d\gamma_{s1}$ is defined and it is substituted into (3.38). Then, by applying partial integration likewise [94, appendix B]

$$P_{SIC}^{(th)}(e) \leq \sum_{i=1}^{N} \left[\varsigma_i Q\left(\sqrt{2\nu_i \rho_s \gamma}\right)\Big|_{\gamma=\phi_{th}}^{\infty} - \int_{\phi_{th}/\rho_s}^{\infty} \frac{d}{d\gamma}\left\{\varsigma_i Q\left(\sqrt{2\nu_i \rho_s \gamma}\right)\right\} u(\gamma) d\gamma \right], \tag{3.39}$$

and with the the Leibniz' rule [89, eq. (0.42)], it turns out to be

$$P_{SIC}^{(th)}(e) \leq \sum_{i=1}^{N} \left[\varsigma_i Q\left(\sqrt{2\nu_i \rho_s \gamma}\right)\Big|_{\gamma=\phi_{th}}^{\infty} + \frac{\varsigma_i \sqrt{2\nu_i \rho_s}}{2\sqrt{2\pi}} \int_{\phi_{th}}^{\infty} \frac{1}{\sqrt{\gamma}} u(\gamma) e^{-\nu_i \rho_s \gamma} d\gamma \right]. \tag{3.40}$$

Since the $\gamma_{s1} \triangleq |h_{s1}|^2$ exponentially distributed and the symbols are forwarded only the condition $SINR_2^{(1)} \geq SINR_{th}$ is succeeded, it is defined as

$$p_{\gamma_{s1}}^{(\phi_{th})} = \begin{cases} 0, & \gamma_{s1} < \phi_{th}, \\ \frac{1}{exp(-\phi_{th}/\sigma_{s1}^2)} \frac{1}{\sigma_{s1}^2} \exp\left(-\gamma/\sigma_{s1}^2\right), & \gamma_{s1} \geq \phi_{th}, \end{cases} \tag{3.41}$$

where $1/exp(-\phi_{th}/\sigma_{s1}^2)$ is scaling factor to ensure PDF to have unit area. Then substituting (3.41) into $u(\gamma)$ and then into (3.40), the average BEP of SIC when $SINR_2^{(1)} \geq SINR_{th}$ is succeeded, is derived as

$$P_{SIC}^{(th)}(e) \leq \sum_{i=1}^{N} \varsigma_i \left[Q\left(\sqrt{2\nu_i \phi_{th}}\right) - \exp\left(\frac{\phi_{th}}{\sigma_{s1}^2}\right) \sqrt{\frac{1}{1 + \frac{1}{\nu_i \rho_s \sigma_{s1}^2}}} Q\left(\sqrt{2\phi_{th}\left(\nu_i \rho_s + \frac{1}{\sigma_{s1}^2}\right)}\right) \right]. \tag{3.42}$$

Lastly, substituting (3.17), (3.21), (3.36) and (3.42) into (3.35), the e2e average BEP of TBS-C-NOMA is derived as

$$
\begin{aligned}
P_{TBS}^{(e2e)}(e) = \sum_{i}^{N} \varsigma_i &\left[\left\{ 1 - \exp\left(-\frac{\phi_{th}}{\rho_s \sigma_{s1}^2} \right) \right\} \times \frac{1}{2} \left(1 - \sqrt{\frac{\nu_i \rho_s \sigma_{s2}^2}{1 + \nu_i \rho_s \sigma_{s1}^2}} \right) + \exp\left(-\frac{\phi_{th}}{\rho_s \sigma_{s1}^2} \right) \right. \\
&\times \left[\left\{ 1 - \left\{ Q\left(\sqrt{2\nu_i \phi_{th}} \right) - \exp\left(\frac{\phi_{th}}{\sigma_{s1}^2} \right) \sqrt{\frac{1}{1 + \frac{1}{\nu_i \rho_s \sigma_{s1}^2}}} Q\left(\sqrt{2\phi_{th}\left(\nu_i \rho_s + \frac{1}{\sigma_{s1}^2} \right)} \right) \right\} \right\} \right. \\
&\times \frac{1}{2} \left\{ 1 - \frac{1}{\nu_i \rho_s \sigma_{s2}^2 - \rho_r \sigma_r^2} \left(\nu_i \rho_s \sigma_{s2}^2 \sqrt{\frac{\nu_i \rho_s \sigma_{s2}^2}{1 + \nu_i \rho_s \sigma_{s2}^2}} - \rho_r \sigma_r^2 \sqrt{\frac{\rho_r \sigma_r^2}{1 + \rho_r \sigma_r^2}} \right) \right\} \\
&+ \left\{ Q\left(\sqrt{2\nu_i \phi_{th}} \right) - \exp\left(\frac{\phi_{th}}{\sigma_{s1}^2} \right) \sqrt{\frac{1}{1 + \frac{1}{\nu_i \rho_s \sigma_{s1}^2}}} Q\left(\sqrt{2\phi_{th}\left(\nu_i \rho_s + \frac{1}{\sigma_{s1}^2} \right)} \right) \right\} \\
&\left. \left. \times \frac{c_{j,M} \rho_r \sigma_r^2}{c_{j,M} \rho_r \sigma_r^2 + \nu_i \rho_s \sigma_{s2}^2} \right] \right].
\end{aligned}
\tag{3.43}
$$

3.3.3.2 Optimum Threshold for TBS-C-NOMA

The optimum threshold for TBS-C-NOMA denotes the threshold value which minimizes the e2e average BEP. Since the e2e average BEP of TBS-C-NOMA is a function of ϕ_{th}, the optimum threshold is given as

$$
SINR_{th}^{opt} = \underset{\phi_{th}}{\operatorname{argmin}} \, P_{TBS}^{(e2e)}(e),
\tag{3.44}
$$

and it is obtained by

$$
\frac{dP_{TBS}^{(e2e)}(e)}{d\phi_{th}} = 0.
\tag{3.45}
$$

After Leibniz' rule [89, eq. (0.42)] is applied to (3.45), with the aid of [97], the optimum value which minimizes e2e BEP is derived as

$$
\phi_{th}^{opt} = \begin{cases} \sum_{i=1}^{N} \frac{1}{2\nu_i} \left(Q^{-1} \left(\delta_i / \varsigma_i \right) \right)^2, & \delta_i < 0.5, \\ 0, & otherwise, \end{cases}
\tag{3.46}
$$

where

$$
\delta_i = \frac{P_{direct}(e|_i) - P_{div}(e|_i)}{P_{prop}(e|_i) - P_{div}(e|_i)}.
\tag{3.47}
$$

After substituting (3.17), (3.21) and (3.36) into (3.48), the optimum threshold value for TBS-C-NOMA is derived by

$$
SINR_{th}^{opt} = \frac{\alpha_2 \phi_{th}^{opt}}{1 + \alpha_1 \phi_{th}^{opt}}.
\tag{3.48}
$$

The derived optimum threshold values ($SINR_{th}^{opt}$) are presented in Table 3.2 with the change of transmit SNR (ρ_s) for two different scenarios for all constellation pairs mode provided in Table 3.1. In Scenario I, $\sigma_{s1}^2 = 3dB$, $\sigma_{s2}^2 = 0dB$, $\sigma_r^2 = 3dB$ where power allocation coefficients are $\alpha_1 = 0.2$ and $\alpha_2 = 0.8$. In Scenario II, $\sigma_{s1}^2 = 10dB$, $\sigma_{s2}^2 = 3dB$, $\sigma_r^2 = 10dB$, $\alpha_1 = 0.1$ and $\alpha_2 = 0.9$ are assumed. It is noteworthy that the condition $\alpha_2 > \alpha_1 SINR_{th}$ is always accomplished otherwise UE_1 would always remains idle in the second phase of TBS-C-NOMA. In both scenarios, $\rho_r = \rho_s/2$ is assumed.

Table 3.2: Optimum threshold values for TBS-C-NOMA

		Scheme I				Scheme II			
		$\rho_s(dB)$				$\rho_s(dB)$			
	mode	0	10	20	30	0	10	20	30
$SINR_{th}^{opt}(dB)$	1	-4.81	1.37	4.31	5.07	-1.61	3.76	6.11	7.14
	2	-4.20	1.17	5.28	5.75	-1.02	5.41	7.76	8.45
	3	-4.56	0.90	3.72	4.62	-1.61	3.22	5.55	6.66
	4	-3.76	1.76	4.84	5.45	-0.86	4.81	7.19	8.04
	5	-4.55	0.83	3.94	4.90	-1.61	3.24	5.69	6.88
	6	-3.76	1.49	5.07	5.68	-0.86	4.80	7.42	8.30

3.4 RELAY-ASSISTED/AIDED-NOMA

3.4.1 System Model

A downlink NOMA scheme is considered where BS is to serve to two legitimate users (i.e. UE_1 and UE_2). However, BS cannot reach out to users because the direct links between BS and users do not exist due to the blockage of path-loss/large-objects. Thus, a DF relay (i.e., R) assists BS to serve users. All nodes are assumed to be equipped with single antenna and relay serves in half-duplex mode to avoid self-interference. Hence, the total communication covers two phases (time slots). In the first phase, BS transmits SC symbols of users to the relay and the received signal is given as
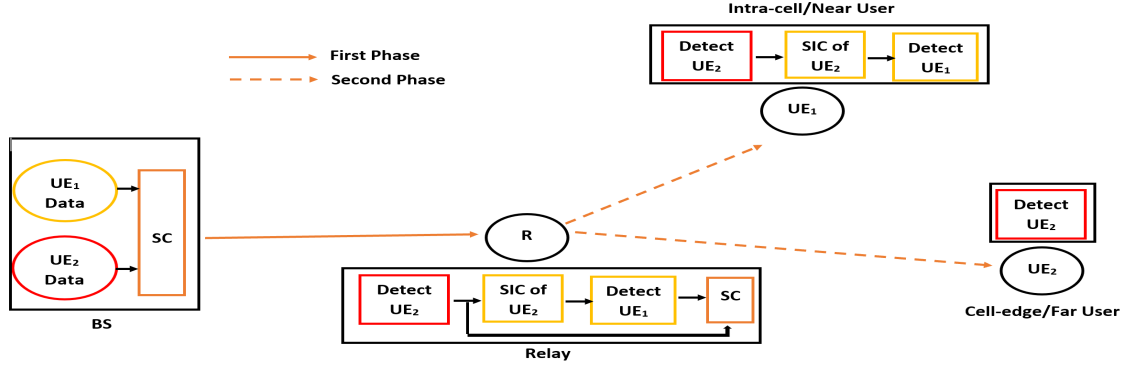
Figure 3.4: The illustration of relay-assisted-NOMA

$$y_{sr} = \sqrt{P_S}h_{sr}\left(\sqrt{\alpha_1}x_1 + \sqrt{\alpha_2}x_2\right) + w_{sr}, \tag{3.49}$$

where P_S is the transmit power of BS and h_{sr} is the channel coefficient between BS and relay which follows $CN(0, \sigma_{sr}^2)$. w_{sr} is AWGN with N_0 variance. α_1, x_1 and α_2, x_2 pairs denoted power allocation coefficient and base-band modulated symbol of related user. $\alpha_1 + \alpha_2 = 1$. Then, the relay forwards the estimated symbols to the users and the received signals by users are given as

$$y_\lambda = \sqrt{P_r}h_\lambda\left(\sqrt{\varrho_1}\hat{x}_1 + \sqrt{\varrho_2}\hat{x}_2\right) + w_\lambda, \quad \lambda = r1, r2, \tag{3.50}$$

where $h_\lambda, i.e., \lambda = r1, r2$ is the complex channel fading coefficient between relay and users with variance σ_λ^2 which is related to the distance between nodes likewise throughout this work. $\sigma_{r1}^2 > \sigma_{r2}^2$ is assumed, hence UE_1 and UE_2 are denoted as near user and far user, respectively. $\hat{x}_1$ and $\hat{x}_2$ estimated symbols of users at relay. Since the channel condition between relay and UE_2 is worse than the one between relay and UE_1, power allocation coefficients at the relay are defined as $\varrho_2 > \varrho_1$ where $\varrho_1 + \varrho_2 = 1$. Based on the received signal, users detects their intended symbols. Whereas UE_1 should implement SIC to detect own symbols, UE_2 implements only ML detector by pretending x_1 symbols as noise since $\varrho_2 > \varrho_1$. The system model of relay-assisted-NOMA is given in Figure 3.4. The power allocation coefficients at the source can be implemented in two ways: $\alpha_2 > \alpha_1$ -conventional relay-assisted-NOMA- or $\alpha_1 > \alpha_2$ -reversed relay-assisted-NOMA-[4]. Relay detects x_1 and x_2 symbols according to power allocation coefficients such ways: if $\alpha_2 > \alpha_1$,

---

[4]Both scenarios can be considered for relay-assisted-NOMA by considering different constraints.

relay firstly detects x_2 symbols with ML detector by pretending x_2 symbols as noise and then, implements SIC for detected x_2 symbols to detect x_1 symbols. On the other hand, if $\alpha_1 > \alpha_2$, relay reverses the detecting order of symbols. In both scenarios, power allocations at the relay are the same as $\varrho_2 > \varrho_1$ since channel condition between relay and UE_2 is worse than that between relay and UE_1.

3.4.2   Performance Analysis

In this section, bit error probability (BEP) analysis is provided to evaluate performance of relay-assisted-NOMA networks when $\alpha_2 > \alpha_1$ -conventional networks-. The provided analysis can be easily modified for $\alpha_1 > \alpha_2$ -reversed network-. Nevertheless, simulation results will be presented for both scenarios in Section 3.6 to compare performances. Ergodic capacity and outage analysis are not provided for relay-assisted-NOMA networks in this thesis since they have been analyzed widely in literature for both HD and FD relaying [124, 125]. Nevertheless, the achievable rate and outage probability of considered network are defined and extensive simulations are provided for performance evaluation.

3.4.2.1   Ergodic Capacity Analysis

Achievable rate for symbols of users in the first phase is given as [127]

$$
\begin{aligned}
R_1^{(sr)} &= \log_2\left(1 + SINR_1^{(sr)}\right), \\
R_2^{(sr)} &= \log_2\left(1 + SINR_2^{(sr)}\right),
\end{aligned}
\tag{3.51}
$$

and in the second phase

$$
\begin{aligned}
R_1^{(r1)} &= \log_2\left(1 + SINR_1^{(r1)}\right), \\
R_2^{(r2)} &= \log_2\left(1 + SINR_2^{(r2)}\right),
\end{aligned}
\tag{3.52}
$$

where $SINR_i^{(sr)}$, $SINR_i^{(ri)}$ $i.e., i = 1, 2$ denote the SINR of users in the first phase and in the second phase, respectively and are defined as

$$
\begin{aligned}
SINR_1^{(sr)} &= \frac{\alpha_1 \rho_s \left|h_{sr}\right|^2}{\beta \alpha_2 \rho_s \left|h_{sr}\right|^2 + 1}, \\
SINR_2^{(sr)} &= \frac{\alpha_2 \rho_s \left|h_{sr}\right|^2}{\alpha_1 \rho_s \left|h_{sr}\right|^2 + 1},
\end{aligned}
\tag{3.53}
$$

and

$$SINR_1^{(r1)} = \frac{\varrho_1 \rho_r |h_{r2}|^2}{\beta \varrho_2 \rho_r |h_{r2}|^2 + 1},$$

$$SINR_2^{(r2)} = \frac{\varrho_2 \rho_r |h_{r2}|^2}{\varrho_1 \rho_r |h_{r2}|^2 + 1},$$

(3.54)

Recalling that the achievable rate for DF relaying is dominated by the weakest link [148], the achievable rates of users for relay-assisted-NOMA are given as[5]

$$R_1^{(RAN)} = \frac{1}{2} \min\{R_1^{(sr)}, R_1^{(r1)}\},$$

$$R_2^{(RAN)} = \frac{1}{2} \min\{R_2^{(sr)}, R_2^{(r1)}\}.$$

(3.55)

Ergodic capacities of each user in the relay-assisted-NOMA are derived by averaging achievable rate as [129]

$$C_1^{(RAN)} = \int\limits_0^\infty R_1^{(RAN)},$$

$$C_2^{(RAN)} = \int\limits_0^\infty R_2^{(RAN)}.$$

(3.56)

3.4.2.2 Outage Probability Analysis

As in all NOMA schemes, the outage occurs when the target rates can not be succeeded. Thus, the OPs of users in relay-assisted-NOMA are given as

$$P_1^{(RAN)}(out) = P(R_1^{(RAN)} < \acute{R}_1^{(RAN)}),$$

$$P_1^{(RAN)}(out) = P(R_2^{(RAN)} < \acute{R}_2^{(RAN)}),$$

(3.57)

where $\acute{R}_i^{(RAN)}, i = 1, 2$ is target rate of user in relay-assisted-NOMA. Likewise, ergodic capacity, OP for relay-assisted-NOMA networks analyzed in [127, 128]. Thus, only simulation results are provided in Section 3.6.

3.4.2.3 Bit Error Probability (BEP) Analysis

Relay-assisted-NOMA network consists of two phases and each phase can be considered as conventional downlink-NOMA network since two different symbols are conveyed to destination (i.e., relay in the first phase and users in the second phase) on the same

---

[5]In equations, RAN is used to refer the relay-assisted-NOMA.

resource block. In addition, error events in two phases are independent. Hence, with the law of total probability, the average BEPs of each user is given as

$$P_1^{(RAN)}(e) = \left(1 - P_1^{(sr)}(e)\right) P_1^{(r1)}(e) + P_1^{(sr)}(e) \left(1 - P_1^{(r1)}(e)\right),$$
$$P_2^{(RAN)}(e) = \left(1 - P_2^{(sr)}(e)\right) P_2^{(r2)}(e) + P_2^{(sr)}(e) \left(1 - P_2^{(r2)}(e)\right),$$

(3.58)

where $P_i^{(sr)}(e)$ and $P_i^{(ri)}(e)$, $i = 1, 2$ denote the BEP of ith user in the first phase between BS and relay and in the second phase between relay and ith user, respectively. As emphasized in Section 2.2.2, the BEP for NOMA schemes is highly dependent to chosen modulation constellation. Thus, likewise in conventional downlink NOMA, it is assumed that QPSK and BPSK are used for the symbols of UE_1 and UE_2, respectively. In this case, the BEP expressions given in (3.58) can be easily obtained by adopting (2.23) and (2.31) -changing channel conditions, power allocation coefficients-. Then, the average e2e BEPs of each user in relay-assisted-NOMA are derived as follow

$$
\begin{aligned}
P_1^{(RAN)}(e) = \frac{1}{2} \Bigg[1 - \frac{1}{2} \Bigg\{ 1 - \sqrt{\frac{\varepsilon_C \sigma_{sr}^2}{N_0 + \varepsilon_C \sigma_{sr}^2}} + \frac{1}{4} \Bigg\{ \sqrt{\frac{\varepsilon_A \sigma_{sr}^2}{N_0 + \varepsilon_A \sigma_{sr}^2}} - \sqrt{\frac{\varepsilon_B \sigma_{sr}^2}{N_0 + \varepsilon_B \sigma_{sr}^2}} \\
- \sqrt{\frac{\varepsilon_D \sigma_{sr}^2}{N_0 + \varepsilon_D \sigma_{sr}^2}} + \sqrt{\frac{\varepsilon_E \sigma_{sr}^2}{N_0 + \varepsilon_E \sigma_{sr}^2}} \Bigg\} \Bigg\} \Bigg] \times \Bigg[1 - \sqrt{\frac{\varepsilon_H \sigma_{r1}^2}{N_0 + \varepsilon_H \sigma_{r1}^2}} + \frac{1}{4} \Bigg\{ \sqrt{\frac{\varepsilon_F \sigma_{r1}^2}{N_0 + \varepsilon_F \sigma_{r1}^2}} \\
- \sqrt{\frac{\varepsilon_G \sigma_{r1}^2}{N_0 + \varepsilon_G \sigma_{r1}^2}} - \sqrt{\frac{\varepsilon_J \sigma_{r1}^2}{N_0 + \varepsilon_J \sigma_{r1}^2}} + \sqrt{\frac{\varepsilon_K \sigma_{r1}^2}{N_0 + \varepsilon_K \sigma_{r1}^2}} \Bigg\} \Bigg] + \Bigg[1 - \sqrt{\frac{\varepsilon_C \sigma_{sr}^2}{N_0 + \varepsilon_C \sigma_{sr}^2}} \\
+ \frac{1}{4} \Bigg\{ \sqrt{\frac{\varepsilon_A \sigma_{sr}^2}{N_0 + \varepsilon_A \sigma_{sr}^2}} - \sqrt{\frac{\varepsilon_B \sigma_{sr}^2}{N_0 + \varepsilon_B \sigma_{sr}^2}} - \sqrt{\frac{\varepsilon_D \sigma_{sr}^2}{N_0 + \varepsilon_D \sigma_{sr}^2}} + \sqrt{\frac{\varepsilon_E \sigma_{sr}^2}{N_0 + \varepsilon_E \sigma_{sr}^2}} \Bigg\} \Bigg] \\
\times \Bigg[1 - \frac{1}{2} \Bigg\{ 1 - \sqrt{\frac{\varepsilon_H \sigma_{r1}^2}{N_0 + \varepsilon_H \sigma_{r1}^2}} + \frac{1}{4} \Bigg\{ \sqrt{\frac{\varepsilon_F \sigma_{r1}^2}{N_0 + \varepsilon_F \sigma_{r1}^2}} - \sqrt{\frac{\varepsilon_G \sigma_{r1}^2}{N_0 + \varepsilon_G \sigma_{r1}^2}} \\
- \sqrt{\frac{\varepsilon_J \sigma_{r1}^2}{N_0 + \varepsilon_J \sigma_{r1}^2}} + \sqrt{\frac{\varepsilon_K \sigma_{r1}^2}{N_0 + \varepsilon_K \sigma_{r1}^2}} \Bigg\} \Bigg\} \Bigg]
\end{aligned}
$$

(3.59)

and

$$
P_2^{(RAN)}(e) =
$$

$$
\begin{aligned}
\frac{1}{4} \Bigg[1 - \frac{1}{4} \Bigg\{ 2 - \sqrt{\frac{\varepsilon_A \sigma_{sr}^2}{N_0 + \varepsilon_A \sigma_{sr}^2}} - \sqrt{\frac{\varepsilon_B \sigma_{sr}^2}{N_0 + \varepsilon_B \sigma_{sr}^2}} \Bigg\} \Bigg] \Bigg[2 - \sqrt{\frac{\varepsilon_F \sigma_{r2}^2}{N_0 + \varepsilon_F \sigma_{r2}^2}} - \sqrt{\frac{\varepsilon_G \sigma_{r2}^2}{N_0 + \varepsilon_G \sigma_{r2}^2}} \Bigg] \\
+ \Bigg[2 - \sqrt{\frac{\varepsilon_A \sigma_{sr}^2}{N_0 + \varepsilon_A \sigma_{sr}^2}} - \sqrt{\frac{\varepsilon_B \sigma_{sr}^2}{N_0 + \varepsilon_B \sigma_{sr}^2}} \Bigg] \Bigg[1 - \frac{1}{4} \Bigg\{ 2 - \sqrt{\frac{\varepsilon_F \sigma_{r2}^2}{N_0 + \varepsilon_F \sigma_{r2}^2}} - \sqrt{\frac{\varepsilon_G \sigma_{r2}^2}{N_0 + \varepsilon_G \sigma_{r2}^2}} \Bigg\} \Bigg] ,
\end{aligned}
$$
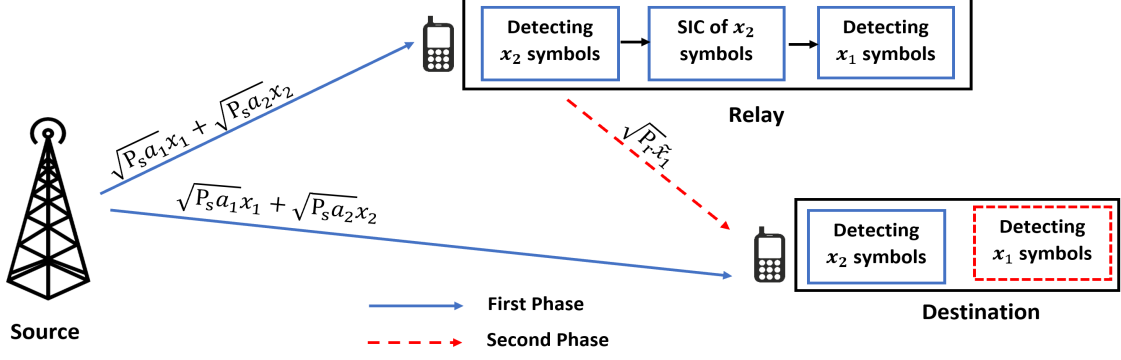
Figure 3.5: NOMA-based cooperative relaying system model

$$(3.60)$$

where ε_A, ε_B, ε_C, ε_D and ε_E are defined in Section 2.2.2 and likewise $\varepsilon_F \triangleq \left(\sqrt{\varrho_2 P_r} + \sqrt{\varrho_1 P_r/2} \right)^2$, $\varepsilon_G \triangleq \left(\sqrt{\varrho_2 P_r} - \sqrt{\varrho_1 P_r/2} \right)^2$, $\varepsilon_H \triangleq \varrho_1 P_r$, $\varepsilon_J \triangleq \left(2\sqrt{\varrho_2 P_r} + \sqrt{\varrho_1 P_r/2} \right)^2$ and $\varepsilon_K \triangleq \left(2\sqrt{\varrho_2 P_r} - \sqrt{\varrho_1 P_r/2} \right)^2$ are defined.

3.5 COOPERATIVE RELAYING SYSTEMS USING NOMA

3.5.1 System Model

A NOMA-based cooperative relaying system (CRS) is considered as in [142] where a source (S) is willing to reach out the destination (D) and a half-duplex relay (R) helps for it. The system model is given in Figure 3.5. All nodes are assumed to be equipped with single antenna and the complex channel fading coefficient between each nodes follows $CN(0, \sigma_\lambda^2)$, i.e., $\lambda = sr, sd, rd$. In order to overcome the inefficiency of the conventional CRS of device-to-device (D2D) communication, NOMA is applied for two intended/consecutive symbols of destination in the first phase of the communication. Then, this total SC symbol is conveyed to both destination and relay, hence the received signals in the first phase are given as

$$y_{sd} = \sqrt{P_s} \left(\sqrt{\alpha_1} x_1 + \sqrt{\alpha_2} x_2 \right) h_{sd} + w_{sd},$$
$$y_{sr} = \sqrt{P_s} \left(\sqrt{\alpha_1} x_1 + \sqrt{\alpha_2} x_2 \right) h_{sr} + w_{sr},$$

$$(3.61)$$

where h_{sd}, w_{sd} and h_{sr}, w_{sr} pairs denote complex channel fading coefficients and AWGN with N_0 variance between the nodes S-D and S-R, respectively. α_1 and α_2 are the power

allocations coefficients for the base-band modulated symbols of x_1 and x_2, respectively. x_1 and x_2 are the two symbols of destination to be transmitted in order. P_s is the transmit power of source, $\alpha_1 + \alpha_2 = 1$ and $\alpha_2 > \alpha_1$ is assumed. Thus, in the first phase of communication, both relay and destination detects x_2 symbol by treating x_1 symbols as noise. Then the relay implements SIC to detect x_1 symbols and forward detected x_1 symbol to the destination in the second phase. The received signal by the destination in the second phase is given as

$$y_{rd} = \sqrt{P_r}\hat{x}_1 h_{srd} + w_{rd}. \tag{3.62}$$

Finally, the destination detects x_1 symbols in the second phase based on the received signal y_{rd}.

3.5.2 Performance Analysis

3.5.2.1 Ergodic Capacity Analysis

The achievable rates for symbols at the relay in the first phase are given as [142]

$$
\begin{aligned}
R_{x_1}^{(sr)} &= \log_2\left(1 + SINR_{x_1}^{(sr)}\right), \\
R_{x_2}^{(sr)} &= \log_2\left(1 + SINR_{x_2}^{(sr)}\right),
\end{aligned}
\tag{3.63}
$$

and achievable rate of x_2 symbols at the destination in the first phase is given as

$$R_{x_2}^{(sd)} = \log_2\left(1 + SINR_{x_2}^{(sd)}\right), \tag{3.64}$$

where $SINR_{x_1}^{(sr)}$, $SINR_{x_2}^{(sr)}$ denote the SINRs of symbols at relay and defined as

$$
\begin{aligned}
SINR_{x_1}^{(sr)} &= \frac{\alpha_1 \rho_s |h_{sr}|^2}{\beta \alpha_2 \rho_s |h_{sr}|^2 + 1}, \\
SINR_{x_2}^{(sr)} &= \frac{\alpha_2 \rho_s |h_{sr}|^2}{\alpha_1 \rho_s |h_{sr}|^2 + 1},
\end{aligned}
\tag{3.65}
$$

where β is the imperfect SIC factor. The SINR of x_2 symbols at destination (i.e., $SINR_2^{(sd)}$) is defined as

$$SINR_{x_2}^{(sd)} = \frac{\alpha_2 \rho_s |h_{sd}|^2}{\alpha_1 \rho_s |h_{sd}|^2 + 1}. \tag{3.66}$$

On the other hand, in the second phase of communication, only the x_1 symbols are transmitted to the destination, the achievable rate of second phase is given

$$R_{x_1}^{(rd)} = \log_2\left(1 + SINR_1^{(rd)}\right),$$ (3.67)

where

$$SNR_{x_1}^{(rd)} = \frac{(1-\beta)\,\rho_r\,|h_{rd}|^2}{\beta\rho_r\,|h_{rd}|^2 + 1}.$$ (3.68)

where β exists since it is assumed that x_2 symbols may not be fully eliminated (imperfect SIC). Thus, the forwarded symbol x_1 includes x_2 symbol as IUI with β coefficient. Since the achievable rate of CRS is dominated by the weakest link [148], the achievable rates of symbols in NOMA-CRS are given as[6]

$$R_{x_1}^{(NCR)} = \frac{1}{2}\min\{R_1^{(sr)}, R_1^{(rd)}\},$$ (3.69)

and

$$R_{x_2}^{(NCR)} = \frac{1}{2}\min\{R_2^{(sr)}, R_2^{(sd)}\}.$$ (3.70)

Ergodic capacity for each symbol is obtained as

$$C_{x_1}^{(NCR)} = \int_0^\infty R_{x_1}^{(NCR)},$$ (3.71)

and

$$C_{x_2}^{(NCR)} = \int_0^\infty R_{x_1}^{(NCR)}.$$ (3.72)

Lastly, ergodic sum rate of NOMA-CRS is obtained as

$$C_{sum}^{(NOMA-CRS)} = C_{x_1} + C_{x_2}.$$ (3.73)

These analysis can be found in [142–144]. Thus, only simulations are provided for EC of NOMA-CRS.

---

[6]In equations, NCR is used to refer the NOMA-CRS.

3.5.2.2 Outage Probability Analysis

In NOMA-CRS, the OP of each symbol is defined as

$$P_{x_1}(out) = P(R_{x_1} < \acute{R}_{x_1}),$$
$$P_{x_2}(out) = P(R_{x_2} < \acute{R}_{x_2}),$$

$$(3.74)$$

where $\acute{R}_{x_1}$ and $\acute{R}_{x_2}$ are the target rates for x_1 and x_2 symbols, respectively. Finally with the law of probability the OP for NOMA-CRS is obtained as [144],

$$P^{(NCR)}(out) = P_{x_1}(out) + P_{x_2}(out) - P_{x_1}(out)P_{x_2}(out). \tag{3.75}$$

Since the OP of NOMA-CRS has been investigated for different conditions, only simulation results are provided.

3.5.2.3 Bit Error Probability (BEP) Analysis

In order to derive total BEP of NOMA-CRS, BEP for two symbols should be firstly derived and should be averaged. Since the x_2 symbols are conveyed to the destination only in the first phase, the BEP for x_2 symbols will be the same with BEP of far user in downlink NOMA. QPSK and BPSK are assumed to be used for the x_1 and x_2 symbols, respectively. Thus, by just adopting channel conditions in (2.23), the average BEP for x_2 symbols is derived as

$$P_{x_2}(e) = \frac{1}{4}\left[2 - \sqrt{\frac{\varepsilon_A\sigma_{sd}^2}{N_0 + \varepsilon_A\sigma_{sd}^2}} - \sqrt{\frac{\varepsilon_B\sigma_{sd}^2}{N_0 + \varepsilon_B\sigma_{sd}^2}}\right]. \tag{3.76}$$

where $\varepsilon_A \triangleq \left(\sqrt{\alpha_2 P_s} + \sqrt{\alpha_1 P_s/2}\right)^2$ and $\varepsilon_B \triangleq \left(\sqrt{\alpha_2 P_s} - \sqrt{\alpha_1 P_s/2}\right)^2$ are defined in Section 2.2.2.

On the other hand, x_1 symbols are firstly detected at the relay and the regenerated form of x_1 symbols are forwarded to the destination. Thus, with the law of total probability, the BEP for x_1 symbols is given as

$$P_{x_1}(e) = \left(1 - P_{x_1}^{(sr)}(e)\right)P_{x_1}^{(rd)}(e) + P_{x_1}^{(sr)}(e)\left(1 - P_{x_1}^{(rd)}(e)\right), \tag{3.77}$$

where $P_{x_1}^{(sr)}(e)$ and $P_{x_1}^{(rd)}(e)$ denote the BEP of x_1 symbols in the first phase and second phase, respectively. In the first phase, since superposition is applied at BS and the relay

implements SIC to detect x_1 symbols, the BEP of x_1 symbols is same with the BEP of near user in downlink NOMA. Thus, by adjusting the BEP given (2.31), the BEP of x_1 symbols in the first phase is derived as

$$P_{x_1}^{(sr)}(e) = \frac{1}{2}\left[1 - \sqrt{\frac{\varepsilon_C \sigma_{sr}^2}{N_0 + \varepsilon_C \sigma_{sr}^2}} + \frac{1}{4}\left\{\sqrt{\frac{\varepsilon_A \sigma_{sr}^2}{N_0 + \varepsilon_A \sigma_{sr}^2}} - \sqrt{\frac{\varepsilon_B \sigma_{sr}^2}{N_0 + \varepsilon_B \sigma_{sr}^2}}\right.\right.$$
$$\left.\left.- \sqrt{\frac{\varepsilon_D \sigma_{sr}^2}{N_0 + \varepsilon_D \sigma_{sr}^2}} + \sqrt{\frac{\varepsilon_E \sigma_{sr}^2}{N_0 + \varepsilon_E \sigma_{sr}^2}}\right\}\right], \tag{3.78}$$

where $\varepsilon_C \triangleq \alpha_1 P_s$, $\varepsilon_D \triangleq \left(2\sqrt{\alpha_2 P_s} + \sqrt{\alpha_1 P_s/2}\right)^2$ and $\varepsilon_E \triangleq \left(2\sqrt{\alpha_2 P_s} - \sqrt{\alpha_1 P_s/2}\right)^2$ are defined in Section 2.2.2. Then in the second phase, only the estimated $\hat{x}_1$ symbols are transmitted and detected at the destination. Since no interference exists in the second phase, the BEP of x_1 symbols in the second phase turns out to be well-known BEP over fading channels. It is given for BPSK over Rayleigh fading channels [90, 149] as

$$P_{x_1}^{(rd)} = \frac{1}{2}\left(1 - \sqrt{\frac{\rho_r \sigma_{rd}^2}{1 + \rho_r \sigma_{rd}^2}}\right). \tag{3.79}$$

Then substituting (3.78) and (3.79) into (3.77), the average BEP of x_1 symbols is derived as

$$P_{x_1}(e) = \frac{1}{2}\left[1 - \frac{1}{2}\left\{1 - \sqrt{\frac{\varepsilon_C \sigma_{sr}^2}{N_0 + \varepsilon_C \sigma_{sr}^2}} + \frac{1}{4}\left\{\sqrt{\frac{\varepsilon_A \sigma_{sr}^2}{N_0 + \varepsilon_A \sigma_{sr}^2}} - \sqrt{\frac{\varepsilon_B \sigma_{sr}^2}{N_0 + \varepsilon_B \sigma_{sr}^2}}\right.\right.\right.$$
$$\left.\left.\left.- \sqrt{\frac{\varepsilon_D \sigma_{sr}^2}{N_0 + \varepsilon_D \sigma_{sr}^2}} + \sqrt{\frac{\varepsilon_E \sigma_{sr}^2}{N_0 + \varepsilon_E \sigma_{sr}^2}}\right\}\right\}\right] \times \left(1 - \sqrt{\frac{\rho_r \sigma_{rd}^2}{1 + \rho_r \sigma_{rd}^2}}\right)$$
$$+ \left\{1 - \frac{1}{2}\left(1 - \sqrt{\frac{\rho_r \sigma_{rd}^2}{1 + \rho_r \sigma_{rd}^2}}\right)\right\} \times \left\{1 - \sqrt{\frac{\varepsilon_C \sigma_{sr}^2}{N_0 + \varepsilon_C \sigma_{sr}^2}} + \frac{1}{4}\left\{\sqrt{\frac{\varepsilon_A \sigma_{sr}^2}{N_0 + \varepsilon_A \sigma_{sr}^2}}\right.\right.$$
$$\left.\left.- \sqrt{\frac{\varepsilon_B \sigma_{sr}^2}{N_0 + \varepsilon_B \sigma_{sr}^2}} - \sqrt{\frac{\varepsilon_D \sigma_{sr}^2}{N_0 + \varepsilon_D \sigma_{sr}^2}} + \sqrt{\frac{\varepsilon_E \sigma_{sr}^2}{N_0 + \varepsilon_E \sigma_{sr}^2}}\right\}\right\} \tag{3.80}$$

Finally, the BEP of NOMA-CRS is obtained by

$$P^{(NCR)}(e) = \frac{P_{x_1}(e) + P_{x_1}(e)}{2}. \tag{3.81}$$

3.5.3 NOMA-based Diamond Relaying Network

In this section, NOMA-based Diamond Relaying Network (NOMA-DRN) proposed in [146] is introduced as a subset of NOMA-CRS.
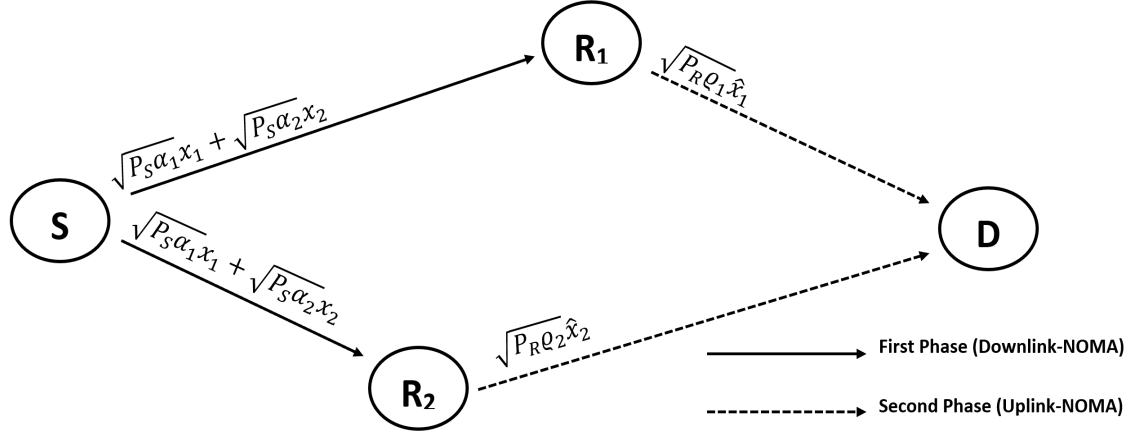
Figure 3.6: The illustration of NOMA-DRN

3.5.3.1 System Model

A NOMA-CRS is considered where two relays (i.e., R_k, $k = 1, 2$) are willing to help to source (S) for conveying symbols to the destination (D). Relays are located between source and destination and the distance of each relay to the source and to the destination differs as shown in Figure 3.6. Hence, the considered model is named as diamond relaying. All nodes are assumed to be equipped with single antenna and the direct link between source and destination does not exist because of large obstacles/path-loss. The fading channel coefficients between nodes follow $CN(0, \sigma_\lambda^2)$ i.e., $\lambda = SR_1, SR_2, R_1D, R_2D$ and since the diamond relaying is assumed, $d_{SR_1} > d_{SR_2}$ while $d_{R_1D} < d_{R_2D}$. Relays operate in half-duplex mode, hence the total communication is completed in two phase. In the first phase, source applies superposition coding for the following two symbols of destination and transmits them on the same resource block (downlink-NOMA). The received signal by the relays is given as

$$y_{sr_k} \sqrt{P_s} \left(\sqrt{\alpha_1} x_1 + \sqrt{\alpha_2} x_2 \right) h_{sr_k} + w_{sr_k}, \quad k = 1, 2, \tag{3.82}$$

where P_s is the transmit power of source. α_1 and α_2 are the power allocation coefficients for the base-band complex symbols x_1 and x_2, respectively. Likewise in conventional NOMA-CRS, x_1 and x_2 are the consecutive symbols of the destination which are intended to transmit in order. $\alpha_1 + \alpha_2 = 1$ and it is assumed[7] $\alpha_1 > \alpha_2$. w_{sr_k} is the AWGN with N_0 variance. In the second phase of communication, R_1 and R_2 forward the detected

---

[7]When two symbols are superimposed, although mostly $\alpha_2 > \alpha_1$ is assumed throughout this PhD dissertation, in this subsection reverse is assumed to make the system model as proposed in [146]

signals x_1 and x_2 to the destination, respectively (uplink-NOMA). It is noteworthy that, R_1 detects x_1 symbols by treating x_2 symbols as noise since $\alpha_1 > \alpha_2$. On the other hand, R_2 should firstly implement SIC to detect x_2 symbols. The received signal at the destination in the second phase is given as

$$y_d = \sqrt{P_r}\left(\sqrt{\varrho_1}\hat{x}_1 h_{r_1 d} + \sqrt{\varrho_2}\hat{x}_2 h_{r_2 d}\right) + w_d, \tag{3.83}$$

where P_r is the total power of relay and allocated[8] by ϱ_1 and ϱ_2 where $\varrho_1 + \varrho_2 = 1$. $\hat{x}_1$ and $\hat{x}_2$ are the detected/estimated symbols at the relays. Finally, the destination firstly detects x_1 symbols and subtracts it from total received signal (i.e., SIC) and detects x_2 symbols.

3.5.3.2 Performance Analysis

In this section, only BEP analysis for NOMA-DRN is provided unlike rest of thesis where three KPIs (BEP, outage and sum rate) are analyzed, since the considered system has been proposed in [146] and some initial analysis has been already provided. In addition, based on our investigations on NOMA-CRS, it is revealed that NOMA-DRN is a non-equiprobable communication and to point out that BEP analysis is provided. Since two independent symbols are transmitted to destination at the same time, end-to-end BEP of NOMA-DRN is given as

$$P^{(e2e)}(e) = \frac{P_{x_1}^{(e2e)}(e) + P_{x_2}^{(e2e)}(e)}{2}, \tag{3.84}$$

where $P_{x_1}^{(e2e)}(e)$ and $P_{x_2}^{(e2e)}(e)$ denote e2e BEP for x_1 and x_2 symbols, respectively. Since the total communication is completed in two phases, with the law of total probability, e2e BEP of each symbol is obtained by

$$\begin{aligned}
P_{x_1}^{(e2e)}(e) &= (1 - P_{x_1}^{(sr_1)}(e))P_{x_1}^{(r_1 d)}(e) + P_{x_1}^{(sr_1)}(e)(1 - P_{x_1}^{(r_1 d)}(e), \\
P_{x_2}^{(e2e)}(e) &= (1 - P_{x_2}^{(sr_2)}(e))P_{x_2}^{(r_2 d)}(e) + P_{x_2}^{(sr_2)}(e)(1 - P_{x_2}^{(r_2 d)}(e),
\end{aligned} \tag{3.85}$$

where $P_{x_k}^{(sr_k)}(e)$ and $P_{x_k}^{(r_k d)}(e)$, $k = 1, 2$ denote the BEP of x_k symbols in the first phase between $S - R_k$ and in the second phase between $R_k - D$, respectively. In order to derive e2e BEP of NOMA-DRN, BEP of each symbol during each phase should be firstly derived.

---

[8]Although the relay nodes could have independent power constraints, for the total power consumption such assumption is reasonable and has been made in existing studies of DRN [146] and uplink NOMA [38].
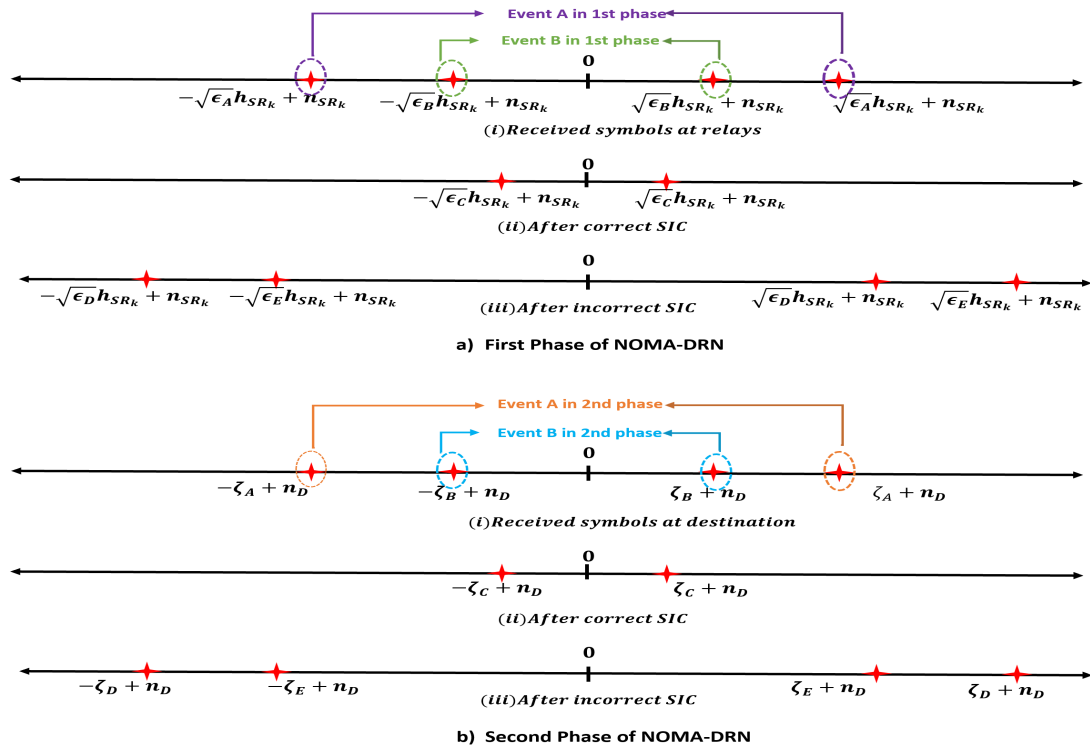
Figure 3.7: The received signal representations for NOMA-DRN

Based on the results of Chapter 2, it is known that error performance of a NOMA involved system is highly dependent to chosen modulation constellation. In this section, both symbols (x_1 and x_2) are assumed to be modulated by BPSK[9]. Since the two symbols are transmitted on the same resource block after superposition coding, the received signal at the relays is given[10] in Figure 3.7.a.*(i).* One can easily see that the received signals have different energy levels according to which x_1 and x_2 symbols are sent (i.e., events A or B). Thus, in error analysis, those two different cases with their priori probabilities should be also considered. In the first phase, relays receive superposition coded symbol as downlink-NOMA. Thus, the BEP at the relays can be obtained by repeating the steps of downlink NOMA considering the new total superposition coded symbol constellation (i.e, BPSK for both symbols as in Figure 3.7.a.*(i)*). Since the R_1 detects x_1 symbols by

---

[9]Although higher level modulation constellation can be considered, we think that this is reasonable assumption since the BEP analysis for cooperative relaying systems is provided for BPSK in almost all literature [97–102] In addition, with higher modulation constellation, the priori probabilities of non-equiprobable communication can be intractable and make the analysis very complex.

[10]For simplicity, the effects of channel fading and noise are not represented.

pretending x_2 symbols as noise, considering the BPSK ML decision rule and with the aid of (2.21)-(2.23), the BEP of x_1 symbols at R_1 is derived as

$$P_{x_1}^{(sr_1)}(e|_{h_{sr_1}}) = \sum_i p(i_{1st}) Q\left(\sqrt{2\epsilon_i \gamma_{sr_1}}\right), \tag{3.86}$$

where $\gamma_{sr_1} \triangleq |h_{sr_1}|^2$ and by averaging over instantaneous channel fading, the average BEP is derived as

$$P_{x_1}^{(sr_1)}(e) = \sum_i p(i_{1st})\left(0.5\left(1 - \sqrt{\frac{\epsilon_i \sigma_{sr_1}^2}{N_0 + \epsilon_i \sigma_{sr_1}^2}}\right)\right), \quad i = A, B, \tag{3.87}$$

where $p(i_{1st})$ $i = A, B$ denotes the priori probability of event i may occur in the first phase which is to be 0.5 since it is mostly assumed that x_1 and x_2 have different symbols with equal probability in communication systems. $\epsilon_A = \left(\sqrt{\alpha_1 P_s} + \sqrt{\alpha_2 P_s}\right)^2$, $\epsilon_B = \left(\sqrt{\alpha_1 P_s} - \sqrt{\alpha_2 P_s}\right)^2$ are defined based on the superposition coded symbols.

On the other hand, R_2 detects x_2 symbols by implementing SIC. Thus, the correct SIC and erroneous SIC cases likewise near user in downlink NOMA should be considered. By taking account of correct detection of x_1 symbols at R_2 and subtracting them from received symbol, with the aid of (2.24)-(2.26), the BEP of x_2 symbols at R_2 under correct SIC (see Figure 3.7.a(ii)) is given as

$$P_{x_2}^{(sr_2)}(e|_{h_{SR_2} \cap correct_{x_1}}) = p(A_{1st})\left(Q\left(\sqrt{2\epsilon_C \gamma_{sr_2}}\right) - Q\left(\sqrt{2\epsilon_A \gamma_{sr_2}}\right)\right) + p(B_{1st})Q\left(\sqrt{2\epsilon_C \gamma_{sr_2}}\right). \tag{3.88}$$

Then, considering the erroneous SIC case, the BEP of x_2 symbols at R_2 under erroneous SIC (see Figure 3.6.a(iii)) is derived as by following steps (2.27)-(2.29),

$$P_{x_2}^{(sr_2)}(e|_{h_{sr_2} \cap error_{x_1}}) = p(A_{1st})Q\left(\sqrt{2\epsilon_D \gamma_{sr_2}}\right) + p(B_{1st})\left(Q\left(\sqrt{2\epsilon_B \gamma_{sr_2}}\right) - Q\left(\sqrt{2\epsilon_E \gamma_{sr_2}}\right)\right), \tag{3.89}$$

$\epsilon_C = \alpha_2 P_s$, $\epsilon_D = \left(2\sqrt{\alpha_1 P_s} + \sqrt{\alpha_2 P_s}\right)^2$ and $\epsilon_E = \left(2\sqrt{\alpha_1 P_s} - \sqrt{\alpha_2 P_s}\right)^2$ are defined. By summing two cases and by averaging over instantaneous channel fading, the total BEP of x_2 symbol at R_2 is derived as

$$P_{x_2}^{(sr_2)}(e) = 0.5\left(1 - \sqrt{\frac{\epsilon_C \sigma_{sr_2}^2}{N_0 + \epsilon_C \sigma_{sr_2}^2}}\right) + \frac{p(A_{1st})}{2}\left(\sqrt{\frac{\epsilon_A \sigma_{sr_2}^2}{N_0 + \epsilon_A \sigma_{sr_2}^2}} - \sqrt{\frac{\epsilon_D \sigma_{sr_2}^2}{N_0 + \epsilon_D \sigma_{sr_2}^2}}\right)$$
$$+ \frac{p(A_{1st})}{2}\left(-\sqrt{\frac{\epsilon_B \sigma_{sr_2}^2}{N_0 + \epsilon_B \sigma_{sr_2}^2}} + \sqrt{\frac{\epsilon_E \sigma_{sr_2}^2}{N_0 + \epsilon_E \sigma_{sr_2}^2}}\right). \tag{3.90}$$

In the second phase of communication, relays forward estimated/detected symbols (i.e., $\hat{x}_1$ and $\hat{x}_2$) on the same resource block. The received signal at destination becomes a superimposed signal from different sources/users likewise in uplink-NOMA. Thus, in order to derive BEP of second phase, the steps in uplink-NOMA (Section 2.3.2) can be repeated. Total received signal at destination is given in Figure 3.7.b(i). x_1 symbols are detected at the destination by treating x_2 symbols as noise. Considering the BPSK decision rule, with the aid of steps (2.52)-(2.54), the BEP of x_1 symbols in the second phase is derived as

$$P_{x_1}^{(r_1 d)}(e|_{\zeta_i}) = \sum_i p(i_{2nd}) Q\left(\sqrt{2}\zeta_i\right) \quad i = A, B, \tag{3.91}$$

where $\zeta_A = \left(\sqrt{\varrho_1 P_r}|h_{r_1 d}| + \sqrt{\varrho_2 P_r}|h_{r_2 d}|\right)/\sqrt{N_0}$ and $\zeta_B = \left(\sqrt{\varrho_1 P_r}|h_{r_1 d}| - \sqrt{\varrho_2 P_r}|h_{r_2 d}|\right)/\sqrt{N_0}$.

On the other hand, the BEP of x_2 symbols should be handled for two cases: correct SIC (see Figure 3.7.b(ii)) and erroneous SIC (see Figure 3.7.a(iii)). By considering the correct/erroneous probability of x_1 symbols at destination and BPSK decision rule, the BEP of x_2 symbols in the second phase under correct SIC with the aid of steps (2.58)-(2.59)

$$P_{x_2}^{(r_2 d)}(e|_{\zeta_i \cap correct_{x_1}}) = p(A_{2nd})\left(Q\left(\sqrt{2}\zeta_C\right) - Q\left(\sqrt{2}\zeta_A\right)\right) + p(B_{2nd})Q\left(\sqrt{2}\zeta_C\right), \tag{3.92}$$

under erroneous SIC with the aid of steps (2.60)-(2.61)

$$P_{x_2}^{(r_2 d)}(e|_{\zeta_i \cap error_{x_1}}) = p(A_{2nd})Q\left(\sqrt{2}\zeta_D\right) + p(B_{2nd})\left(Q\left(\sqrt{2}\zeta_B\right) - Q\left(\sqrt{2}\zeta_E\right)\right), \tag{3.93}$$

where $\zeta_C = \sqrt{\varrho_2 P_r/N_0}|h_{r_2 d}|$, $\zeta_D = \left(2\sqrt{\varrho_1 P_r}|h_{r_1 d}| + \sqrt{\varrho_2 P_r}|h_{r_2 d}|\right)/\sqrt{N_0}$ and $\zeta_E = \left(2\sqrt{\varrho_1 P_r}|h_{r_1 d}| - \sqrt{\varrho_2 P_r}|h_{r_2 d}|\right)/\sqrt{N_0}$. Then, by summing two cases the BEP of x_2 symbols in the second phase is obtained as

$$\begin{aligned} P_{x_2}^{(r_2 d)}(e) = & Q\left(\sqrt{2}\zeta_C\right) + p(A_{2nd})\left(-Q\left(\sqrt{2}\zeta_A\right) + Q\left(\sqrt{2}\zeta_D\right)\right) \\ & + p(B_{2nd})\left(Q\left(\sqrt{2}\zeta_B\right) - Q\left(\sqrt{2}\zeta_E\right)\right). \end{aligned} \tag{3.94}$$

In the BEP analysis of uplink NOMA (Section 2.3.2.3), some assumptions/approximations have been provided to derive closed-form expressions. Since, to the best of our knowledge, eq. (3.94) cannot be derived in the closed-form, with the aid of Corollary 2.1, the term $Q\left(\sqrt{2}\zeta_A\right)$ in (3.91) and (3.94) and the term $Q\left(\sqrt{2}\zeta_D\right)$ in (3.94) can be neglected. Then, with the aid of provided approximation in Lemma 2.1, the approximated BEPs in the second phase become as

$$P_{x_1}^{(r_1 d)}(e) \approx p(B_{2nd})\frac{\varrho_2 P_r \sigma_{r_2 d}^2}{\varrho_1 P_r \sigma_{r_1 d}^2 + \varrho_2 P_r \sigma_{r_2 d}^2}, \tag{3.95}$$

and

$$P_{x_2}^{(r_2 d)}(e) \approx$$
$$0.5\left(1 - \sqrt{\frac{\varrho_2 P_r \sigma_{r_2 d}^2}{1 + \varrho_2 P_r \sigma_{r_2 d}^2}}\right) + p(B_{2nd})\left(\frac{\varrho_2 P_r \sigma_{r_2 d}^2}{\varrho_1 P_r \sigma_{r_1 d}^2 + \varrho_2 P_r \sigma_{r_2 d}^2} - \frac{\varrho_2 P_r \sigma_{r_2 d}^2}{4\varrho_1 P_r \sigma_{r_1 d}^2 + \varrho_2 P_r \sigma_{r_2 d}^2}\right). \tag{3.96}$$

Corollary 3.1. *Based on the exact and approximated analysis, one can easily see that the priori probabilities of the superimposed symbols in the second phase have dominant effect on the error performance. Hence, the priori probabilities should be derived.*

Lemma 3.1. *It is mostly expected that the priori probabilities of events A and B have equal probability in the first phase. However, in the second phase of communication $p(A_{2nd}) \geq p(B_{2nd})$ even if $p(A_{1st}) = p(B_{1st})$ in the first phase. In particular in the low SNR regime, hence the error performance of second phase is dominated by the symbols which belong to event A or B. These priori probabilities are provided for two different channel realizations and power allocations in Table 3.3.*

Table 3.3: Priori probabilities of the non-equiprobable communication in the second phase

	$\alpha_1 = 0.8$, $\sigma_{sr_1}^2 = 1$, $\sigma_{sr_2}^2 = 2$				$\alpha_1 = 0.7$, $\sigma_{sr_1}^2 = 2$, $\sigma_{sr_2}^2 = 10$			
	$SNR = P_s/N_0 (dB)$				$SNR = P_s/N_0 (dB)$			
	0	5	10	15	0	5	10	15
$p(A_{2nd})$	0.6021	0.5949	0.5559	0.5223	0.6415	0.6100	0.5588	0.5237

Proof. Let consider the probability of the event A may occur in the second phase of communication. One can easily see that this event depends on the detections on the relays and the priori probability of events in the first phase. Firstly, it is assumed that the event A has already occurred in the first phase. In this case, the event A occurs in the second phase only if both relays detect correctly or erroneously their related symbols $(R_1 \rightarrow x_1$ and $R_2 \rightarrow x_2)$ at the same time, and the conditional probability is given as

$$p(A_{2nd}|A_{1st}) = (1 - P_{x_1}^{(sr_1)}(e|A_{1st}))(1 - P_{x_2}^{(sr_2)}(e|A_{1st})) + P_{x_1}^{(sr_1)}(e|A_{1st})P_{x_2}^{(sr_2)}(e|A_{1st}), \quad (3.97)$$

On the other hand, if B occurs in the first phase, the event A occurs in the second phase only if one of the relays detects erroneously the related symbols. It is given as

$$p(A_{2nd}|B_{1st}) = P_{x_1}^{(SR_1)}(e|B_{1st})(1 - P_{x_2}^{(SR_2)}(e|B_{1st})) + (1 - P_{x_1}^{(SR_1)}(e|B_{1st}))P_{x_2}^{(SR_2)}(e|B_{1st}),$$
$$(3.98)$$

where conditional probabilities denote the error probability when the related condition event occurred. Total probability is given as

$$p(A_{2nd}) = p(A_{1st})p(A_{2nd}|A_{1st}) + p(B_{1st})p(A_{2nd}|B_{1st}), \quad (3.99)$$

and with the aid of total probability law

$$p(B_{2nd}) = 1 - p(A_{2nd}). \quad (3.100)$$

Substituting related expressions from (3.86) and (2.39) into (3.99) and (3.100), the priori probabilities are derived and so the proof is completed. □

3.6 NUMERICAL RESULTS

In this section, validations of the derived expressions are provided for all three concepts of the interplay between NOMA and cooperative communications. Firstly, validations of derived EC, OP and BEP expressions are provided for C-NOMA and TBS-C-NOMA. Extended simulations for C-NOMA and TBS-C-NOMA are presented in Chapter 5 to compare conventional NOMA networks. Then, validations for derived expressions and extended simulations are presented for both relay-assisted-NOMA and NOMA-CRS schemes in this section.
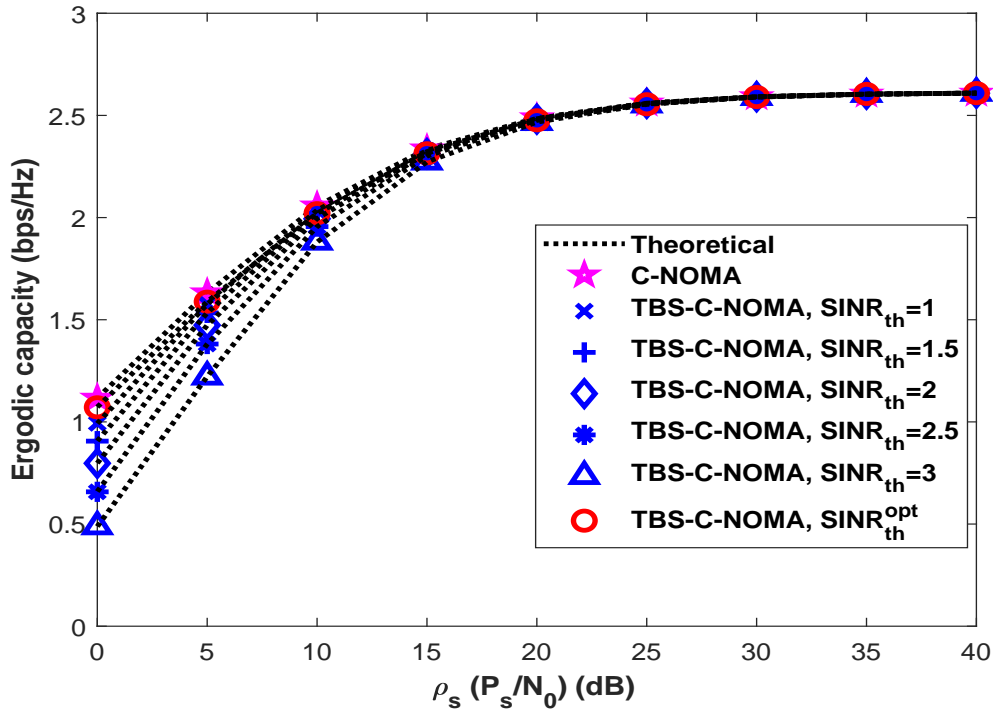
Figure 3.8: Ergodic capacity of C-NOMA and TBS-C-NOMA when $\alpha_1 = 0.2$, $\alpha_2 = 0.8$

Cooperative-NOMA networks: Theoretical curves and simulations of EC for C-NOMA and TBS-NOMA[11] are presented when $\sigma_{s1}^2 = 10dB$, $\sigma_{s2}^2 = 0dB$ and $\sigma_r^2 = 10dB$ and it is also assumed $P_r = P_s/2$. The power allocation coefficients are assumed to be $\alpha_1 = 0.2, \alpha_2 = 0.8$ and $\alpha_1 = 0.1, \alpha_2 = 0.9$ in Figure 3.8 and Figure 3.9, respectively. The results of TBS-C-NOMA are given for five different fixed-threshold values $SINR_{th} = 1, 1.5, 2, 2.5, 3$ and $SINR_{th} = 2, 4, 6, 7, 8$ for figures, respectively. The results of TBS-C-NOMA are also presented for the derived optimum threshold value given in Section 3.3.3.2. One can easily see that, introducing threshold values causes relay to be silent in some cases, hence the achievable rate may decrease since only direct link remains. Nevertheless, with the use of optimum threshold, the same ergodic capacity performance with C-NOMA is obtained.

Then, the outage performance of both C-NOMA and TBS-C-NOMA are provided for the

---

[11] C-NOMA and TBS-C-NOMA are proposed to enhance performance of UE_2 in donwlink NOMA networks. Hence, the analytical deductions and simulations of C-NOMA and TBS-C-NOMA are provided only for UE_2. Results of UE_1 are not presented since they will be same with conventional downlink NOMA networks.
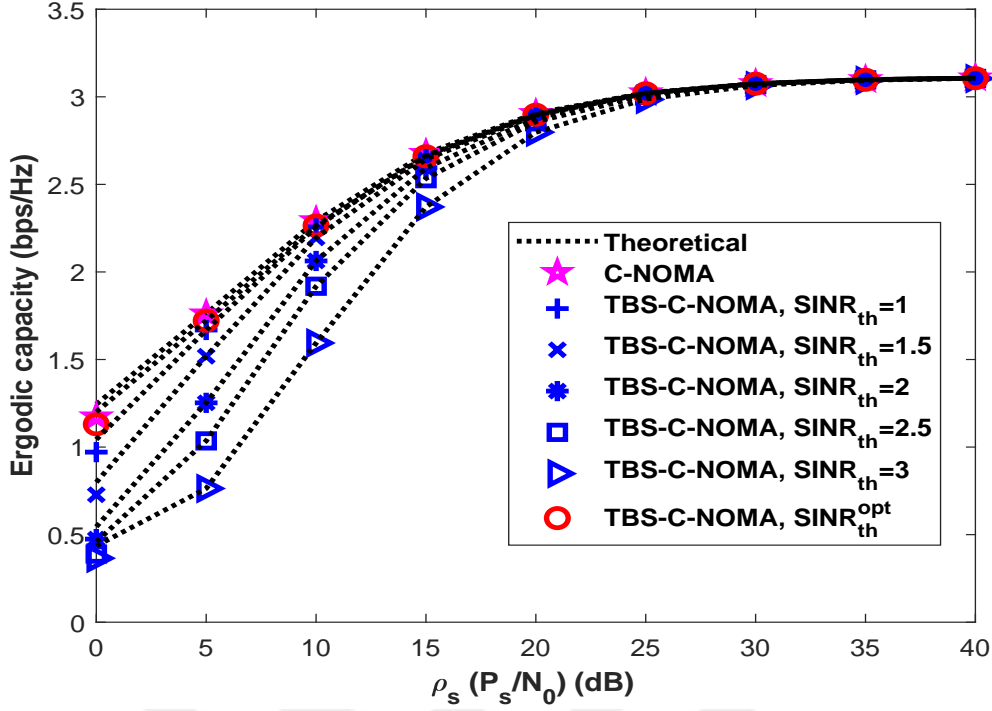
Figure 3.9: Ergodic capacity of C-NOMA and TBS-C-NOMA when $\alpha_1 = 0.1$, $\alpha_2 = 0.9$

same conditions in Figure 3.10 and Figure 3.11.

The error performances of C-NOMA and TBS-C-NOMA are evaluated for all six modes given in Table 3.1 in Figure 3.12 and Figure 3.13, respectively. The channel conditions are assumed to be same as in EC and OP results. The power allocation coefficient pairs are chosen as $\alpha_1 = 0.2$, $\alpha_2 = 0.8$ and the threshold value for TBS-C-NOMA is assumed to be $SINR_{th} = 2$. One can see that derived expressions match perfectly with simulations for both C-NOMA and TBS-C-NOMA. As seen from Figure 3.12, C-NOMA cannot achieve full diversity order (i.e., 2) although cooperative communication is applied. This is caused by the error propagation from UE_1 to UE_2. This can be resolved by TBS-C-NOMA as seen in Figure 3.13. Nevertheless, TBS-C-NOMA is also affected by error propagation in high SNR regime and the diversity order can not be achieved by fixed-threshold value. Thus, comparison of C-NOMA and TBS-C-NOMA are provided also with different threshold values in Figure 3.14. The channel conditions are assumed to be same with previous figures. As constellations mode 3 is chosen (i.e., QPSK and BPSK). One can easily see that TBS-C-NOMA with optimum threshold outperforms all fixed
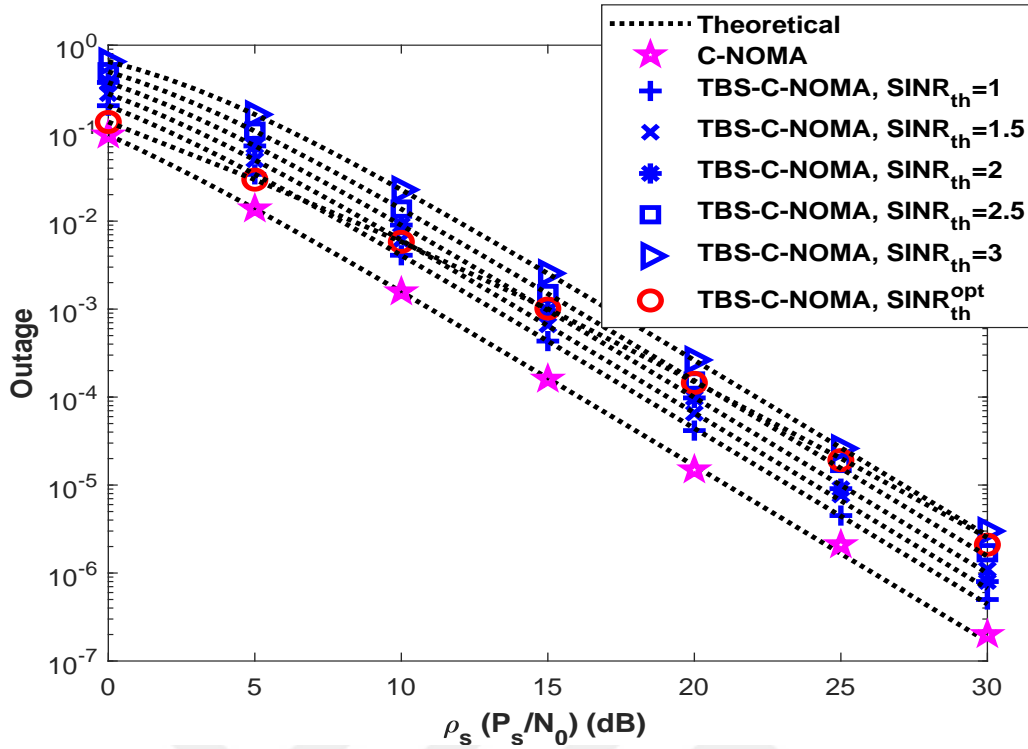
Figure 3.10: Outage performances of C-NOMA and TBS-C-NOMA when $\alpha_1 = 0.2$, $\alpha_2 = 0.8$ and $\acute{R}_{CN} = \acute{R}_{SCN} = 0.5 BPCU$
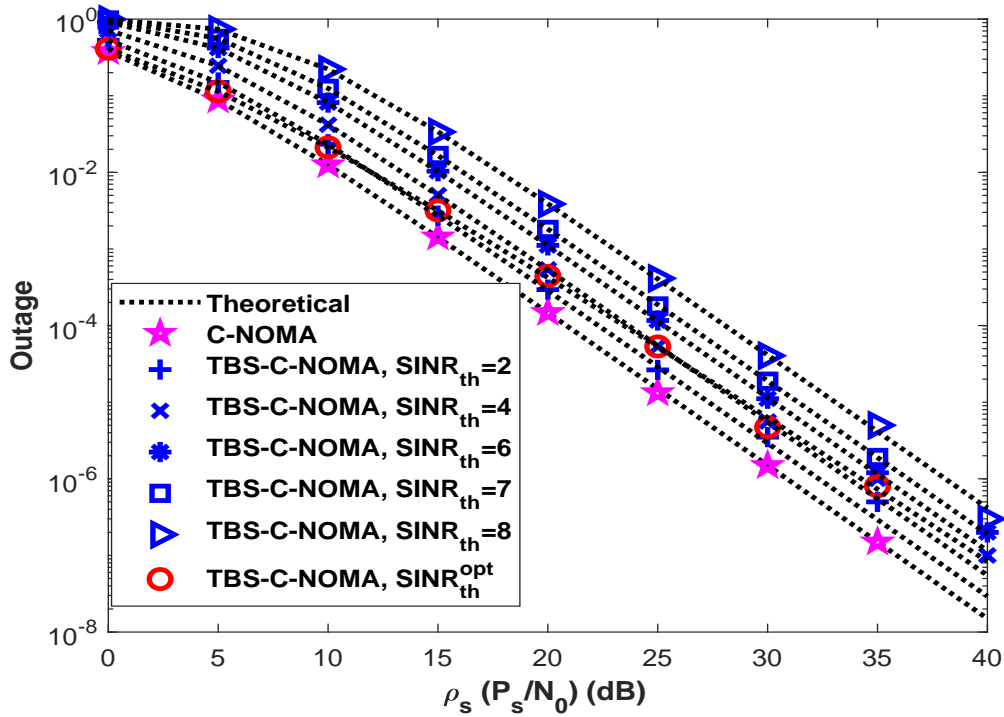
Figure 3.11: Outage performances of C-NOMA and TBS-C-NOMA when $\alpha_1 = 0.1$, $\alpha_2 = 0.9$ and $\acute{R}_{CN} = \acute{R}_{SCN} = 1 BPCU$
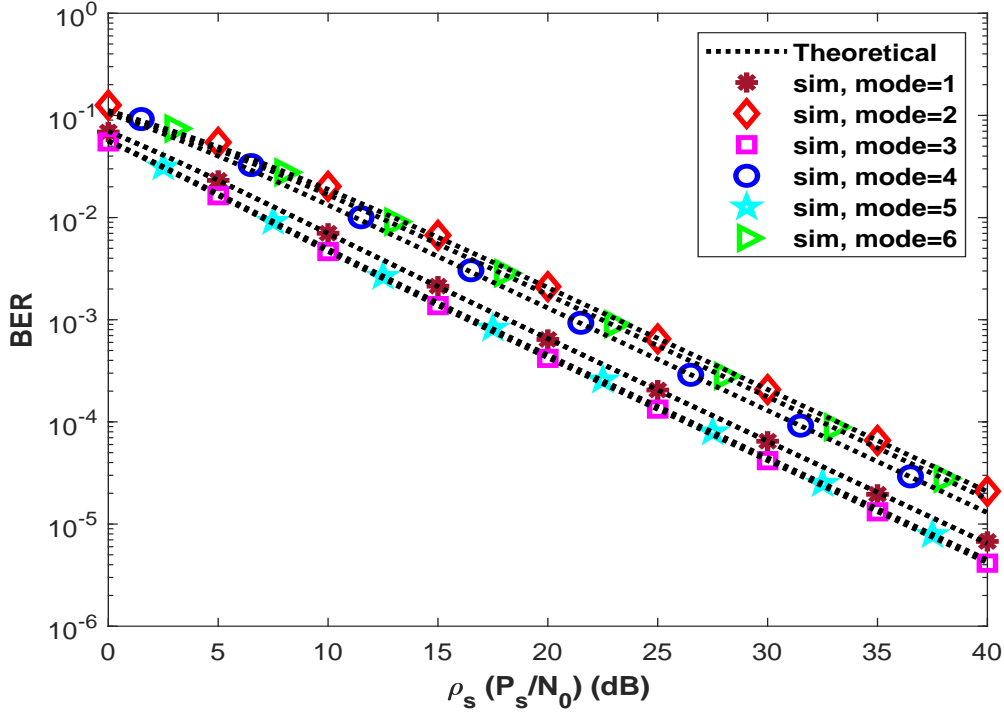
Figure 3.12: Error performance of C-NOMA when $\alpha_1 = 0.2$, $\alpha_2 = 0.8$

values in all SNR regime and provides full diversity order.

Relay-assisted-NOMA networks: As the second concept, numerical results for relay-assisted-NOMA networks are provided and derived BER expressions are validated via simulations. In this section, $\alpha_2 > \alpha_1$ is firstly assumed as defined in the system model -conventional relay-assisted-NOMA- and $\alpha_2 = \varrho_2$ is assumed. Error performances of users are provided for different channel conditions. In Figure 3.15, BER performances are provided when $\sigma_{sr}^2 = 3dB$, $\sigma_{r1}^2 = 3dB$, $\sigma_{r2}^2 = 0dB$ and $P_r = {}^{P_s}/2$. As expected, with the change of power allocations error performances of users change inversely.

Then, the effect of relay power on the error performances of users is investigated in Figure 3.16. The conditions are assumed to be same with previous Figure 3.15 and the power allocations are $\alpha_2 = \varrho_2 = 0.3$. As seen from Figure 3.16, relay power has the main role on the error performances since there is no direct link between BS and users.

Numerical results for the error performances of users for different σ_{sr}^2 are given in Figure
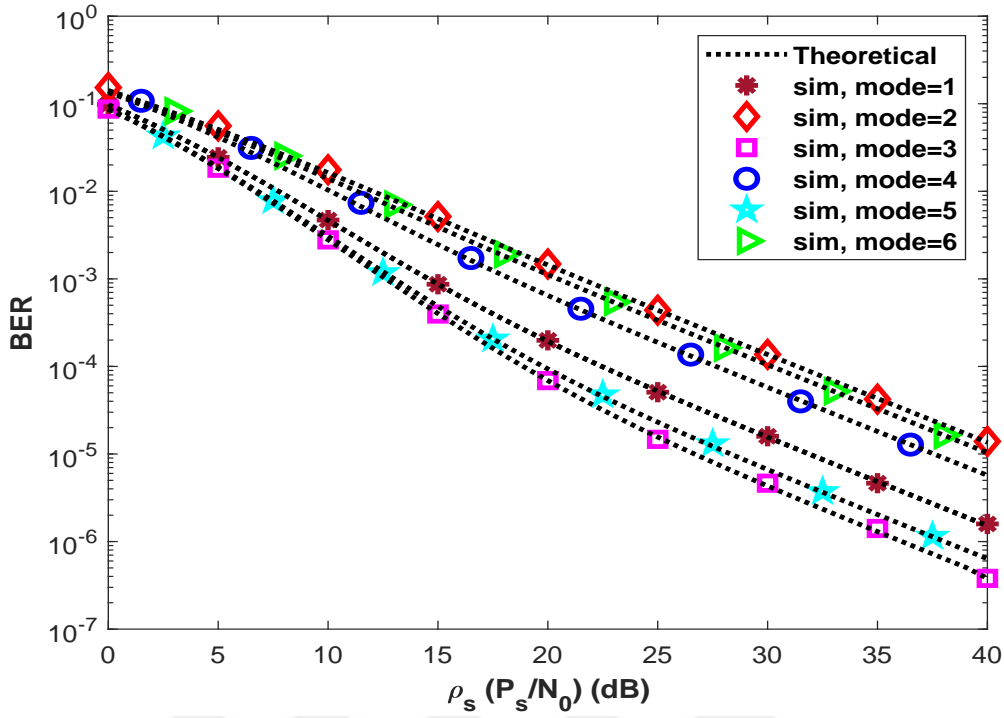
Figure 3.13: Error performance of TBS-C-NOMA when $\alpha_1 = 0.2$, $\alpha_2 = 0.8$ and $SINR_{th} = 2$
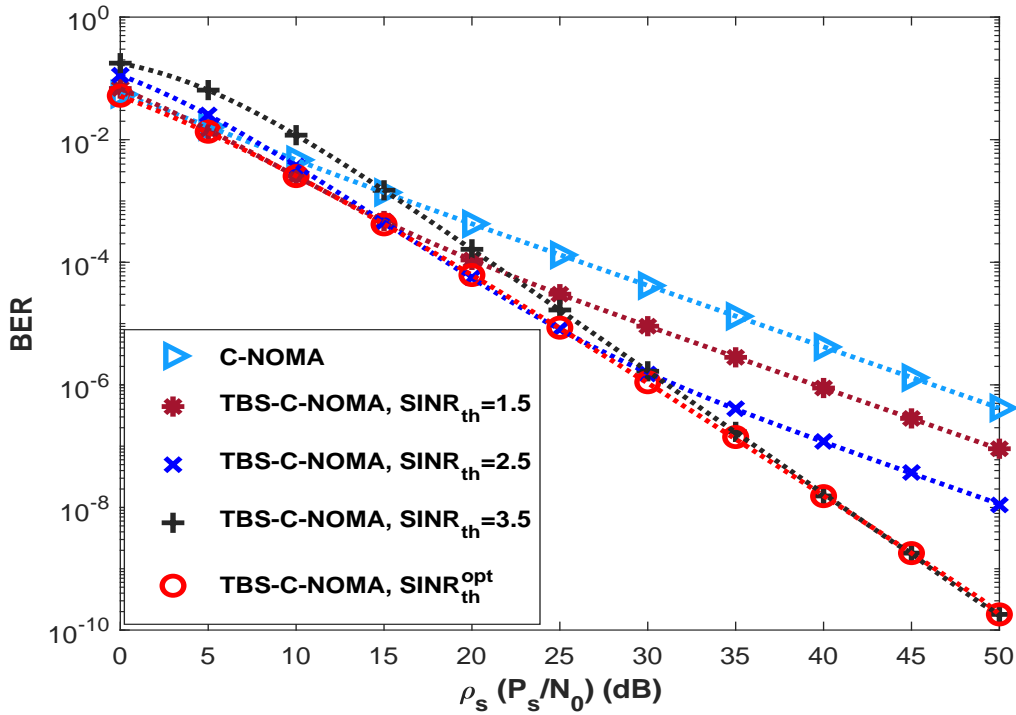
Figure 3.14: Error performance comparison between C-NOMA and TBS-C-NOMA with different threshold values when $\alpha_1 = 0.2$, $\alpha_2 = 0.8$
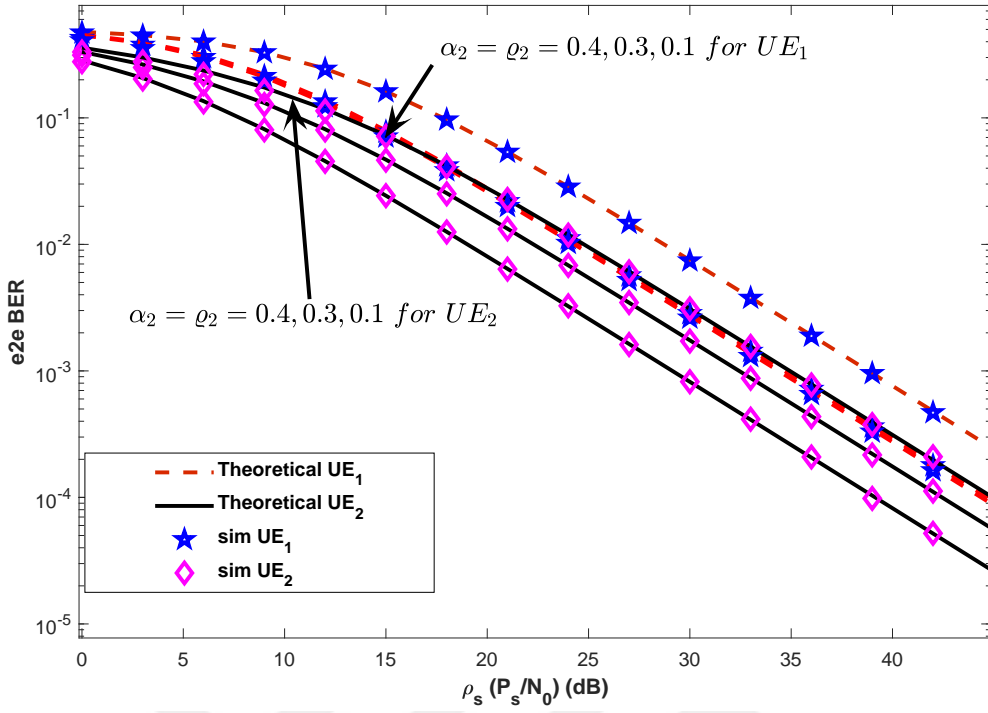
Figure 3.15: Error performance of relay-assisted-NOMA when $\sigma_{sr}^2 = 3dB$, $\sigma_{r1}^2 = 3dB$, $\sigma_{r2}^2 = 0dB$ and $P_r = {}^{P_s}/_2$
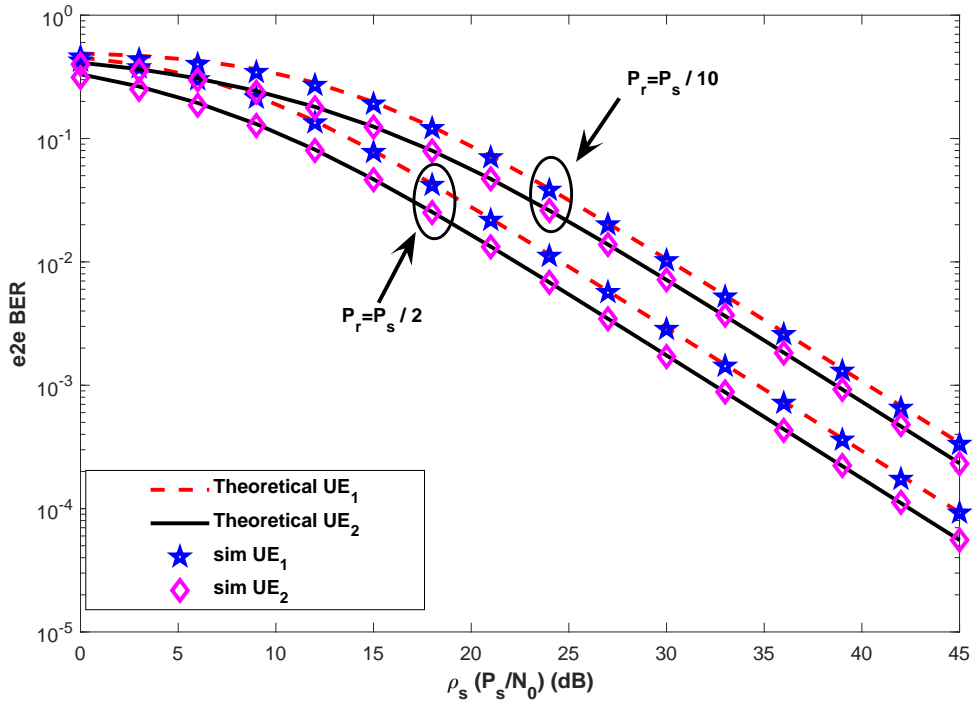
Figure 3.16: Error performance of relay-assisted-NOMA when $\sigma_{sr}^2 = 3dB$, $\sigma_{r1}^2 = 3dB$, $\sigma_{r2}^2 = 0dB$ and $\alpha_2 = \varrho_2 = 0.3$
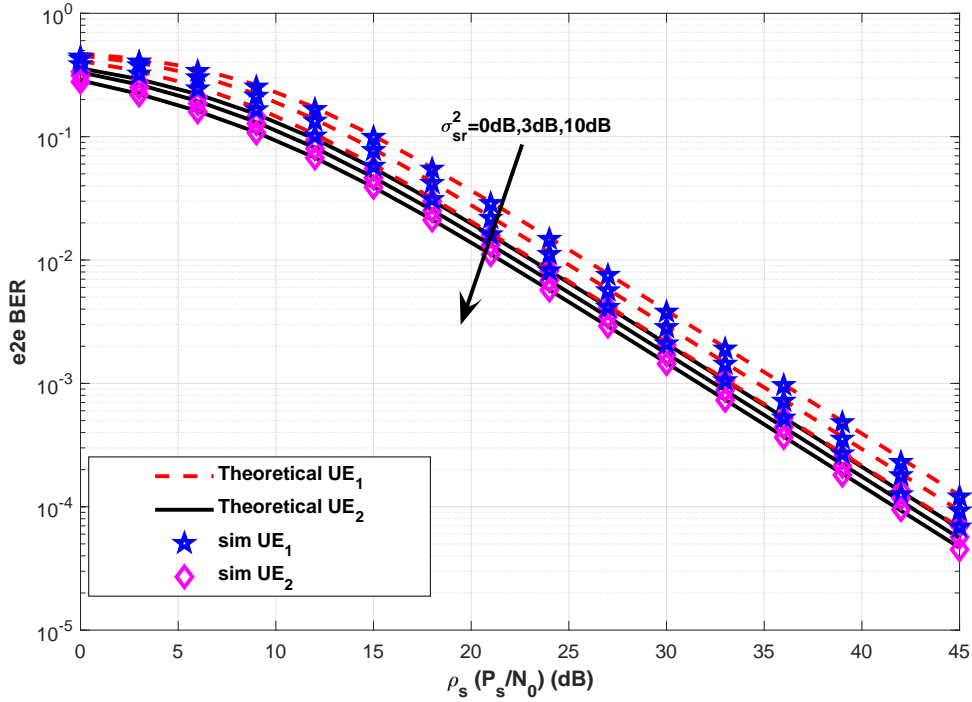
Figure 3.17: Error performance of relay-assisted-NOMA when $\sigma_{r1}^2 = 3dB$, $\sigma_{r2}^2 = 0dB$, $\alpha_2 = \varrho_2 = 0.3$ and $P_r = {}^{P_s}\!/\!_2$

3.17. Since both users' symbols are detected at relay and then forwarded, increase in channel quality between source and relay provides performance gain for both users. In Figure 3.17, $\sigma_{r1}^2 = 3dB$, $\sigma_{r2}^2 = 0dB$, $\alpha_2 = \varrho_2 = 0.3$ and $P_r = {}^{P_s}\!/\!_2$ are assumed.

The performances of reversed relay-assisted-NOMA are investigated when power allocation at the BS is reversed (i.e., $\alpha_1 > \alpha_2$).

In the given above results, one can easily see that derived BEP expressions match perfectly with simulations. Nevertheless, it is hereby noteworthy that relay-assisted-NOMA networks can be applied in reverse by changing power allocations at the source -detecting order at relay-. The performances of reversed relay-assisted-NOMA are investigated when power allocation at the BS is reversed (i.e., $\alpha_1 > \alpha_2$). In the following simulations, performances of both considered relay-assisted-networks: conventional ($\alpha_2 > \alpha_1$) and reversed ($\alpha_1 > \alpha_2$) are investigated. Then, the optimum power allocation pairs for both scenarios is discussed under EC, OP and BER constraints. Firstly in Figure 3.18, EC comparison between conventional and reversed relay-assisted-NOMA networks are provided when
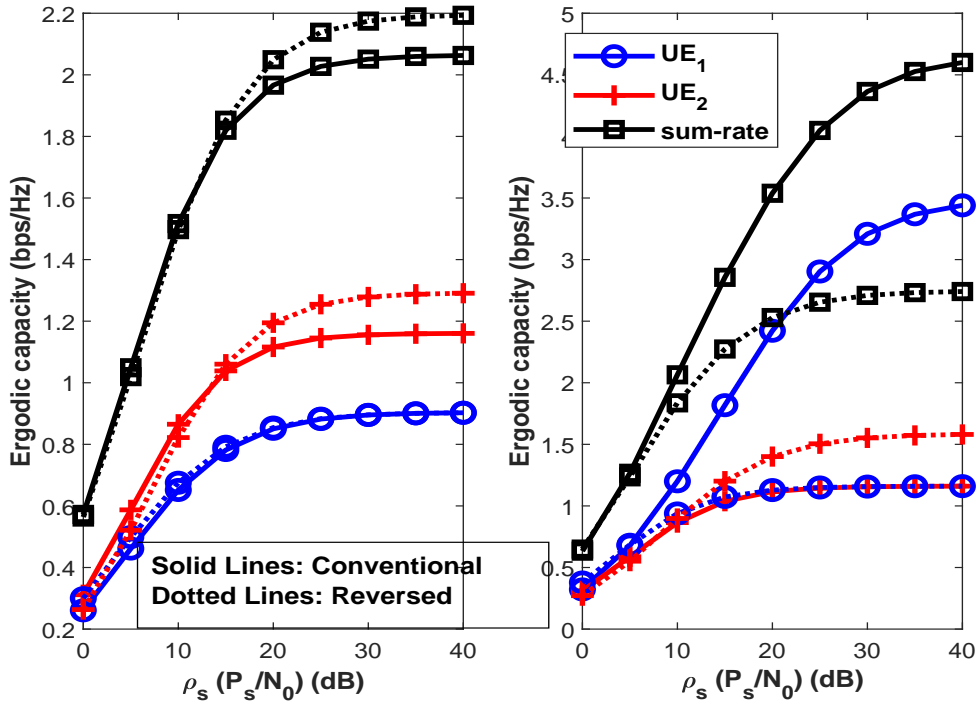
Figure 3.18: Ergodic rate comparison between conventional and reversed relay-assisted-NOMA a) $\beta = 0.05$ b)$\beta = 0.001$

$\sigma_{sr}^2 = 10dB$, $\sigma_{r1}^2 = 10dB$, $\sigma_{r2}^2 = 0dB$ and $\alpha_2 = \varrho_2 = 0.8$ for conventional relay-assisted-NOMA -in reversed network, complementary of α_2 is used (i.e., $\alpha_1 = \varrho_2 = 0.8$)-. It is clear that when the imperfect SIC factor gets higher, reversed scheme provides better individual rates and sum-rate.

Then, for the same conditions, outage performance comparison between conventional and reversed relay-assisted-NOMA networks is provided in Figure 3.19. For both imperfect SIC factor (β), reversed network offers better outage performance for UE_1. On the other hand, UE_2 has almost the same outage performance in both networks.

BER comparisons are provided for conventional and reversed relay-assisted-NOMA networks in Figure 3.20. The channel conditions and power allocation pairs are assumed to be same within the figures EC and outage comparisons. One can easily see from Figure 3.20 that reversed network provides better BER performance.
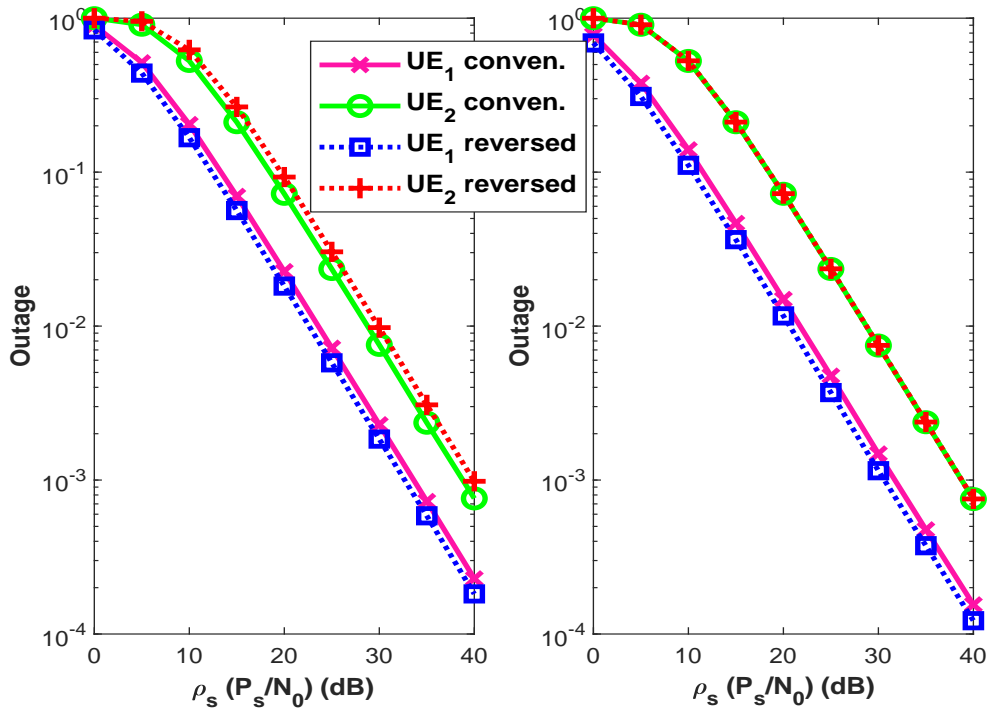
Figure 3.19: Outage performance comparison between conventional and reversed relay-assisted-NOMA when $\acute{R}_1 = 0.5$ and $\acute{R}_2 = 1$ a) $\beta = 0.05$ b)$\beta = 0.001$
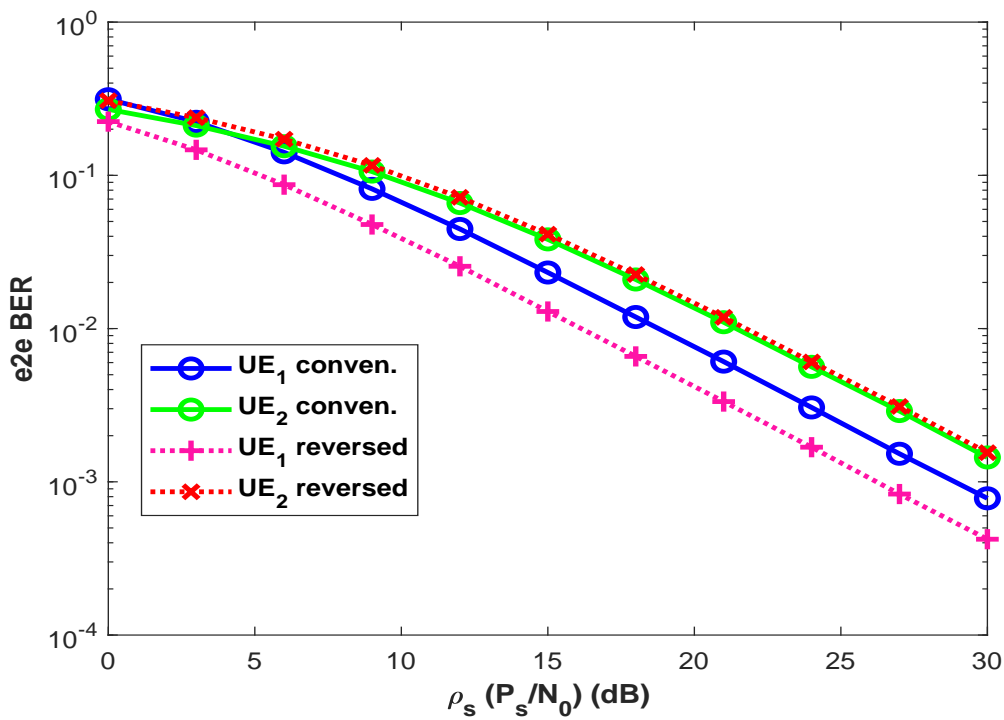
Figure 3.20: Error performance comparison between conventional and reversed relay-assisted-NOMA

Figure 3.21: Optimum power allocation pairs for relay-assisted-NOMA under maximum EC constraint when $\rho_s = 20dB$ and $\beta = 0.05$ a) conventional network b) reversed network

In addition, the effect of power allocation pairs is investigated for both conventional and reversed relay-assisted-NOMA under different constraints. Firstly, EC maximization is considered, hence sum-rates of networks are provided with the change of power allocation pairs in Figure 3.21 when $\sigma_{sr}^2 = 10dB$, $\sigma_{r1}^2 = 10dB$, $\sigma_{r2}^2 = 0dB$, $\rho_s = 20dB$ and $\beta = 0.05$. In this case, one can see that conventional network achieves maximum sum rate when $\alpha_1 \sim 0.3$ and $\varrho_1 \sim 0.45$ whereas reversed network achieves its maximum sum rate $\alpha_1 \sim 0.55$ and $\varrho_1 \sim 0.1$.

For the same conditions, outage comparisons of the users are provided with the change of power allocation coefficients in Figure 3.22 and Figure 3.23, respectively. In Figure 3.22, in terms of the outage of UE_1 when $\acute{R}_1 = 0.5BPCU$, the optimum power allocation pairs are $\alpha_1 \sim 0.45$, $\varrho_1 \sim 0.45$ and $\alpha_1 \sim 0.9$, $\varrho_1 \sim 0.45$ for conventional and reversed networks, respectively. In Figure 3.23, in terms of the outage of UE_2 when $\acute{R}_2 = 1BPCU$, optimum power allocation pairs are seen as $\alpha_1 \sim 0.05$, $\varrho_1 \sim 0.05$ and $\alpha_1 \sim 0.55$, $\varrho_1 \sim 0.05$ for conventional and reversed networks, respectively.
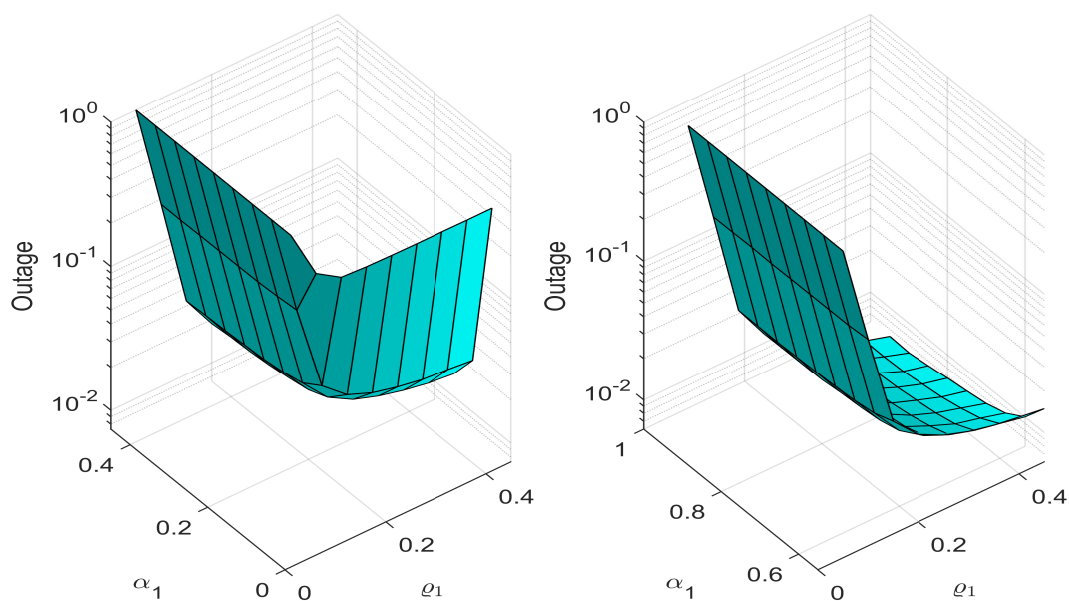
Figure 3.22: Optimum power allocation pairs for relay-assisted-NOMA under minimum OP of UE_1 constraint when $\rho_s = 20dB$, $\beta = 0.05$ and $\acute{R}_1 = 0.5BPCU$ a) conventional network b) reversed network
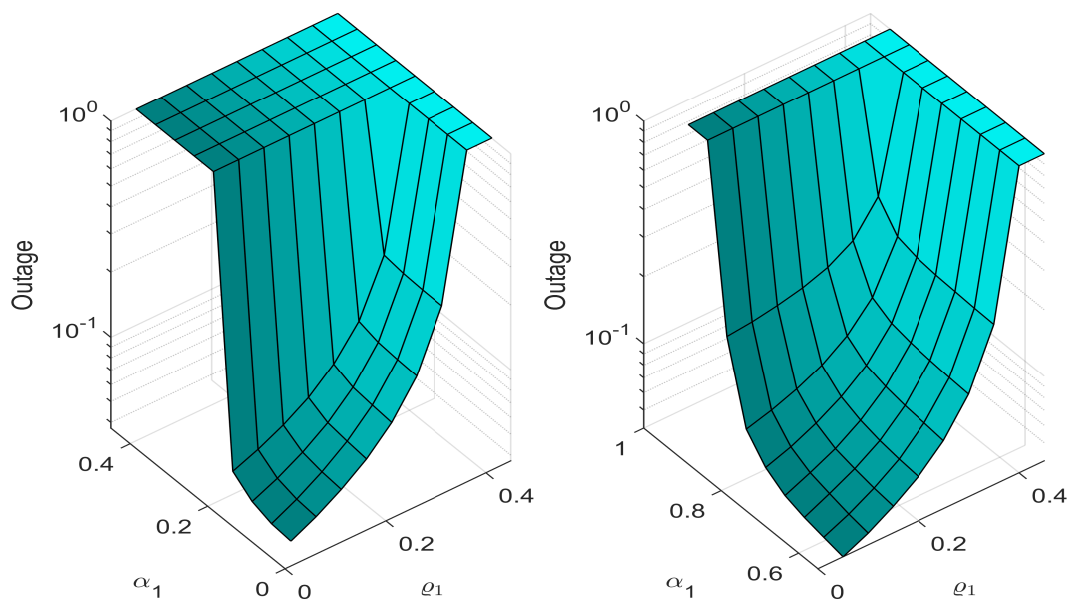
Figure 3.23: Optimum power allocation pairs for relay-assisted-NOMA under minimum OP of UE_2 constraint when $\rho_s = 20dB$, $\beta = 0.05$ and $\acute{R}_2 = 1BPCU$ a) conventional network b) reversed network
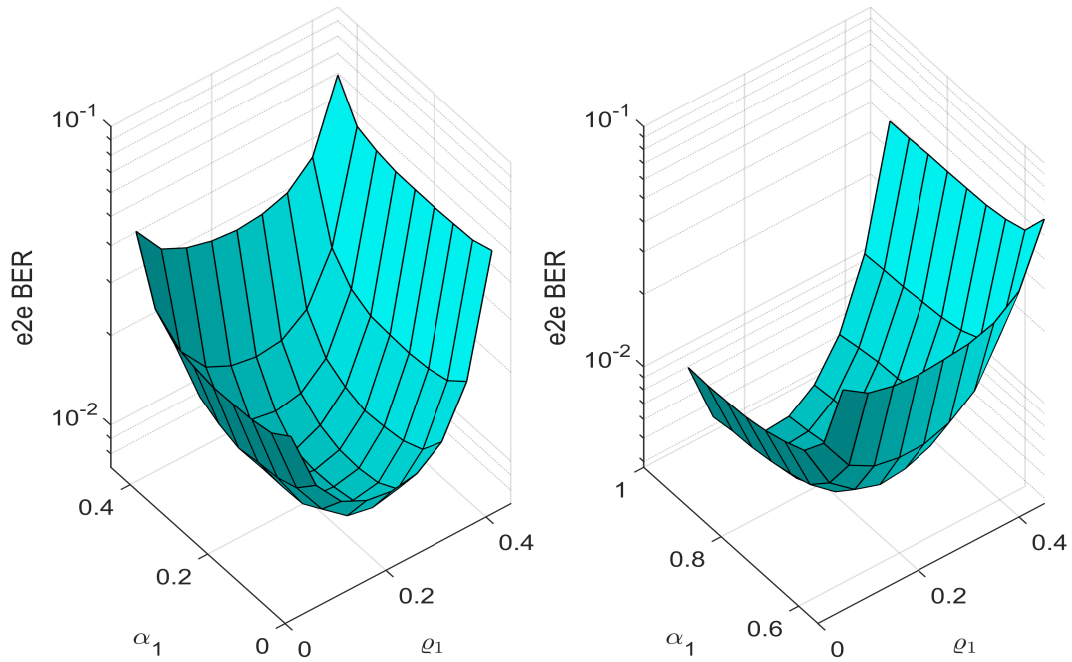
Figure 3.24: Optimum power allocation pairs for relay-assisted-NOMA under minimum BER of UE_1 constraint when $\rho_s = 20dB$ a) conventional network b) reversed network

Lastly, optimum power allocation pair discussion is provided under BER constraints of users. E2e BER of users are presented according to power allocation pairs in Figure 3.24 and Figure 3.25 for UE_1 and UE_2, respectively. The channel conditions are the same with previous comparisons. According to figures, optimum power allocation pairs for UE_1 are $\alpha_1 \sim 0.25$, $\varrho_1 \sim 0.25$ and $\alpha_1 \sim 0.95$, $\varrho_1 \sim 0.2$ for conventional and reversed networks, respectively. On the other hand, optimum power allocation pairs for UE_2 are $\alpha_1 \sim 0.05$, $\varrho_1 \sim 0.05$ and $\alpha_1 \sim 0.8$, $\varrho_1 \sim 0.05$ for conventional and reversed networks, respectively.

Considering all these discussions on optimum power allocation, it is worthy to note that power allocation pairs cause a trade-off between performances of users. Hence, it is not possible to provide a global optimum power allocation pair. It should be determined according to used scheme and the users' demands (QoS criteria). In some cases, data reliability (BER) has priority and in some cases to be reached out (not to be in outage) has that priority, hence it should be designed what user demands.
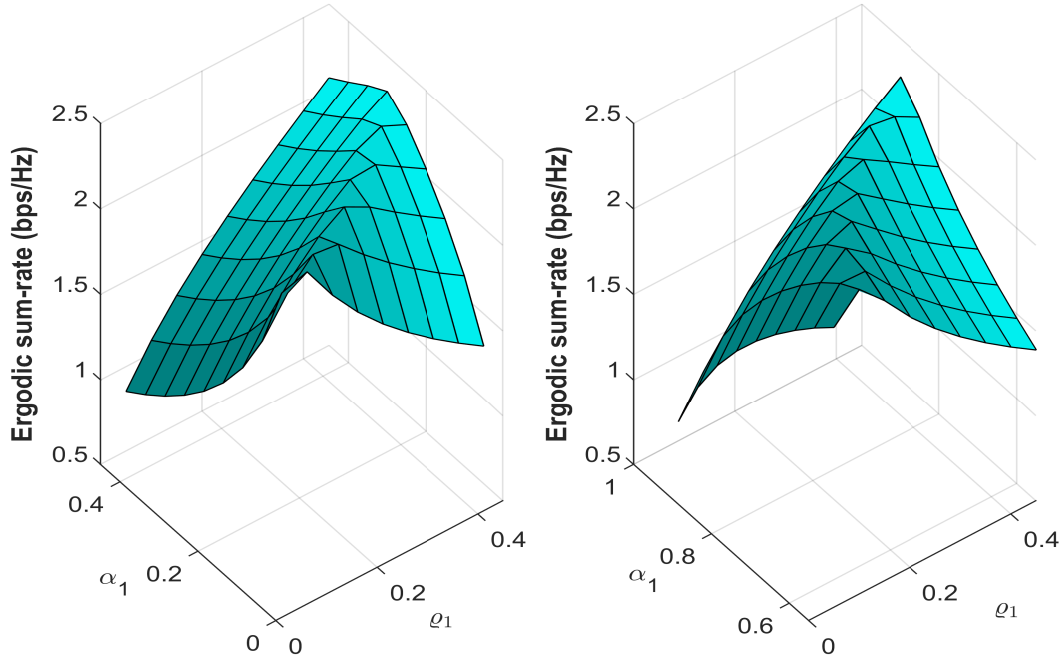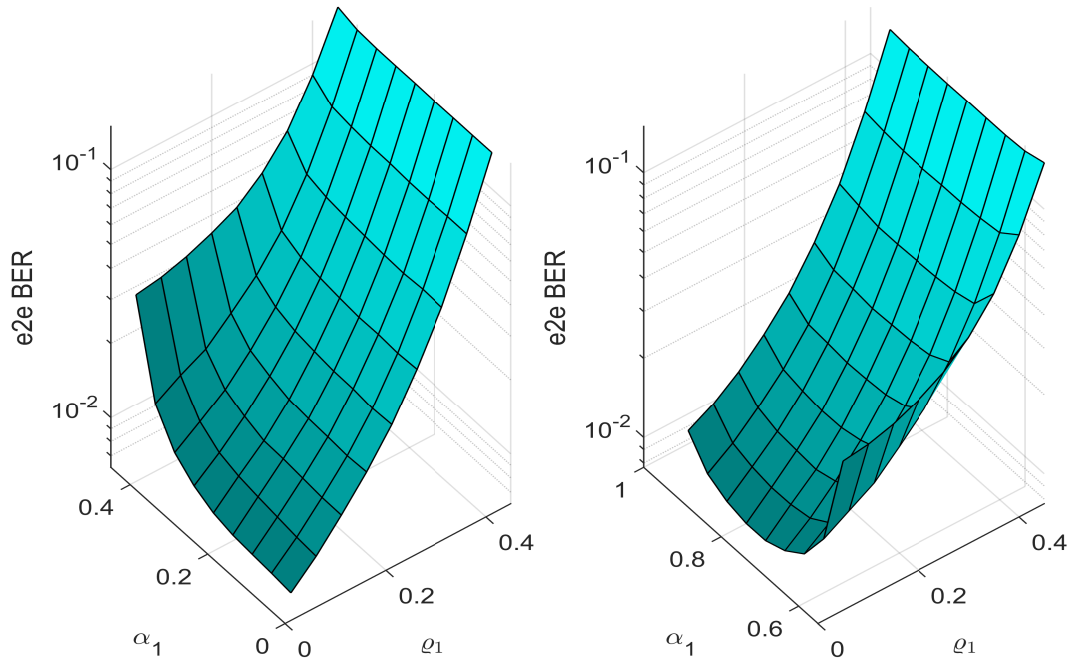
Figure 3.25: Optimum power allocation pairs for relay-assisted-NOMA under minimum BER of UE_2 constraint when $\rho_s = 20dB$ a) conventional network b) reversed network

NOMA-based cooperative relaying systems (NOMA-CRS): As the third/last concept for the interplay between NOMA and cooperative communication, numerical results for NOMA-CRS are presented in the following. As mentioned previously, EC and OP of NOMA-CRS schemes have been investigated widely in the literature, hence only simulations are presented briefly for them. However, to the best of our knowledge, BEP of NOMA-CRS is firstly investigated in the literature, hence extended simulations are provided on BER of NOMA-CRS in order to both validate analysis and to investigate error performance of NOMA-CRS in detail. EC and OP of NOMA-CRS are provided in Figure 3.26 and Figure 3.27, respectively. $\sigma_{sr}^2 = 10dB$, $\sigma_{sd}^2 = 0dB$ and $\sigma_{rd}^2 = 10dB$ are assumed. The power allocation coefficients are chosen as $\alpha_1 = 0.1$, $\alpha_2 = 0.9$ and the power of the nodes are equal $P_s = P_r$ as in [142]. In the capacity and outage comparisons, results for conventional cooperative relaying systems with HD such as [97] are also provided. One can see from the results that NOMA-CRS outperforms conventional CRS in terms of both EC and OP.
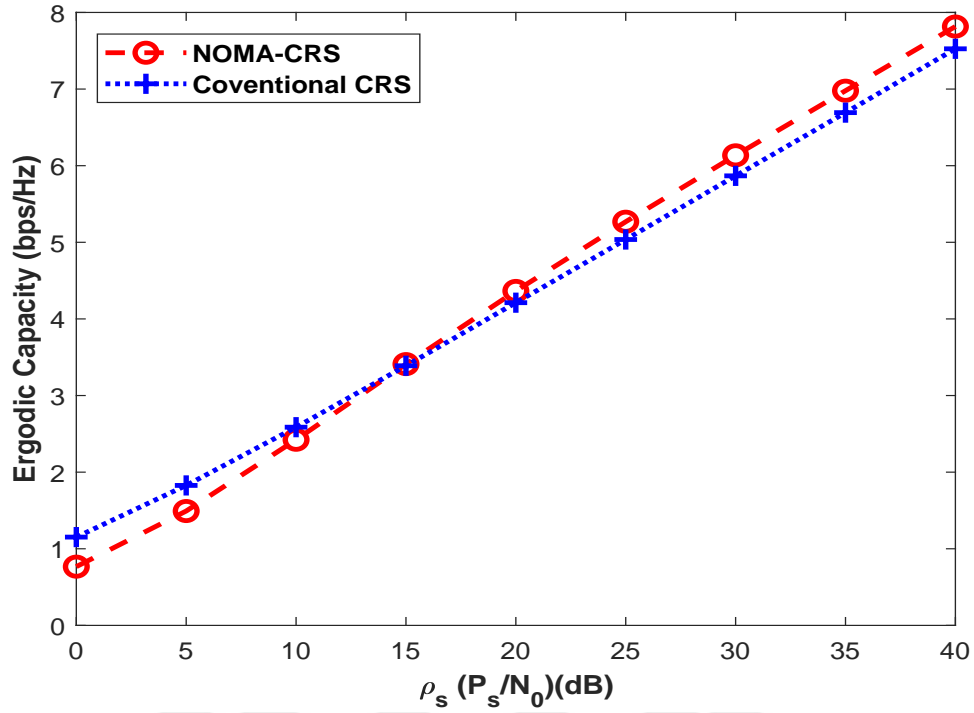
Figure 3.26: EC comparison for NOMA-CRS and conventional CRS
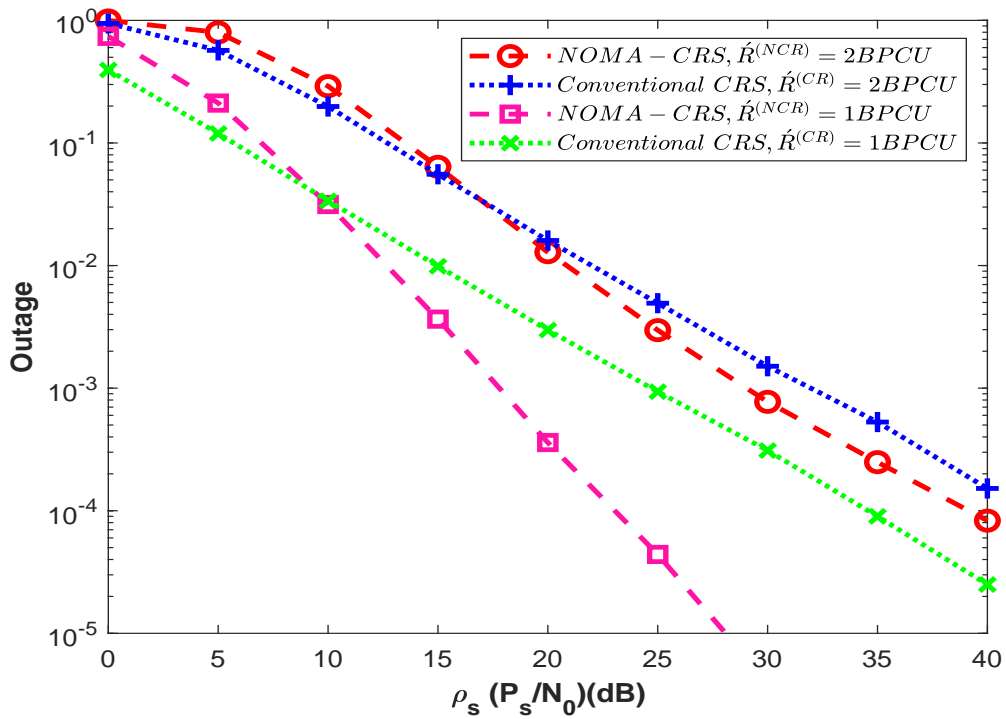
Figure 3.27: OP comparison for NOMA-CRS and conventional CRS

The derived BEP expressions are validated in Figure 3.28. The channel conditions are assumed to be the same with previous EC and OP comparisons. The results are provided for different power allocation coefficients. Based on the results, one can say that power allocation has not always same effect on BER performance since with the increase of α_1, BER performance of NOMA-CRS firstly increases and then decreases. It can be explained as: Increasing α_1 provides better BER for x_1 symbols and overall BER performance is increased, however when this increase continues, it will pull down the BER performance of x_2 symbols and it dominates the overall performance. In addition, for all power allocation coefficients, NOMA-CRS has worse BER performance than conventional CRS which is expected since conventional CRS has no inter-symbol-interference (ISI). Considering the system model of NOMA-CRS, one can easily say that link qualities between nodes have dominant effect on error performance of NOMA-CRS as in all communications systems. Nevertheless, in NOMA-CRS, since NOMA is implemented in the first phase, optimum power allocation should be considered according to channel qualities. One can easily see that in the second phase of NOMA-CRS, there is no ISI, hence the performance of x_1 symbols is dominated by link between source and relay. Thus, if this link is good enough, the power allocated to x_2 symbols should be increased and vice versa. In order to emphasize this, optimum power allocation is investigated with the channel qualities between source-relay-destination. Letting the linear sum of the average channel powers between source-relay and relay-destination (i.e., $\sigma_{sr}^2 + \sigma_{rd}^2$) does not change, e.g. in the previous figure, $\sigma_{sr}^2 = 10$ and $\sigma_{rd}^2 = 10$ is assumed, hence if $\sigma_{sr}^2 = 5$ is assumed then, it will be $\sigma_{rd}^2 = 15$. With this assumption, mutual optimum power allocation is provided for NOMA-CRS in Figure 3.29 when $\rho_s = 20dB$. One can easily see that if the relay is close to the source (high σ_{sr}^2), it should be used lower α_1, if it is close to the destination (low σ_{sr}^2), higher α_1 should be chosen.

Lastly in this chapter, numerical results are provided for NOMA-DRN as a subset of NOMA-CRS. In Figure 3.30, error performance of NOMA-DRN is presented for two different scenarios. In Scenario I, $\sigma_{sr_1}^2 = 1$, $\sigma_{sr_2}^2 = 10$, $\sigma_{r_1d}^2 = 9$, $\sigma_{r_2d}^2 = 2$ and, Scenario II, $\sigma_{sr_1}^2 = 2$, $\sigma_{sr_2}^2 = 10$, $\sigma_{r_1d}^2 = 9$, $\sigma_{r_2d}^2 = 3$. The power allocation coefficients are given $\alpha_1 = 0.9602$, $\varrho_1 = 0.8011$ and $\alpha_1 = 0.8816$, $\varrho_1 = 0.6055$ which are given as sub-optimum coefficients for given scenarios, respectively [146]. In the results, bit error rate (BER)
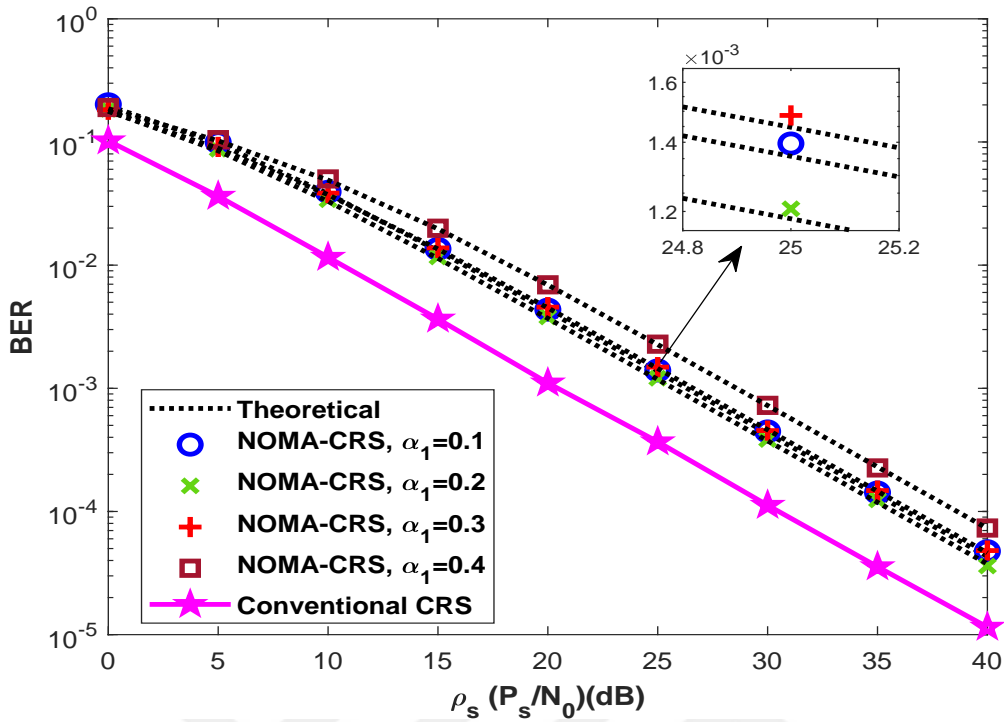
Figure 3.28: BER performance comparison for NOMA-CRS and conventional CRS
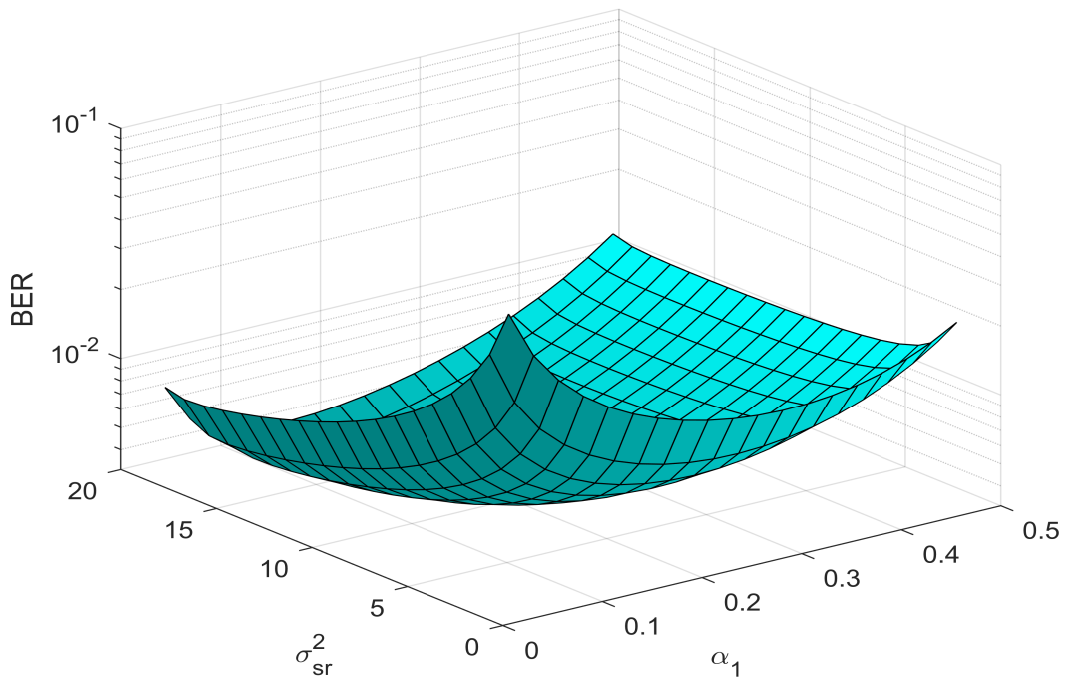
Figure 3.29: BER performance of NOMA-CRS with the change of average power of source-relay link (σ_{sr}^2) and power allocation (α)
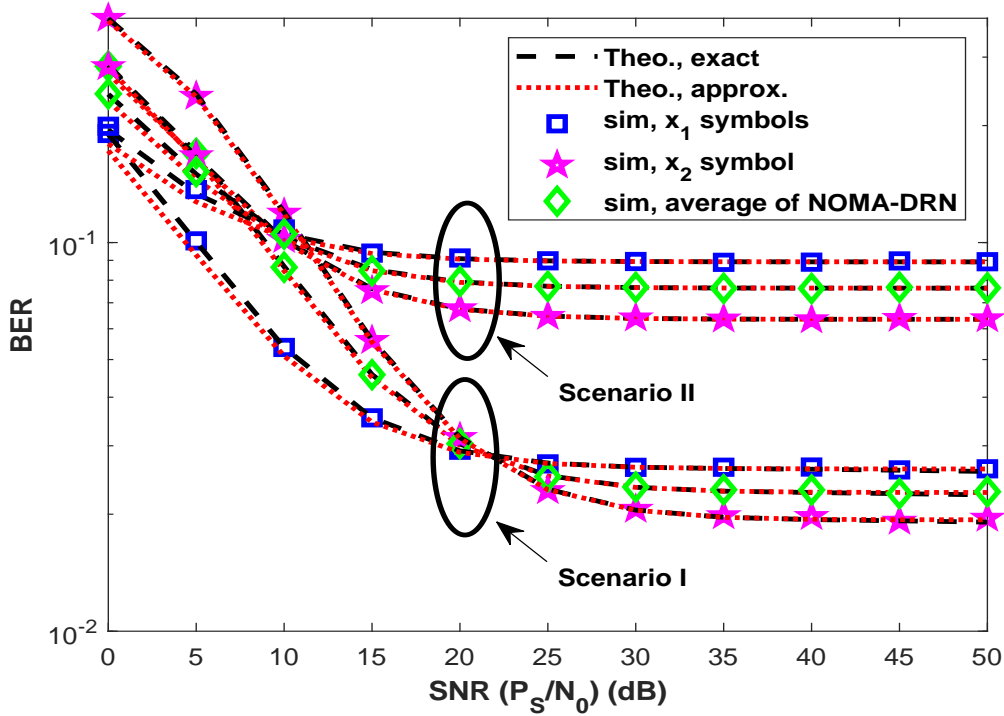
Figure 3.30: BER performance of NOMA-DRN

for x_1, x_2 symbols and average BER for NOMA-DRN are provided. Based on the simulations, it is noteworthy that derived one-degree integral form of exact BEP matches perfectly with simulation. In addition, provided approximate expression matches well also. Furthermore, in order to show the effect of power allocation coefficients (i.e., α_k, ϱ_k, $k = 1, 2$), e2e BER of NOMA-DRN is provided with the change of α_1 and ϱ_1, in Figure 3.31 when $SNR = 15dB$ and $SNR = 20dB$. Based on provided simulation results, optimum power allocation pairs which minimize e2e BER of NOMA-DRN for given scenarios are $\alpha_1 \simeq .875$, $\varrho_1 \simeq .925$, and $\alpha_1 \simeq .900$, $\varrho_1 \simeq .925$, respectively.

In order to validate derived priori probabilities (i.e., $p(A_{2nd})$, $p(B_{2nd})$) and to emphasize their effect, error performance for second phase of NOMA-DRN is provided in Figure 3.32. Simulation results are given for two different schemes. In Scenario III, $\alpha_1 = 0.8$, $\sigma_{sr_1}^2 = 1$, $\sigma_{sr_2}^2 = 2$, $\beta_1 = 0.8$, $\sigma_{r_1d}^2 = 2$, $\sigma_{r_2d}^2 = 1$ and in Scenario IV, $\alpha_1 = 0.7$, $\sigma_{sr_1}^2 = 2$, $\sigma_{sr_2}^2 = 10$, $\beta_1 = 0.7$, $\sigma_{r_1d}^2 = 10$, $\sigma_{r_2d}^2 = 2$. Theoretical curves for non-equiprobable communication are provided according to derived priori probabilities in Lemma 3.1. Theoretical curves for equiprobable communication are also presented as if $p(A_{2nd}) = p(B_{2nd})$. One can easily
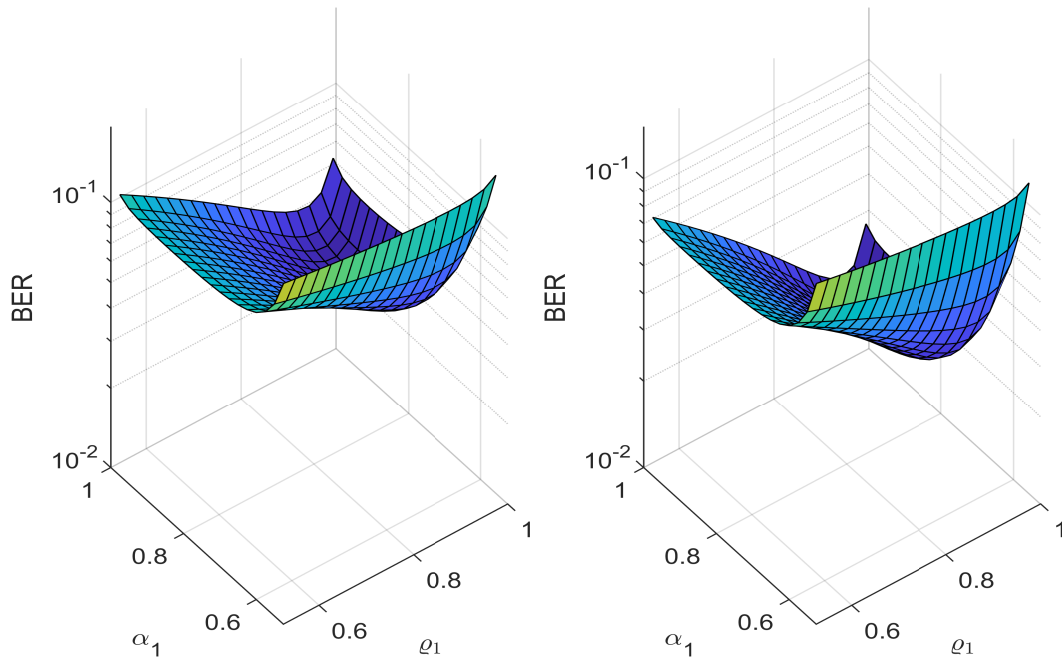
Figure 3.31: Optimum power allocation pairs for NOMA-DRN under minimum BER constraint a) $\rho_s = 15dB$ b) $\rho_s = 20dB$
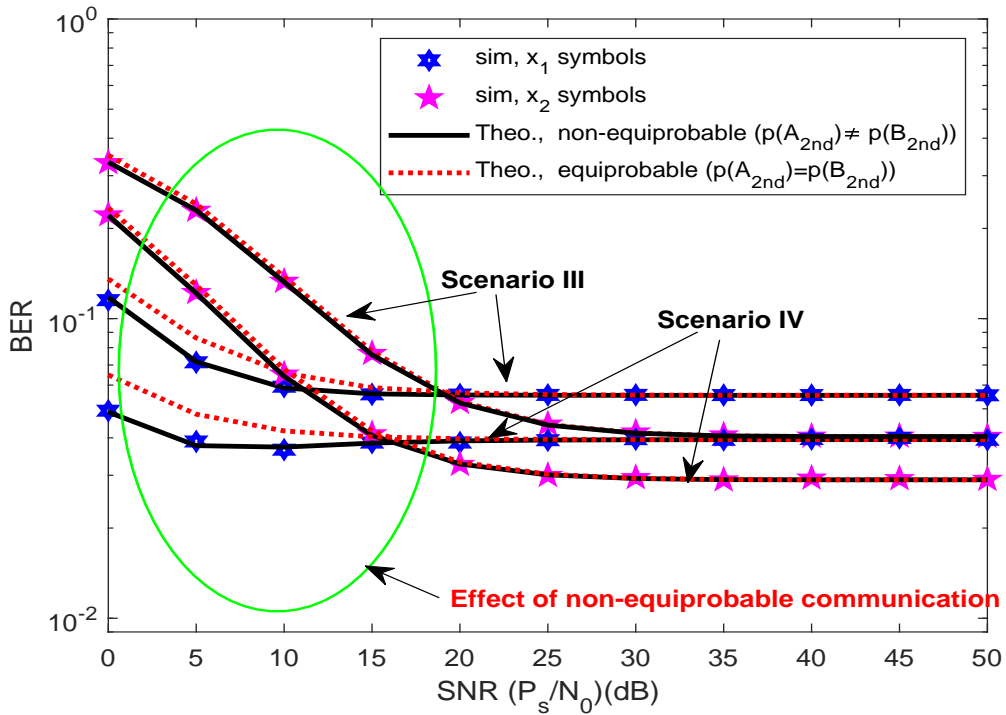
Figure 3.32: BER performance in the second phase of NOMA-DRN (uplink NOMA)

see that derived priori probabilities are correct and analytical analysis matches perfectly with simulations. The effect of this non-equiprobable communication has dominant effect especially in the low SNR regime (green circle in Figure 3.32).

CHAPTER 4

INTERPLAY BETWEEN NOMA AND SPATIAL MODULATION

4.1 BACKGROUND FOR SPATIAL MODULATION

Index modulation (IM) techniques [150, 151] have attracted tremendous attention where information bits are conveyed to the destination by not only conventional modulation schemes (M-ary) but also mapping to different indexes such as antenna [152], sub-carrier [153], RF mirror [154] etc. Spatial modulation is a subset of IM. In SM [155, 156], unlike in V-BLAST, only one transmit antenna is activated during one symbol duration and this active antenna index is determined according to information bits. Remaning information bits are modulated by M-ary modulation and transmitted by activated antenna. An illustration of SM is shown in Table 4.1, where $k = 4$ bits are intended to be transmitted in one symbol duration. The transmitter has $N_r = 4$ transmit antennas, hence $n = log_2(N_t) = 2$ bits are mapped into transmit antenna index and renaming $m = 2$ bits are modulated by QPSK/4-QAM.

SM is a very promising technique owing to following superiority to conventional MIMO systems

- In SM, channel correlations are eliminated, hence SM requires much less complex receivers compared to conventional MIMO systems such as V-BLAST.

- Only one Radio Frequency (RF) chain is required in SM.

- It is not required to synchronize antennas and any limit for receiver antenna number exists no more.

- Capacity is increased since additional bits are conveyed through the antenna index.

Table 4.1: SM for $N_r = 4$ and $M = 4$

Information bits	Bits conveyed in Antenna Index	Bits conveyed by QPSK	Activated Antenna Index	Transmitted Base-band Symbols
{0000}	{00}	{00}	1	$\{-1/2, -j/2\}$
{0001}	{00}	{01}	1	$\{-1/2, j/2\}$
{0010}	{00}	{10}	1	$\{1/2, -j/2\}$
{0011}	{00}	{11}	1	$\{1/2, j/2\}$
{0100}	{01}	{00}	2	$\{-1/2, -j/2\}$
{0101}	{01}	{01}	2	$\{-1/2, j/2\}$
{0110}	{01}	{10}	2	$\{1/2, -j/2\}$
{0111}	{01}	{11}	2	$\{1/2, j/2\}$
{1000}	{10}	{00}	3	$\{-1/2, -j/2\}$
{1001}	{10}	{01}	3	$\{-1/2, j/2\}$
{1010}	{10}	{10}	3	$\{1/2, -j/2\}$
{1011}	{10}	{11}	3	$\{1/2, j/2\}$
{1100}	{11}	{00}	4	$\{-1/2, -j/2\}$
{1101}	{11}	{01}	4	$\{-1/2, j/2\}$
{1110}	{11}	{10}	4	$\{1/2, -j/2\}$
{111}	{11}	{11}	4	$\{1/2, j/2\}$

On the other hand, main disadvantages of SM can be considered as follow: if the channels are not totaly uncorrelated (within transmit antennas), the error performance of SM gets worse. When the bits conveyed in antenna index increase, the number of transmit antenna increase exponentially.

Space Shift Keying (SSK) is a spacial case of SM where the information bits are only mapped into transmit antenna index. SSK requires even less complex receivers than SM and it can perform as SM [157]. Hence, SSK has been widely analyzed in literature and various SSK schemes have been investigated such as Generalized-SSK (GSSK) [158]. In addition to SSK, SM/IM variants have attracted recent attention such as space time block coded SM (STBC-SM) [159], trellis coded SM (TCSM) [160,161], space time chan-

nel modulation (STCM) /media-based modulation (MBM) [154,162] .

Thanks to its advantages, IM techniques are very promising for future wireless networks. In addition, its implementation with other physical layer techniques is relatively simple. Hence, in this chapter, SM is applied for multiple access and SSK as a subset of IM and NOMA are implemented together.

4.2 RELATED WORKS AND MOTIVATION

As two promising techniques for future wireless networks, the integration of SM and NOMA together have been investigated in literature. The authors in [163] propose to apply NOMA with finite alphabets into MIMO SM to improve spectral efficiency of conventional SM. In [163], after applying SM for each user's symbols, the symbols of two users are transmitted by two selected antennas (according to SM applied for each user) simultaneously. The mutual information is analyzed for proposed scheme (NOMA-MIMO-SM) and it is proved that NOMA-MIMO-SM is superior to conventional MIMO-OMA and SM. Then, the combination of SM and NOMA for the vehicle networks has been proposed in [164] where a cooperative communication is considered. In the first phase of cooperative communication, NOMA is implemented for two vehicles' symbols and the superposition coded symbol is transmitted by BS -infrastructure to vehicles (I2V)-. In the second phase of communication, one of the vehicle -relay- operates as a relay for both mobile user in that vehicle and other vehicle (V2V). The relay applies SM for other vehicles symbols and transmits superposition coded symbol (NOMA) of user and vehicle by activated antenna. The spectral efficiency is analyzed for the proposed system and BER simulations are provided.

The aforementioned studies consider NOMA implementation in SM to increase spectral efficiency of conventional SM. However, the considered model in this chapter much differs from this concept and the motivation of this chapter is much beyond. As proved in Chapter 2, NOMA suffers from IUI and this IUI causes poor BER performance compared to OMA [85]. In addition to poor BER performance, when the number of user in a resource block is increased, the advantage of NOMA may also be trivial in terms of achievable rate. Thus, most of studies in literature and the standards consider only two NOMA

users in a resource block [7–9]. To this end, a new or hybrid multiple access design which can compete with OMA in terms of BER and with NOMA in terms of achievable rate, is required. Hence, for two users networks, SM aided multiple antenna network is considered in [165] which is called as spatial multiple access [166] and detail performance analysis is provided for three of KPIs (i.e., EC, OP, BER). Nevertheless, [165] and [166] still consider two users in a resource block. Thus, the combination of SSK/GSSK with NOMA is introduced where cell-edge user(s) is(are) multiplexed in spatial domain [167, 168]. Although the proposed concepts in [167, 168] are promising, the considered models have unrealistic assumptions such as NOMA symbols are known at cell-edge user(s), thus the provided detector cannot detect symbols when this strict-assumption is relaxed and there is no analytical evaluation for considered models. To this end, SSK-NOMA is proposed with a optimum detector at the cell-edge user [169]. In addition, closed-from expressions of EC, OP and BEP are derived for the proposed models.

4.3 SPATIAL MULTIPLE ACCESS (SMA)

4.3.1 System Model

A downlink MIMO scenario is considered where a base station (BS) and two mobile users (i.e., UE_1 and UE_2) are located. BS and users are equipped with N_t and N_r antennas, respectively. The channel gain between BS and each user are defined as $\mathbf{H_i}, i = 1, 2$ where $\mathbf{H_i} \subset \mathbb{C}^{N_r \times N_t}$. $\mathbf{H_i}$ consists of $\mathbf{h_{i,j}} = [h_{i,j,1}, \ h_{i,j,2}, \ldots, h_{i,j,N_r}]^T, \quad j = 1, 2, \ldots, N_t$ vectors. $h_{i,j,k}, \ j = 1, 2, \ldots, N_t, \ k = 1, 2, \ldots, N_r$ are assumed to be independent and identical distributed. $h_{i,j,k}$ follow $CN(0, \sigma_{si}^2), \ i = 1, 2$ where σ_{si}^2 denotes the average channel power which is related to distance between BS and user i likewise throughout this dissertation. $\sigma_{s1}^2 > \sigma_{s2}^2$ is assumed. Thus, likewise in all NOMA schemes, the UE_1 and UE_2 can be considered as intra-cell user and cell-edge user, respectively. As shown in Figure 4.1, BS implements Spatial Multiple Access (SMA) to convey the symbols of users. SMA is based on applying Spatial Modulation (SM) principles for the symbols of different users. Hence, the binary symbols of UE_1 are modulated according to an M-ary modulation constellation whereas binary symbols of UE_2 are mapped into transmit antenna index -Space Shift

100
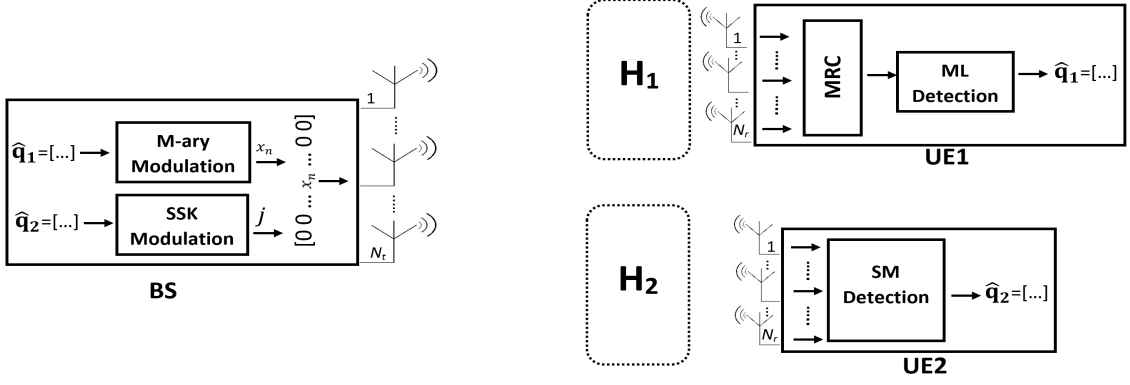
Figure 4.1: The illustration of SMA

Keying (SSK)- only which be activated during symbol duration[1]. The resulting transmit vector for BS is given as

$$\mathbf{x} = [\overbrace{0\ 0...x_1...0\ 0}^{N_t}]^T,$$
$$\uparrow v^{th} position$$

(4.1)

where x_1 is modulated base-band signal of UE_1 and v is the activated transmit antenna index which is determined according to binary symbol of UE_2 intended to be transmitted. The revived signal vector for each user is given as

$$\mathbf{y_i} = \sqrt{P_s}\mathbf{H_i}\mathbf{x} + \mathbf{w_i}, i = 1, 2,$$

(4.2)

where P_s is the transmit power of BS and $\mathbf{w_i}$ N_r-dim AWGN and each dimension follows $CN(0, N_0)$.

4.3.1.1 Detection at Users

4.3.1.1.1 Detection at UE_1 -intra-cell user- (ML detection)

Since the symbols of UE_1 are transferred according to chosen M-ary constellation, UE_1 implements a ML detector for received vector by N_r receive antennas. Thus, it implements MRC and detects own symbols as

$$\hat{x}_1 = \underset{n}{\operatorname{argmin}} \left\| \mathbf{y_1} - \sqrt{P_s}\mathbf{h_{1,v}}x_{1,n} \right\|^2, \quad n = 1, 2, ..M_1,$$

(4.3)

---

[1]Although the users are assigned into different domains and power allocation is not implemented likewise conventional NOMA, SMA is a NOMA scheme since two users are served in the same resource block.

where $x_{1,n}$ denotes the complex base-band signal at the point of n for M_1-ary modulation constellation.

4.3.1.1.2 Detection at UE_2 -cell-edge user- (SM detection)

The symbols of UE_2 are mapped into transmit antenna index. Thus, in order to obtain transmitted symbols of UE_2, it should be estimated which transmit antenna is activated. This can be done by SSK demodulation given in [157]. However, complex base-band x_2 symbols are transmitted from the selected/activated transmitted antenna in SMA likewise SM rather than only the transmit SNR in SSK. Thus, optimum detector for SMA is SM detector in [155] rather than SSK detector [157] although SSK is used to transmit symbols of UE_2 -mapped into only transmit antenna index-. The optimum ML detector for UE_2 symbols is given as

$$[\hat{v}, \hat{x}_1] = \underset{v,n}{\operatorname{argmin}} \sqrt{\rho_s} \left\| \mathbf{g_{v,n}} \right\|_F^2 - 2Re\{\mathbf{y_2}^H \mathbf{g_{v,n}}\}, \tag{4.4}$$

where $v = 1, 2, ..N_t$ and $n = 1, 2, \ldots M_1$. $\mathbf{g_{v,n}} = \mathbf{h_{2,v}} x_{1,n}$ is defined and $\rho_s = {}^{P_s}/_{N_0}$ is the average SNR for each antenna.

4.3.2 Performance Analysis

4.3.2.1 Ergodic Capacity Analysis

The achievable (Shannon) capacities of the users for the proposed SMA system are

$$\begin{aligned}
R_1^{(SMA)} &= \log_2\left(1 + SNR_1\right), \\
R_2^{(SMA)} &= \log_2\left(N_t\right),
\end{aligned} \tag{4.5}$$

where

$$SNR_1 = \rho_s \left\| \mathbf{h_{1,v}} \right\|^2, \tag{4.6}$$

Letting $\gamma_{s1} \triangleq \left\| \mathbf{h_{1,v}} \right\|^2$, in this case γ_{s1} will be chi-square distributed with $2N_r$ degree of freedom and the PDF is given [149] as

$$p_{\gamma_{s1}}(\gamma_{s1}) = \frac{\gamma_{s1}^{N_r-1} e^{-\gamma_{s1}/\sigma_{s1}^2}}{\Gamma(N_r)\sigma_{s1}^{2\,N_r}}, \tag{4.7}$$

where $\Gamma(.)$ is the Gamma function [89, eq. (8.32)].

The ergodic capacity for UE_1 is given by

$$C_1^{(SMA)} = \int_0^\infty \log_2\left(1 + \rho_s \gamma_{s1}\right) p_{\gamma_{s1}}(\gamma_{s1}) d\gamma_{s1}. \tag{4.8}$$

By substituting PDF given (4.7) into (4.8), with utilizing [89, eq. (4.337.5)] and after some simplifications, ergodic capacity for UE_1 is derived as

$$
\begin{aligned}
C_1^{(SMA)} =& \frac{\log_2 e}{\Gamma(N_r)} \sum_{\lambda=0}^{N_r-1} \frac{(N_r-1)!}{(N_r-\lambda-1)!} \\
&\times \left(\frac{(-1)^{N_r-\lambda-2}}{(\rho_s\sigma_{s1}^2)^{N_r-\lambda-1}} e^{1/(\rho_s\sigma_{s1}^2)} E_i\left(-\frac{1}{\rho_s\sigma_{s1}^2}\right) + \sum_{\eta=1}^{N_r-\lambda-1} \frac{(\eta-1)!}{(-\rho_s\sigma_{s1}^2)^{N_r-\lambda-\eta-1}} \right).
\end{aligned}
\tag{4.9}
$$

Although the achievable rate of UE_2 only depends on the number of transmit antenna (4.5), some researches/studies assume that the achievable rate of SSK is defined as the binary bits detected correctly. Hence, the achievable rate of UE_2 is modified as

$$R_2^{(SMA)} = \log_2 N_t \left[1 - P_2\left(e|\mathbf{h_{2,v}}\right)\right], \tag{4.10}$$

where $P_2(e|\mathbf{h_{2,v}})$ is the conditional BEP of UE_2. Thus, the ergodic rate for UE_2 is derived by averaging achievable rate over $\mathbf{h_{2,v}}$. Then, it is derived as

$$C_2^{(SMA)} = \log_2 N_t \left[1 - P_2\left(e\right)\right], \tag{4.11}$$

where $P_2\left(e\right)$ is the average BEP of UE_2 and it will be derived in the next subsections. Finally, likewise all schemes, the ergodic sum rate of SMA is obtained by

$$C_{sum}^{(SMA)} = C_1^{(SMA)} + C_2^{(SMA)}. \tag{4.12}$$

4.3.2.2   Outage Probability Analysis

The outage event occurs when the target rate cannot be achieved. Thus OPs of users are defined as

$$
\begin{aligned}
P_1^{(SMA)}(out) &= P(R_1^{(SMA)} < \acute{R}_1^{(SMA)}), \\
P_1^{(SMA)}(out) &= P(R_2^{(SMA)} < \acute{R}_2^{(SMA)}),
\end{aligned}
\tag{4.13}
$$

where $\acute{R}_i^{(SMA)}, i = 1, 2$ are target rates of users. For UE_1, by substituting (4.5) into (4.13), OP is obtained as

$$P_1(out) = P\left(\rho_s \gamma_{s1} < \phi_1^{(SMA)}\right), \tag{4.14}$$

where $\phi_1^{(SMA)} = 2^{\acute{R}_1^{(SMA)}} - 1$. By using CDF of γ_{s1} [90], it is derived as

$$P_1(out) = 1 - exp\left(-\phi_1^{(SMA)}/(\rho_s\sigma_{s1}^2)\right) \sum_{\lambda=1}^{N_r} \frac{\left(\phi_1^{(SMA)}/(\rho_s\sigma_{s1}^2)\right)^{\lambda-1}}{(\lambda-1)!}. \tag{4.15}$$

For UE_2, substituting (4.10) into (4.13), OP is obtained as

$$\begin{aligned} P_2(out) &= P\left(\log_2 N_t\left[1 - P_2(e|\mathbf{h_{2,v}})\right] < \acute{R}_2^{(SMA)}\right) \\ &= P\left(P_2(e|\mathbf{h_{2,v}}) \geq \psi_2^{(SMA)}\right), \end{aligned} \tag{4.16}$$

where $\psi_2^{(SMA)} = 1 - \frac{\acute{R}_2^{(SMA)}}{\log_2 N_t}$. Then, the OP is derived as

$$\begin{aligned} P_2(out) &= \int_{\psi_2^{(SMA)}}^{\infty} P_2(e|\gamma_{s2})p_{\gamma_{s2}}(\gamma_{s2})d\gamma_{s2} \\ &= \int_0^{\infty} P_2(e|\gamma_{s2})p_{\gamma_{s2}}(\gamma_{s2})d\gamma_{s2} - \int_0^{\psi_2^{(SMA)}} P_2(e|\gamma_{s2})p_{\gamma_{s2}}(\gamma_{s2})d\gamma_{s2}, \end{aligned} \tag{4.17}$$

where $\gamma_{s2} \triangleq \|\mathbf{h_{2,v}}\|^2$. However, the second integral in (4.17) cannot be solved in closed-form. Nevertheless, it is worthy to note that the OP of UE_2 turns out to be average BEP of UE_2 when $\acute{R}_2^{(SMA)} = \log_2 N_t$ which is such reasonable assumption. The average BEP of UE_2 is derived in the next subsection.

4.3.2.3 Bit Error Probability (BEP) Analysis

Since only one transmit antenna is activated by BS according to UE_2 symbols and modulated x_1 symbols are transmitted by that activated antenna, the system model turns out to be well-know $1 \times N_r$ single-input-multiple-output (SIMO) system in terms of UE_1. Hence, the conditional BEP for UE_1 is given by

$$P_1\left(e|\mathbf{h_{1,v}}\right) = \varsigma Q\left(\sqrt{\nu\rho_s\gamma_{s1}}\right), \tag{4.18}$$

where ς and ν changes according to chosen M_1-ary modulation constellation which can be found in [170] for various constellations. The average BEP of x_1 symbols is obtained by

$$P_1(e) = \int_0^{\infty} P_1\left(e|\mathbf{h_{1,v}}\right)p_{\gamma_{s1}}(\gamma_{s1})d\gamma_{s1}. \tag{4.19}$$

After substituting given PDF (4.7) into (4.19), with the aid of [149, eq. (64)], average BEP of UE_1 is derived as

$$P_2(e) = \varsigma \left(\frac{1 - \mu_1}{2} \right)^{N_r} \sum_{\lambda=0}^{N_r-1} \binom{N_r + \lambda - 1}{\lambda} \left(\frac{1 + \mu_1}{2} \right)^{\lambda}, \tag{4.20}$$

where $\mu_1 = \sqrt{\frac{\nu \rho_s \sigma_{s1}^2}{2 + \nu \rho_s \sigma s1^2}}$.

On the other hand, in order to derive BEP of UE_2, well-known union bound technique which is commonly used for SM/SSK schemes in the literature is used since exact BEP for SM/SSK schemes cannot be derived, to the best of our knowledge. The union bound for SM detection is given [155] as

$$P(e) \leq \sum_{v=1}^{N_t} \sum_{\hat{v}=1}^{N_t} \sum_{n=1}^{M_1} \sum_{\hat{n}=1}^{M_1} \frac{N(x_{1,n} \to \hat{x}_{1,n}) PEP(\mathbf{x}_{v,n} \to \mathbf{x}_{\hat{v},\hat{n}})}{M_1 N_t}, \tag{4.21}$$

where $\mathbf{x}_{v,n}$ denotes that the $x_{1,n}$ symbol is transmitted by the vth transmit antenna. $N(x_{1,n} \to \hat{x}_{1,n})$ is the number of different bits (Hamming distance) between $x_{1,n}$ and $\hat{x}_{1,n}$. $PEP(\mathbf{x}_{v,n} \to \mathbf{x}_{\hat{v},\hat{n}})$ is the pairwise error probability (PEP). Although the detector given (4.4) detects both transmit antenna index and modulated x_1 symbols mutually, the symbols of UE_2 are mapped into only the transmit antenna index. Thus, the given union bound is simplified as

$$P(e) \leq \sum_{v=1}^{N_t} \sum_{\hat{v}=1}^{N_t} \frac{PEP(\mathbf{x}_{v,n} \to \mathbf{x}_{\hat{v},\hat{n}})}{N_t}. \tag{4.22}$$

The conditional PEP for real constellations (i.e., BPSK) is given in [155] as $Q(\sqrt{\kappa})$ where $\kappa \triangleq \frac{\rho_s}{2} \|\mathbf{g_{v,n}} - \mathbf{g_{\hat{v},\hat{n}}}\|_F^2$. Considering this, PEP for general constellations is extended by using [171, eq. (7)] and with the aid of [149, eq. (64)],

$$PEP(\mathbf{x}_{v,n} \to \mathbf{x}_{\hat{v},\hat{n}}) = \mu_2^{N_r} \log_2 M_1 \sum_{\lambda=0}^{N_r-1} \binom{N_r - 1 + \lambda}{\lambda} (1 - \mu_2)^{\lambda}, \tag{4.23}$$

where $\mu_2 = \frac{1}{2} \left(1 - \sqrt{\frac{\sigma_a^2}{1 + \sigma_a^2}} \right)$ and $\sigma_a^2 = \frac{\rho_s \sigma_2^2 \left(|x_{1,n}|^2 + |x_{1,\hat{n}}|^2 \right)}{4}$. By substituting (4.23) into (4.22), average BEP of UE_2 is derived as

$$P_2(e) \leq \frac{N_t}{2} \mu_2^{N_r} \log_2 M_1 \sum_{\lambda=0}^{N_r-1} \binom{N_r - 1 + \lambda}{\lambda} (1 - \mu_2)^{\lambda}. \tag{4.24}$$

105

4.4 SSK-NOMA

In this section, it is proposed to extend the SMA system model by combining SSK and NOMA to serve more than two users in a resource block.

4.4.1 System Model

A downlink MIMO scheme is considered where a BS and L users (i.e., UE_1, UE_2, UE_3, ... , UE_L) are located. In order to achieve better performance than conventional NOMA, both SSK and NOMA are involved together. Likewise in SMA, BS and users are equipped with N_t and N_r antennas, respectively. The channel gain between BS and each user is defined as $\mathbf{H_i}, i = 1, 2, \ldots, L$ where $\mathbf{H_i} \subset \mathbb{C}^{N_r \times N_t}$. $\mathbf{H_i}$ consists of $\mathbf{h_{i,j}} = [h_{i,j,1}, \ h_{i,j,2}, \ldots, h_{i,j,N_r}]^T$, $\quad j = 1, 2, \ldots, N_t$ vectors. $h_{i,j,k}$, $j = 1, 2, \ldots, N_t$, $k = 1, 2, \ldots, N_r$ are assumed to be independent and identical distributed. $h_{i,j,k}$ follow $CN(0, \sigma_{si}^2)$, $i = 1, 2, \ldots, L$ where σ_{si}^2 denotes the average channel power which is related to distance between BS and user i. Without loss of generality, users are assumed to be sorted in ascending order of average channel powers [2] i.e., $\sigma_{s1}^2 \leq \sigma_{s2}^2 \leq \sigma_{s3}^2 \leq \cdots \leq \sigma_{sL}^2$. The illustration of SSK-NOMA is presented in Figure 4.2. As shown in Figure 4.2, first user (UE_1) is assigned into spatial domain and the binary symbol of UE_1 determined the transmit antenna index which will be activated during one symbol duration. On the other hand, the other users ($UE_2, UE_3, \ldots, UE_L$) are multiplexed in power domain by NOMA. Thus, the total superposition coded symbol which will be conveyed to the users by selected/activated transmit antenna is given as

$$\chi = \sum_{i=2}^{L} \sqrt{\alpha_i} x_i, \tag{4.25}$$

where $\chi \subset \mathbb{C}^{M_T}$ and $M_T = \prod_{i=2}^{L} M_i$ is defined where M_i refers the chosen M_i-ary modulation level/order/size for the symbols of UE_i. x_i is the complex base-band symbol of users. α_i is the power allocation for the x_i symbol. $\sum_{i=2}^{L} \alpha_i = 1$. Since the users are ordered in ascending order according to CQI, it is assumed to be $\alpha_2 > \alpha_3 > \cdots > \alpha_L$. Then, the SC symbol χ is transmitted by the activated antenna index v which is determined by

---

[2]Unlike throughout this dissertation, first user (UE_1) denotes cell-edge user in this section for the notation simplicity of the equations in the performance analysis of this section.
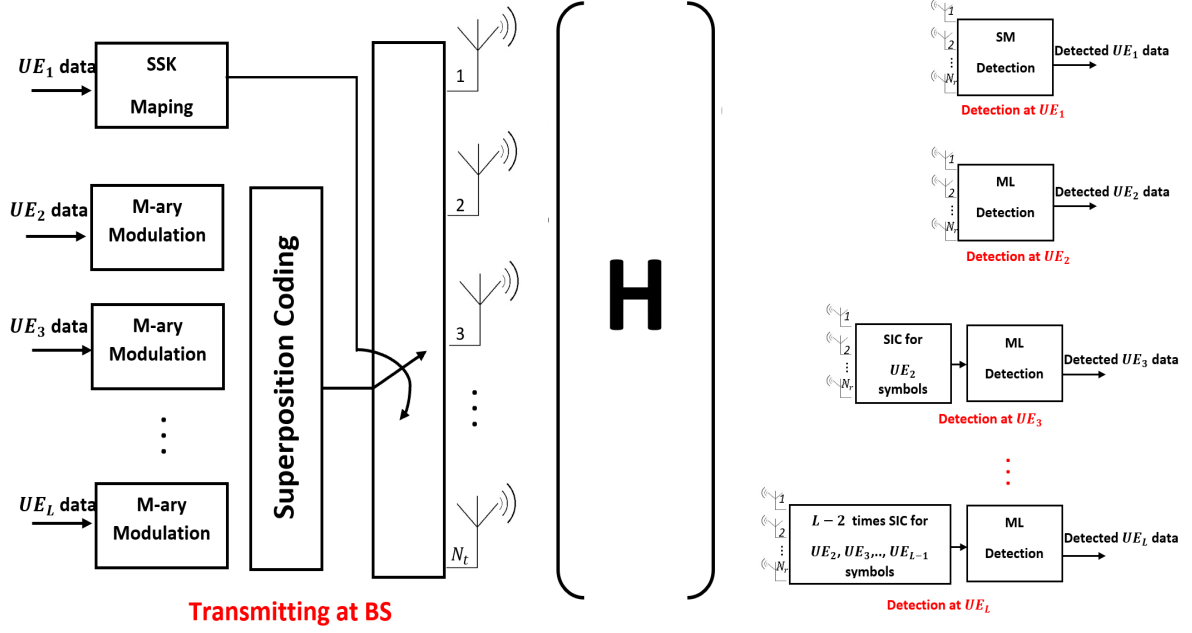
Figure 4.2: The illustration of SSK-NOMA

mapping binary symbols of UE_1. The transmitted vector by BS is given as

$$\mathbf{x} = [\overbrace{0\ 0\ 0\ \ldots\ \chi\ \ldots\ 0\ 0\ 0}^{N_t}]^T.$$

$$\uparrow v^{th} position$$

$$(4.26)$$

Thus, the received vector by each user is given as

$$\mathbf{y_i} = \sqrt{P_s}\mathbf{H_i}\mathbf{x} + \mathbf{w_i} \quad i = 1, 2, ...L, \tag{4.27}$$

where P_s is the transmit power of BS and $\mathbf{w_i}$ is N_r-dim AWGN at users and each dimension of it follows $CN(0, N_0)$. Based on the received signal, users detect their own symbols by implementing proper detectors. Since both SSK and NOMA/SC are implemented, the required detectors change according to users likewise in SMA.

4.4.1.1 Detection at Users

4.4.1.1.1 Detection at the first user (UE_1) (cell-edge user-SM)

The binary symbols of UE_1 are assigned into transmit antenna index by SSK modulation. Hence, such a detector should be implemented at UE_1 that can estimate by which transmit antenna the complex SC symbol (χ) is transferred to the air. Hence, just as in

107

SMA, SM detector should be implemented rather than SSK detector although the SSK modulation is used on BS side. In addition, since the transmitted symbol is a SC symbol which consists of symbols of users with different power allocation coefficient, optimal SM detector given (4.4) should be modified. The optimal SM detector for SSK-NOMA is given as

$$[\hat{v}, \hat{\chi}_k] = \underset{v,k}{\operatorname{argmin}} \sqrt{\rho_s} \|\mathbf{g_{v,k}}\|_F^2 - 2Re\{\mathbf{r_1}^H \mathbf{g_{v,k}}\}, \tag{4.28}$$

where $v = 1, 2, ..N_t$ and $k = 1, 2, \ldots, \prod_{i=2}^{L} M_i$. $\mathbf{g_{v,k}} = \mathbf{h_{1,v}}\chi_k$ is defined and $\rho_s = P_s/N_0$ is the average SNR for each antenna. Here, χ_k denotes the symbol of the point k on the total SC symbol constellation.

4.4.1.1.2   Detection at the users for UE_i, $i \geq 2$ (intra-cell users-NOMA)

SSK-NOMA system model can be considered as a SIMO-NOMA for the intra-cell users $(UE_i, \ i \geq 2)$. Thus, the users $UE_i, \ i \geq 2$ should detect their own symbols by using principles of conventional downlink NOMA schemes. The second user (UE_2) -with the highest power allocation coefficient- implements ML detector to detect its own symbols by treating symbols of remaining users noise. Then, the users with lower power allocation coefficients $(UE_i, \ i =, 3, 4, \ldots, L)$ implement iterative SIC detectors to detect their own symbols. The ML detection for UE_2 is given as

$$\hat{x}_2 = \underset{n}{\operatorname{argmin}} \left\| \mathbf{y_2} - \sqrt{\alpha_2 P_s}\mathbf{h_{2,v}}x_{2,n} \right\|^2, \quad n = 1, 2, ..M_2, \tag{4.29}$$

where $x_{i,n}$ is the symbol on the nth point of M_i-ary modulation constellation. The $UE_i, \ i = 3, 4, \ldots, L$ users implement $i - 2$ times iterative SIC processes to eliminate the effect of symbol of users with higher power allocation (i.e., $m < i$). The ML detection for $UE_i, \ i = 3, 4, \ldots, L$ users is given as

$$\hat{x}_i = \underset{n}{\operatorname{argmin}} \left\| \mathbf{y_i'} - \sqrt{\alpha_i P_s}\mathbf{h_{i,v}}x_{i,n} \right\|^2, \quad n = 1, 2, ..M_i, \tag{4.30}$$

where

$$\mathbf{y_i'} = \mathbf{y_i} - \sum_{m=2}^{i-1} \mathbf{h_{i,v}} \sqrt{\alpha_m P_s}\hat{x}_m, \tag{4.31}$$

where $\hat{x}_m$ is the estimated symbol of user UE_m at UE_i.

4.4.1.2 Complexity

In this section, receiver complexity is analyzed for both SMA and SSK-NOMA to provide comparisons with conventional NOMA networks. The complexity analysis is provided in terms of the number of complex operations at the users. Thus, the complexity for detectors should be derived. Let firstly analyze the complexity of SM detectors for both SMA (4.4) and SSK-NOMA (4.28). With the aid of [155], the complexity of SM detectors is given as

$$\delta_{SM} = 2N_r N_t + N_t M_\ell + M_\ell, \quad \ell = SMA, SSK - NOMA. \tag{4.32}$$

where M_ℓ is the total constellation size transmitted by active antenna and it was defined as $M_{SMA} \triangleq M_1$ and $M_{SSK-NOMA} \triangleq M_T \triangleq \prod_{i=2}^{L} M_i$ in Section 4.2.1 and in the previous subsection, respectively.

The receiver complexity for intra-cell users (i.e., UE_2 in SMA, UE_i, $i = 2, 3, \ldots, L$) is computed according by the required ML and SIC operations. The receiver complexity for ML detection is defined as

$$\delta_{ML,i} = 4N_r M_i, \tag{4.33}$$

where M_i is the modulation size of ith user. Whereas only the ML detection is required in SMA and for the UE_2 in SSK-NOMA, the users UE_i, $i = 3, 4, \ldots, L$ should implement SIC to detect own symbols. Hence, the complexity of a SIC process given (4.31) in SSK-NOMA is obtained as

$$\delta_{SIC,i} = \sum_{m=2}^{i-1} (4N_r M_m + 2N_r) \quad m < i, \ i = 3, 4, \ldots, L. \tag{4.34}$$

It is noteworthy that given complexity of a SIC process for SSK-NOMA includes the required ML detection complexities for detecting and subtracting symbols of users which are before in the detecting order ($m < i$).

In order to obtain total complexity of SMA and SSK-NOMA, the numbers of the required SM detector, ML detector and SIC operations should be derived. In SMA, since only two users are served and no IUI is introduced, the required operations are given

$$\mathcal{O}_{SM}^{SMA} = 1,$$
$$\mathcal{O}_{ML}^{SMA} = 1. \tag{4.35}$$

On the other hand, in SSK-NOMA, the intra-cell users $-UE_i, \; i = 3, 4, \ldots, L-$ should implement $i-2$ times iterative SIC processes to subtract effect of the other users' symbols in addition to ML detector. UE_2 should implement only ML detector and cell-edge user $-UE_1-$ should implement only SM detector. Thus, the numbers of required operations for SSK-NOMA are given as

$$
\begin{aligned}
\mathcal{O}_{SM}^{SSK-NOMA} &= 1, \\
\mathcal{O}_{ML}^{SSK-NOMA} &= L - 1, \\
\mathcal{O}_{SIC}^{SSK-NOMA} &= \sum_{i=3}^{L}(i-2) = \frac{(L-2)(L-1)}{2}.
\end{aligned}
\tag{4.36}
$$

By using (4.32), (4.33), (4.35) and (4.36), total receiver complexity for SMA and SSK-NOMA are derived as

$$
\delta_{SMA} = \underbrace{2N_rN_t + N_tM_1 + M_1}_{SM\ detection} + \underbrace{4N_rM_1}_{ML\ detection},
\tag{4.37}
$$

and

$$
\delta_{SSK-NOMA} = \underbrace{2N_rN_t + N_tM_T + M_T}_{SM\ detection} + \underbrace{\sum_{i=2}^{L} 4N_rM_i}_{ML\ detection} + \underbrace{\sum_{i=3}^{L}\sum_{m=2}^{i-1}(4N_rM_m + 2N_r)}_{SIC\ processes}.
\tag{4.38}
$$

In order to provide comparison with conventional NOMA schemes, receiver complexity for conventional NOMA is also derived. It is hereby noted that complexity of conventional NOMA is provided for SIMO (i.e., $1 \times N_r$) case for fairness since SSK-NOMA activates only one transmit antenna during one symbol duration. Otherwise the complexity of conventional NOMA would increase exponentially with N_t. All users in conventional NOMA are split into power domain with different power allocation coefficients. Thus, the first user in NOMA -cell-edge user- implements ML and the other users implement iterative SIC processes and ML to detect their symbols. The required numbers of operations in conventional NOMA are given as

$$
\begin{aligned}
\mathcal{O}_{ML}^{NOMA} &= L, \\
\mathcal{O}_{SIC}^{NOMA} &= \sum_{i=2}^{L}(i-1) = \frac{L(L-1)}{2}.
\end{aligned}
\tag{4.39}
$$

By using the complexities (4.33) and (4.34), total receiver complexity of conventional NOMA is derived as

$$
\delta_{NOMA} = \underbrace{\sum_{i=1}^{L} 4N_rM_i}_{ML\ detection} + \underbrace{\sum_{i=2}^{L}\sum_{m=1}^{i-1}(4N_rM_m + 2N_r)}_{SIC\ processes}.
\tag{4.40}
$$

110

Total receiver complexity comparison between SSK-NOMA and conventional NOMA is given in Table 4.2. This comparison also includes the comparison between SMA and NOMA when the number of users $L = 2$. In comparisons, all intra-cell users in SSK-NOMA and all users in NOMA are modulated by the same M-ary modulation constellations (i.e., $M_i = M$). Thus, for fairness in terms of achievable rate, the number of transmit antenna in SSK-NOMA or SMA is also equal to that (i.e., $N_t = M$). It is clear that SMA is superior to NOMA in terms of complexity. Based on the comparisons, one can easily say that SSK-NOMA is also superior to conventional NOMA schemes in terms of receiver complexity in particular when the number of users (L) and the modulation level (M) are relatively lower. On the other hand, the more number of users and the higher modulations sizes are chosen, the more complexity is required in SSK-NOMA since the complexity of SM detection at the cell-edge user in SSK-NOMA will increase with the total SC symbol size (M_T). Nevertheless, considering the gain in performance of SSK-NOMA compared to conventional NOMA which is provided in Section 4.4, this complexity can be considered as affordable. In addition, in all cases, the other users except cell-edge user require much less complexity since the number of SIC process is decreased by assigning one user into spatial domain.

Table 4.2: Complexity comparison of SMA/SSK-NOMA with NOMA

L	M	N_r	Complexity		
			δ_{SMA}	$\delta_{SSK-NOMA}$	δ_{NOMA}
2	2	2	30	-	52
2	4	4	116	-	200
3	2	2	-	72	108
3	4	4	-	312	408
4	2	2	-	140	184
4	4	4	-	760	688
5	2	2	-	240	280
5	4	4	-	2000	1040

4.4.2 Performance Analysis

4.4.2.1 Ergodic Capacity Analysis

Ergodic capacity analysis of UE_1 in SSK-NOMA is very similar to ergodic capacity of UE_2 in SMA (section 4.2.2). Hence, the ergodic capacity for UE_1 is derived as by taking steps between (4.10)-(4.11)

$$C_1 = \log_2 N_t \left[1 - P_1(e) \right], \tag{4.41}$$

where $P_1(e)$ is the average BEP for UE_1 and it is derived in the following subsections for SSK-NOMA.

In order to derive ergodic capacities of intra-cell users in SSK-NOMA, the achievable rates are defined in terms of Shannon limit and it is given as

$$R_i = \log_2 \left(1 + SINR_i \right) \quad i = 2, 3, \ldots, L, \tag{4.42}$$

where $SINR_i$ is defined as

$$SINR_i = \frac{\alpha_i \rho_s \gamma_{si}}{1 + \left\{ \beta \sum_{m=2}^{i-1} \alpha_m + \sum_{p=i+1}^{L} \alpha_p \right\} \rho_s \gamma_{si}}, \tag{4.43}$$

where β denotes the imperfect SIC factor for the symbols of users which are before in the detecting order $(m < i)$. The second sum operator in the denominator is defined the IUI for the symbols of users which are later in the detection order $(p > i)$. One can easily see that, for $i = 2$ the the term for imperfect SIC effect and for $i = L$ the term for IUI become zero "0". Thus, with some simplifications, the achievable rates of intra-cell users turn out to be

$$\begin{aligned} R_i = & \log_2 \left(1 + \left\{ \sum_{\ell=i}^{L} \alpha_\ell + \beta \sum_{m=2}^{i-1} \alpha_m \right\} \rho_s \gamma_{si} \right) \\ & - \log_2 \left(1 + \left\{ \sum_{p=i+1}^{L} \alpha_p + \beta \sum_{m=2}^{i-1} \alpha_m \right\} \rho_s \gamma_{si} \right), \quad i = 2, 3, \ldots, L. \end{aligned} \tag{4.44}$$

Ergodic capacity of each user is derived by

$$C_i = \int_0^\infty \log_2 R_i p_{\gamma_{si}}(\gamma_{si}) d\gamma_{si} \quad i = 2, 3, \ldots, L. \tag{4.45}$$

112

Letting $\theta_1 = \left\{ \sum_{\ell=i}^{L} \alpha_\ell + \beta \sum_{m=2}^{i-1} \alpha_m \right\} \rho_s \sigma_{si}^2$ and $\theta_2 = \left\{ \sum_{p=i+1}^{L} \alpha_p + \beta \sum_{m=2}^{i-1} \alpha_m \right\} \rho_s \sigma_{si}^2$, by substituting PDF of γ_{si} (4.7) into (4.45), with the aid of [89, eq. (4.337.5)], ergodic capacity of each intra-cell user in SSK-NOMA is derived as

$$
C_i = \sum_{j=1}^{2} (-1)^{j-1} \frac{\log_2 e}{\Gamma(N_r)} \sum_{\lambda=0}^{N_r-1} \frac{(N_r-1)!}{(N_r-1-\lambda)!}
$$
$$
\left[\frac{(-1)^{N_r-\lambda-2}}{\theta_j^{N_r-1-\lambda}} e^{1/\theta_j} \mathbf{Ei} \left(-\frac{1}{\theta_j} \right) + \sum_{\kappa=1}^{N_r-1-\lambda} \frac{(\kappa-1)!}{(-\theta_j)^{N_r-1-\lambda-\kappa}} \right], i = 2, 3, \ldots, L.
$$
(4.46)

Lastly, ergodic sum rate of SSK-NOMA is given as

$$
C_{sum}^{(SSK-NOMA)} = \sum_{i=1}^{L} C_i.
$$
(4.47)

4.4.2.2   Outage Probability Analysis

Likewise the ergodic rate, OP of UE_1 in SSK-NOMA is derived as the OP of UE_2 in SMA. Hence, repeating steps between (4.16)-(4.17), the OP of UE_1 in SSK-NOMA is obtained as

$$
P_1(out) = \int_{\psi_1}^{\infty} P_1(e|\gamma_{s1}) p_{\gamma_{s1}}(\gamma_{s1}) d\gamma_{s1}
$$
$$
= \int_{0}^{\infty} P_1(e|\gamma_{s1}) p_{\gamma_{s1}}(\gamma_{s1}) d\gamma_{s1} - \int_{0}^{\psi_1} P_1(e|\gamma_{s1}) p_{\gamma_{s1}}(\gamma_{s2}) d\gamma_{s1},
$$
(4.48)

where $\psi_1 = 1 - \frac{\acute{R}_1}{\log_2 N_t}$. Just as in SMA, when the target rate is equal to $\acute{R}_1 = \log_2 N_t$, the OP of UE_1 turns out to be average BEP of UE_1 which is derived in the next subsection.

The outage events for intra-cell users in SSK-NOMA is given by

$$
P_i(out) = P(R_i < \acute{R}_i),
$$
(4.49)

where $\acute{R}_i$ is the target-rate/QoS-requirement for each user.

Theorem 4.1. *The OP of ith user is given by*

$$
P_i(out) = P_r(\gamma_{si} < \psi_i)
$$
$$
= F_{\gamma_{si}}(\psi_i),
$$
(4.50)

where $F_{\gamma_{si}}(\psi_i)$ is the CDF of γ_{si} and

$$\psi_i = \frac{1}{\rho_s}max\left(\frac{\phi_i}{\alpha_i - \left\{\beta\sum_{\ell=2}^{i-1}\alpha_\ell + \sum_{p=i+1}^{L}\alpha_p\right\}\phi_i}, \cdots \frac{\phi_m}{\alpha_m - \left\{\beta\sum_{\ell=2}^{m-1}\alpha_\ell + \sum_{p=m+1}^{L}\alpha_p\right\}\phi_m},\right.$$
$$\left.\cdots, \frac{\phi_2}{\alpha_2 - \sum_{p=3}^{L}\alpha_p\phi_2}\right), \ m < i, \ i = 2,3\ldots,L.$$

$$(4.51)$$

Proof. Outage event at user i occurs when the target rate of user i cannot be achieved. In addition to this, user i remains in outage if any symbols of users cannot be detected during iterative SIC process (Hereby, it is not meant correct or erroneous SIC. It means that target rate (QoS) for the users which are before in the detecting order ($m < i$) cannot be succeeded at user i.). Thus, the OP of user i is revised as

$$P_i(out) = P(R_i < \acute{R}_i)\cup P(R_{i\to i-1} < \acute{R}_{i-1})\cup\cdots\cup P(R_{i\to m} < \acute{R}_m)\cup\cdots\cup P(R_{i\to 2} < \acute{R}_2),$$

$$(4.52)$$

where $R_{i\to m}$ is the achievable rate for the symbols of user m during SIC at user i, and it is given as

$$R_{i\to m} = \log_2\left(1 + SINR_{i\to m}\right)$$
$$= \log_2\left(1 + \frac{\alpha_m\rho_s\gamma_{si}}{1 + \left\{\beta\sum_{\ell=2}^{m-1}\alpha_\ell + \sum_{p=m+1}^{L}\alpha_p\right\}\rho_s\gamma_{si}}\right). \qquad (4.53)$$

Hence, the OP of user i becomes as

$$P_i(out) = P\left(\frac{\alpha_i\rho_s\gamma_{si}}{1 + \left\{\beta\sum_{\ell=2}^{i-1}\alpha_\ell + \sum_{p=i+1}^{L}\alpha_p\right\}\rho_s\gamma_{si}} < \phi_i\right)\cup\ldots$$
$$\cup P\left(\frac{\alpha_m\rho_s\gamma_{si}}{1 + \left\{\beta\sum_{\ell=2}^{m-1}\alpha_\ell + \sum_{p=m+1}^{L}\alpha_p\right\}\rho_s\gamma_{si}} < \phi_m\right)\cup\ldots \qquad (4.54)$$
$$\cup P\left(\frac{\alpha_2\rho_s\gamma_{si}}{1 + \sum_{p=3}^{L}\alpha_p\rho_s\gamma_{si}} < \phi_2\right) \ m < i, \ i = 2,3\ldots,L,$$

and with some algebraic manipulations, it is derived as in (4.50) so the proof is completed.

$\square$

Finally, substituting CDF of γ_{si} into (4.50), the OP of user i in SSK-NOMA is derived as

$$P_i(out) = 1 - e^{-\psi_i/\sigma_{si}^2}\sum_{\lambda=1}^{N_r}\frac{(\psi_i/\sigma_{si}^2)^{\lambda-1}}{(\lambda-1)!}. \qquad (4.55)$$

114

4.4.2.3 Bit Error Probability (BEP) Analysis

The BEP of UE_1 is obtained by union bound likewise in SMA. Since the optimal SM detector is modified in SSK-NOMA, the BEP is given SM detection should be revised also. Considering the total SC symbol with dimension M_T is transmitted by BS in SSK-NOMA, the BEP of UE_1 is derived by repeating steps between (4.21)-(4.24). The BEP for UE_1 is derived as

$$P_1(e) \leq \frac{N_t}{2} \mu_1^{N_r} \log_2 M_T \sum_{\lambda=0}^{N_r-1} \binom{N_r - 1 + \lambda}{\lambda} (1 - \mu_1)^{\lambda}, \tag{4.56}$$

where $\mu_1 = \frac{1}{2}\left(1 - \sqrt{\frac{\sigma_a^2}{2+\sigma_a^2}}\right)$ and $\sigma_a^2 = \frac{\rho_s \sigma_{s1}^2 \left(|\chi_k|^2 + |\hat{\chi}_k|^2\right)}{4}$. It is noteworthy that σ_a^2 changes according to transmitted χ_k and estimated $\hat{\chi}_k$. χ_k includes symbols with different energy levels since SC of users' symbols is applied. Thus, given average BEP should be averaged considering all scenarios.

In order to derive BEP for intra-cell users, the total constellation of transmitted SC symbol should be considered. In addition, for users i.e., $UE_i, i = 3, 4, \ldots, L$, correct SIC and erroneous SIC cases should be handled likewise in downlink NOMA. However, when $L > 3$, the analysis of erroneous SIC becomes intractable. Hence, exact analysis is provided for $L = 3$ whereas a union bound is derived for $L > 3$.

4.4.2.3.1 Exact Analysis for $L = 3$

Let firstly assume $L = 3$. In this case, the number of users multiplexed by NOMA is only two and for two-user NOMA networks, exact BEP analysis is provided in Section 2.2.2. when QPSK and BPSK are used for users' symbols. In this section, it is assumed that both users are modulated by QPSK.

Proposition 4.1. *If QPSK is used for both NOMA users (i.e., UE_2 and UE_3) and Gray mapping is applied, the conditional BEP of UE_2 is given as*

$$P_2(e|\gamma_{s2}) = \sum_{j=1}^{2} \frac{1}{2} Q\left(\sqrt{2\rho_s \epsilon_j \gamma_{s2}}\right), \tag{4.57}$$

where $\epsilon_1 = {}^1\!/\!{}_2 \left(\sqrt{\alpha_2} + \sqrt{\alpha_3}\right)^2$ and $\epsilon_2 = {}^1\!/\!{}_2 \left(\sqrt{\alpha_2} - \sqrt{\alpha_3}\right)^2$.

Table 4.3: Base-band SC symbols (χ) for L=3 and QPSK at BS

			Binary symbols of UE_3			
			00	01	10	11
Binary symbols of UE_2	00	Re	$\sqrt{\alpha_2/2}+\sqrt{\alpha_3/2}$	$\sqrt{\alpha_2/2}-\sqrt{\alpha_3/2}$	$\sqrt{\alpha_2/2}+\sqrt{\alpha_3/2}$	$\sqrt{\alpha_2/2}-\sqrt{\alpha_3/2}$
		Im	$\sqrt{\alpha_2/2}+\sqrt{\alpha_3/2}$	$\sqrt{\alpha_2/2}+\sqrt{\alpha_3/2}$	$\sqrt{\alpha_2/2}-\sqrt{\alpha_3/2}$	$\sqrt{\alpha_2/2}-\sqrt{\alpha_3/2}$
	01	Re	$-\sqrt{\alpha_2/2}+\sqrt{\alpha_3/2}$	$-\sqrt{\alpha_2/2}-\sqrt{\alpha_3/2}$	$-\sqrt{\alpha_2/2}+\sqrt{\alpha_3/2}$	$-\sqrt{\alpha_2/2}-\sqrt{\alpha_3/2}$
		Im	$\sqrt{\alpha_2/2}+\sqrt{\alpha_3/2}$	$\sqrt{\alpha_2/2}+\sqrt{\alpha_3/2}$	$\sqrt{\alpha_2/2}-\sqrt{\alpha_3/2}$	$\sqrt{\alpha_2/2}-\sqrt{\alpha_3/2}$
	10	Re	$\sqrt{\alpha_2/2}+\sqrt{\alpha_3/2}$	$\sqrt{\alpha_2/2}-\sqrt{\alpha_3/2}$	$\sqrt{\alpha_2/2}+\sqrt{\alpha_3/2}$	$\sqrt{\alpha_2/2}-\sqrt{\alpha_3/2}$
		Im	$-\sqrt{\alpha_2/2}+\sqrt{\alpha_3/2}$	$-\sqrt{\alpha_2/2}+\sqrt{\alpha_3/2}$	$-\sqrt{\alpha_2/2}-\sqrt{\alpha_3/2}$	$-\sqrt{\alpha_2/2}-\sqrt{\alpha_3/2}$
	11	Re	$-\sqrt{\alpha_2/2}+\sqrt{\alpha_3/2}$	$-\sqrt{\alpha_2/2}-\sqrt{\alpha_3/2}$	$-\sqrt{\alpha_2/2}+\sqrt{\alpha_3/2}$	$-\sqrt{\alpha_2/2}-\sqrt{\alpha_3/2}$
		Im	$-\sqrt{\alpha_2/2}+\sqrt{\alpha_3/2}$	$-\sqrt{\alpha_2/2}+\sqrt{\alpha_3/2}$	$-\sqrt{\alpha_2/2}-\sqrt{\alpha_3/2}$	$-\sqrt{\alpha_2/2}-\sqrt{\alpha_3/2}$

Proof. When QPSK is used for both users, the transmitted total SC symbol (χ) at BS is given in Table 4.3. Considering the ML decision rules for QPSK, if the steps given BEP analysis for downlink NOMA (2.21)-(2.22) are repeated, the BEP is derived as in (4.57).

$\square$

Substituting PDF of γ_{s2} into (4.57), with the aid of [149, eq. (64)], the average BEP for UE_2 is derived as

$$P_2(e) = \sum_{j=1}^{2} \frac{\left(\frac{1-\mu_2}{2}\right)^{N_r}}{2} \sum_{\lambda=0}^{N_r-1} \binom{N_r-1+\lambda}{\lambda} \left(\frac{1+\mu_2}{2}\right)^{\lambda}, \tag{4.58}$$

$\mu_2 = \sqrt{\frac{\epsilon_j \sigma_{s2}^2}{1+\epsilon_j \sigma_{s2}^2}}$.

Proposition 4.2. *The conditional BEP of UE_3 is given as*

$$P_3(e|\gamma_3) = \frac{1}{2}\left[2Q\left(\sqrt{2\epsilon_3 \rho_s \gamma_{s3}}\right)\right.$$
$$\left.-Q\left(\sqrt{2\epsilon_1 \rho_s \gamma_{s3}}\right) + Q\left(\sqrt{2\epsilon_2 \rho_s \gamma_{s3}}\right) + Q\left(\sqrt{2\epsilon_4 \rho_s \gamma_{s3}}\right) - Q\left(\sqrt{2\epsilon_5 \rho_s \gamma_{s3}}\right)\right], \tag{4.59}$$

where $\epsilon_3 = {\alpha_3}/{2}$, $\epsilon_4 = {}^1/_2\left(2\sqrt{\alpha_2}+\sqrt{\alpha_3}\right)^2$ and $\epsilon_5 = {}^1/_2\left(2\sqrt{\alpha_2}-\sqrt{\alpha_3}\right)^2$.

Proof. Considering correct SIC, remained signal after SIC is only symbols of UE_3 with α_3 coefficients and channel fading γ_{s3}. Recalling this is conditional probability on correct

SIC and the probability of correct SIC can be derived by adopting (4.57). Then, by taking steps between (2.24) and (2.26) for QPSK decision rule, the conditional BEP under correct SIC is derived as

$$P_3(e|correct_{x_2}) = \frac{1}{2}\left[2Q\left(\sqrt{2\epsilon_3\rho_s\gamma_{s3}}\right) - Q\left(\sqrt{2\epsilon_1\rho_s\gamma_{s3}}\right)\right].\tag{4.60}$$

In the second case, under erroneous SIC, the remained signal at UE_3 is given by $\mathbf{y_3'} = \Upsilon\sqrt{P_s}\mathbf{h_{3,v}} + \mathbf{w_3}$. Constellation for Υ is given in Table 4.4.

Table 4.4: Base-band symbols at UE_3 after erroneous detection of x_2 symbols

		Υ	
		Re	Im
Binary symbols of UE_2	00	$2\sqrt{\alpha_2/2} + \sqrt{\alpha_3/2}$	$2\sqrt{\alpha_2/2} + \sqrt{\alpha_3/2}$
	01	$2\sqrt{\alpha_2/2} - \sqrt{\alpha_3/2}$	$2\sqrt{\alpha_2/2} + \sqrt{\alpha_3/2}$
	10	$2\sqrt{\alpha_2/2} + \sqrt{\alpha_3/2}$	$2\sqrt{\alpha_2/2} - \sqrt{\alpha_3/2}$
	11	$2\sqrt{\alpha_2/2} - \sqrt{\alpha_3/2}$	$2\sqrt{\alpha_2/2} - \sqrt{\alpha_3/2}$

Recalling the QPSK decision rule and the priori probability of erroneous detection of x_2 symbol, the conditional BEP for UE_3 under the condition erroneous SIC is obtained by repeating steps between (2.27) and (2.29). It is derived as

$$P_3(e|error_{x_2}) = \frac{1}{2}\left[Q\left(\sqrt{2\epsilon_2\rho_s\gamma_{s3}}\right) + Q\left(\sqrt{2\epsilon_4\rho_s\gamma_{s3}}\right) - Q\left(\sqrt{2\epsilon_5\rho_s\gamma_{s3}}\right)\right].\tag{4.61}$$

The total conditional BEP for UE_3 is obtained by $P_3(e|\gamma_3) = P_3(e|correct_{x_2}) + P_3(e|error_{x_2})$ as in (4.59), so the proof is completed. □

Substituting PDF of γ_{s3} into (4.59), the average BEP of UE_3 is derived as

$$P_3(e) = \sum_{j=1}^{5} \frac{A_j(-1)^j\left(\frac{1-\mu_3}{2}\right)^{N_r}}{2} \sum_{\lambda=0}^{N_r-1}\binom{N_r-1+\lambda}{\lambda}\left(\frac{1+\mu_3}{2}\right)^{\lambda},\tag{4.62}$$

where $A_j = -2 \; if, c = 3, \; otherwise \; 1$ and $\mu_3 = \sqrt{\frac{\epsilon_j\sigma_{s3}^2}{1+\epsilon_j\sigma_{s3}^2}}$.

4.4.2.3.2 Union Bound Analysis for $L \geq 3$

On the other hand, secondly $L > 3$ is assumed. In this case, the union bound for BEP is derived for SISO-NOMA networks based on the pairwise error probability (PEP) in [172]. By utilizing given PEP in [172], conditional PEP for intra-cell users in SSK-NOMA is given as

$$PEP(x_i \rightarrow \hat{x}_i | \mathbf{h_{i,v}}) = Q\left(\frac{\varphi_i \sqrt{\mathbf{h_{i,v} h_{i,v}^H}}}{\vartheta}\right), \tag{4.63}$$

where

$$\varphi_i = \sqrt{\alpha_i \rho_s} \left|\triangle_i\right|^2 + 2[Re\{\triangle_i \underbrace{\sum_{p=i+1}^{L} \sqrt{\alpha_p \rho_s} x_p^*}_{noise\ term\ for\ p>i}\} + Re\{\triangle_i \underbrace{\sum_{q=2}^{i-1} \sqrt{\alpha_q \rho_s} \triangle_q^*}_{SIC\ errors\ for\ q<i}\}]. \tag{4.64}$$

It is given as $\vartheta = \sqrt{2} \left|\triangle_i\right|$ and $\triangle_i = x_i - \hat{x}_i$ [172, Eq. (17)- Eq. (20)]. Then, by averaging PEP over instantaneous γ_{si} by using PDF (4.7), the average PEP is obtained as

$$PEP(x_i \rightarrow \hat{x}_i) = \left(\frac{1-\xi_i}{2}\right)^{N_r} \sum_{\lambda=0}^{N_r-1} \binom{N_r - 1 + \lambda}{\lambda} \left(\frac{1+\xi_i}{2}\right)^{\lambda}, \tag{4.65}$$

where $\xi_i = \sqrt{\frac{\sigma_{si}^2 \varphi_i^2}{2\vartheta^2 + \sigma_{si}^2 \varphi_i^2}}$. Then the union BER is derived by averaging all possibilities of PEP as

$$BER_i^{union} \leq \sum_{x_i} N(x_i \rightarrow \hat{x}_i) \sum_{x_i \neq \hat{x}_i} PEP(x_i \rightarrow \hat{x}_i | x_p, \triangle_p) \quad \forall p \neq i, \tag{4.66}$$

where $N(x_i \rightarrow \hat{x}_i)$ is the Hamming distance between x_i and $\hat{x}_i$.

4.5 NUMERICAL RESULTS

In this section, derived analytical expressions for SMA and SSK-NOMA are validated with computer simulations.

Spatial Multiple Access (SMA): Firstly, validations of SMA in terms of EC are presented. $\sigma_{s1}^2 = \sigma_{s2}^2 = 0dB$ is assumed. In SMA, it is assumed to be $N_r = N_t$. In Figure 4.3, ergodic capacities of users and sum-rate of SMA are presented. It is shown that derived expressions match perfectly with simulations.
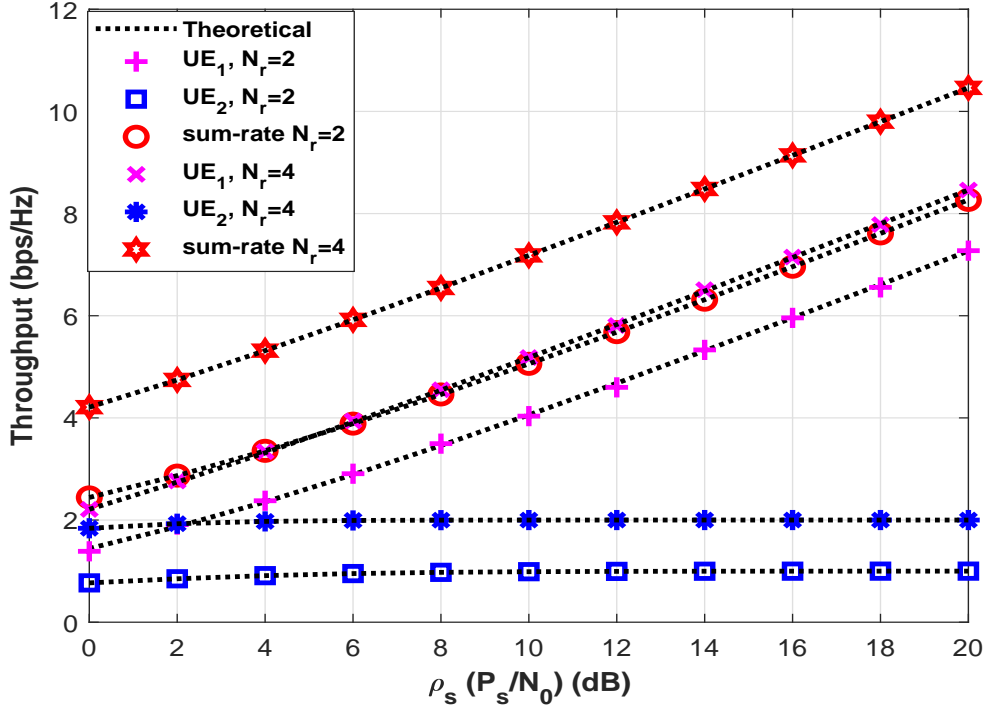
Figure 4.3: Capacity performance of SMA when $\sigma_{s1}^2 = \sigma_{s2}^2 = 0dB$ and $N_r = N_t$

Then, outage performances of users in SMA are provided in Figure 4.4. Target rates are chosen according to receive antenna number such as $\acute{R}_1 = \acute{R}_2 = \log_2 N_r$. Likewise in EC, $N_t = N_r$ is assumed. One can see that analysis matches perfectly with simulations.

Lastly for SMA, validations of derived BEP expressions are provided for the same channel conditions above in Figure 4.5. One can easily see that derived BEP expression for UE_1 matches perfectly with simulations. In addition, provided union bound for UE_2 is also very tight.

SSK-NOMA: Secondly in this section, derived expressions of SSK-NOMA networks are validated. In the validations, it is assumed that $\sigma_{si}^2 = 2\sigma_{s(i-1)}^2$ and $\sigma_{s1}^2 = 0dB$. The power allocation coefficients for NOMA users are fixed and chosen as $\alpha_i = [0.8, \ 0.2]$, $\alpha_i = [0.7, \ 0.2, \ 0.1]$ and $\alpha_i = [0.6, \ 0.25, \ 0.1, \ 0.05]$ according to number of NOMA users. Likewise SMA, $N_t = N_r$ is assumed.

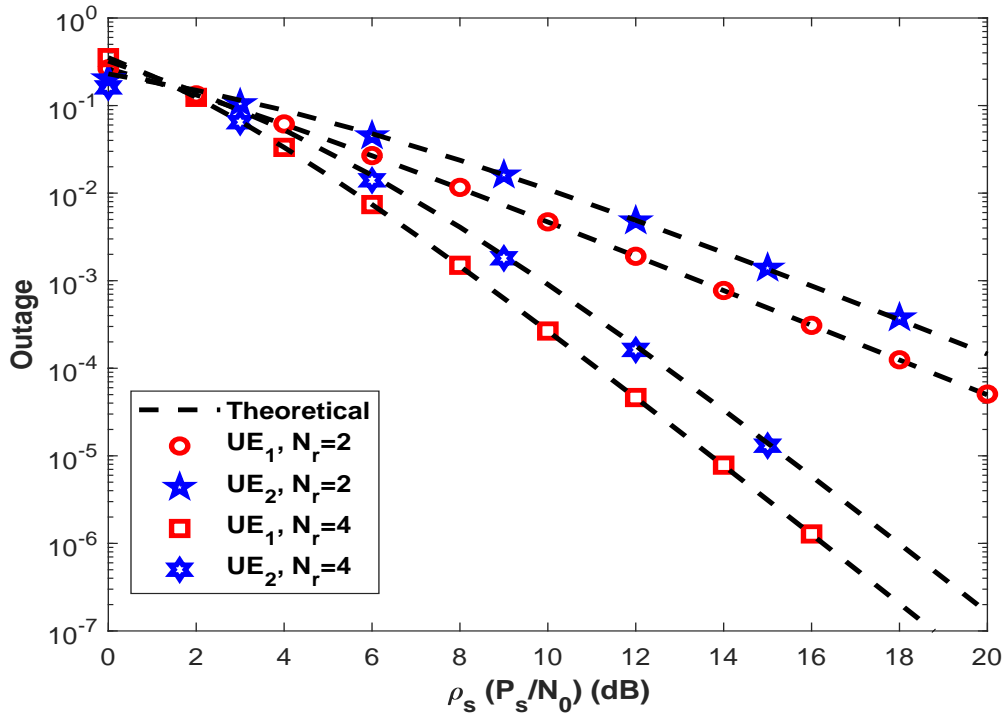In Figure 5.6, sum-rates of SSK-NOMA are presented when the number of users is equal

Figure 4.4: Outage performance of SMA when $\sigma_{s1}^2 = \sigma_{s2}^2 = 0dB$, $N_r = N_t$ and $\acute{R}_1 = \acute{R}_2 = \log_2 N_r$
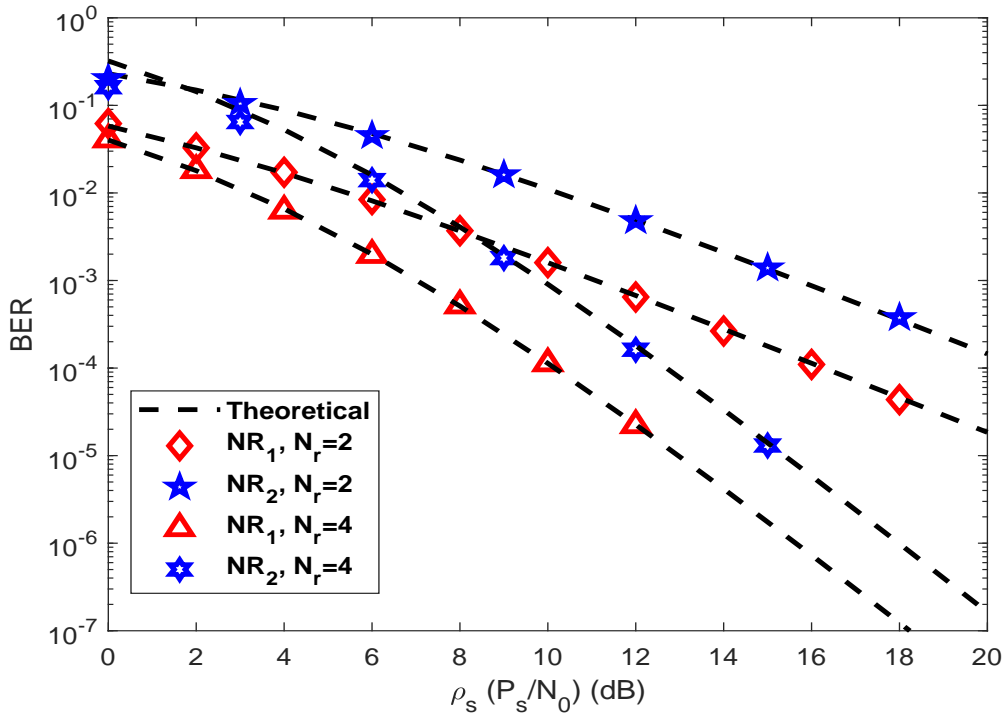

Figure 4.5: BER performance of SMA when $\sigma_{s1}^2 = \sigma_{s2}^2 = 0dB$ and $N_r = N_t$
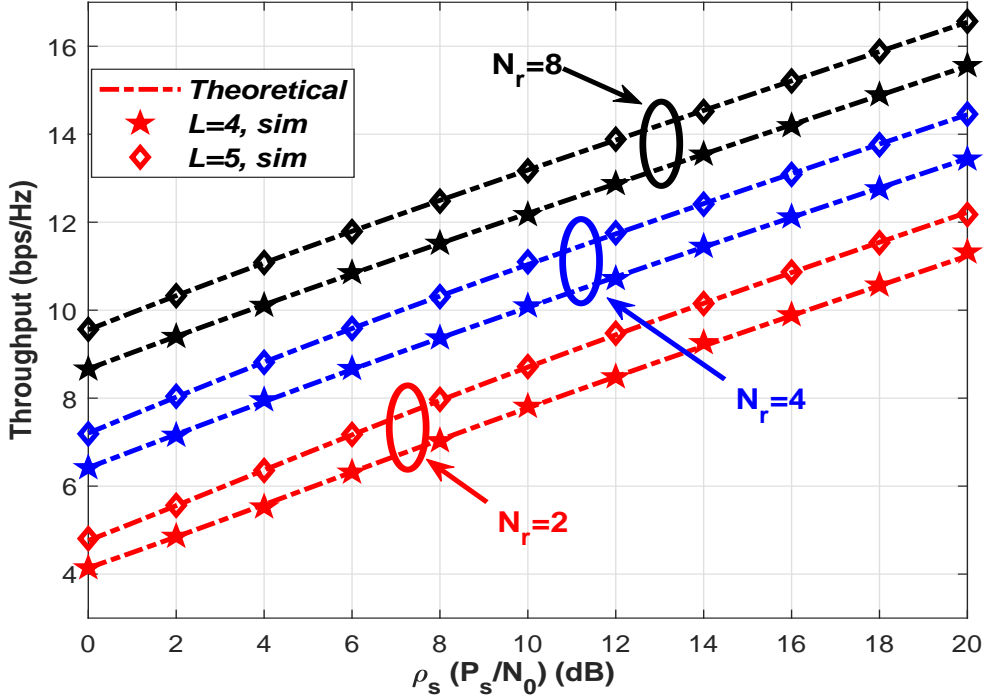
Figure 4.6: Capacity performance of SSK-NOMA when $L = 4, 5$ and $N_r = N_t = 2, 4, 8$

to $L = 4, 5$ and the number of antennas is equal to $N_r = 2, 4, 8$. It is proved that derived expressions for EC match perfectly with simulations.

Then, outage performances of users in SSK-NOMA are provided in Figure 5.7 when the number of users is equal to $L = 4$. Likewise in SMA, the target rates of users are assumed to be $\acute{R}_2 = \acute{R}_3 = \acute{R}_3 = \log_2 N_r$. In outage comparisons, outage performance of UE_1 is not presented since it is equal to error performance (BER) of UE_1 as explained in section 4.4.2.2 which are given in the next figures.

Finally, validations for derived BEP expressions of SSK-NOMA are presented in Figure 5.8 and Figure 5.9. In Figure 5.8, it is assumed that $L = 3$ and QPSK is used for NOMA users (i.e., $i \geq 2$). In this case, derived exact BEP expressions for NOMA users are validated and they match perfectly with simulations. For UE_1, derived union bound is also validated. It matches well and it is very tight in the medium-high SNR regime such as in conventional SSK networks. In Figure 5.9, validations for union bound analysis of NOMA users are presented when $L = 4$. One can easily see that derived union bound for
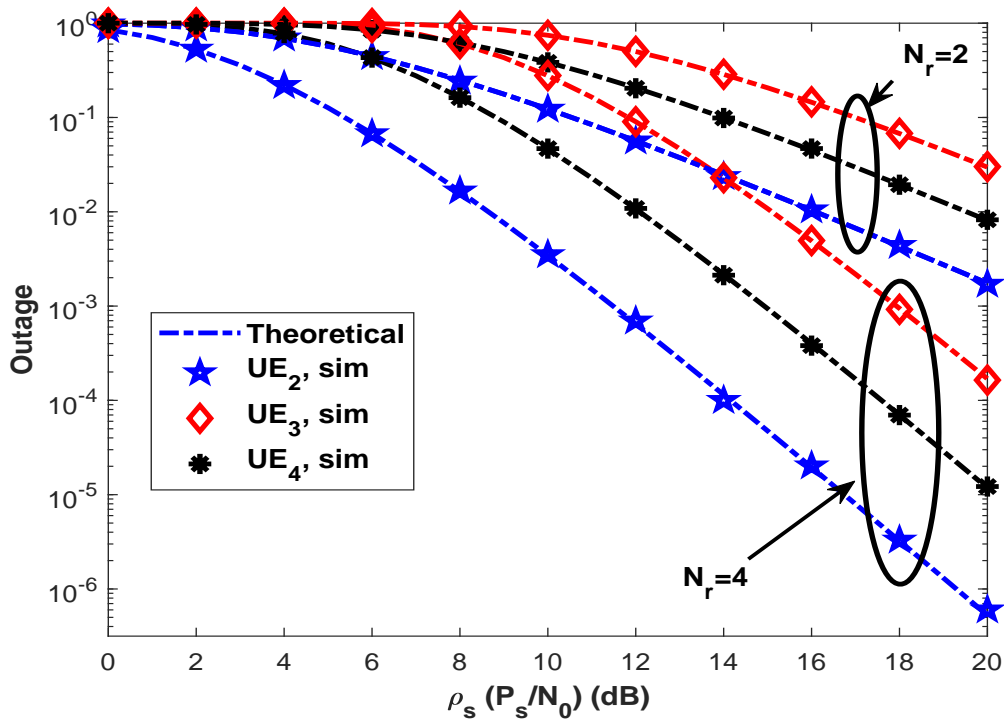
Figure 4.7: Outage performance of SSK-NOMA when $L = 4$, $N_r = N_t = 2, 4$ and $\acute{R}_2 = \acute{R}_3 = \acute{R}_4 = \log_2 N_r$
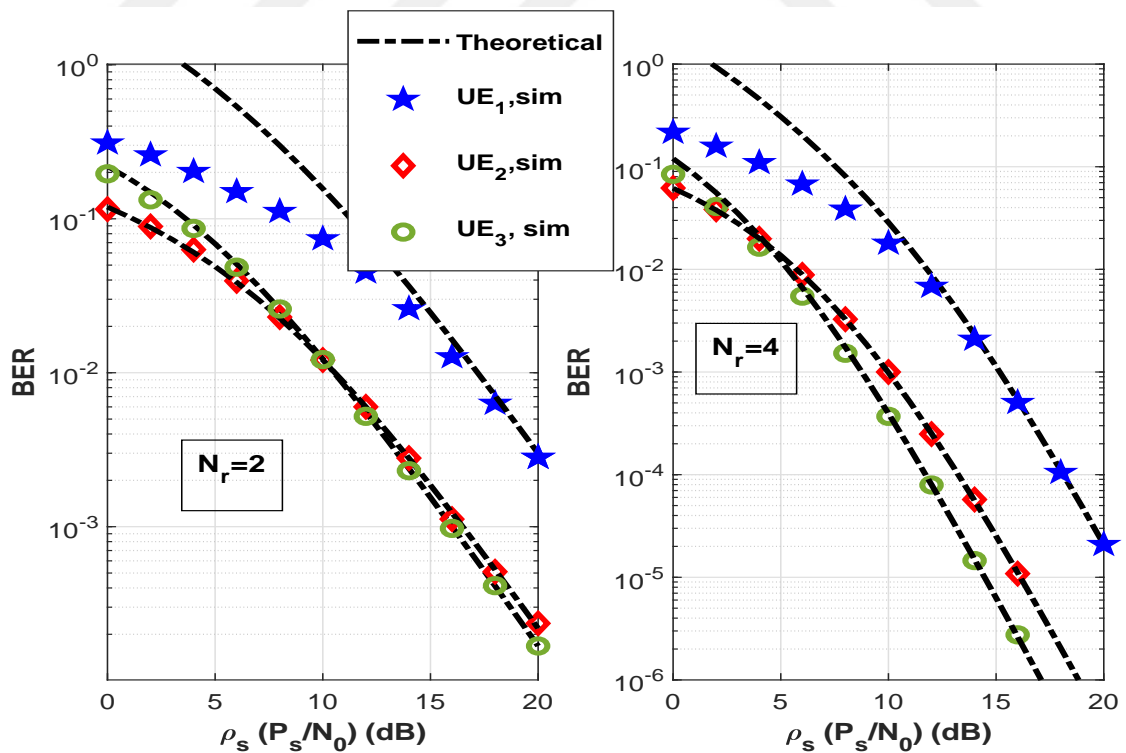

Figure 4.8: Error performance of SSK-NOMA when $L = 3$ a) $N_r = N_t = 2$ b) $N_r = N_t = 4$
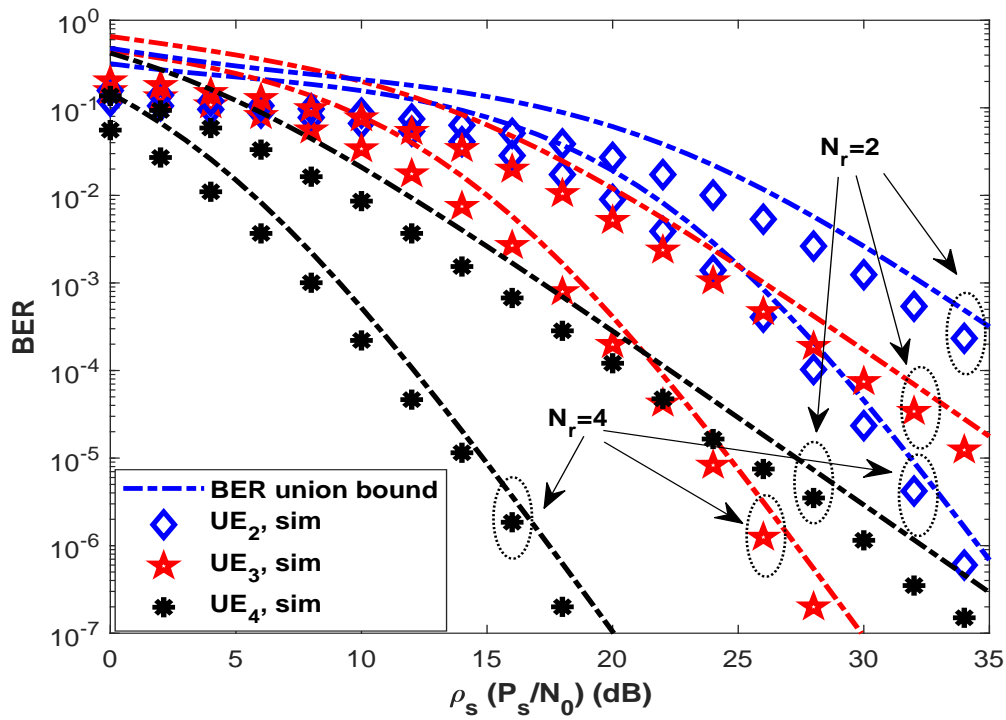
Figure 4.9: Error performance of NOMA users in SSK-NOMA when $L = 4$, $N_r = N_t = 2, 4$

NOMA users in SSK-NOMA also matches well with simulations.

CHAPTER 5

SIMULATION RESULTS AND PERFORMANCE EVALUATION

In this chapter, extensive simulations are presented to evaluate performances of NOMA involved systems and to compare them with the OMA counterparts.

Conventional NOMA networks: Let firstly present results for both conventional SISO downlink and uplink networks. In Figure 5.1 and in Figure 5.2, EC is presented in downlink network where $\sigma_{s1}^2 = 3dB$ and $\sigma_{s2}^2 = 0dB$ for $\alpha_1 = 0.1$ and $\alpha_1 = 0.3$, respectively. NOMA results are given for various imperfect SIC factors (i.e., $\beta = 0.05$, $\beta = 0.001$, $\beta = 0$). Results for OMA networks[1] are also provided. Based on given results, one can see that NOMA outperforms OMA in terms of sum-rate. Nevertheless, considering the users' individual achievable rate, UE_2 in NOMA has worse achievable rate than OMA in the medium-high SNR regime. This can be explained that achievable rate of UE_2 in NOMA is limited by the IUI in high SNR regime. On the other hand, UE_1 in NOMA can outperform significantly OMA according to chosen power allocation coefficient (α_1) and the success of SIC (β). For instance for $\beta = 0.05$, EC of UE_1 in NOMA is worse than OMA in all SNR regime when $\alpha_1 = 0.1$ whereas EC of UE_1 in NOMA outperforms OMA until $\rho_s = 20dB$ than it is limited by imperfect SIC when $\alpha_1 = 0.3$. Nevertheless, with a better SIC (i.e., $\beta = 0.001$), EC of UE_1 in NOMA always outperforms OMA and this performance gain is more significant when $\alpha_1 = 0.3$. Thus, in designing power allocation, user fairness and maximization of sum-rate should be considered with the other KPIs (i.e., outage and BER). This discussion will be presented in the next simulations of this chapter by considering all constraints.

Then, outage performances of users are presented in downlink NOMA considering the same channel conditions given above. Outage performance of users are given for $\alpha_1 = 0.1$

---

[1]In OMA networks, users are assumed to by spitted by TDMA, hence the achievable rate for a user is given by $R_k = {}^1\!/\!{}_2 \log_2{(1 + \rho_s \gamma_k)}$.
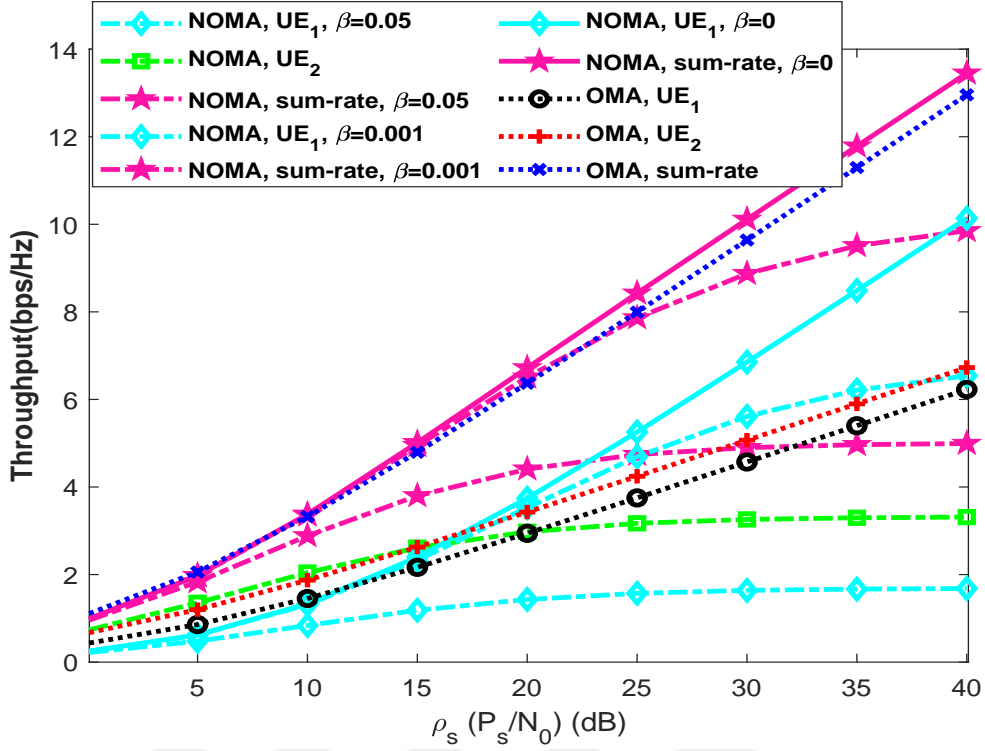
Figure 5.1: Capacity comparison between downlink NOMA and OMA when $\sigma_{s1}^2 = 3dB$, $\sigma_{s2}^2 = 0dB$ and $\alpha_1 = 0.1$
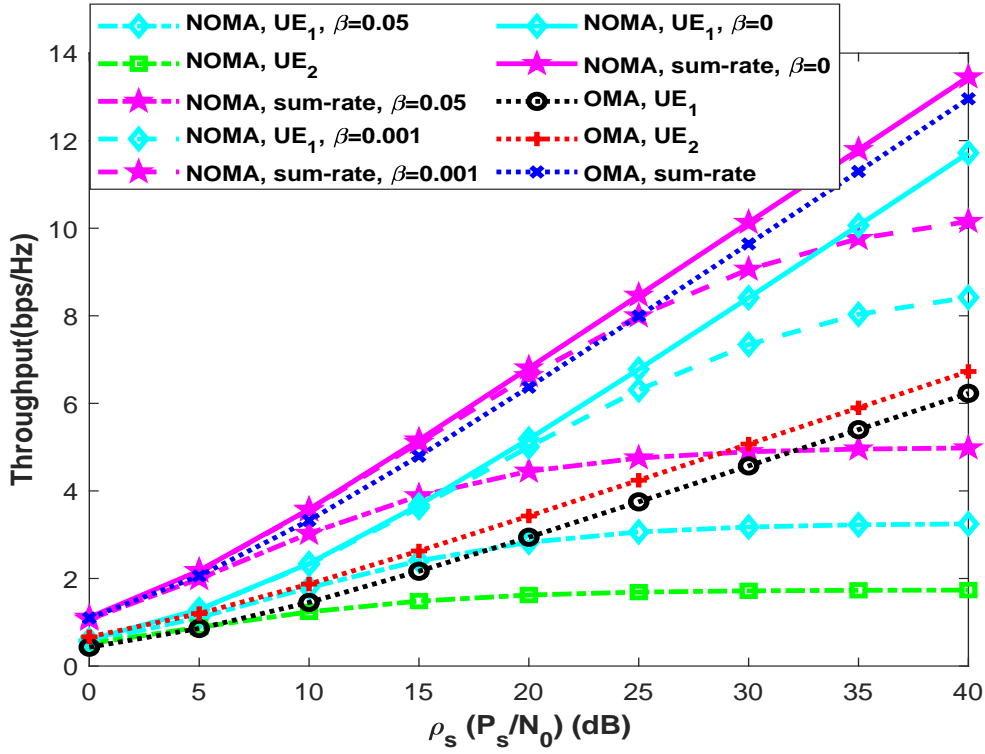

Figure 5.2: Capacity comparison between downlink NOMA and OMA when $\sigma_{s1}^2 = 3dB$, $\sigma_{s2}^2 = 0dB$ and $\alpha_1 = 0.3$
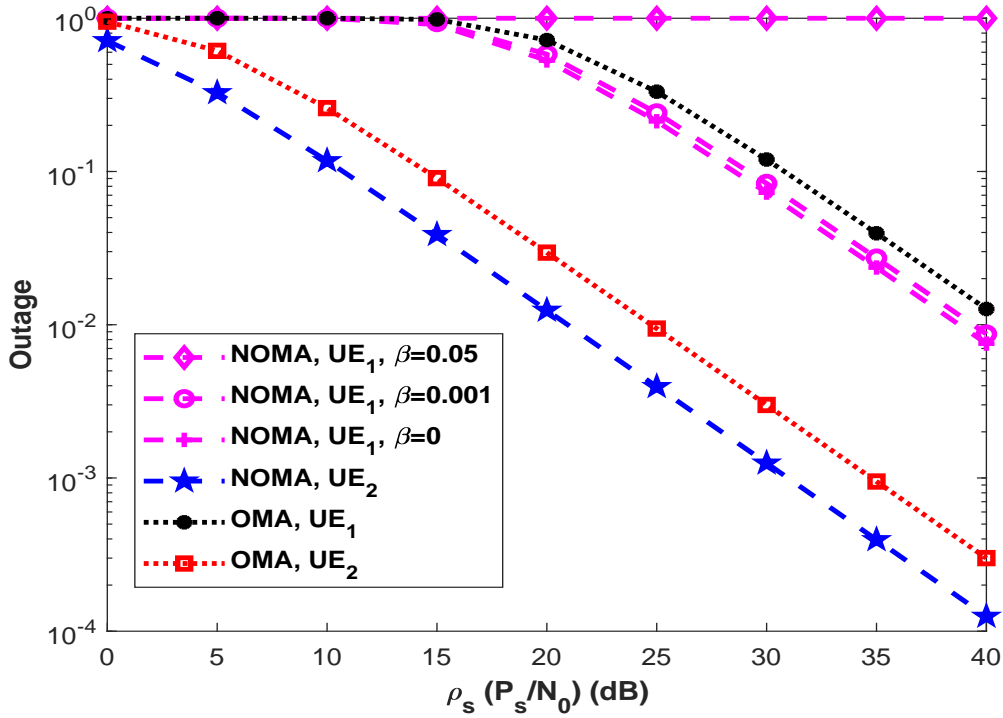
Figure 5.3: Outage comparison between downlink NOMA and OMA when $\sigma_{s1}^2 = 3dB$, $\sigma_{s2}^2 = 0dB$, $\alpha_1 = 0.1$, $\acute{R}_1 = 4BPCU$ and $\acute{R}_2 = 1BPCU$

and $\alpha_1 = 0.3$ in Figure 5.3 and Figure 5.4, respectively. Likewise in EC comparisons, outage performance of UE_1 in NOMA is presented for various imperfect SIC factors and related OMA performances are also presented. In Figure 5.3 and Figure 5.4, target rates of users are assumed to be $\acute{R}_1 = 4BPCU$ and $\acute{R}_2 = 1BPCU$. Based on simulations, one can easily see that NOMA outperforms OMA for both users for given target rates. Nevertheless, as expected, outage performance of UE_1 highly depends on success of SIC process. If the SIC process is not good enough, UE_1 can be always in outage (i.e., $\beta = 0.05$). One can easily see that, the increase in α_1 provides better outage performance for UE_1 since the allocated power for its symbols is increased so that the performance gain to the OMA is increased. The opposite can be said for UE_2. Nevertheless, it is worthy to be noted that if the allocated power to the UE_2 is decreased too much (i.e., higher α_1 lower α_2), both users can be in outage since UE_1 should also detect symbols of UE_2 to accomplish SIC.

In addition to power allocation (α) and the imperfect SIC factor (β), target rates of users
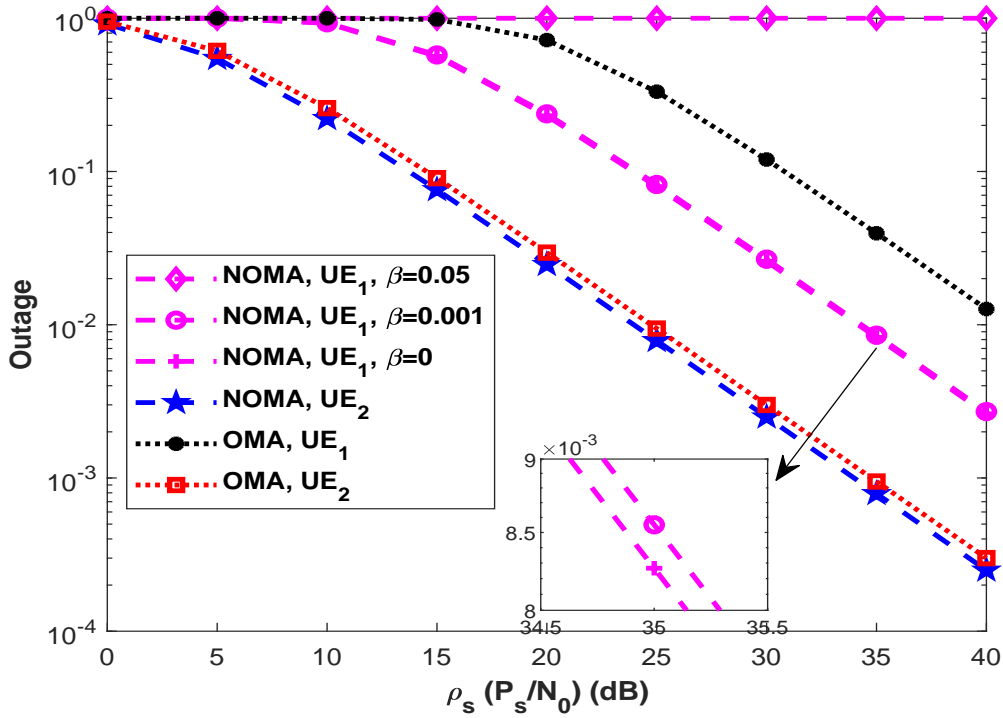
Figure 5.4: Outage comparison between downlink NOMA and OMA when $\sigma_{s1}^2 = 3dB$, $\sigma_{s2}^2 = 0dB$, $\alpha_1 = 0.3$, $\acute{R}_1 = 4BPCU$ and $\acute{R}_2 = 1BPCU$

have dominant effect on the outage performance of NOMA. Thus, outage performances of users are provided with different target rates in Figure 5.5. In Figure 5.5, it is assumed that channel conditions are the same and the imperfect SIC factor is $\beta = 0.001$. The power allocation is chosen as $\alpha_1 = 0.1$. Based on given results, it is concluded that in terms of UE_2, NOMA always outperforms OMA for various target rate. However, if such a target rate which does not fulfill the condition $\alpha_2 > \alpha_1\phi_2$ where $\phi_2 = 2^{\acute{R}_2} - 1$, is chosen, UE_2 always remains in outage (see result for $\acute{R}_2 = 3.5BPCU$ in Figure 5.5). On the other hand, one can easily see that in terms of UE_1, NOMA outperforms OMA when the target rate is relatively high. In the low target rates, OMA outperforms NOMA. Nevertheless, it is hereby noted that if the above mentioned condition for power allocation is not satisfied, UE_1 will be also in outage since SIC should be implemented at UE_1. For instance, when the target rates equal to $\acute{R}_1 = 5BPCU$ and $\acute{R}_2 = 3.5BPCU$, UE_1 in NOMA has better outage performance than that in OMA. Nevertheless, without changing target rates of UE_1, if the target rate for UE_2 is updated as $\acute{R}_2 = 3.5BPCU$, UE_1 is also always in outage due to the SIC process.
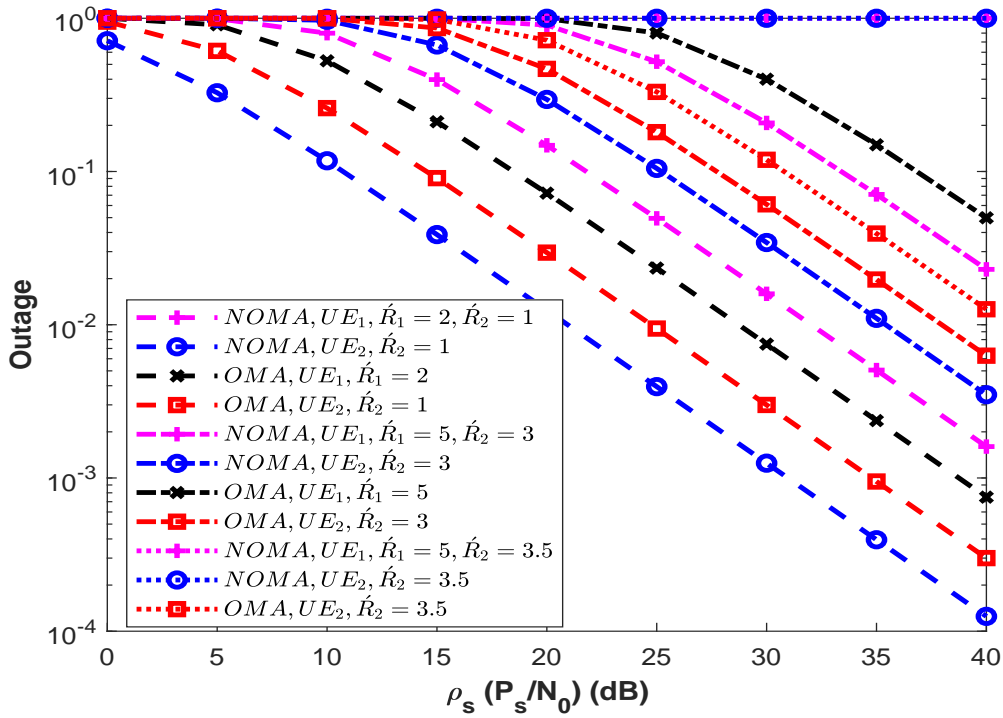
Figure 5.5: Outage comparison between downlink NOMA and OMA when $\sigma_{s1}^2 = 3dB$, $\sigma_{s2}^2 = 0dB$, $\alpha_1 = 0.1$ and $\beta = 0.001$

Error performances of users in donwlink NOMA are presented in Figure 5.6 where QPSK and BPSK are chosen for UE_1 and UE_2, respectively. Channel conditions are chosen as in EC and OP comparisons given above. Simulations are provided for $\alpha_1 = 0.1$ and $\alpha_1 = 0.3$. OMA performances are also presented to compare. Based on simulations, it is seen that UE_2 has better error performance than UE_1 in NOMA although it has worse channel conditions. This is caused by more power is allocated to symbols of UE_2. As expected when α_1 is increased, error performance of UE_1 also increases whereas performance of UE_2 decreases. However, both user cannot compete their OMA counterparts in terms of error performance because of the IUI interference by which they are affected. This decay in error performance in NOMA can be seen as the cost which has to be paid for better achievable rate and better outage performance. There is a trade-off between error and capacity/outage performances of NOMA users. Thus, it is noteworthy that the decay in error performance should be considered when designing a NOMA scheme and it is clear that NOMA may not be the ideal solution for such applications where high data
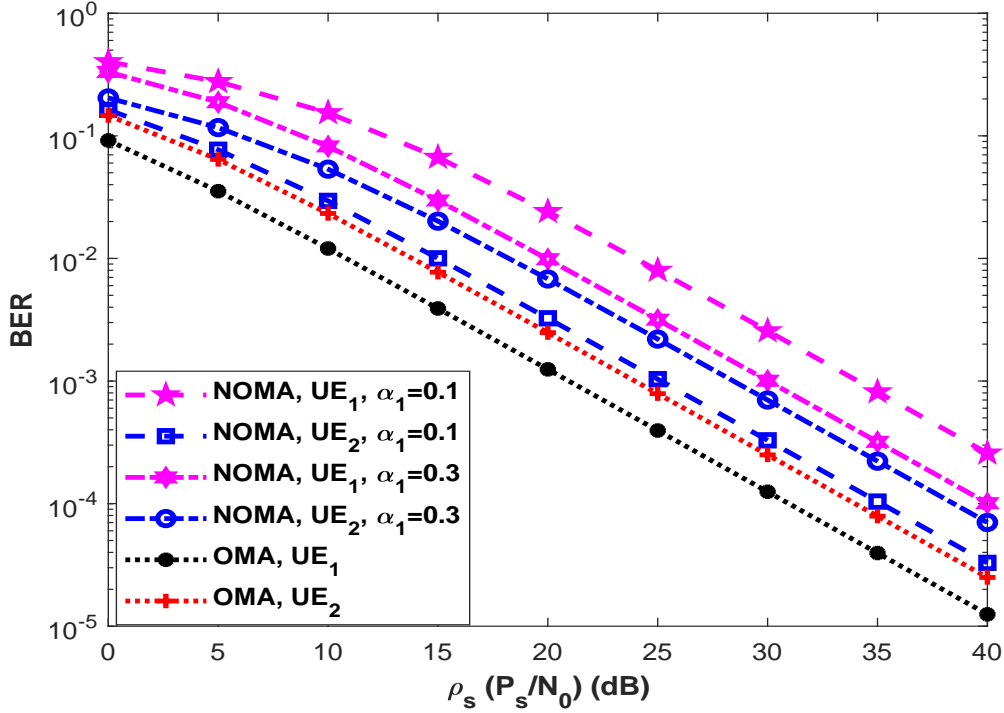
Figure 5.6: BER comparison between downlink NOMA and OMA when $\sigma_{s1}^2 = 3dB$ and $\sigma_{s2}^2 = 0dB$

reliability has a priority such as uRRLC.

Lastly for downlink NOMA, the effect of power allocation on performances of users is emphasized. Thus, for all considered KPIs, performances of users are presented with the change of power allocation coefficient α_1 for the same channel conditions given above comparisons. In EC and OP comparisons, results are provided for both $\beta = 0.001$ and $\beta = 0$. EC performances are presented with respect to α_1 for $\rho_s = 15dB, 30dB$ in Figure 5.7. Then in Figure 5.8, outage performance of users are given with respect to α_1 for two different target rates. In the first scenario, $\acute{R}_1 = 2BPCU$ and $\acute{R}_1 = 1BPCU$ are assumed. In the second scenario, it is assumed that $\acute{R}_1 = 4BPCU$ and $\acute{R}_1 = 2BPCU$. The results are presented for $\rho_s = 30dB$. Moreover, error performances of users are presented in donwlink with respect to α_1 for $\rho_s = 15dB, 30dB$ in Figure 5.9. Based on given results for all three metrics (i.e., EC, OP and BER), one can easily say that increasing α_1 mostly provides performance gain for UE_1 and causes decay in performances of UE_2. However, it can be easily observed that too much increase in α_1 may also cause the worst
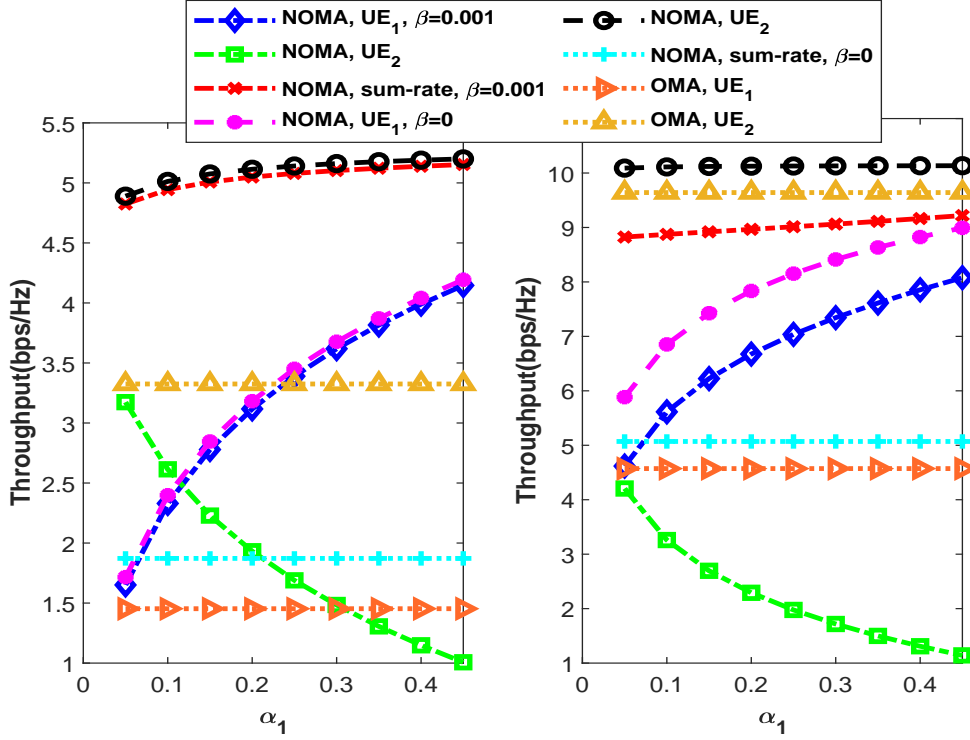
Figure 5.7: Capacity comparison between downlink NOMA and OMA respect to power allocation when $\sigma_{s1}^2 = 3dB$ and $\sigma_{s2}^2 = 0dB$ a) $\rho_s = 15dB$ b) $\rho_s = 30dB$

performance for UE_1 since SIC should be implemented firstly at UE_1 (see outage performance in Figure 5.8.b OP=1 after $\alpha_1 \approx 0.3$). In addition to this, considering user fairness which can be explained as: Both users in NOMA should not have worse performance in terms of capacity and outage than OMA counterparts and both of them should have an affordable decay in error performance, it can be said that optimum power allocation for downlink NOMA should be in range $0.2 \leq \alpha_1 \leq 0.3$.

As the second scheme for conventional NOMA networks, simulations for uplink NOMA are provided in the following figures. Likewise in donwlink NOMA, performances of users in uplink NOMA are evaluated for various conditions in terms of ergodic capacity, outage and bit error rate. Simulations for OMA are also provided to compare with NOMA. Firstly in uplink NOMA, ECs for users are presented when $\sigma_{s1}^2 = 3dB$ and $\sigma_{s2}^2 = 0dB$ in Figure 5.10. Transmit powers of users are assumed to be $P_2 = P_1/5$. Except for worse SIC performance (i.e., $\beta = 0.05$), UE_2 in NOMA always outperforms OMA counterpart. On the other hand, UE_1 in NOMA has worse achievable rate than OMA counterpart in

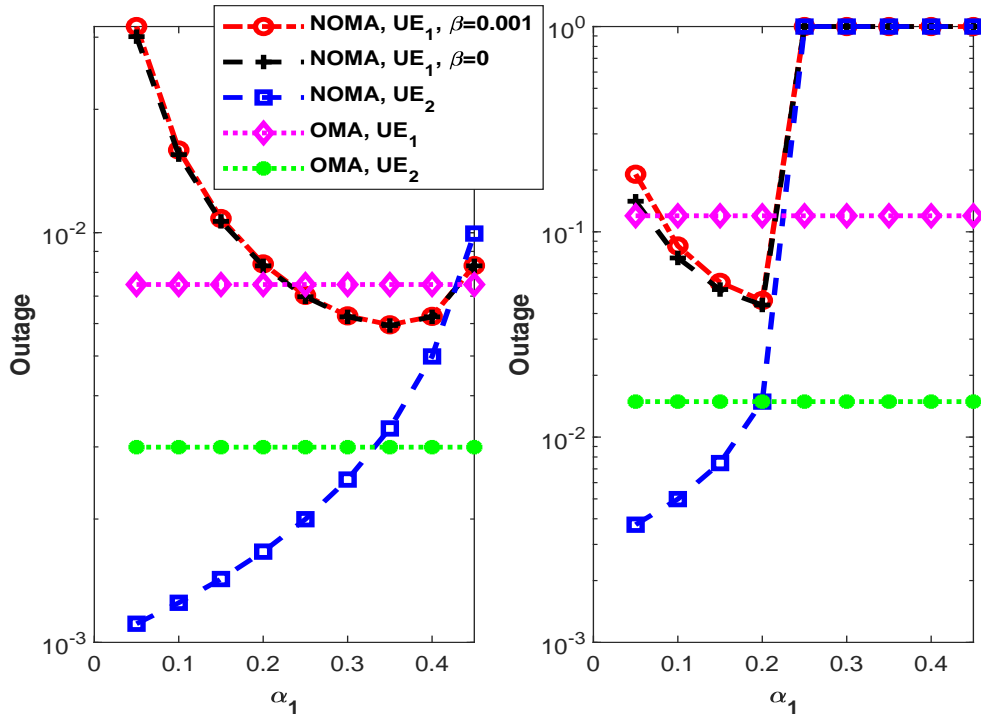**Figure 5.8:** Outage comparison between downlink NOMA and OMA respect to power allocation when $\sigma_{s1}^2 = 3dB$, $\sigma_{s2}^2 = 0dB$ and $\rho_s = 30dB$ a) $\acute{R}_1 = 2BPCU$ and $\acute{R}_2 = 1BPCU$ b) $\acute{R}_1 = 4BPCU$ and $\acute{R}_2 = 2BPCU$
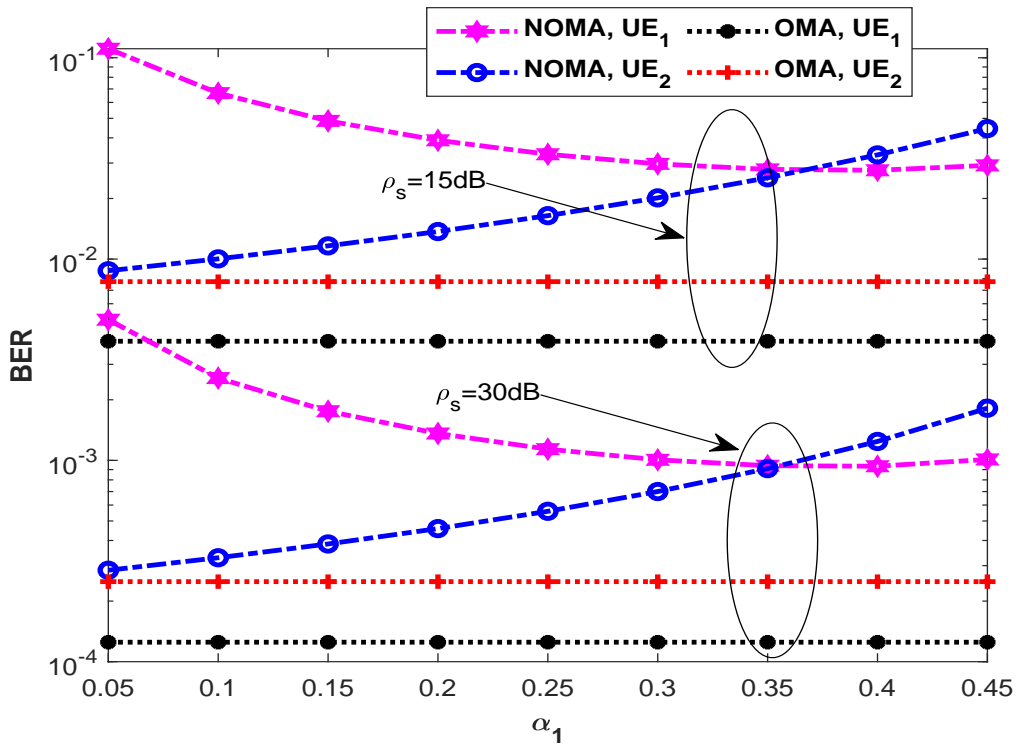

Figure 5.9: BER comparison between downlink NOMA and OMA respect to power allocation when $\sigma_{s1}^2 = 3dB$ and $\sigma_{s2}^2 = 0dB$

medium-high SNR regime although it has better performance in the low SNR regime. As mentioned in Section 2.3, it is caused by the IUI and it can be seen that achievable rate performance of UE_1 is limited even if its power is increased since the interference power (power of UE_2) also increases in this scenario. Hence, NOMA is much more reasonable in uplink when the difference between powers of users or channel qualities is relatively high. To emphasize effectiveness of NOMA, simulations are provided for two different scenarios in Figure 5.11 and Figure 5.12. In Figure 5.11, it is assumed that channel conditions are the same with Figure 5.10 and the transmit SNR for UE_1 is fixed as $\rho_1 = 20dB$. ECs of users are presented with respect to transmit SNR of UE_2 (i.e., ρ_2). One can easily see that, NOMA outperforms OMA counterpart for both users and sum rate when the power difference is relatively high (until $\sim 13dB$). Then, simulations are presented when the users have equal transmit SNR as $\rho_1 = \rho_2 = 20dB$ in Figure 5.12. It is assumed that the average channel quality of UE_1 is fixed as $\sigma_{s1}^2 = 10dB$ and σ_{s2}^2 differs. Although NOMA outperforms OMA in terms of sum rate and the achievable rate of UE_2, UE_1 in NOMA can outperform OMA counterpart until only $\sigma_{s2} \sim 1.5$ since the users have equal power and the difference between channel qualities cannot over IUI penalty.

Likewise in EC comparisons between uplink NOMA and OMA, outage simulations are provided for the same above scenarios in Figure 5.13, Figure 5.14 and Figure 5.15, respectively. Target rates of users are assumed to be $\acute{R}_1 = 2$ and $\acute{R}_2 = 1$. In Figure 5.13, both users in NOMA outperform OMA counterparts until $\sim 15dB$, after that point IUI limits the performance of UE_1 so that of UE_2 since SIC should be succeeded to obtain symbols of UE_2. In Figure 5.14, the effect of IUI can be easily observed. After $\rho_2 \sim 10dB$, the performance of UE_2 in NOMA gets worse although its transmit power increase. It is exactly dominated by the performance of SIC process where UE_1 remains in outage with higher probability. Based on results in Figure 5.14, one can easily see that NOMA outperforms OMA in terms of outage performance of both users when the transmit SNR difference within user is above $\sim 15dB$ which proves our assertion that NOMA is much more reasonable in uplink when the users have different power levels. In Figure 5.15, for better illustration, it is updated as $\rho_1 = 10dB$ and $P_2 = {}^{P_1}/_5$. Likewise in EC comparisons, it can be seen that NOMA can only outperform OMA when the channel quality difference is relatively high when the users have fixed power.
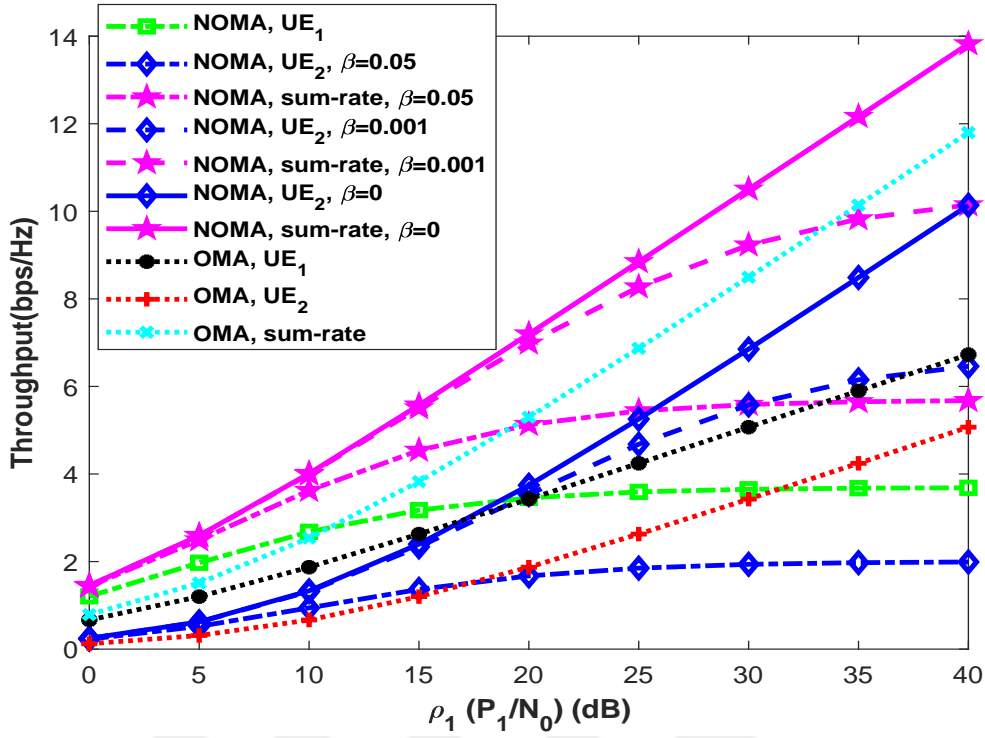
Figure 5.10: Capacity comparison between uplink NOMA and OMA vs. ρ_1 when $\sigma_{s1}^2 = 3dB$, $\sigma_{s2}^2 = 0dB$ and $P_2 = \frac{P_1}{5}$

Figure 5.11: Capacity comparison between uplink NOMA and OMA vs. ρ_2 when $\sigma_{s1}^2 = 3dB$, $\sigma_{s2}^2 = 0dB$ and $\rho_1 = 20dB$

Figure 5.12: Capacity comparison between uplink NOMA and OMA vs. σ_{s2}^2 when $\sigma_{s1}^2 = 10dB$ and $\rho_1 = \rho_2 = 20dB$
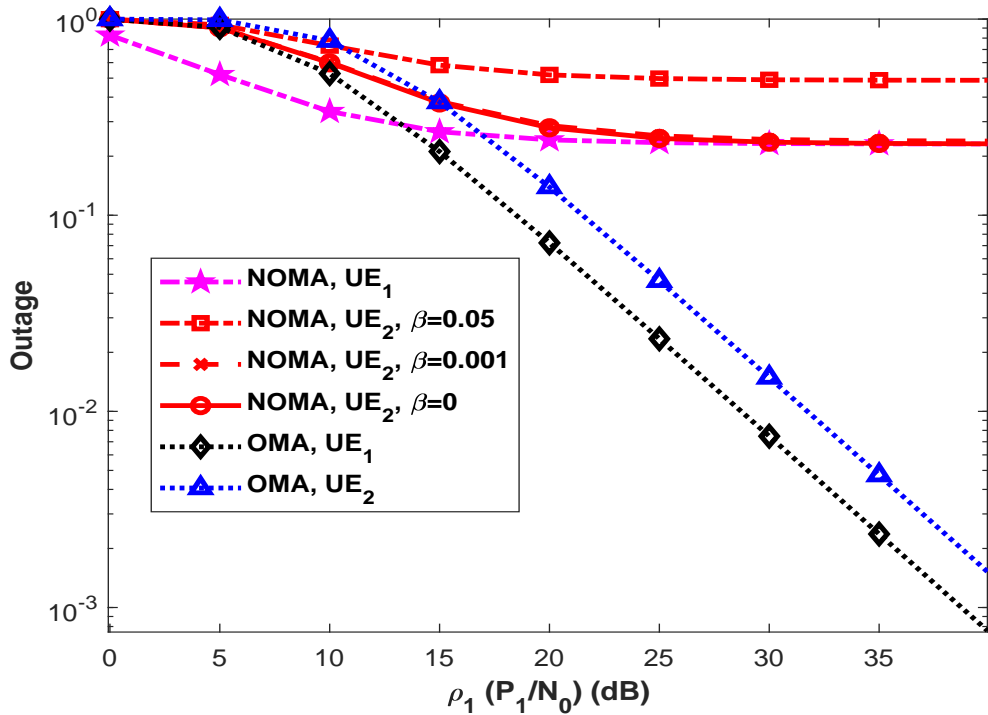
Figure 5.13: Outage comparison between uplink NOMA and OMA vs. ρ_1 when $\sigma_{s1}^2 = 3dB$, $\sigma_{s2}^2 = 0dB$, $P_2 = {}^{P_1}/_5$, $\acute{R}_1 = 2$ and $\acute{R}_2 = 1$
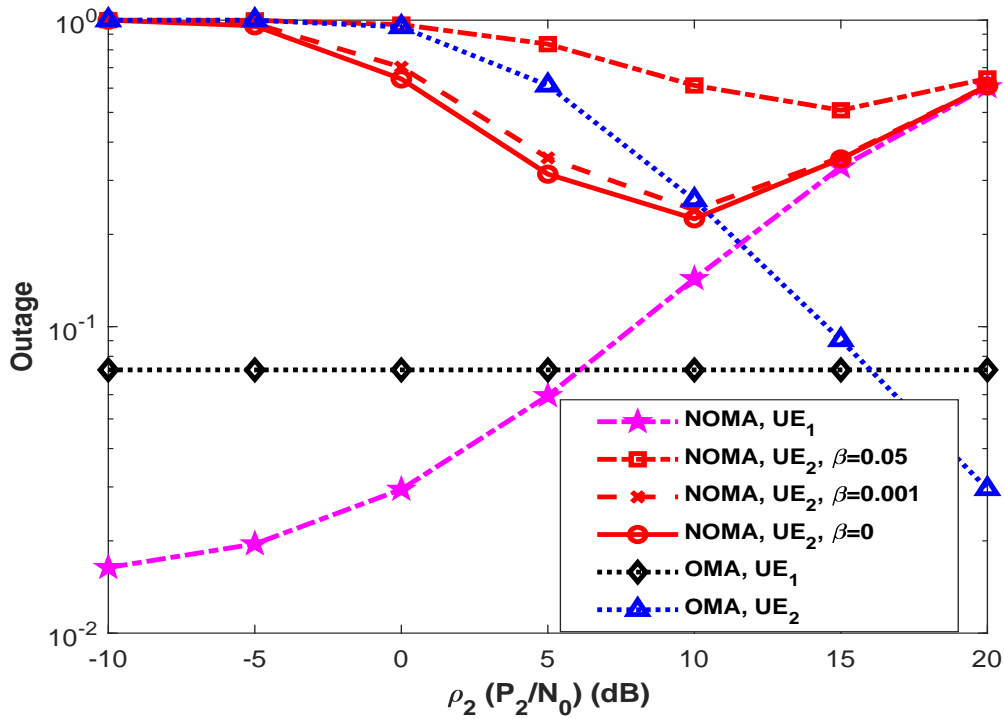
Figure 5.14: Outage comparison between uplink NOMA and OMA vs. ρ_2 when $\sigma_{s1}^2 = 3dB$, $\sigma_{s2}^2 = 0dB$, $\rho_1 = 20dB$, $\acute{R}_1 = 2$ and $\acute{R}_2 = 1$
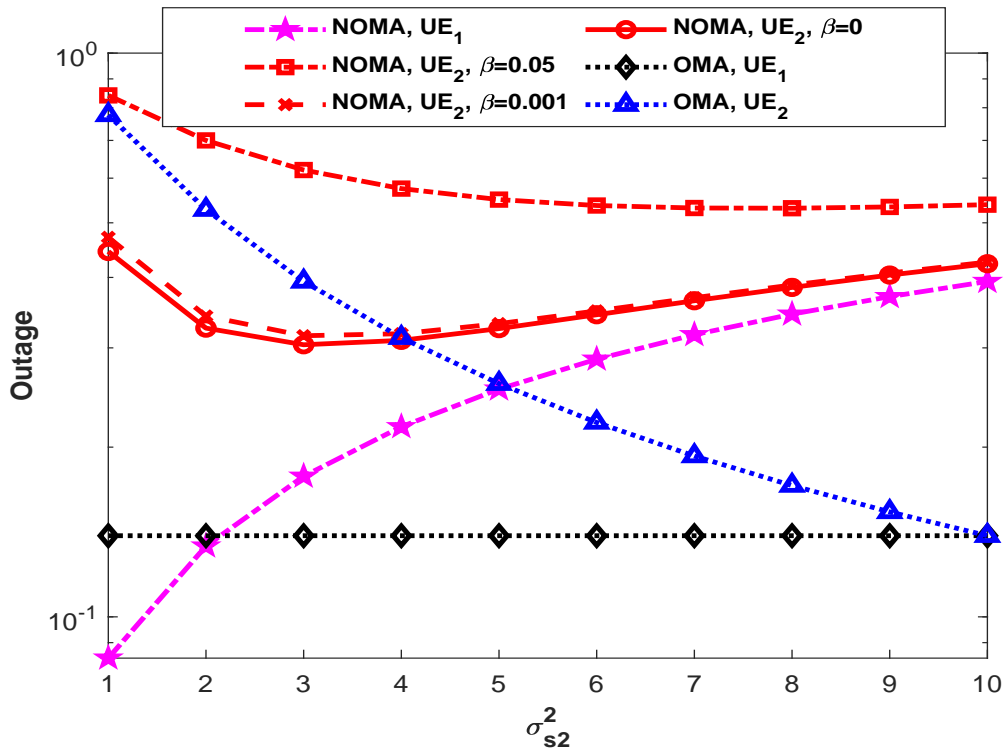
Figure 5.15: Outage comparison between uplink NOMA and OMA vs. σ_{s2}^2 when $\sigma_{s1}^2 = 10dB$, $\rho_1 = 10dB$, $P_2 = {}^{P_1}/_5$, $\acute{R}_1 = 2$ and $\acute{R}_2 = 1$

Finally, BER performances of users are provided for the same scenarios of EC and outage comparison in Figure 5.16, Figure 5.17 and Figure 5.18, respectively. As expected NOMA cannot outperform OMA in any scenario because of IUI. Likewise in downlink, it can be considered that there is trade-off between error and capacity/outage performances in also uplink NOMA. This should be taken into consideration when designing a NOMA scheme. In Figure 5.16, NOMA users have poor performance since the performance of UE_1 is dominated by IUI even if the transmit SNR is increased. Hence, the performance of UE_2 gets worse since it is affected by SIC performance. In Figure 5.17, one can see that increasing transmit power of UE_2 causes worse error performance of UE_1 since it increases IUI whereas it provides performance gain for UE_2 as expected. Nevertheless, too much increase in ρ_2 affects error performance of UE_2 also in a negative manner since then error performance of UE_2 is dominated by erroneous detection of UE_1's symbols during SIC. Unlike in EC and OP comparisons, one can easily see from Figure 5.18 that channel quality difference does not affect error performance of users significantly as being in EC an OP.

Cooperative-NOMA: In this part of the chapter, simulations for Cooperative-NOMA networks given in Section 3.3 are presented and compared with conventional NOMA networks. In comparisons, simulations for the proposed TBS-C-NOMA are also provided to emphasize its superiority and TBS-C-NOMA performances are given for derived optimum threshold. In comparisons, the fairness is also taken into consideration in terms of energy consumption. In relay networks, relay -it is UE_1 in C-NOMA and TBS-C-NOMA- also consumes energy to forward symbols. Thus, the total power consumption at the nodes is fixed and the total power is shared[2] by source (BS) and relay (UE_1). On the other hand, conventional NOMA and OMA networks use total power at the source. Firstly, EC comparisons[3] are provided for two different total energy sharing strategy between source and relay in Figure 5.19 and Figure 5.20. Let the total power is represented by P_T, it is assumed that $P_s = P_r = {}^{P_T}/_2$ in Figure 5.19 whereas it is shared as $P_s = {}^{4P_T}/_5$

---

[2]Relay can harvest its own energy by simultaneous wireless information and power transfer (SWIPT). However, SWIPT is not considered in this work and beyond the scope.

[3]In C-NOMA and TBS-C-NOMA, it is assumed that short range communication is applied like Bluetooth as proposed in [108], hence $^1/_2$ coefficient does not exist in achievable rates of them which is explained before in related sections.

Figure 5.16: BER comparison between uplink NOMA and OMA vs. ρ_1 when $\sigma_{s1}^2 = 3dB$, $\sigma_{s2}^2 = 0dB$ and $P_2 = {}^{P_1}/_5$
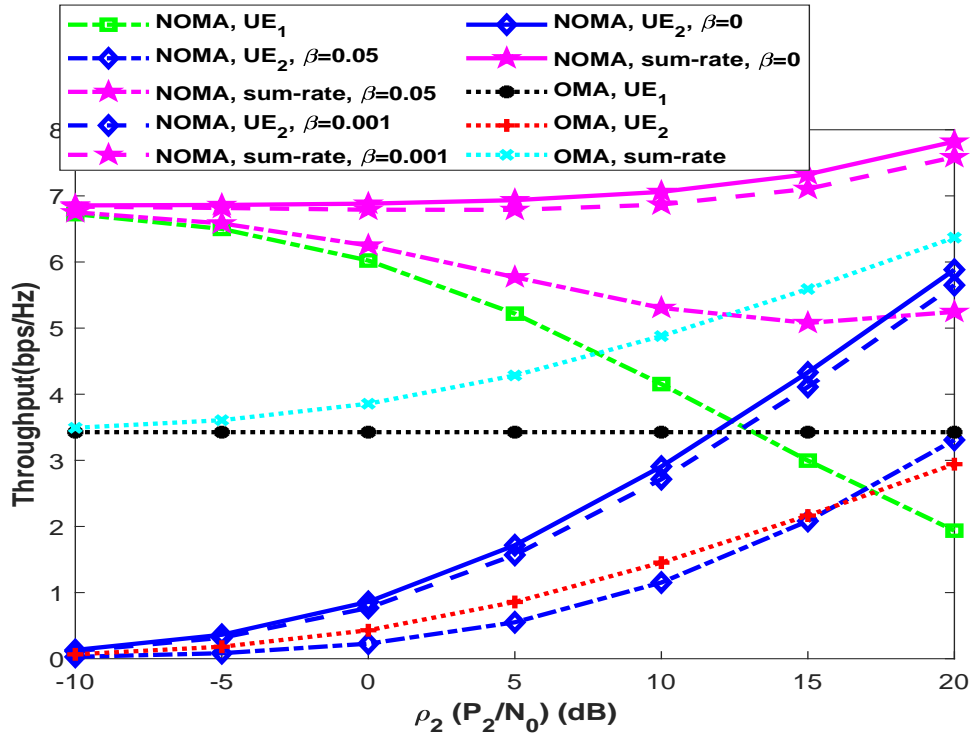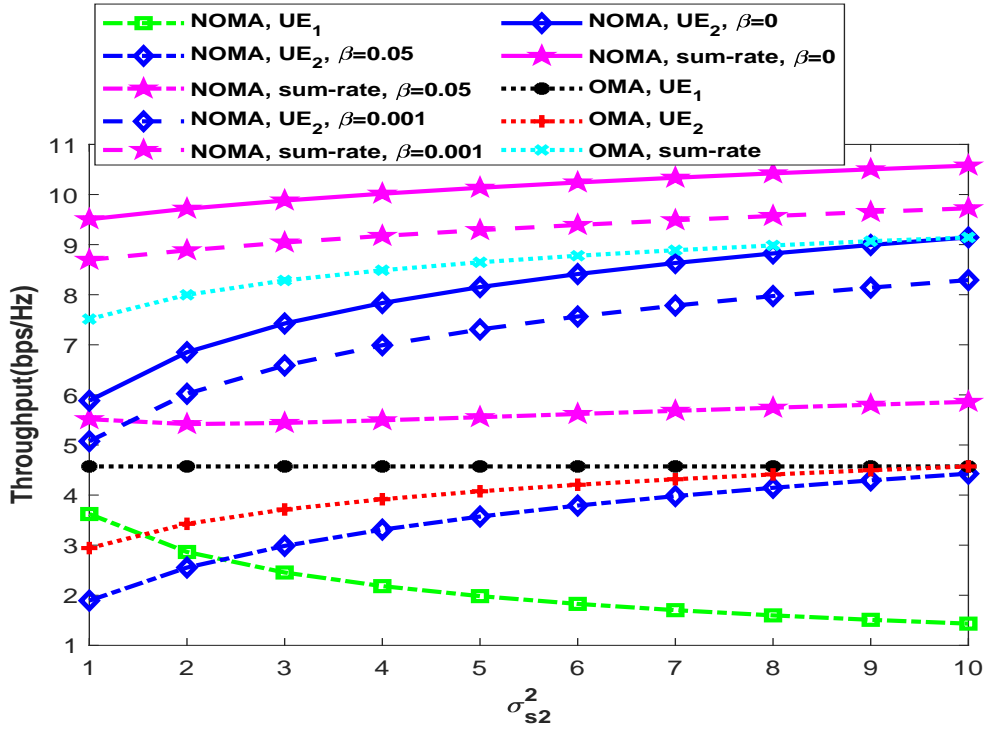

Figure 5.17: BER comparison between uplink NOMA and OMA vs. ρ_2 when $\sigma_{s1}^2 = 3dB$, $\sigma_{s2}^2 = 0dB$ and $\rho_1 = 20dB$
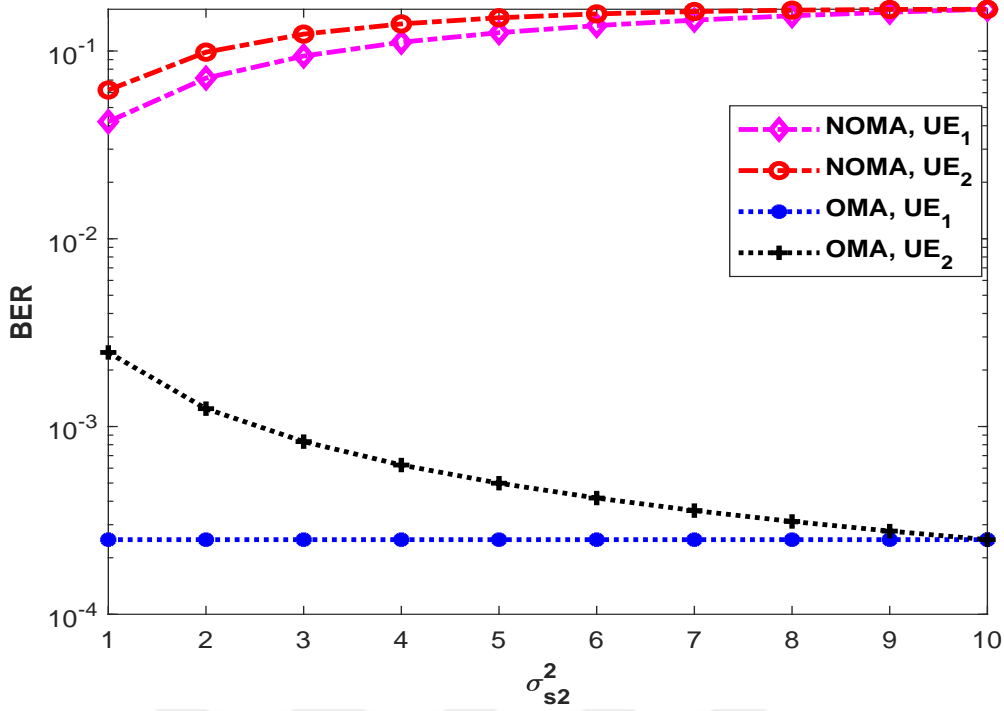
Figure 5.18: BER comparison between uplink NOMA and OMA vs. σ_{s2}^2 when $\sigma_{s1}^2 = 10dB$ and $\rho_1 = \rho_2 = 20dB$
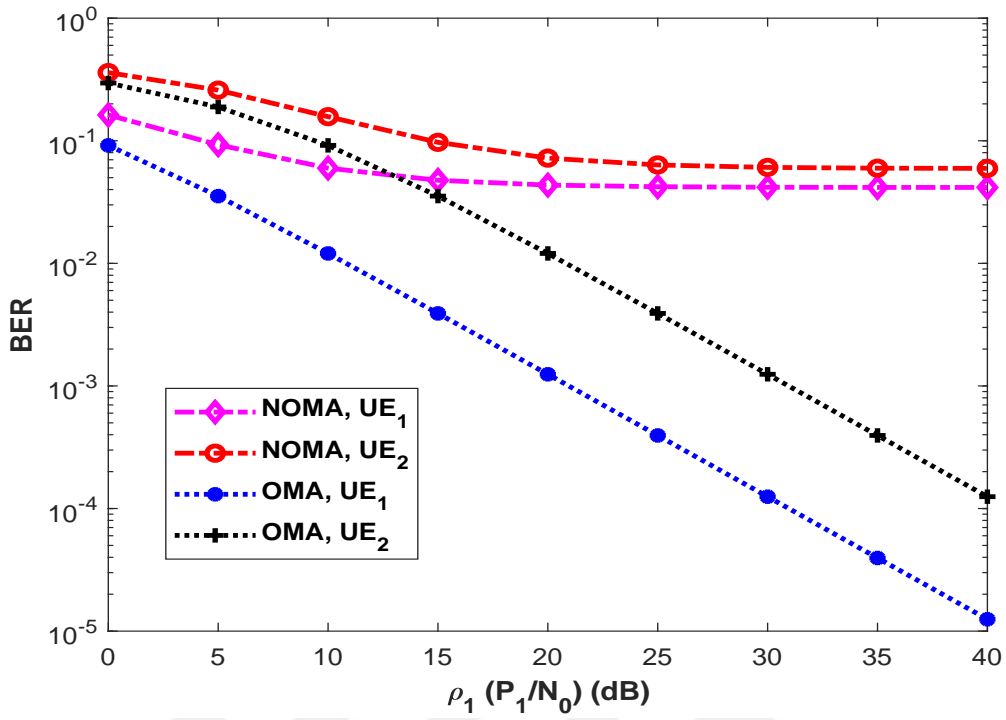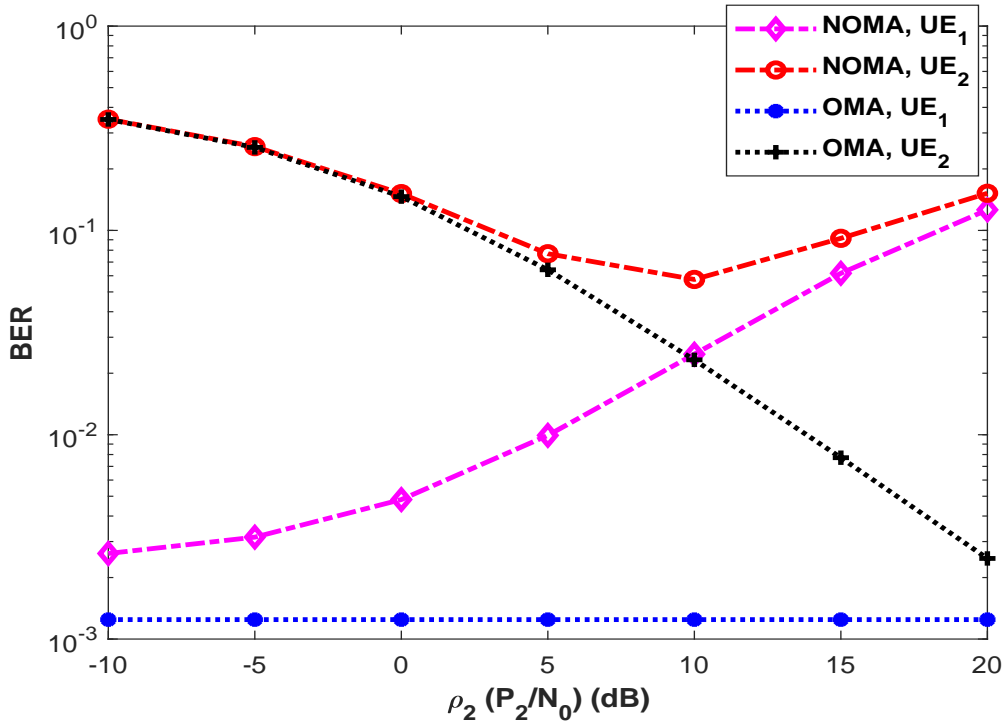
and $P_r = {}^{P_T}\!/_5$ in Figure 5.20. The channel conditions are $\sigma_{s1}^2 = 10dB$, $\sigma_{s2}^2 = 0dB$ and $\sigma_r^2 = 10dB$. The power allocation coefficient for NOMA is chosen as $\alpha_1 = 0.1$ and the imperfect SIC factor for UE_1 is assumed as $\beta = 0.001$. Based on given simulations, one can easily say that C-NOMA and TBS-C-NOMA has almost the same EC performance and they outperform both conventional NOMA and OMA networks in terms of UE_2. UE_1 has exactly the same performance since TBS-C-NOMA does not affect UE_1, hence its performance is presented only one cooperative-NOMA scheme. As expected, the more power is consumed by relay the more EC is achieved by UE_1 whereas the less EC is achieved by UE_2 since the total power (P_T) is shared and UE_1 symbols have been transmitted with less power from source. The power allocation has also important role on performances of C-NOMA and TBS-C-NOMA. However, considering the total energy consumption which is shared by source and relay, it is very complex to provide an optimum power allocation for cooperative-NOMA schemes. In optimum power allocation, total power sharing and the position of the relay -UE_1- also should be considered such as provided for NOMA-CRS in Section 3.6. Nevertheless, in the next simulations, there will

Figure 5.19: Capacity comparisons for TBS-C-NOMA, C-NOMA, NOMA and OMA when $\sigma_{s1}^2 = 10dB$, $\sigma_{s2}^2 = 0dB$, $\sigma_r^2 = 10dB$, $\alpha_1 = 0.1$, $\beta = 0.001$ and $P_s = P_r = {}^{P_T}/{}_2$

be also a discussion on the effect of power allocation for C-NOMA and TBS-C-NOMA.

Then, outage performances of C-NOMA and TBS-C-NOMA are given in Figure 5.21 and Figure 5.22 for the same conditions in EC comparisons. The target rates of users are assumed as $\acute{R}_1 = 4BPCU$ and $\acute{R}_2 = 3BPCU$. Likewise in EC comparison, C-NOMA and TBS-COMA outperform both conventional NOMA and OMA networks in terms of outage performance of UE_2 since it is strengthened by a cooperative phase. Once more power is consumed at the source, UE_1 in C-NOMA and TBS-C-NOMA can compete with conventional NOMA, in this case TBS-C-NOMA also performs much more similar to C-NOMA in terms of UE_2's outage. As discussed above, optimum power allocation should be also considered in terms of individual outage performances of users.

Furthermore, BER comparisons are presneted for TBS-C-NOMA, C-NOMA, NOMA and OMA for $P_s = P_r = {}^{P_T}/{}_2$ and $P_s = {}^{4P_T}/{}_5$, $P_r = {}^{P_T}/{}_5$ in Figure 5.23 and Figure 5.24, respectively. It is hereby emphasized that TBS-C-NOMA outperforms significantly C-

Figure 5.20: Capacity comparisons for TBS-C-NOMA, C-NOMA, NOMA and OMA when $\sigma_{s1}^2 = 10dB$, $\sigma_{s2}^2 = 0dB$, $\sigma_r^2 = 10dB$, $\alpha_1 = 0.1$, $\beta = 0.001$, $P_s = {}^{4P_T}/_5$ and $P_r = {}^{P_T}/_5$

Figure 5.21: Outage comparisons for TBS-C-NOMA, C-NOMA, NOMA and OMA when $\sigma_{s1}^2 = 10dB$, $\sigma_{s2}^2 = 0dB$, $\sigma_r^2 = 10dB$, $\alpha_1 = 0.1$, $\beta = 0.001$, $P_s = P_r = {}^{P_T}/_2$, $\acute{R}_1 = 4BPCU$ and $\acute{R}_2 = 3BPCU$
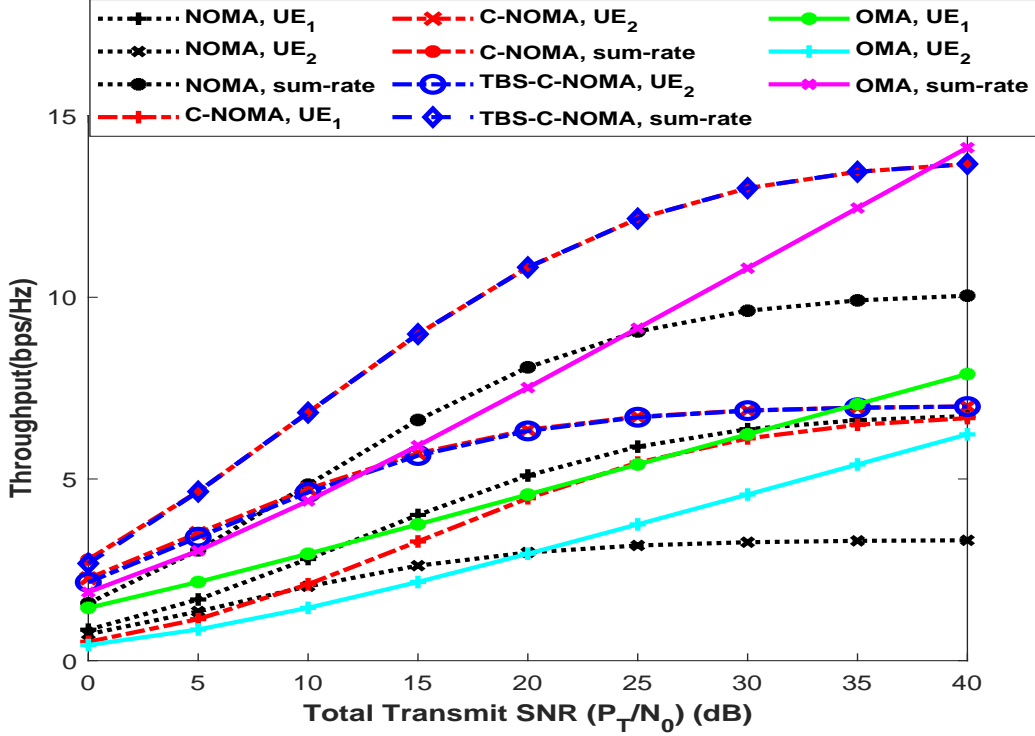
Figure 5.22: Outage comparisons for TBS-C-NOMA, C-NOMA, NOMA and OMA when $\sigma_{s1}^2 = 10dB$, $\sigma_{s2}^2 = 0dB$, $\sigma_r^2 = 10dB$, $\alpha_1 = 0.1$, $\beta = 0.001$, $P_s = {}^{4P_T}/_5$, $P_r = {}^{P_T}/_5$, $\acute{R}_1 = 4BPCU$ and $\acute{R}_2 = 3BPCU$

NOMA for both power sharing schemes since TBS-C-NOMA removes the effect of error propagation in C-NOMA by increasing reliability of forwarded symbol from UE_1 to UE_2. TBS-C-NOMA achieves full diversity order (*i.e.*, 2) and its error performance gets very close to genie-aided/perfect-SIC C-NOMA case where it is assumed that UE_1 detects perfectly symbols of UE_2 before forwarding and no error propagation occurs. Considering this spectacular gain in error performance, a slight decay in EC and OP of TBS-C-NOMA can be easily ignored compared to C-NOMA. In addition, this performance gain can be provided when the total power mostly consumed by source hence, the UE_1 in TBS-C-NOMA does not also loose any performance compared to OMA (see Figure 5.24). One can easily see that TBS-C-NOMA achieves full diversity order. Thus, by implementing TBS-C-NOMA, better achievable rate, outage performance and error performance can be achieved than both conventional NOMA and OMA networks. This provides us to defeat the trade-off between capacity and error performances in conventional NOMA networks compared to OMA.
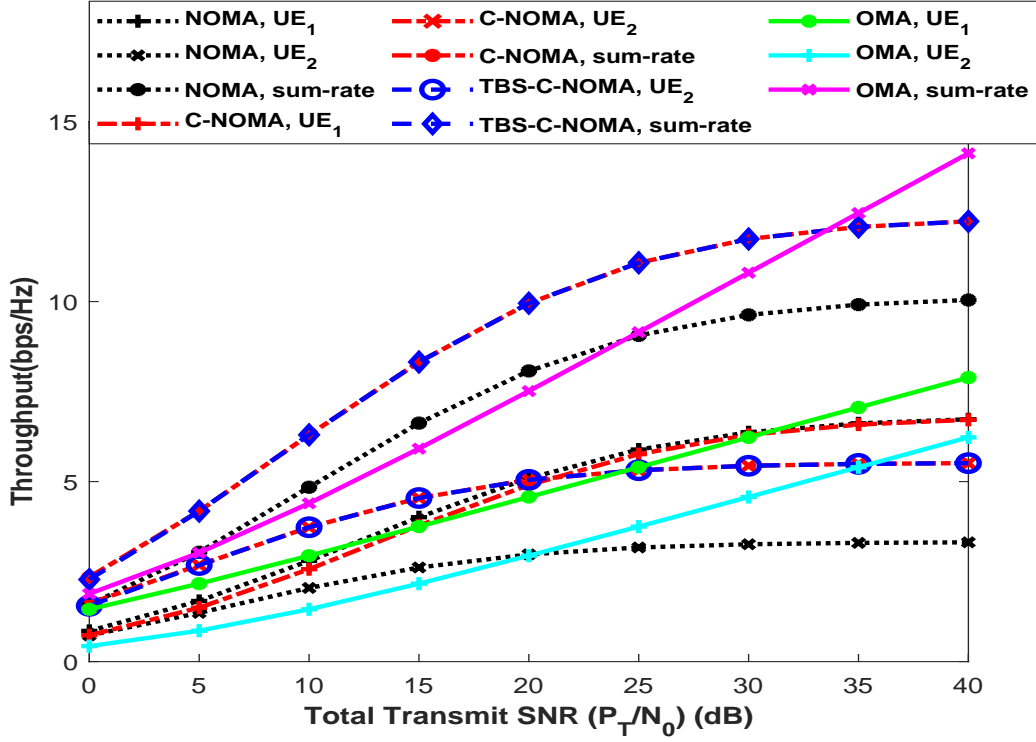
Figure 5.23: BER comparisons for TBS-C-NOMA, C-NOMA, NOMA and OMA when $\sigma_{s1}^2 = 10dB$, $\sigma_{s2}^2 = 0dB$, $\sigma_r^2 = 10dB$, $\alpha_1 = 0.1$ and $P_s = P_r = {}^{P_T}\!/_2$

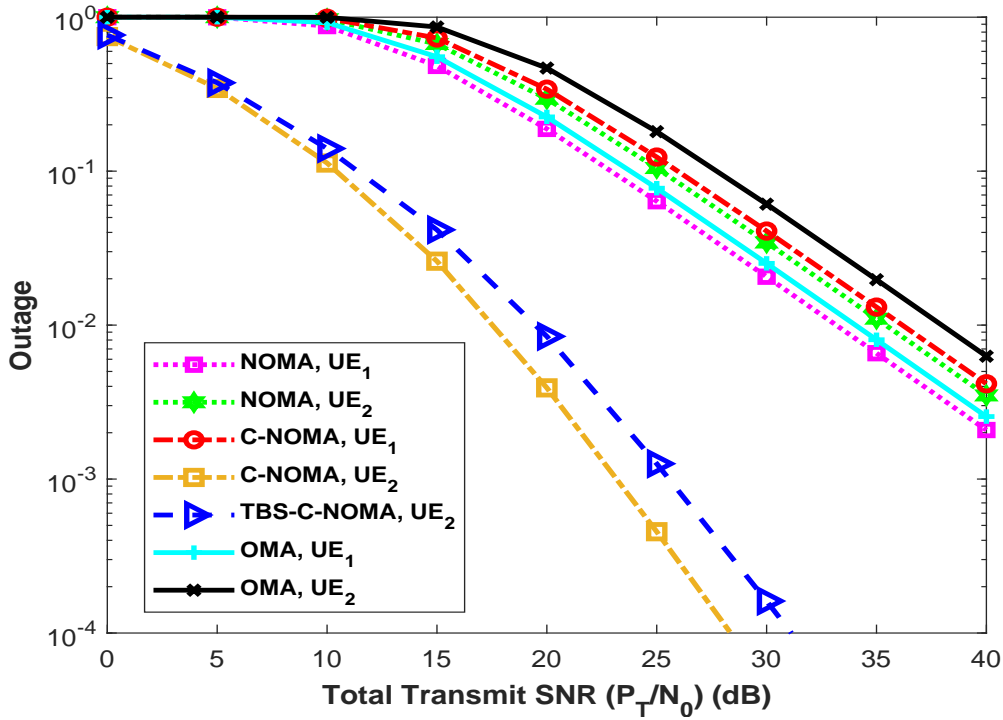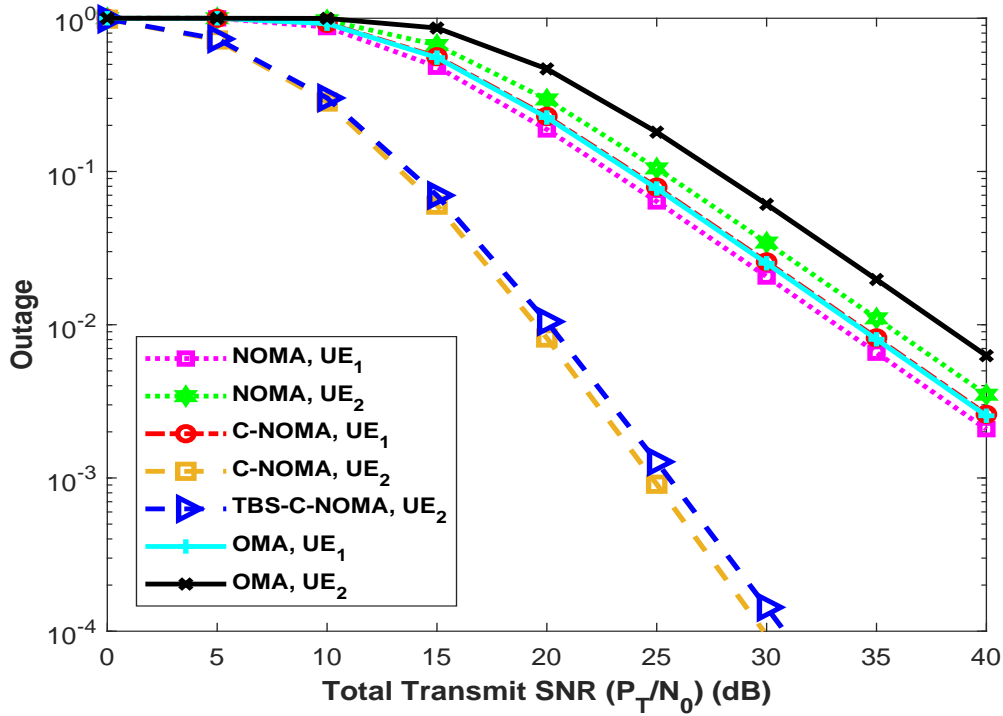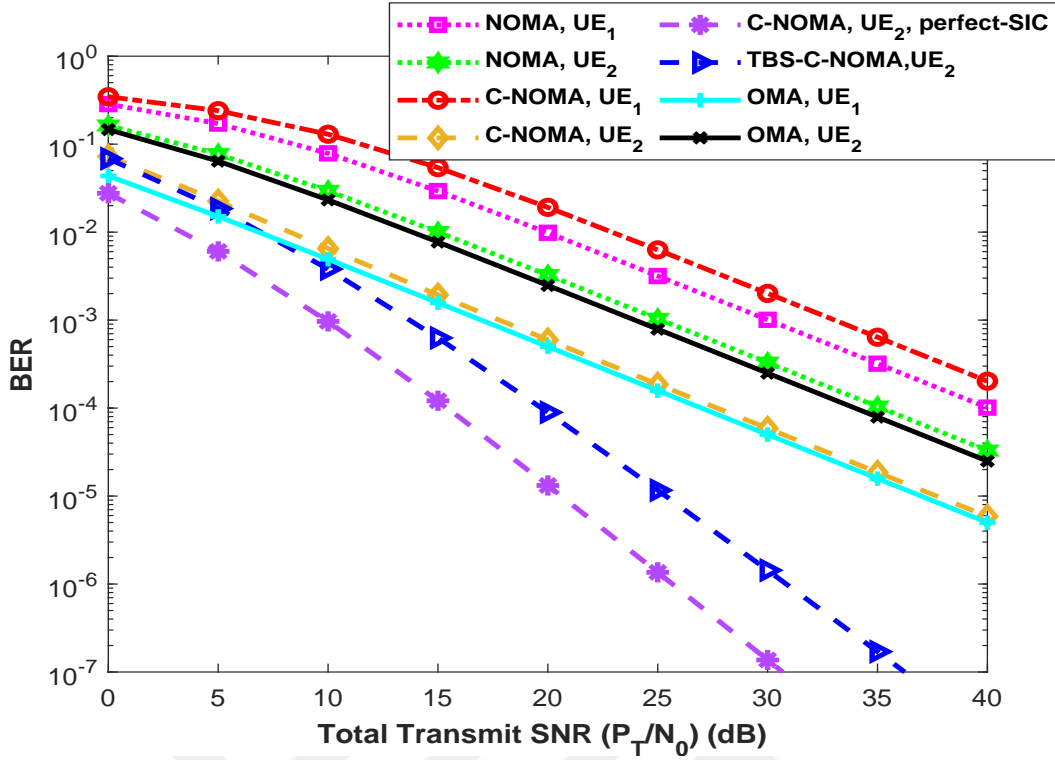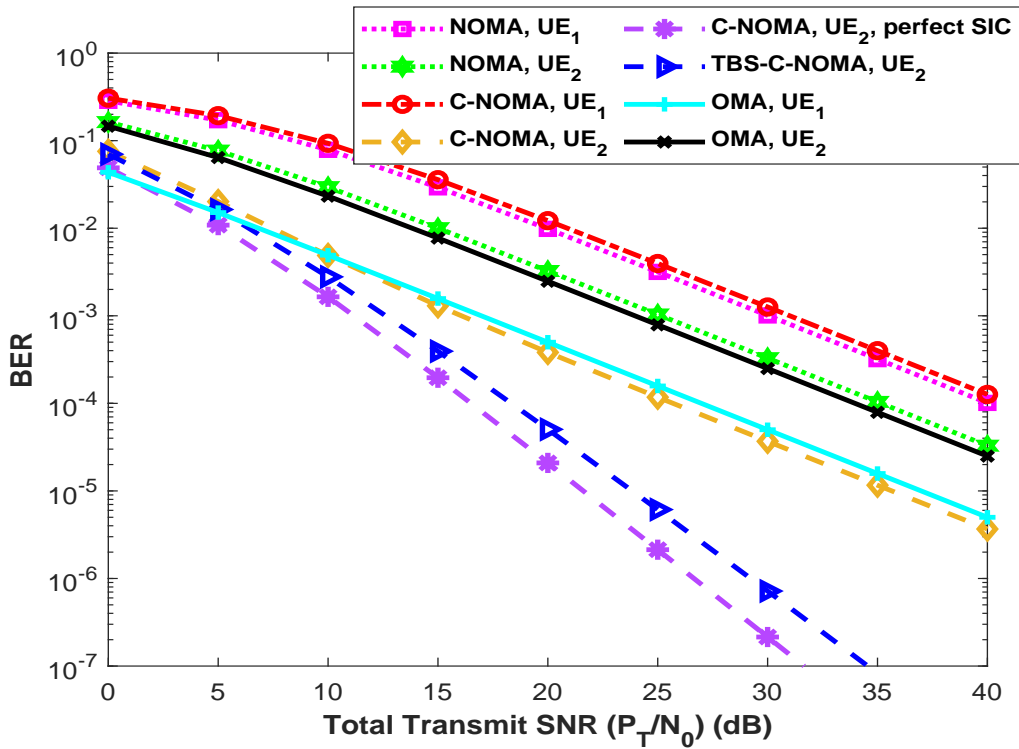**Figure 5.24:** BER comparisons for TBS-C-NOMA, C-NOMA, NOMA and OMA when $\sigma_{s1}^2 = 10dB$, $\sigma_{s2}^2 = 0dB$, $\sigma_r^2 = 10dB$, $\alpha_1 = 0.1$, $P_s = {}^{4P_T}\!/_5$ and $P_r = {}^{P_T}\!/_5$

Finally for cooperative-NOMA networks, power allocation design in TBS-C-NOMA is discussed in the following figures -from Figure 5.25 to Figure 5.27-. As mentioned above, obtaining an optimum power allocation for TBS-C-NOMA is a very complex task since it should be considered in terms of energy consumption sharing at the nodes (i.e., source and relay) and the location of the relay -average channel quality between nodes- in addition to individual performances of users in terms of EC, OP and BEP. Moreover, when considering users' performances, user fairness should be also taken into account in a way that none of user meet non-affordable decay in any performance compared to their conventional NOMA or OMA counterparts. Furthermore, since users' performances in NOMA networks change oppositely each other, optimum power allocation is not a concave optimization problem either. Nevertheless, to draw a general scheme for optimizing power allocation, simulations of TBS-C-NOMA are provided in terms of maximizing sum-rate, minimizing outage and error performances of users in Figure 5.25, Figure 5.26 and Figure 5.27, respectively. The channel conditions are considered as given above comparisons and the imperfect SIC factor ($\beta = 0.001$). The performances of TBS-C-NOMA are investigated with respect to power allocation coefficient (α_1) and to the power consumed by source. For better illustration, let defining Θ and it denotes to be consumed rate of total power by source (BS) (i.e., $P_s = \Theta P_T$), hence $P_r = (1 - \Theta)P_T$. The total transmit SNR is fixed as $P_T/N_0 = 25dB$. The results for ECs of users in TBS-C-NOMA are presented in Figure 5.25. It is seen that EC performances of users change exactly in opposite way according to Θ and α_1. It is explained as increasing power of relay or decreasing α_1 decreases IUI at UE_2, thus it provides performance gain for UE_2 whereas it causes decrease in energy for the symbols of UE_1 so that performance of UE_1 gets worse. In Figure 5.26, outage performances of users are presented for $\acute{R}_1 = 4BPCU$ and $\acute{R}_2 = 1.5BPCU$. $\acute{R}_2$ is chosen relatively lower compared to above given comparisons otherwise in the higher α_1 values, UE_1 will always be in outage due to IUI by implementing SIC. Outage performance of UE_2 can be interpreted in a linear way such that the more power is consumed by relay, the better performance it has. It is also valid for lower α_1. On the other hand, outage performance of UE_1 changes non-linearly according to α_1. With the increase of α_1, it is usually expected UE_1 to have better performance since it affects the energy of UE_1' symbol. However, if it is increased too much, UE_1 will be in outage with highly probability since it cannot succeed SIC. When it comes to Θ, UE_1 also performs linearly
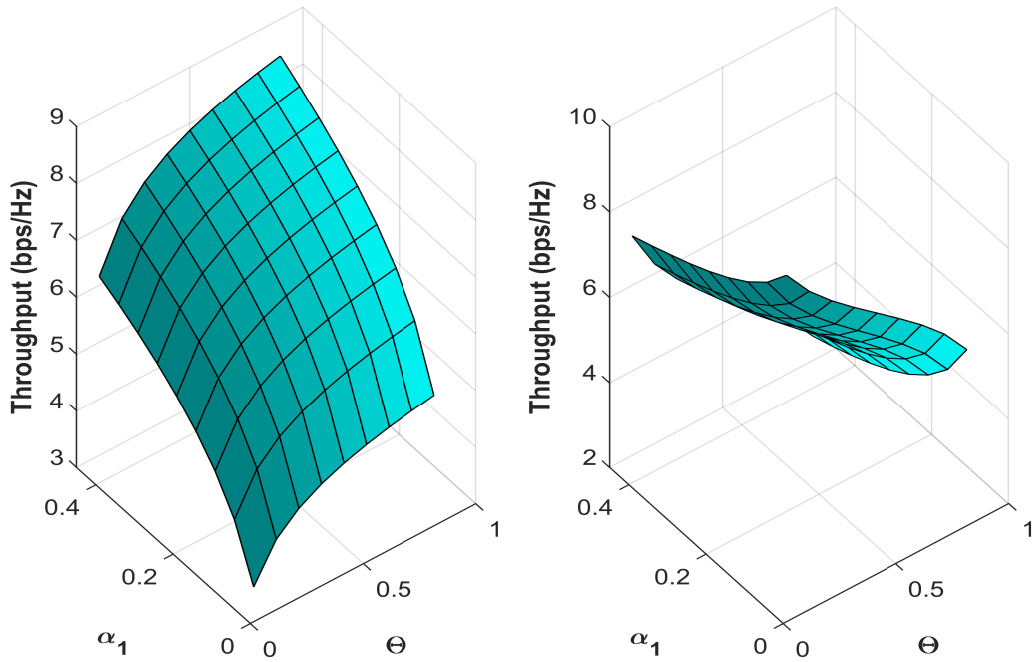
Figure 5.25: Ergodic capacities in TBS-C-NOMA vs. Θ and α_1 when $\sigma_{s1}^2 = 10dB$, $\sigma_{s2}^2 = 0dB$, $\sigma_r^2 = 10dB$ and $\beta = 0.001$ a) UE_1 b) UE_2

with the change of it. If Θ is increased, it means the power of UE_1 is increased since it only receives symbol from source so that its performance gets better. From Figure 5.27, one can easily see that the discussions on outage performance of TBS-C-NOMA are also valid in BER for both users. Considering all these constraints, Θ and α_1 pair should be chosen what the priority performance metrics of users are. Based on simulations, without decreasing any performance metrics dramatically for each user, it can be said that $0.7 \leq \Theta \leq 0.8$ and $0.2 \leq \alpha_1 \leq 0.3$ can be chosen.

SMA and SSK-NOMA: In this part of the chapter, simulations are presented to compare proposed SMA and SSK-NOMA with their NOMA/OMA counterparts. In comparisons, since only one transmit antenna is selected and one RF chain is required, the comparisons for conventional NOMA and OMA networks are given for $1 \times N_r$ SIMO case with MRC as explained in the complexity analysis in Section 4.4.1.1.2.

Firstly, comparisons between SMA and two users NOMA/OMA networks are presented.
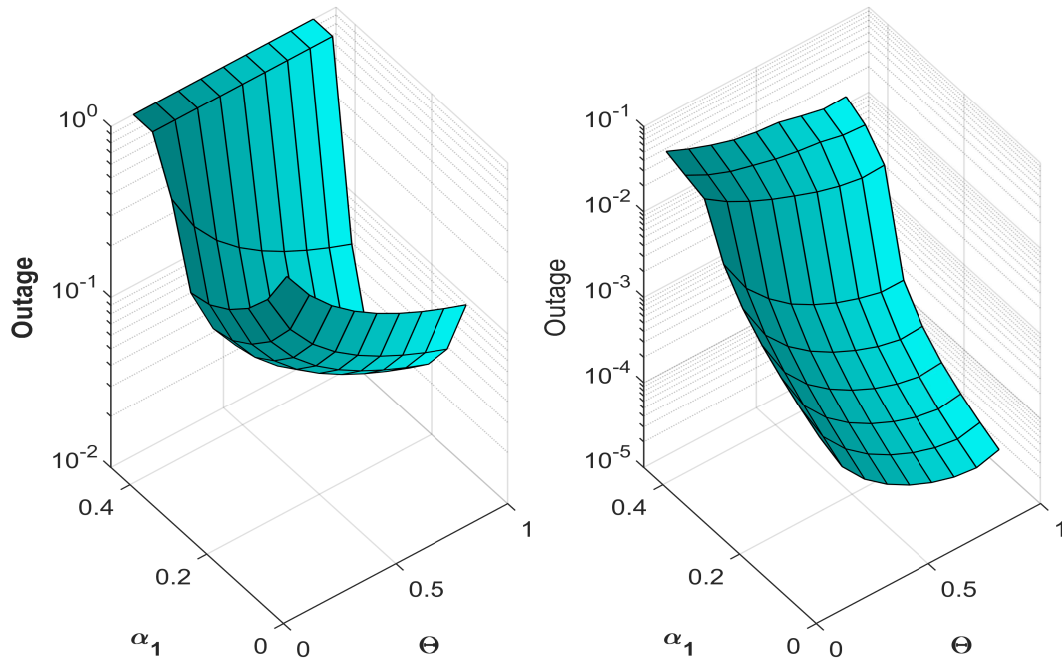
Figure 5.26: Outage performances in TBS-C-NOMA vs. Θ and α_1 when $\sigma_{s1}^2 = 10dB$, $\sigma_{s2}^2 = 0dB$, $\sigma_r^2 = 10dB$, $\beta = 0.001$, $\acute{R}_1 = 4BPCU$ and $\acute{R}_2 = 1.5BPCU$ a) UE_1 b) UE_2
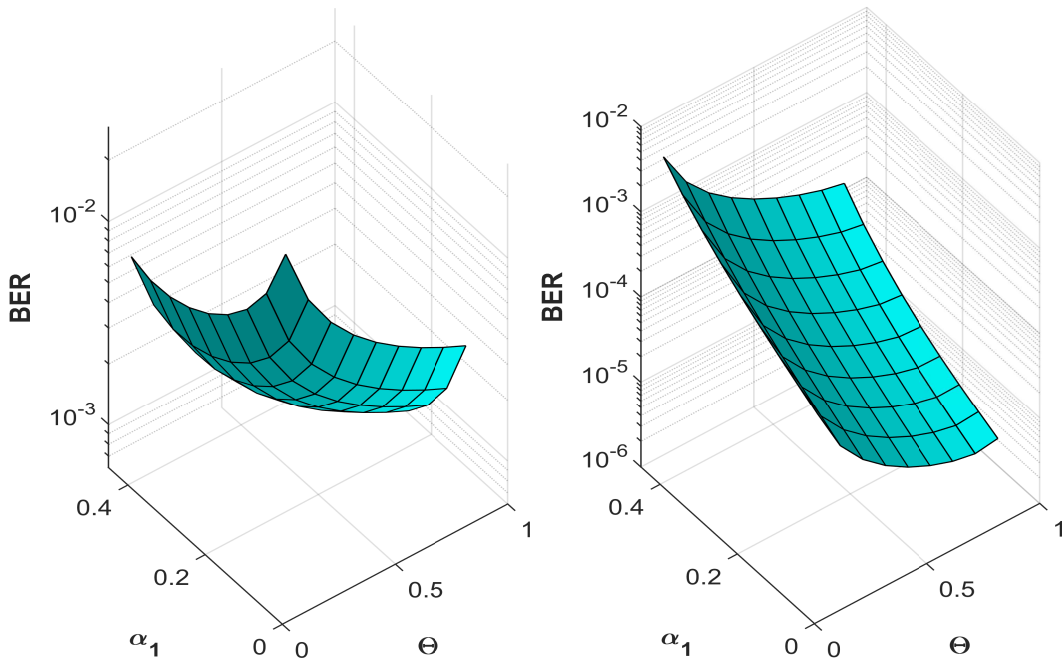
Figure 5.27: BER performances in TBS-C-NOMA vs. Θ and α_1 when $\sigma_{s1}^2 = 10dB$, $\sigma_{s2}^2 = 0dB$ and $\sigma_r^2 = 10dB$ a) UE_1 b) UE_2

146
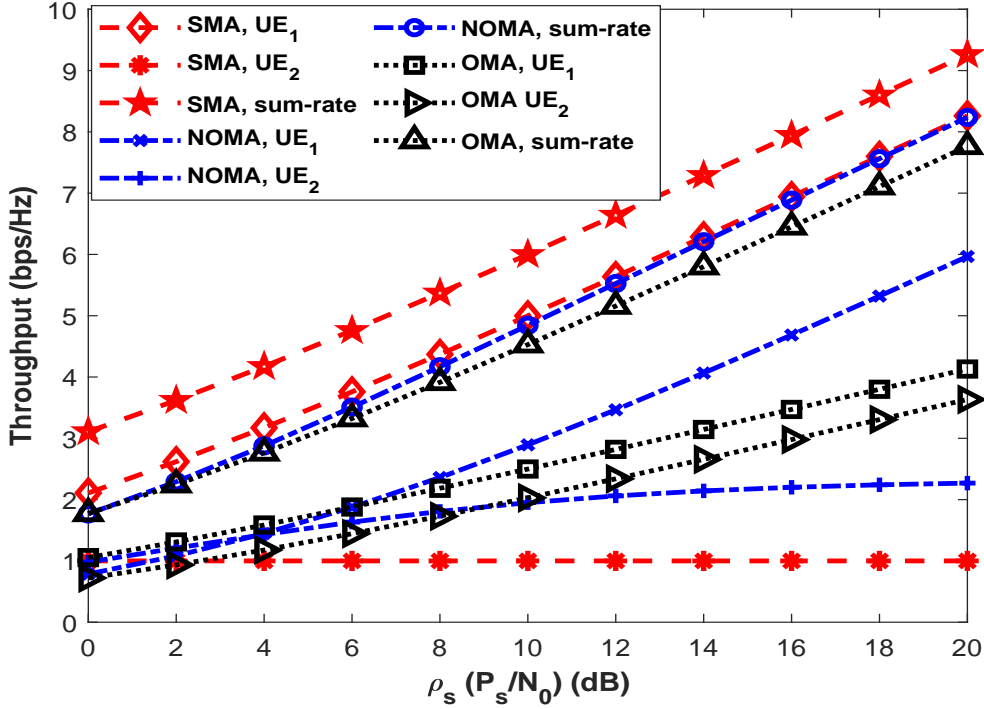
Figure 5.28: Ergodic capacity comparisons for SMA, NOMA and OMA when $\sigma_{s1}^2 = 3dB$, $\sigma_{s2}^2 = 0dB$ and $N_r = 2$

$\sigma_{s1}^2 = 3dB$ and $\sigma_{s1}^2 = 0dB$ are assumed. Simulation results are presented for $N_t = N_r = 2$ and $N_t = N_r = 4$ in Figure 5.28 and Figure 5.29, respectively. Power allocation coefficients for NOMA are chosen as $\alpha_1 = 0.2$ and $\alpha_2 = 0.8$. In both figures, one can easily see that SMA outperforms NOMA and OMA networks in terms of EC of UE_1 and sum-rate. It is hereby noted that NOMA performances are given for perfect SIC case ($\beta = 0$) and it is obvious that performance gain in SMA will be higher when this assumption is relaxed. EC of UE_2 in SMA is dominated by the number of transmit antennas (N_t) -it actually only depends on N_t, only correct detected bits change according to SNR-, it is almost constant in whole SNR regime. Although, it seems that UE_2 in SMA has worse capacity performance than NOMA and OMA in low SNR regime, it can be easily increased by implementing more transmit antennas without increasing implementation complexity/cost.

Then, the same comparisons are given in terms of outage performances of users in Figure 5.30 and Figure 5.31. Target rates of users are chosen as $\acute{R}_1 = \acute{R}_2 = \log_2 N_r$. Based on simulations, when the number of receive antennas is increased OMA can outperform
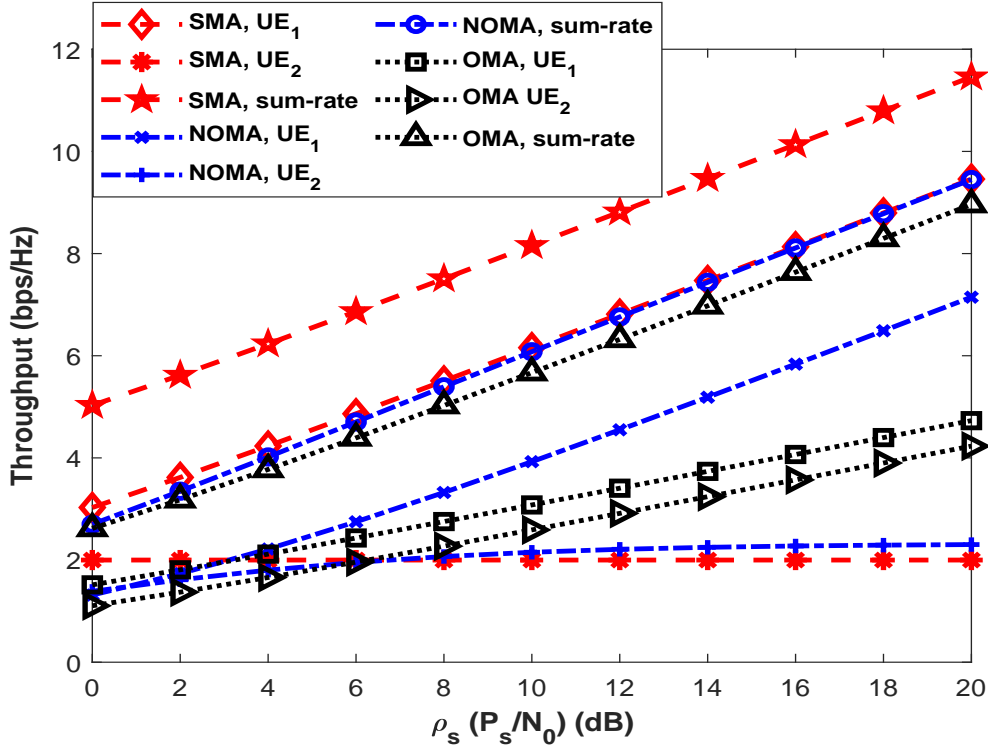
Figure 5.29: Ergodic capacity comparisons for SMA, NOMA and OMA when $\sigma_{s1}^2 = 3dB$, $\sigma_{s2}^2 = 0dB$ and $N_r = 4$

NOMA in terms of outage. Nevertheless, it is clear that SMA outperforms both OMA and NOMA in all cases even if perfect SIC ($\beta = 0$) is assumed in simulations.

Lastly for SMA, BER simulations are presented in Figure 5.32 and Figure 5.33 for the same channel conditions above in EC and OP comparisons. Based on simulations, SMA outperforms NOMA in terms of both users and this is very promising considering the decay in error performance of NOMA networks which is explained previous section and it is defined as the cost to be paid for NOMA networks. In SMA, error performance of UE_2 takes place between NOMA and OMA and this can afford the trade-off between error and capacity/outage performance of NOMA. In addition, it can be seen from the previous comparisons that UE_2 reaches that error performance besides gain in EC and outage. When it comes to UE_1, the performance gain is much more, it is beyond affording the decay in error performance, its error performance is the same with OMA as seen from figures. Hence, it is noteworthy that, SMA is much more reasonable multiple access scheme than multiple antenna NOMA considering all performance metrics.
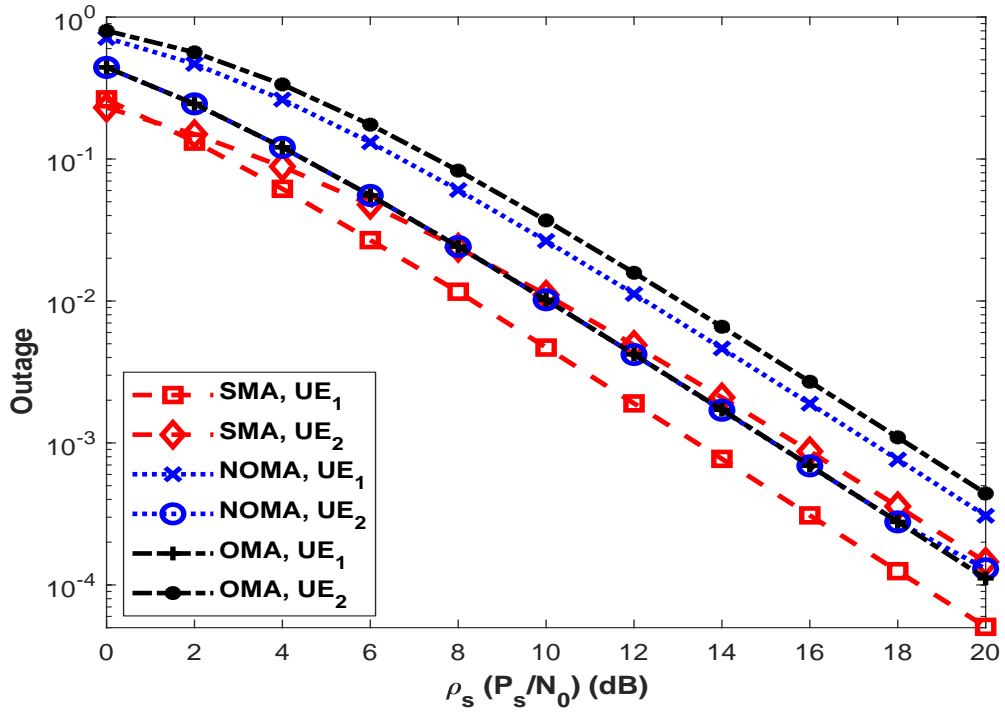
Figure 5.30: Outage comparisons for SMA, NOMA and OMA when $\sigma_{s1}^2 = 3dB$, $\sigma_{s2}^2 = 0dB$, $\acute{R}_1 = \acute{R}_2 = \log_2 N_r$ and $N_r = 2$
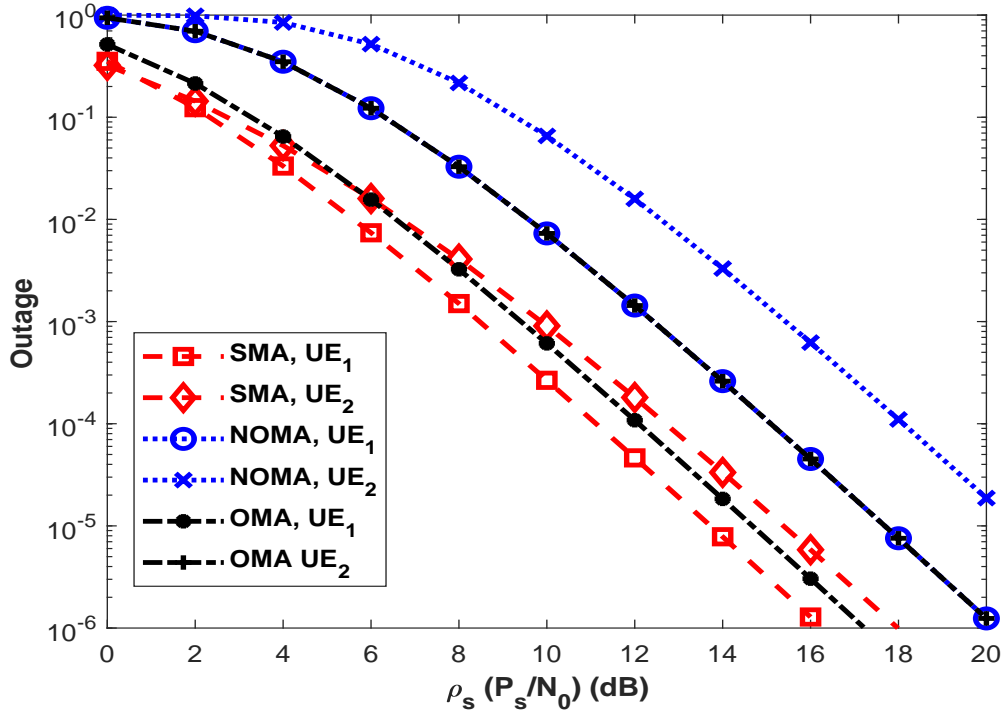
Figure 5.31: Outage comparisons for SMA, NOMA and OMA when $\sigma_{s1}^2 = 3dB$, $\sigma_{s2}^2 = 0dB$, $\acute{R}_1 = \acute{R}_2 = \log_2 N_r$ and $N_r = 4$
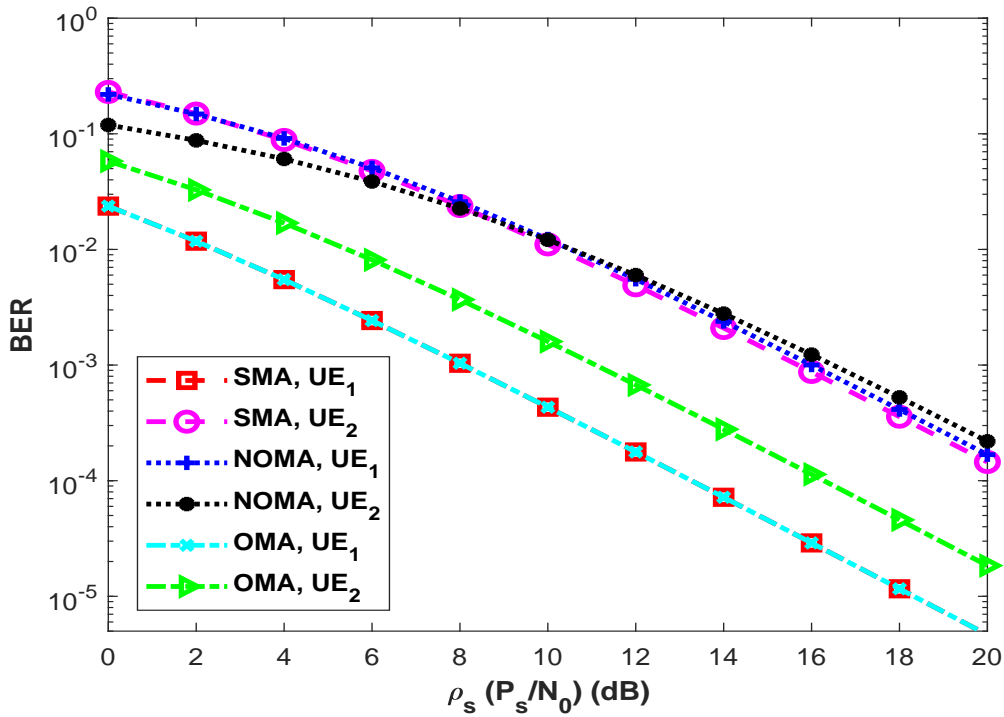
Figure 5.32: Error performance (BER) comparisons for SMA, NOMA and OMA when $\sigma_{s1}^2 = 3dB$, $\sigma_{s2}^2 = 0dB$ and $N_r = 2$
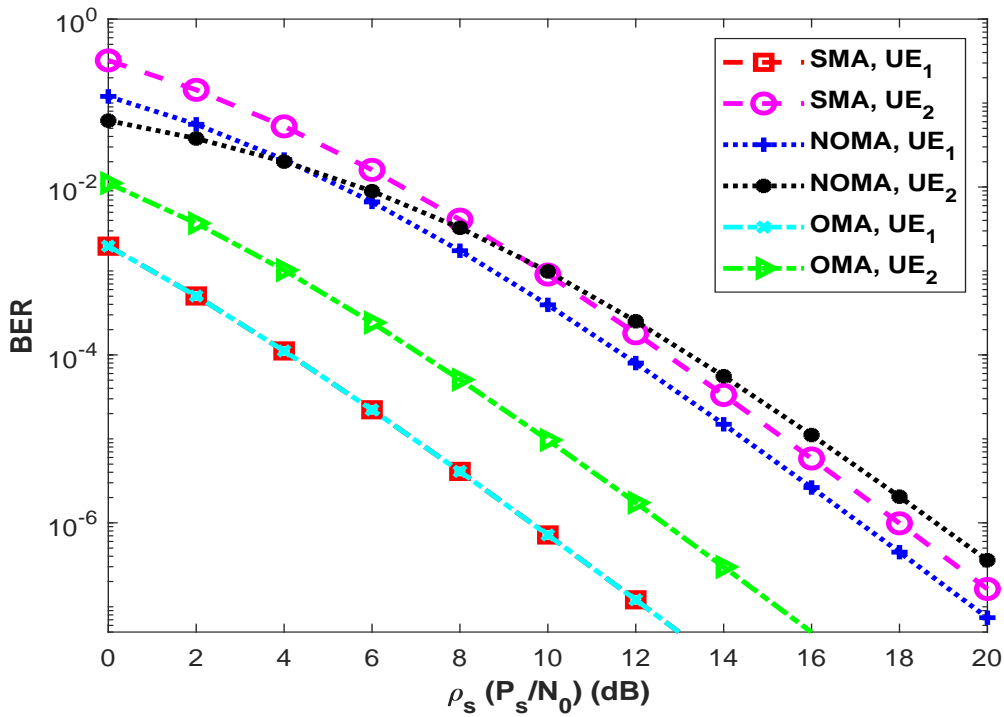
Figure 5.33: Error performance (BER) comparisons for SMA, NOMA and OMA when $\sigma_{s1}^2 = 3dB$, $\sigma_{s2}^2 = 0dB$ and $N_r = 4$
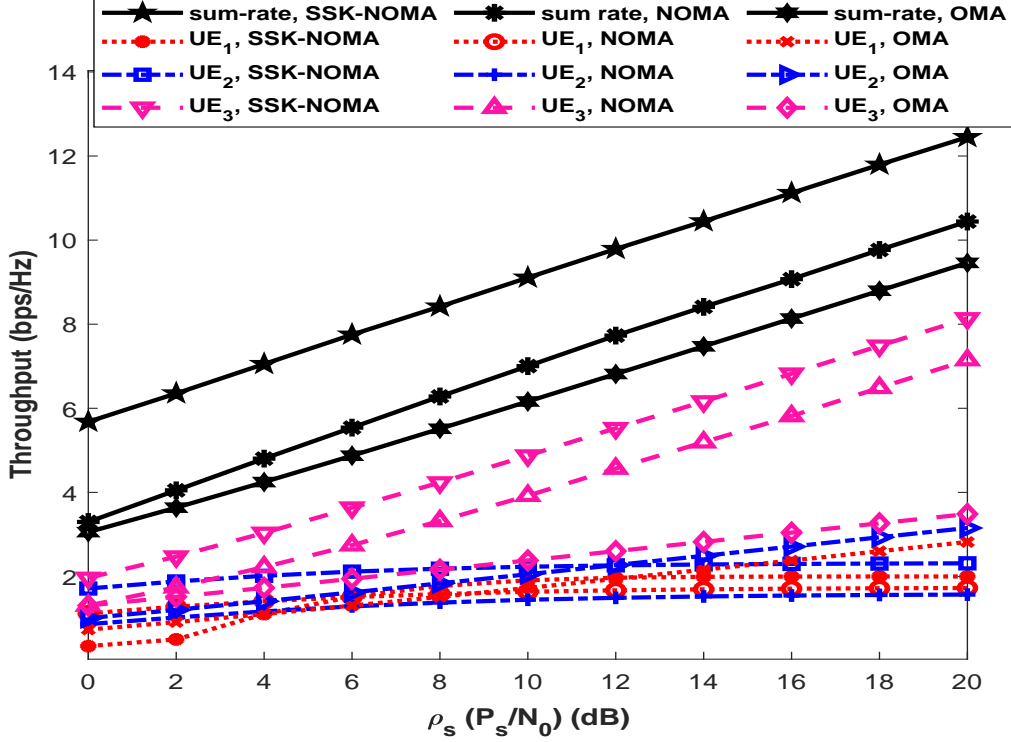
Figure 5.34: Capacity comparisons for SSK-NOMA, NOMA and OMA when $L = 3$ and $N_r = 2$

Finally, simulations are presented for SSK-NOMA and comparisons with NOMA/OMA counterpart are given for performance evaluation. In all simulations, it is assumed that $\sigma_{si}^2 = 2\sigma_{s(i-1)}^2$ and $\sigma_{s1}^2 = 0dB$. The power allocation coefficients for NOMA users are fixed and chosen as $\alpha_i = [0.8,\ 0.2]$, $\alpha_i = [0.7,\ 0.2,\ 0.1]$, $\alpha_i = [0.6,\ 0.25,\ 0.1,\ 0.05]$ and $\alpha_i = [0.4,\ 0.25,\ 0.2,\ 0.1,\ 0.05]$ when the number of NOMA users is equal to, 2, 3, 4 and 5, respectively.

In Figure 5.34, capacity comparisons of users within SSK-NOMA, NOMA and OMA are given when $L = 3$ and $N_r = 4$. As seen that, although NOMA is proposed due to its potential in terms of achievable capacity, this gain is increased by SSK-NOMA. All users in SSK-NOMA have better ergodic capacity performance than those counterparts in NOMA. It can be explained as users in SSK-NOMA encounter less IUI than NOMA counterparts since number of users multiplexed in power domain is decreased by introducing SSK.
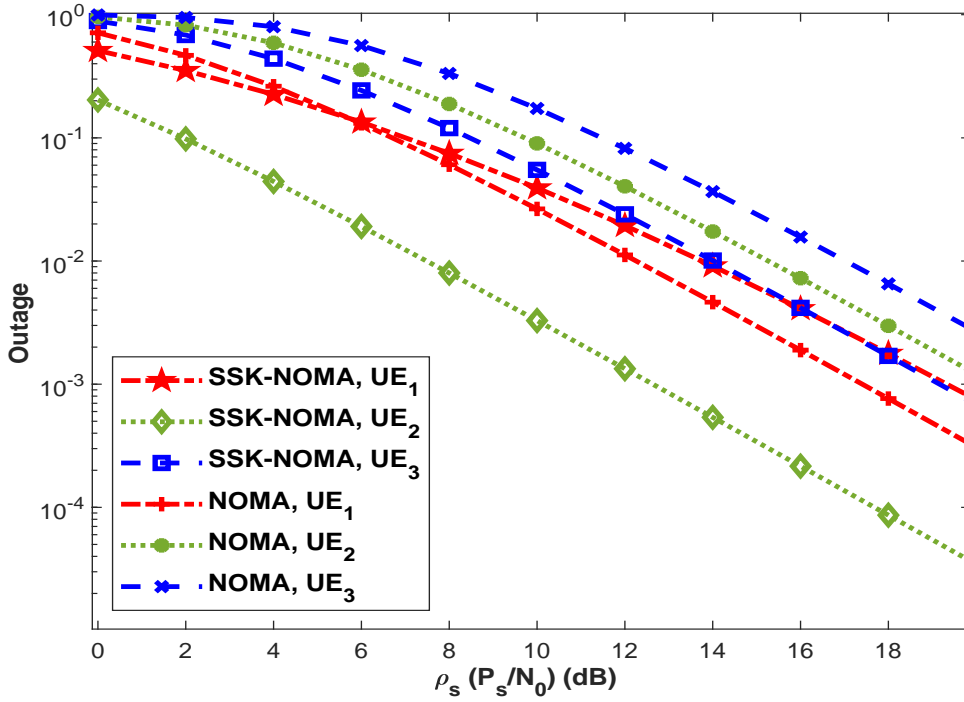
Figure 5.35: Outage comparisons for SSK-NOMA and NOMA when $L = 3$, $N_r = 2$, $\acute{R}_1 = 1BPCU$, $\acute{R}_2 = 1BPCU$ and $\acute{R}_3 = 2BPCU$

Then, in Figure 5.35 and Figure 5.36, outage performances are presented for two different target rates of users when $L = 3$ and $N_r = 2$. In Figure 5.35, it is assumed that $\acute{R}_1 = 1BPCU$, $\acute{R}_2 = 1BPCU$ and $\acute{R}_3 = 2BPCU$. SSK-NOMA outperforms NOMA in terms of outage performance of NOMA users (i.e., UE_2 and UE_3) whereas NOMA seems superior slightly to SSK-NOMA in terms of first user (UE_1). Nevertheless, if the target rates of users are updated as $\acute{R}_1 = 2BPCU$, $\acute{R}_2 = 2BPCU$ and $\acute{R}_3 = 4BPCU$ as in Figure 5.36, outage performance of UE_1 in SSK-NOMA almost does not change. On the other hand, UE_1 in NOMA remains in outage till $\sim 10dB$ and after that point SSK-NOMA still outperforms NOMA. Furthermore, this target rate increase also causes other users in NOMA to be in outage because of iterative SIC procedures and the performance gap between SSK-NOMA and NOMA gets larger for UE_2 and UE_3. It is noteworthy that achievable rate of UE_1 in SSK-NOMA is increased by just placing $N_t = 4$ without any further changes which does not cost any implementation complexity.
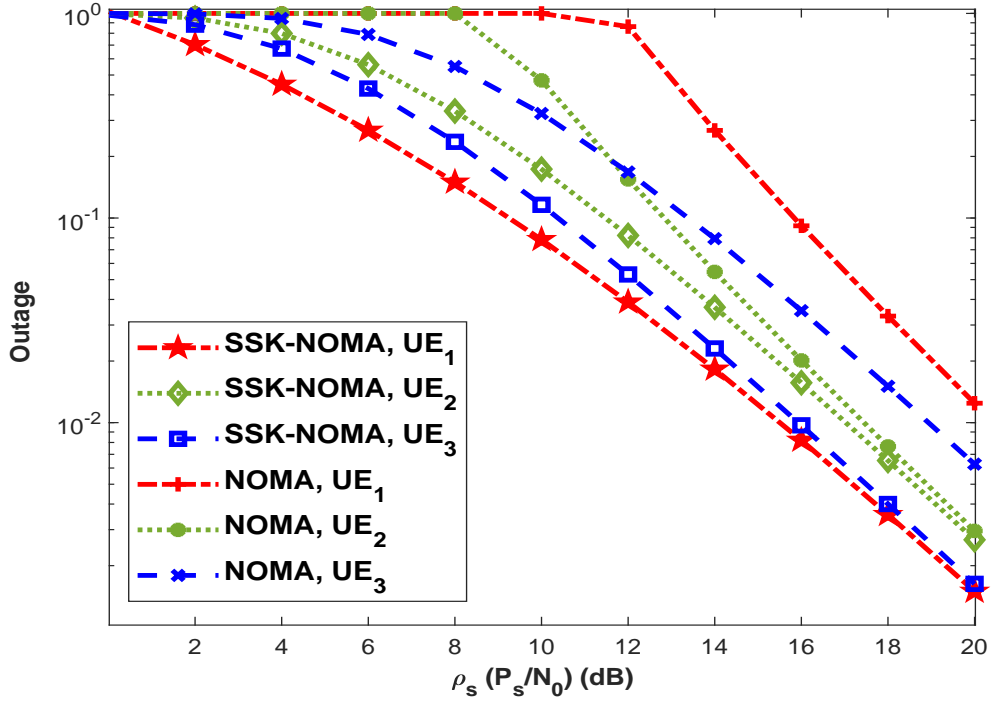
Figure 5.36: Outage comparisons for SSK-NOMA and NOMA when $L = 3$, $N_r = 2$, $\acute{R}_1 = 2BPCU$, $\acute{R}_2 = 2BPCU$ and $\acute{R}_3 = 2BPCU$

Moreover, BER simulations are provided for SSK-NOMA and NOMA to compare them. In addition, OMA results are also provided to highlight that SSK-NOMA can reduce performance decay in NOMA due to IUI. Simulation result are given for $N_r = 2$ and $N_r = 4$ in Figure 5.37 and Figure 5.38, respectively when $L = 3$. One can easily see that conventional NOMA has severe error performance when the number of users is increased to $L = 3$ even if number of receive antennas is increased. In addition, it is usually expected as N_r diversity order for users performances. However, it is not valid for NOMA due to IUI at UE_1 and erroneous detection during SIC procedures in UE_2 and UE_3. On the other hand, SSK-NOMA has much more acceptable/affordable error performance for all users and all users achieve full diversity order (i.e., N_r). SSK-NOMA outperforms NOMA about $10 - 15dB$ and this is very promising for energy efficiency. One can easily see that SSK-NOMA offers a reliable communication compared to NOMA although it cannot also achieve error performance of OMA networks since OMA does not encounter any IUI. Nevertheless, considering the performance gain in achievable rate compared to OMA and its potential to support massive connection -e.g for $L = 3$ number of users in
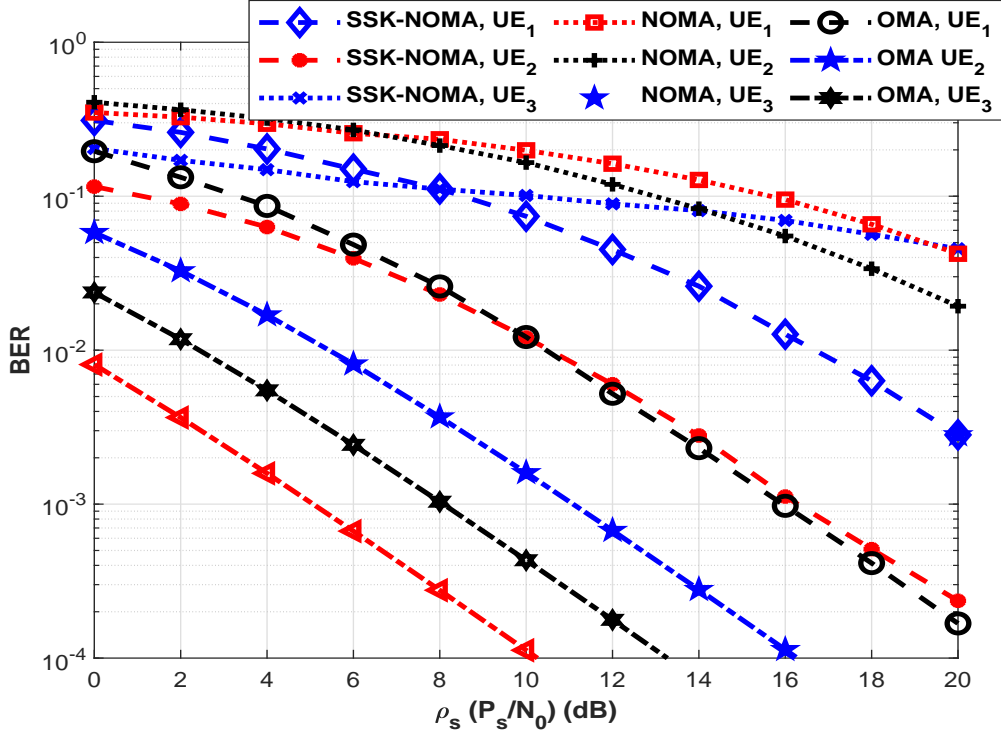
Figure 5.37: Error performance (BER) comparisons for SSK-NOMA, NOMA and OMA when $L = 3$ and $N_r = 2$

a resource block is increased by 3 times with an affordable decay in error performance-SSK-NOMA seems a major candidate for future networks.

Finally, optimum power allocation discussions for conventional NOMA networks still valid for also SSK-NOMA. Optimum power allocation should be handled considering priority in performance metrics of users. Thus, power allocation can change from application to application. If the data reliability is essential, power allocation should be arranged in a way minimizing users' bit error rate. On the other hand, if the continuity in connection is important, power allocation should be designed in way users become in outage with very low probability. To highlight this in SSK-NOMA, outage and BER performances of NOMA users (i.e., UE_2 and UE_3) are represented with respect to α_2 when $N_r = 2$ and $\rho_s = 20dB$ in Figure 5.49 and Figure 5.40, respectively. In Figure 5.39, results are presented for two different target rates. Based on simulations, it can be concluded that when α_2 is low (i.e., ~ 0.5), both users can remain in outage and have poor error performance. Nevertheless, when α_2 is high (i.e., above ~ 0.85), performance of both
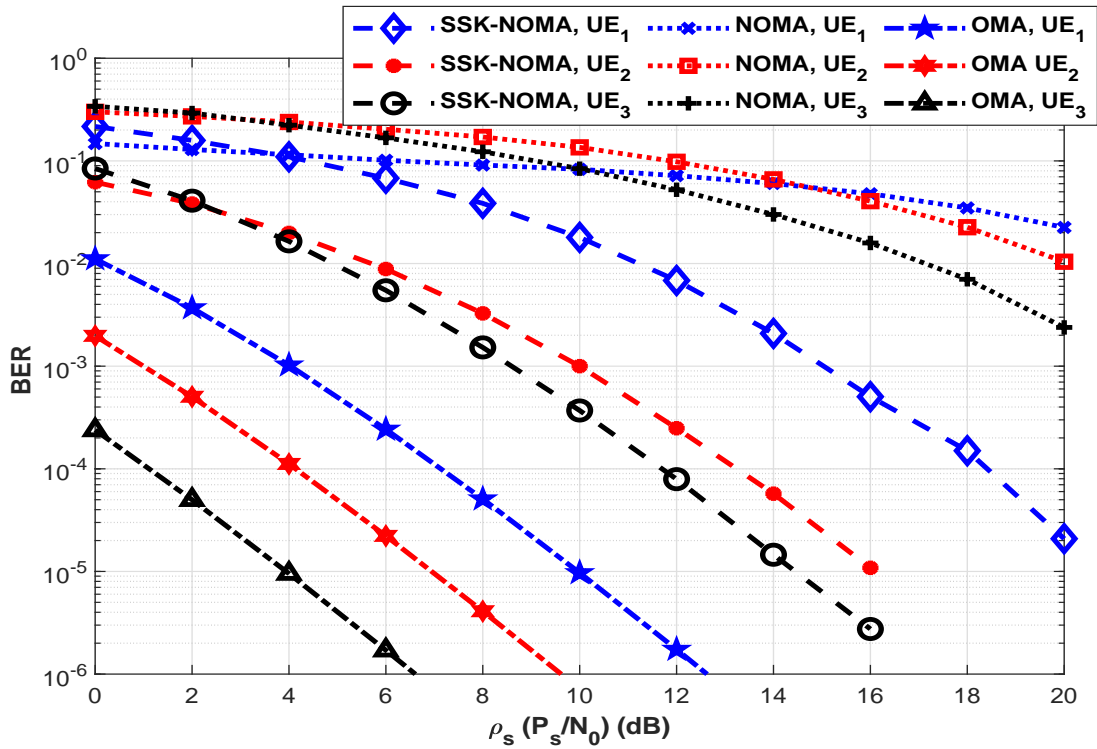
Figure 5.38: Error performance (BER) comparisons for SSK-NOMA, NOMA and OMA when $L = 3$ and $N_r = 4$

users decreases again because of SIC procedure. Thus, optimum power allocation should be in range $0.7 \leq \alpha_2 \leq 0.8$ by considering performances of both users.
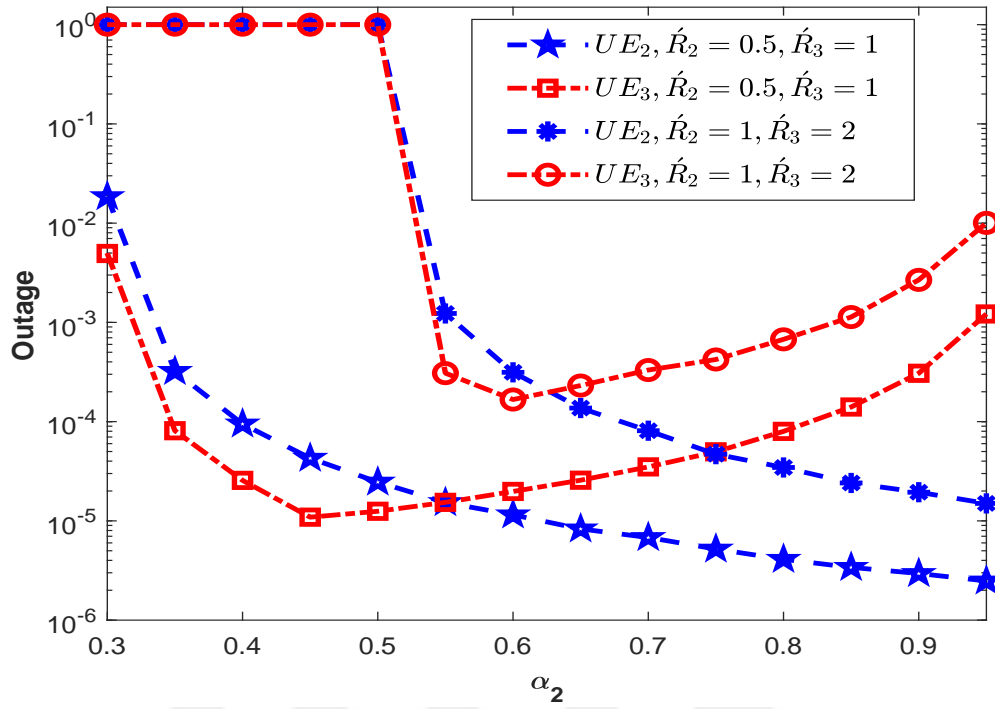
Figure 5.39: Outage performance of NOMA users in SSK-NOMA vs. α_2 when $L = 3$, $N_r = 2$, $\rho_s = 20dB$
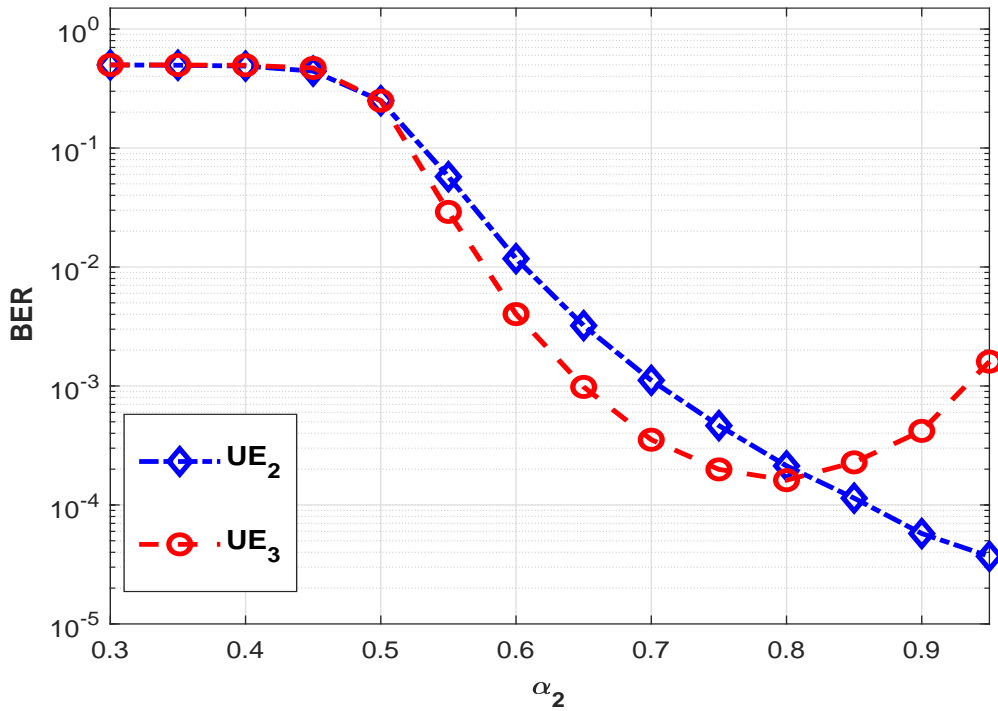
Figure 5.40: Error performance (BER) of NOMA users in SSK-NOMA vs. α_2 when $L = 3$, $N_r = 2$, $\rho_s = 20dB$

CHAPTER 6

CONCLUSIONS

In this chapter, the contributions of this thesis are summarized and discussions on results are provided. Based on accomplished works and detailed literature research for future wireless networks, insights are also presented for what future directions of researches on NOMA involved networks are to be.

6.1 SUMMARY AND CONTRIBUTIONS

In this thesis, NOMA involved systems have been analyzed under imperfect SIC. Analysis consists of three chapter according to considered NOMA system models. Hereby, the contributions in each chapter are summarized and discussions on them are provided.

In Chapter 2, conventional downlink and uplink NOMA networks are studied and closed-form expressions are derived for ergodic capacity (EC), outage probability and bit error probability (BEP). All analyses are validated via computer simulations.

In Chapter 3, the interplay between NOMA and cooperative communication is considered in three major concepts. Firstly, the cooperative-NOMA (C-NOMA) is analyzed where users are in cooperation and the intra-cell user also acts as a relay as well for the cell-edge user to improve its performance. The closed form expressions of EC, OP and BEP for C-NOMA are derived and validated with simulations. Then, threshold-based selective cooperative-NOMA (TBS-C-NOMA) is proposed where transmission in the second phase is conditioned on the reliability of SIC process at the intra-cell user to improve error performance of C-NOMA. Then, optimum threshold for TBS-C-NOMA is derived and it is proved that TBS-C-NOMA achieves full diversity order and minimum BER nearly perfect SIC case. In addition, the EC and OP of TBS-C-NOMA remain the same with C-NOMA by introducing optimum threshold. In this chapter, relay-assisted/aided-NOMA networks

are analyzed with imperfect SIC unlike previous studies, and the derived expressions are validated via simulations. Considering user fairness, reversed relay-assisted-NOMA is proposed where detection at the relay is reversed by changing power allocation coefficients for users' symbols. It is seen that, in some cases, proposed reversed network provide better performance and higher user fairness than conventional relay-assisted-NOMA network. Considering users' demands (QoS) under various constraints (i.e., EC, OP and BEP), optimum power allocation is discussed for both conventional and reversed relay-assisted-NOMA networks. Moreover, NOMA-based cooperative relaying systems (CRS) are analyzed. Analytical results are validated via simulations. Then, NOMA based diamond relaying network (DRN) is also investigated as a subset of NOMA-CRS in terms of BEP. Based on simulations, it is pointed out that NOMA-DRN turns out to be a non-equiprobable communication and again pointed out that NOMA-DRN has a poor error performance though it has been proposed for achievable rate. Lastly, based on the simulation results, the trade-off between capacity and reliability of NOMA-CRS is emphasized and it is discussed how the optimal power allocation should be handled in terms of BER constraints.

In chapter 4, spatial multiple access (SMA) and space shift keying (SSK)-NOMA are proposed as alternatives to the two users and multiple users NOMA networks, respectively. SMA and SSK-NOMA are analyzed in terms of EC, OP and BEP. The derived expressions are validated with simulations. In addition, complexity comparisons between SSK-NOMA and NOMA are provided and it is shown that only cell-edge user in SSK-NOMA has higher computational complexity than NOMA and it is only if the number of users and modulation order are both relatively high. Nevertheless, this is an affordable complexity considered the performance gain in all three KPIs. SSK-NOMA allows serving more than three users without decreasing any performance metric and increasing complexity. This is very promising for mMTC.

In chapter 5, extensive simulations are provided to compare performances of NOMA networks with OMA counterparts in terms of all performance metrics. Based on extensive simulations it is proved that NOMA is superior to OMA networks in terms of EC and OP. However, NOMA cannot compete with OMA counterparts in terms of bit error

rate (BER) due to the inter-user-interferences (IUI). In addition, this performance decay in error performance get worse when the number of users served in a resource block is increased. Thus, the trade-off between capacity and reliability of NOMA networks is raised and it is emphasized that target error probability should be considered when designing NOMA schemes. In addition, numerous efforts on optimum power allocation and user pairing algorithms in the literature should be adopted by considering BER constraints and user fairness in terms of error performance. Then, comparison between C-NOMA and proposed TBS-C-NOMA are also provided and it is proved that TBS-C-NOMA outperforms C-NOMA in terms of error performance without decreasing EC or outage performance. Then, optimum power allocation is discussed for TBS-C-NOMA in terms of energy efficiency, sum-rate maximization, outage and BEP minimization. Furthermore, performances of proposed SMA and SSK-NOMA models are evaluated and comparisons with NOMA counterparts are provided. Based on extensive simulations, both proposed models outperform conventional NOMA networks in terms of all three KPIs. Thus, SMA as a new multiple access provides higher spectral efficiency than NOMA and is competitive to OMA for two user networks. In addition, the hybrid SSK-NOMA achieves higher spectral efficiency without decreasing error performance of users compared to NOMA for more than three users networks.

6.2 FUTURE WORKS

Firstly as related to this thesis, all analysis throughout this thesis can be easily extended for different fading channels/multiple-antenna situations and the BEP analysis can be extended for different modulation constellations. In addition, as mentioned above optimum power allocation and user pairing algorithms should be adopted according to error performance targets of users to provide a reliable communication. The proposed SMA and SSK-NOMA schemes can be extended for other index modulation (IM) techniques where our insight is that using media based modulation (MBM) rather than SSK can be a good solution to limit the number of required antennas at BS. In addition, since the proposed models in thesis (i.e., SMA and SSK-NOMA) are easily applicable with other physical layer techniques, the models can be extended with the usage of cooperative communication, cognitive radio etc.

Secondly, all considered NOMA models should be evaluated in terms of other KPIs which are physical security, secrecy rate, energy efficiency and based on these constraints, NOMA involved systems can be evolved.

Lastly, based on our insights during this research, NOMA indeed is a promising technique for future networks. However, due to the penalty of the error performance, NOMA may not be a reasonable solution to serve mobile users in a cellular network in a conventional way and NOMA should be considered something else than conventional multiple access techniques. Recalling the trade-off between capacity and reliability in NOMA networks, NOMA is not a reasonable solution for uRLLC concept of 5G and beyond due to the reliability although it is still strong candidate for mMTC thanks to high spectral efficiency. Nevertheless, if the error performance of NOMA networks can be improved, this insight will be invalid. This improvement may be succeeded with the use of new techniques for modulation/demodulation such as machine learning algorithms. Their first attempts in NOMA seem promising [173–175].

NOMA will take the role in more challenging tasks such as mobile edge computing (MEC) [176–178], coordinated multipoint (CoMP) [179–181] or in more flexible situations such as grant-free access [182–184], unnamed aerial vehicles/drone networks [185–187]. Thus, future researches of NOMA are expected to be on those topics and further researches will evolve to investigate the role of NOMA on those challenging issues.

BIBLIOGRAPHY

[1] Andrews J J G, Buzzi S, Choi W, Hanly S V S, Lozano A, Soong A A C K and Zhang J J C (2014) What Will 5G be? *IEEE Journal of Selected Areas in Communications,* 32 (6): 1065-1082.

[2] White paper (2017) Cisco Visual Networking Index: Global Mobile Data Traffic Forecast Update, 2017-2022

[3] Boccardi F, Heath R, Lozano A, Marzetta T and Popovski P (2014) Five Disruptive Technology Directions for 5G. *IEEE Communications Magazine.,* 52 (2): 74-80.

[4] Hossain E and Hasan M (2015) 5G Cellular: Key Enabling Technologies and Research Challenges. *IEEE Instrumentation and Measurement Magazine,* 18 (21):11-21.

[5] Popovski P, Trillingsgaard K F, Simeone O and Durisi G (2018) 5G Wireless Network Slicing for eMBB, URLLC, and MMTC: A Communication-Theoretic View. *IEEE Access,* 6: 55 765-55 779.

[6] Cai Y, Qin Z, Cui F, Li G Y and McCann J A (2018) Modulation and Multiple Access for 5G Networks. *IEEE Communications Surveys and Tutorials,* 20 (1): 629- 646.

[7] 3GPP (2019) Technical Specification Group Services and System Aspects; Release 15 Description.

[8] 3GPP (2015) TR 36.859: Study on Downlink Multiuser Superposition Transmission (MUST) for LTE (Release 13).

[9] 3GPP (2016) RP-160680: Downlink Multiuser Superposition Transmission for LTE.

[10] Dai L, Wang B, Yuan Y, Han S, Lin C and Wang Z (2015) Non-Orthogonal Multiple Access for 5G: Solutions, Challenges, Opportunities, and Future Research Trends. *IEEE Communications Magazine,* 53 (9): 74-81.

[11] Ding Z, Lei X, Karagiannidis G K, Schober R, Yuan J and Bhargava V K (2017) A Survey on Non-Orthogonal Multiple Access for 5G Networks: Research Challenges and Future Trends. *IEEE Journal on Selected Areas in Communications,* 35 (10): 2181-2195.

[12] Nikopour H, Yi E, Bayesteh A, Au K, Hawryluck M, Baligh H and Ma J (2014) SCMA for Downlink Multiple Access of 5G Wireless Networks. *IEEE Global Communications Conference,* Dec. 2014, Austin, TX, USA, 3940-3945.

BIBLIOGRAPHY (continued)

[13] Chen S, Ren B, Gao Q, Kang S, Sun S and Niu K (2017) Pattern Division Multiple Access (PDMA)-A Novel Non-Orthogonal Multiple Access for 5G Radio Networks. *IEEE Transactions on Vehicular Technology,* 66 (4): 3185-3196.

[14] Peng W, Jun X and Li P (2006) Comparison of Orthogonal and Non-Orthogonal Approaches to Future Wireless Cellular Systems. *IEEE Vehicular Technology Magazine,* September: 4-11.

[15] Yuan Z, Yu G, Li W, Yuan Y, Wang X and Xu J (2016) Multi-user Shared Access for Internet of Things. *IEEE Vehicular Technology Conference,* 15-18 May 2016, Nanjing, China, 1-5.

[16] Shirvanimoghaddam M, Dohler M and Johnson S. J (2017) Massive Non- Orthogonal Multiple Access for Cellular loT: Potentials and Limitations. *IEEE Communications Magazine,* 55 (9): 55-61.

[17] Verdu S (1988) *Multiuser Detection.* 1st edition, ISBN: 9780521593731 Cambridge Press, Cambridge, 451 pp.

[18] Wang X and Poor H V (2004) *Wireless communication systems: advanced techniques for signal reception,* lst edition, ISBN: 978-0137020805, Prentice Hall, New Jersey, 704 pp.

[19] Saito Y, Kishiyama Y, Benjebbour A, Nakamura T, Li A and Higuchi K (2013) Non-Orthogonal Multiple Access (NOMA) for Cellular Future Radio Access. *IEEE 77th Vehicular Technology Conference (VTC Spring),* 2-5 June 2013, Dresden, Germany, 1-5.

[20] Ding Z, Liu Y, Choi J, Sun Q, Elkashlan M, Lin C and Poor H V (2017) Application of Non-Orthogonal Multiple Access in LTE and 5G Networks. *IEEE Communications Magazine,* 55 (2): 185-191.

[21] Liu Y, Qin Z, Elkashlan M, Ding Z, Nallanathan A and Hanzo L (2017) Non-Orthogonal Multiple Access for 5G. *Proceedings of IEEE,* 105 (12): 2347-2381

[**22] Shin W, Vaezi M, Lee B, Love D J, Lee J and Poor H V** (2017) Non-Orthogonal Multiple Access in Multi-Cell Networks: Theory, Performance, and Practical Challenges. *IEEE Communications Magazine,* 55 (10): 176-183.

[23] Ding Z, Peng M and Poor H V (2015) Cooperative Non-Orthogonal Multiple Access in 5G Systems. *IEEE Communications Letters,* 19 (8): 1462-1465.

[24] Kim J B and Lee I H (2015) Capacity Analysis of Cooperative Relaying Systems Using Non-Orthogonal Multiple Access. *IEEE Communications Letters,* 19 (11): 1949-1952.

[25] Ding Z, Adachi F and Poor H V (2016) The Application of MIMO to Non- Orthogonal Multiple Access. *IEEE Transactions on Wireless Communications,* 15 (1): 537-552.

[26] Ding Z, Fan P and Poor H V (2017) Random Beamforming in Millimeter-Wave NOMA Networks. *IEEE Access,* 5: 7667-7681.

[27] Cui J, Liu Y, Ding Z, Fan P and Nallanathan A (2018) Optimal User Scheduling and Power Allocation for MillimeterWave NOMA Systems. *IEEE Transactions on Wireless Communications,* 17 (3): 1502-1517.

[28] Liu Y, Ding Z, Elkashlan M and Yuan J (2016) Nonorthogonal Multiple Access in Large-Scale Underlay Cognitive Radio Networks. *IEEE Transactions on Vehicular Technology,* 65 (12): 152-10157.

[29] Marshoud H, Kapinas V M, Karagiannidis G K and Muhaidat S (2015) Non-Orthogonal Multiple Access for Visible Light Communications. *IEEE Photonics Technology Letters,* 28 (1): 51-54.

[30] Ding Z, Ng D W K, Schober R and Poor V H (2018) Delay Minimization for NOMA-MEC offloading. *IEEE Signal Processing Letters,* 25 (12): 1875-1879.

[31] Saito Y, Benjebbour A, Kishiyama Y and Nakamura T (2013) System-level Performance Evaluation of Downlink Non-Orthogonal Multiple Access (NOMA). *IEEE 24th Annual International Symposium on Personal, Indoor, and Mobile Radio Communications (PIMRC),* 8-11 Sep. 2013, London, United Kingdom, 611-615.

[32] Ding Z, Yang Z, Fan P and Poor H V (2014) On the Performance of Non- Orthogonal Multiple Access in 5G Systems with Randomly Deployed Users. *IEEE Signal Processing Letters,* 21 (12): 1501-1505.

[33] Timotheou S and Krikidis I (2015) Fairness for Non-Orthogonal Multiple Access in 5G Systems. *IEEE Signal Processing Letters,* 22 (10): 1647-1651.

[34] Ding Z, Fan P and Poor H V (2016) Impact of User Pairing on 5G Nonorthogonal Multiple Access Downlink Transmissions. *IEEE Transactions on Vehicular Technology,* 65 (8): 6010-6023.

[35] Yang Z, Ding Z, Fan P and Karagiannidis G K (2016) On the Performance of Non-Orthogonal Multiple Access Systems with Partial Channel Information. *IEEE Transactions on Communications,* 64 (2): 654-667.

[36] Xu P, Yuan Y, Ding Z, Dai X and Schober R (2016) On the Outage Performance of Non-Orthogonal Multiple Access with 1-bit Feedback. *IEEE Transactions on Wireless Communications,* 15 (10): 6716-6730.

[37] Benjebbour A, Li A, Kishiyama Y, Jiang H and Nakamura T (2014) System-level Performance of Downlink NOMA Combined with SU-MIMO for Future LTE Enhancements. *IEEE Globecom Workshops (GC Wkshps),* 8-12 Dec. 2014, Austin, Texas, USA, 706-710.

[38] **Ding Z, Schober R, and Poor H V (**2016) A General MIMO Framework for NOMA Downlink and Uplink Transmission Based on Signal Alignment. *IEEE Transactions on Wireless Communications,* 15 (6): 4438-4454.

[39] **Ding Z, Adachi F and Poor H V** (2016) The Application of MIMO to Non-Orthogonal Multiple Access. *IEEE Transactions on Wireless Communications,* 15 (1): 537-552.

[40] **Sun Q, Han S, Lin C and Pan Z** (2015) On the Ergodic Capacity of MIMO NOMA Systems. *IEEE Wireless Communications Letters,* 4 (4): 405-408.

[41] **Liu Y, Pan G, Zhang H, and Song M** (2016) On the Capacity Comparison between MIMO-NOMA and MIMO-OMA. *IEEE Access,* 4: 2123-2129.

[42] **Zeng M, Yadav A, Dobre O A, Tsiropoulos G I and Poor H V** (2017) On the Sum Rate of MIMO-NOMA and MIMO-OMA Systems. *IEEE Wireless Communications Letters,* 6 (4): 534-537.

[43] **Ding Z, Dai L and Poor H V** (2016) MIMO-NOMA Design for Small Packet Transmission in the Internet of Things. *IEEE Access,* 4: 1393-1405.

[44] **Sun Y, Ng D W K, Ding Z and Schober R** (2016) Optimal Joint Power and Subcarrier Allocation for MC-NOMA Systems. *IEEE Global Communications Conference (GLOBECOM),* 4-8 Dec. 2016, Washington DC, USA, 1-6.

[45] **Wei Z, Ng D W K, Yuan J and Wang H** (2017) Optimal Resource Allocation for Power Efficient MC-NOMA with Imperfect Channel State Information. *IEEE Transactions on Communications,* 65 (9): 3944-3961.

[46] **Lei H, Zhang J, Park K, Xu P, Ansari I S, Pan G, Alomair B and Alouini M** (2017) On Secure NOMA Systems with Transmit Antenna Selection Schemes. *IEEE Access,* 5: 17 450-17464.

[47] **Chen Z, Ding Z, Dai X and Karagiannidis G K** (2016) On the Application of Quasi-degradation to MISO-NOMA Downlink. *IEEE Transactions on Signal Processing,* 64 (23): 6174-6189.

[48] **Choi J** (2016) Power Allocation for Max-sum Rate and Max-min Rate Proportional Fairness in NOMA. *IEEE Communications Letters,* 20 (10): 2055-2058.

[49] **Li C, Zhang Q, Li Q and Qin J** (2016) Price-based Power Allocation for Non-Orthogonal Multiple Access Systems. *IEEE Wireless Communications Letters,* 5 (6,): 664-667.

[50] **Choi J** (2016) On the Power Allocation for a Practical Multiuser Superposition Scheme in NOMA Systems. *IEEE Communications Letters,* 20 (3): 438-441.

[51] **Zhu J, Wang J, Huang Y, He S, You X and Yang L** (2017) On Optimal Power Allocation for Downlink Non-Orthogonal Multiple Access Systems. *IEEE Journal on Selected Areas in Communications,* 35 (12): 2744-2757.

[52] **Oviedo J A and Sadjadpour H R** (2017) A Fair Power Allocation Approach to NOMA in Multiuser SISO Systems. *IEEE Transactions on Vehicular Technology,* 66 (9): 7974-7985.

[53] **Xu P and Cumanan K** (2017) Optimal Power Allocation Scheme for Non-Orthogonal Multiple Access with *a*-fairness. *IEEE Journal on Selected Areas in Communications,* 35 (10): 2357-2369.

[54] **Yang Z, Xu W, Pan C, Pan Y and Chen M** (2017) On the Optimality of Power Allocation for NOMA Downlinks with Individual QoS Constraints. *IEEE Communications Letters,* 21 (7): 1649-1652.

[55] **Wang C, Chen J and Chen Y** (2016) Power Allocation for a Downlink Non-Orthogonal Multiple Access System. *IEEE Wireless Communications Letters,* 5 (5): 532-535.

[56] **Yang Z, Ding Z, Fan P and Al-Dhahir N** (2016) A General Power Allocation Scheme to Guarantee Quality of Service in Downlink and Uplink NOMA Systems. *IEEE Transactions on Wireless Communications,* 15 (11): 7244-7257.

[57] **Lei L, Yuan D, Ho C. K and Sun S** (2016) Power and Channel Allocation for Non-Orthogonal Multiple Access in 5G Systems: Tractability and Computation. *IEEE Transactions on Wireless Communications,* 15 (12): 8580-8594.

[58] **Cui J, Ding Z and Fan P** (2016) A Novel Power Allocation Scheme under Outage Constraints in NOMA Systems. *IEEE Signal Processing Letters,* 23 (9): 1226-1230.

[59] **Cui J, Ding Z and Fan P** (2018) Outage Probability Constrained MIMO-NOMA Designs under Imperfect CSI. *IEEE Transactions on Wireless Communications,* 17 (12): 8239-8255.

[60] **Lei L, Yuan D and Vrbrand P** 2016 On Power Minimization for Non-Orthogonal Multiple Access (NOMA). *IEEE Communications Letters,* 20 (12): 2458-2461.

[61] **Hanif M F, Ding Z, Ratnarajalı T and Karagiannidis G K** (2016) A Minorization-Maximization Method for Optimizing Sum Rate in the Downlink of Non-Orthogonal Multiple Access Systems. *IEEE Transactions on Signal Processing,* 64 (1): 76-88.

[62] **Di B, Song L and Li Y** (2016) Sub-channel Assignment, Power Allocation, and User Scheduling for Non-Orthogonal Multiple Access Networks. *IEEE Transactions on Wireless Communications,* 15 (11): 7686-7698.

[63] **Ali M. S, Tabassum H and Hossain E** (2016) Dynamic User Clustering and Power Allocation for Uplink and Downlink Non-Orthogonal Multiple Access (NOMA) Systems. *IEEE Access,* 4: 6325-6343.

[64] **Chen Z, Ding Z, Dai X and Zhang R** (2017) An Optimization Perspective of the Superiority of NOMA Compared to Conventional OMA. *IEEE Transactions on Signal Processing,* 65 (19): 5191-5202.

[65] **Hojeij M, Faralı J, Nour C A and Douillard C** (2015) Resource Allocation in Downlink Non-Orthogonal Multiple Access (Noma) for Future Radio Access. *IEEE 81st Vehicular Technology Conference (VTC Spring),* 11-14 May. 2015, Glasgow, Scotland, 1-6.

[66] **Islam S M R, Zeng M, Dobre O A and Kwak K** (2018) Resource Allocation for Downlink NOMA Systems: Key Techniques and Open Issues. *IEEE Wireless Communications,* 25 (2): 40-47.

[67] **Qin Z, Liu Y, Ding Z, Gao Y and Elkashlan M** (2016) Physical Layer Security for 5G Non-Orthogonal Multiple Access in Large-scale Networks. *IEEE International Conference on Communications,* 23-27 May. 2016, Kuala Lumpur, Malaysia, 1-6.

[68] **Chen J, Yang and Alouini** M (2018) Physical Layer Security for Cooperative NOMA Systems. *IEEE Transactions on Vehicular Technology,* 67 (5): 4645-4649.

[69] **Zhang Y, Wang H, Yang Q and Ding Z** (2016) Secrecy Sum Rate Maximization in Non-Orthogonal Multiple Access. *IEEE Communications Letters,* 20 (5): 930-933.

[70] **Li Y, Jiang M, Zhang Q, Li Q and Qin J** (2017) Secure Beamforming in Downlink MISO Nonorthogonal Multiple Access Systems. *IEEE Transactions on Vehicular Technology,* 66 (8): 7563-7567.

[71] **Zhang H, Yang N, Lang K, Pan M, Karagiannidis G K and Leung V C M** (2018) Secure Communications in NOMA System: Subcarrier Assignment and Power Allocation. *IEEE Journal on Selected Areas in Communications,* 36 (7): 1441-1452.

[72] **Lv L, Ding Z, Ni Q and Chen J** (2018) Secure MISO-NOMA Transmission with Artificial Noise. *IEEE Transactions on Vehicular Technology,* 67 (7): 6700-6705.

[73] **Al-Imari M, Xiaa P, Imran M A and Tafazalli R** (2014) Uplink Non-Orthogonal Multiple Access for 5G Wireless Networks. *11th International Symposium on Wireless Communications Systems (JSWCS),* 26-29 Aug. 2014, Barcelona, Spain, 781-785.

[74] **Zhang N, Wang J, Kang G and Liu Y** (2016) Uplink Nonorthogonal Multiple Access in 5G Systems. *IEEE Communications Letters,* 20 (3): 458-461.

[75] **Kim B, Chung W, Lim S, Suh S, Kwun J, Chai S and Hang D** (2015) Uplink Noma with Multi-antenna. *IEEE 81st Vehicular Technology Conference (VTC Spring),* 11-14 May. 2015, Glasgow, Scotland, 1-5.

[76] **Gao Y, Xia B, Xiao K, Chen Z, Li X and Zhang S** (2017) Theoretical Analysis of the Dynamic Decode Ordering SIC Receiver for Uplink NOMA Systems. *IEEE Communications Letters,* 21 (10): 2246-2249.

[77] **Liu Y, Derakhshani M and Lambotharan S** (2018) Outage Analysis and Power Allocation in Uplink Non-Orthogonal Multiple Access Systems. *IEEE Communications Letters,* 22 (2): 336-339.

[78] **Chen X, Benjebbour A, Li A and Harada A** (2014) Multi-user Proportional Fair Scheduling for Uplink Non-Orthogonal Multiple Access (NOMA). *IEEE 79th Vehicular Technology Conference (VTC Spring),* 18-21 May. 2014, Seoul, Korea, 1-5.

[79] **Wang H, Zhang R, Song R and Leung S** (2018) A Novel Power Minimization Precoding Scheme for MIMO-NOMA Uplink Systems. *IEEE Communications Letters,* 22 (5): 1106-1109.

[80] **Chen S, Peng K and Jin H** (2015) A Suboptimal Scheme for Uplink NOMA in 5G Systems. *International Wireless Communications and Mobile Computing Conference (IWCMC),* 24-28 Aug. 2015, Dubrovnik, Crotia 1429-1434.

[81] **Al-Imari M, Xiao P and Imran M A** (2015) Receiver and Resource Allocation Optimization for Uplink NOMA in 5G Wireless Networks. *International Symposium on Wireless Communication Systems (ISWCS),* 25-28 Aug. 2015, Brussels, Belgium, 151-155.

[82] **Haci H, Zhu H and Wang J** (2017) Performance of Non-Orthogonal Multiple Access with A Novel Asynchronous Interference Cancellation Technique. *IEEE Transactions on Communications,* 65 (3): 1319-1335.

[83] **Usman M R, Khan A, Usman M A, Jang Y S and Shin S Y** (2016) On the Performance of Perfect and Imperfect SIC in Downlink Nonorthogonal Multiple Access (NOMA). *International Conference on Smart Green Technology in Electrical and Information Systems (ICSGTEIS),* 6-8 Oct. 2016, Bali, Indonesia, 102-106.

[84] **Wang X, Labeau F and Mei L** (2017) Closed-form BER Expressions of QPSK Constellation for Uplink Non-Orthogonal Multiple Access. *IEEE Communications Letters,* 21 (10): 2242-2245.

[85] **Kara F and Kaya H** (2018) BER Performances of Downlink and Uplink NOMA in the Presence of SIC Errors over Fading Channels. *IET Communications* 12 (15): 1834-1844.

[86] **Kara F and Kaya H** (2018) "Derivation of the Closed-form BER Expressions for DL-NOMA over Nakagami-m Fading Channels. *IEEE 26th Signal Processing Communications Applications Conference*, 2-5 May. 2018, İzmir, Turkey, 1-4.

[87] **Gokceli S and Karabulut Kurt G** (2018) Superposition Coded-Orthogonal Frequency Division Multiplexing. *IEEE Access,* 6: 14842-14856.

[88] **Shannon C E** (1956) The Zero-Error Capacity of a Noisy Channel. *IRE Transactions on Information Theory,* 2: 8-19.

[89] **Gradshteyn I and Ryzhik I** (1994) *Table of Integrals, Series, and Products,* 5th edition, ISBN: 9780123849335, Academic Press, California, 1184 pp.

[90] **Simon M K and Alouini M S** (2004) *Digital Communication over Fading Channels,* 2nd edition, ISBN: 9780471649533, John Wiley & Sons, New Jersey, 936 pp.

[91] **Ross S** (2012) *A First Course in Probability.* 9th edition, ISBN: 978-0321794772, Pearson, London, 480 pp.

[92] **Archer C O** (1967) Some Properties of Rayleigh Distributed Random Variables and of Their Sums and Products. Naval Missile Center, Point Mugu, California

[93] **Laneman J N, Tse D N C and Wornell G W** (2004) Cooperative Diversity in Wireless Networks: Efficient protocols and outage behavior. *IEEE Transactions on Information Theory,* 50 (12): 3062-3080.

[94] **Herhold P, Zimmermann E and Fettweis G** (2004) "A Simple Cooperative Extension to Wireless Relaying. *International Zurich Seminar on Digital Communications,* 18-20 Feb. 2004, Zurich, Switzerland, 36-39.

[95] **Rankov B and Wittneben A** (2007) Spectral Efficient Protocols for Half-duplex Fading Relay Channels. *IEEE Journal on Selected Areas in Communications,* 25 (2): 379-389.

[96] **Zhang Z, Chai X, Long K, Vasilakos A V and Hanzo L** (2015) Full Duplex Techniques for 5G Networks: Self-interference Cancellation, Protocol Design, and Relay Selection. *IEEE Communications Magazine,* 53 (5): 128-137.

[97] **Onat F A, Adinoyi A, Fan Y, Yanikomeroglu H, Thompson J S and Marsland I D** (2008) Threshold Selection for SNR-based Selective Digital Relaying in Cooperative Wireless Networks. *IEEE Transactions on Wireless Communications,* 7 (11): 4226-4237.

[98] **Kara F, Kaya H, Erkaymaz O and Ozturk E** (2016) Prediction of the Optimal Threshold Value in DF Relay Selection Schemes Based on Artificial Neural Networks. *International Symposium on Innovations Intelligent Systems and Applications*, 2-5 Aug. 2016, Sinaia, Romania, 1-6.

[99] **Bletsas A, Khisti A, Reed D and Lippman A** (2006) A Simple Cooperative Diversity Method Based on Network Path Selection. *IEEE Journal on Selected Areas in Communications,* 24 (3): 659-672.

[100] **Ikki S S and Ahmed M H** (2010) On the Performance of Cooperative-diversity Networks with the Nth Best-relay Selection Scheme. *IEEE Transactions on Communications,* 58 (11): 3062-3069.

[101] **Ikki S S and Ahmed M H** (2010) Performance Analysis of Generalized Selection Combining for Decode-and-Forward Cooperative-Diversity Networks. *IEEE 72nd Vehicular Technology Conference (VTC Fall),* 6-9 Sep. 2010, Ottawa, Canada, 1-5.

[102] **Öztürk E and Kaya H** (2015) Performance Analysis of Distributed Turbo Coded Scheme with Two Ordered Best Relays. *IET Communications,* 9 (5): 638-648.

BIBLIOGRAPHY (continued)

[103] **Boyer J, Falconer D D and Yanikomeroglu H** (2004) Multihop Diversity in Wireless Relaying Channels. *IEEE Transactions on Communications,* 52 (10): 1820-1830.

[104] **Maric I and Yates R D** (2004) Cooperative Multihop Broadcast for Wireless Networks. *IEEE Journal on Selected Areas in Communications,* 22 (6): 1080-1088.

[105] **Krikidis I, Suraweera H A, Smith P J and Yuen C** (2012) Full-duplex Relay Selection for Amplify-and-Forward Cooperative Networks. *IEEE Transactions on Wireless Communications,* 11 (12): 4381-4393.

[106] **Riihonen T, Werner S and Wichman R** (2011) Hybrid Full-duplex/Half-duplex Relaying with Transmit Power Adaptation. *IEEE Transactions on Wireless Communications,* 10 (9): 3074-3085.

[107] **Azarian K, El Gama H and Schniter P** (2005) On the Achievable Diversity-multiplexing Tradeoff in Half-duplex Cooperative Channels. *IEEE Transactions on Information Theory,* 51 (12): 4152-4172.

[108] **Ding Z, Peng M, and Poor H V** (2015) Cooperative Non-orthogonal Multiple Access in 5G Systems. *IEEE Communications Letters,* 19 (8): 1462-1465.

[109] **Janghel K and Prakriya S** (2018) Performance of Adaptive OMA/Cooperative-NOMA Scheme with User Selection. *IEEE Communications Letters,* 22 (10): 2092-2095.

[110] **Zhang Z, Ma Z, Xiao M, Ding Z and Fan P** (2017) Full-duplex Device-to-Device-aided Cooperative Nonorthogonal Multiple Access. *IEEE Transactions on Vehicular Technology,* 66 (5): 4467-4471.

[111] **Yue X, Liu Y, Kang S, Nallanathan A and Ding Z** (2018) Exploiting Full/Half- duplex User Relaying in NOMA Systems. *IEEE Transactions on Communications,* 66 (2): 560-575.

[112] **Liu G, Chen X, Ding Z, Ma Z and Yu F R** (2018) Hybrid Half-duplex/Full- duplex Cooperative Non-Orthogonal Multiple Access with Transmit Power Adaptation. *IEEE Transactions on Wireless Communications,* 17 (1): 506-519.

[113] **Liau Q Y and Leow C Y** (2019) Successive User Relaying in Cooperative NOMA System *IEEE Wireless Communications Letters,* 8 (3): 921-924.

[114] **Do T N, Da Costa D B, Duong T Q and An B** (2018) Improving the Performance of Cell-edge Users in NOMA Systems Using Cooperative Relaying. *IEEE Transactions on Communications,* 66 (5): 1883-1901.

[115] **Li Y, Jiang M, Zhang Q, Li Q and Qin J** (2018) Cooperative Non-Orthogonal Multiple Access in Multiple-Input-Multiple-Output Channels. *IEEE Transactions on Wireless Communications,* 17 (3): 2068-2079.

[116] **Zhang J, Tao X, Wu H and Zhang X** (2018) Performance Analysis of User Pairing in Cooperative NOMA Networks. *IEEE Access,* 6: 74288-74302.

[117] **Ning B, Hao W, Zhang A, Zhang J and Gui G** (2019) Energy Efficiency Delay Tradeoff for A Cooperative NOMA System. *IEEE Communications Letters,* 23 (4,): 732-735.

[118] **Alsaba Y, Leow C Y and Abdul Rahim S K** (2018) Full-duplex Cooperative Non-Orthogonal Multiple Access with Beamforming and Energy Harvesting. *IEEE Access,* 6: 19726-19738.

[119] **Liu Y, Ding Z, Elkashlan M and Poor H V** (2016) Cooperative Non-Orthogonal Multiple Access with Simultaneous Wireless Information and Power Transfer. *IEEE Journal on Selected Areas in Communications,* 34 (4,): 938-953.

[120] **Do T N, Da Costa D B, Duong T Q and An B** (2018) Improving the Performance of Cell-edge Users in MISO-NOMA Systems Using TAS and SWIPT-based Cooperative Transmissions," *IEEE Transactions on Green Communications and Networking,* 2 (1): 49-62.

[121] **Kara F and Kaya H** (2019) On the Error Performance of Cooperative-NOMA with Statistical CSIT. *IEEE Communications Letters,* 23 (1): 128-131.

[122] **Kara F and Kaya H** (2019) Error Analysis of Cooperative-Non-Orthogonal Multi- ple Access (NOMA) over Nakagaıni-m Fading Channels. *Karaelmas Science Engineering Journal,* 9 (1): 130-141.

[123] **Kara F and Kaya H** (2019) Threshold-based Selective Cooperative-NOMA. *IEEE Communications Letters,* 23 (7): 1263-1266.

[124] **Xiao Y, Hao L, Ma Z, Ding Z, Zhang Z and Fan P** (2018) Forwarding Strategy Selection in Dual-hop NOMA Relaying Systems. *IEEE Communications Letters,* 22 (8): 1644-1647.

[125] **Liu Y, Pan G, Zhang H and Song M** (2016) Hybrid Decode-Forward Amplify-Forward Relaying with Non-Orthogonal Multiple Access. *IEEE Access,* 4: 4912-4921.

[126] **Liu Y, Lu W, Shi S, Wu Q, Li B, Li Z and Zhu H** (2018) Performance Analysis of A Downlink Cooperative NOMA Network over Nakagami-m Fading Channels. *IEEE Access,* 6: 53034-53043.

[127] **Yue X, Liu Y, Kang S and Nallanathan A** (2017) Performance Analysis of NOMA with Fixed Gain Relaying over Nakagami-*m* Fading Channels. *IEEE Access,* 5: 5445-5454.

[128] **Liang X, Wu Y, Ng D W K, Zuo Y, Jin S and Zhu H** (2017) Outage Performance for Cooperative NOMA Transmission with An AF Relay. *IEEE Communications Letters,* 21 (11): 2428-2431.

[129] Zhang Q, Liang Z, Li Q and Qin J (2017) Buffer-aided Non-Orthogonal Multiple Access Relaying Systems in Rayleigh Fading Channels. *IEEE Transactions on Communications,* 65 (1): 95-106.

[130] Luo S and Teh K C (2017) Adaptive Transmission for Cooperative NOMA System with Buffer-aided Relaying. *IEEE Communications Letters,* 21 (4): 937-940.

[131] Wan D, Wen M, Ji F, Liu Y and Huang Y (2018) Cooperative NOMA Systems with Partial Channel State Information over Nakagami- *m* Fading Channels. *IEEE Transactions on Communications,* 66 (3): 947-958.

[**132] Men J, Ge J and Zhang C** (2017) Performance Analysis for Downlink Relaying aided Non-Orthogonal Multiple Access Networks with Imperfect CSI over Nakagami- *m* Fading. *IEEE Access,* 5: 998-1004.

[133] Ding Z, Dai H and Poor H V (2016) Relay Selection for Cooperative NOMA. *IEEE Wireless Communications Letters,* 5 (4): 416-419.

[134] Yang Z, Ding Z, Wu Y and Fan P (2017) Novel Relay Selection Strategies for Cooperative NOMA. *IEEE Transactions on Vehicular Technology,* 66 (11): 10114-10123.

[135] Xu P, Yang Z, Ding Z and Zhang Z (2018) Optimal Relay Selection Schemes for Cooperative NOMA. *IEEE Transactions on Vehicular Technology,* 67 (8): 7851-7855.

[136] Deng D, Fan L, Lei X, Tan W and Xie D (2017) Joint User and Relay Selection for Cooperative NOMA Networks. *IEEE Access,* 5: 20220-20227.

[137] Xu Y, Sun H, Hu R Q and Qian Y (2015) Cooperative non-orthogonal multiple access in heterogeneous networks. *IEEE Global Communications Conference (GLOBECOM),* 6-10 Dec. 2015, San Diego, California, USA, 1-6

[138] Kader M F, Shahab M B and Shin S Y (2017) Exploiting Non-Orthogonal Multiple Access in Cooperative Relay Sharing. *IEEE Communications Letters,* 21 (5): 1159-1162.

[139] Kader M F, Shin S Y and Leung V C M (2018) Full-duplex Non-Orthogonal Multiple Access in Cooperative Relay Sharing for 5G Systems. *IEEE Transactions on Vehicular Technology,* 67 (7): 5831-5840.

[140] Yue X, Liu Y, Kang S, Nallanathan A and Chen Y (2018) Modeling and analysis of two-way relay non-orthogonal multiple access systems. *IEEE Transactions on Communications,* 66 (9): 3784-3796.

[141] Kara F and Kaya H (In Press) The Error Performance Analysis of the Decode-forward Relay-aided-NOMA Systems and A Power Allocation Scheme for User Fairness. *Journal of Faculty of Engineering and. Architecture of Gazi University*

BIBLIOGRAPHY (continued)

[142] **Kim J B and Lee I H** (2015) Capacity Analysis of Cooperative Relaying Systems Using Non-Orthogonal Multiple Access. *IEEE Communications Letters,* 19 (11): 1949-1952.

[143] **Jiao R, Dai L, Zhang J, Mackenzie R and Hao M** (2017) On the Performance of NOMA-based Cooperative Relaying Systems Over Rician Fading Channels. *IEEE Transactions on Vehicular Technology,* 66 (12): 11409-11413.

[144] **Zhang Y, Yang Z, Feng Y and Yan S** (2018) Performance Analysis of Cooperative Relaying Systems with Power-Domain Non-Orthogonal Multiple Access. *IEEE Access,* 6: 39839-39848.

[145] **Abbasi O, Ebrahimi A and Mokari N** (2019) NOMA Inspired Cooperative Relaying System Using an AF Relay. *IEEE Wireless Communications Letters,* 8 (1): 261-264.

[146] **Wan D, Wen M, Ji F, Yu H and Chen F** (2019) On the Achievable Sum-rate of NOMA-based Diamond Relay Networks. *IEEE Transactions on Vehicular Technology,* 68 (2): 1472-1486.

[147] **Proakis J G** (2008) *Digital Communications.* 5th edition, ISBN: 9780072957167, McGraw-Hill, New York, 1150 pp.

[148] **Bhatnagar M R** (2013) On the Capacity of Decode-and-Forward Relaying over Rician Fading Channels. *IEEE Communications Letters,* 17 (6): 1100-1103.

[149] **Alouini M S and Goldsmith A J** (1999) A Unified Approach for Calculating Error Rates of Linearly Modulated Signals over Generalized Fading Channels. *IEEE Transactions on Communications,* 47 (9): 1324-1334.

[150] **Basar E** (2016) Index Modulation Techniques for 5G Wireless Networks. *IEEE Communications Magazine,* 54 (7): 168-175.

[151] **Basar E, Wen M, Mesleh R, Renzo M D, Xiao Y and Haas H** (2017) Index Modulation Techniques for Next-Generation Wireless Networks. *IEEE Access,* 5: 16693-16746.

[152] **Mesleh R, Haas H, Ahn C W and Yun S** (2006) Spatial Modulation- A new Low Complexity Spectral Efficiency Enhancing Technique. *First International. Conference on Communications and Networking in China,* 25-27 Oct. 2006, Beijing, China, 1-5.

[153] **Basar E, Aygolu U, Panayirci E and Poor H V** (2013) Orthogonal Frequency Division Multiplexing with Index Modulation. *IEEE Transactions on Signal Processing,* 61 (22): 5536-5549.

[154] **Basar E** (2019- Early Access) Media-Based Modulation for Future Wireless Systems: A Tutorial. *IEEE Wireless Communications*

[155] **Jeganathan J, Ghrayeb A and Szczecinski L** (2008) Spatial modulation: Optimal Detection and Performance Analysis. *IEEE Communications Letters,* 12 (8): 545-547.

[156] **Mesleh R Y, Haas H, Sinanovic S, Ahn C W and Yun S Y** (2008) Spatial Modulation. *IEEE Transactions on Vehicular Technology,* 57 (4): 2228-2241.

[157] **Jeganathan J, Ghrayeb A, Szczecinski L and Ceron A** (2009) Space Shift Keying Modulation for MIMO Channels," *IEEE Transactions on Wireless Communications,* 8 (7): 3692-3703.

[158] **Jeganathan J, Ghrayeb A and Szczecinski L** (2008) Generalized Space Shift Keying Modulation for MIMO Channels," *IEEE 19th International Symposium on Personal Indoor Mobile and Radio Communications,* 15- 18 Sep. 2008, Cannes, France, 1-5.

[159] **Basar E, Aygölü Ü, Panayirci E and Poor H V** (2011) Space-time Block Coded Spatial Modulation. *IEEE Transactions on Communications,* 59 (3): 823-832.

[160] **Mesleh R, Stefan I, Haas H and Grant P** (2009) On the Performance of Trellis Coded Spatial Modulation. *International ITG Workshop on Smart Antennas,* 2: 235-241.

[161] **Mesleh R Y, Renzo M D, Haas H and Grant P M** (2010) Trellis Coded Spatial Modulation," *IEEE Transactions on Wireless Communications,* 9 (7): 2349-2361.

[162] **Basar E and Altunbas İ** (2017) Space-Time Channel modulation. *IEEE Transactions on Vehicular Technology,* 66 (8): 7609-7614.

[163] **Wang X, Wang J, He L and Song J** (2017) Spectral Efficiency Analysis for Down- link NOMA Aided Spatial Modulation with Finite Alphabet Inputs. *IEEE Transactions on Vehicular Technology,* 66 (11): 10562-210566.

[164] **Chen Y, Wang L, Ai Y, Jiao B and Hanzo L** (2017) Performance Analysis of NOMA-SM in Vehicle-to-Vehicle Massive MIMO Channels. *IEEE Journal on Selected Areas in Communications,* 35 (12): 2653-2666.

[165] **Zhong C, Hu X, Chen X, Ng D W K and Zhang Z** (2018) Spatial Modulation Assisted Multi-Antenna Non-Orthogonal Multiple Access *IEEE Wireless Communications,* 25 (2): 61-67.

[166] **Kara F and Kaya H** (2019) Spatial Multiple Access (SMA): Enhancing Performances of MIMO-NOMA Systems. *42nd International Conference on Telecommunications and Signal Processing,* 1-3 July, Budapest, Hungary, 466-471.

[167] **Irfan M, Kim B S and Shin S Y** (2015) A Spectral Efficient Spatially Modulated Non-Orthogonal Multiple Access for 5G. *International Symposium on Intelligent Signal Processing and Communications Systems ISPACS,* 9-12 Nov. 2015, Nusa Dua, Indonesia, 625-628.

[168] **Kim J W, Shin S Y and Leung V C M** (2018) Performance Enhancement of Downlink NOMA by Combination with GSSK. *IEEE Wireless Communications Letters,* 7 (5): 860-863.

BIBLIOGRAPHY (continued)

[169] Kara F and Kaya H (2019) Performance Analysis of SSK-NOMA. *IEEE Transactions on Vehicular Technology,* 68 (7): 6231-6242.

[170] Goldsmith A J (2005) *Wireless Communications,* lst edition, ISBN: 9780521837163, Cambridge Press, Cambridge, 644 pp.

[171] Di Renzo M and Haas H (2012) Bit Error Probability of SM-MIMO over Generalized Fading Channels. *IEEE Transactions on Vehicular Technology,* 61 (3): 1124-1144.

[172] Bariah L, Mıhaidat S and Al-Dweik A (2019), Error Probability Analysis of Non-Orthogonal Multiple Access over Nakagami-m Fading Channels. *IEEE Transactions on Communications,* 67 (2): 1586-1599.

[173] Gui G, Huang H, Song Y and Sari H (2018) Deep Learning for an Effective Nonorthogonal Multiple Access Scheme. *IEEE Transactions on Vehicular Technology,* 67 (9): 8440-8450.

[174] Emir A, Kara F and Kaya H (2019) Deep Learning-based Joint Symbol Detection for NOMA. in *27th Signal Processing and Communications Applications Conference,* 24-26 Apr. 2019, Sivas, Turkey, 1-4.

[175] Lin C, Chang Q and Li X (2019) A Deep Learning Approach for MIMO-NOMA Downlink Signal Detection. *Sensors,* 19 (11): 2526.

[176] Kiani A and Ansari N (2018) Edge Computing Aware NOMA for 5G Networks. *IEEE Internet of Things Journal,* 5 (2): 1299-1306.

[177] Ding Z, Fan P and Poor H V (2019) Impact of Non-Orthogonal Multiple Access on the Offloading of Mobile Edge Computing. *IEEE Transactions on Communications,* 67 (1): 375-390.

[178] Wu Y, Ni K, Zhang C, Qian L P and Tsang D H K (2018) Noma-Assisted Multi-Access Mobile Edge Computing: A Joint Optimization of Computation Offloading and Time Allocation. *IEEE Transactions on Vehicular Technology,* 67 (12): 12244-12258.

[179] Tian Y, Nix A R and Beach M (2016) On the Performance of Opportunistic NOMA in Downlink CoMP Networks. *IEEE Communications Letters,* 20 (5): 998-1001.

[180] Beylerian A and Ohtsuki T (2016) Coordinated Non-Orthogonal Multiple Access (CO-NOMA). *IEEE Global Communications Conference (GLOBECOM),* 4-6 Dec. 2016, Washington DC, USA, 1-5.

[181] Ali M S, Hossain E, Al-Dweik A and Kim D I (2018) Downlink Power Allocation for CoMP-Noma in Multi-cell Networks. *IEEE Transactions on Communications,* 66 (9): 3982-3998.

[182] Wang B, Dai L, Zhang Y, Mir T and Li J (2016) Dynamic Compressive Sensing-based Multi-user Detection for Uplink Grant-free NOMA. *IEEE Communications Letters,* 20 (11): 2320-2323.

[183] Du Y, Dong B, Chen Z, Wang X, Liu Z, Gao P and Li S (2017) Efficient Multi-user Detection for Uplink Grant-free NOMA: Prior-information Aided Adaptive Compressive Sensing Perspective. *IEEE Journal on Selected Areas in Communications,* 35 (12): 2812-2828.

[184] Dogan S, Tusha A and Arslan H (2019-Early Access) Noma with Index Modulation for Uplink URLLC through Grant-free Access. *IEEE Journal of Selected Topics in Signal Processing*

[185] Sohail M. F, Leow C Y and Won S (2018) Non-Orthogonal Multiple Access for Unmanned Aerial Vehicle Assisted Communication. *IEEE Access,* 6: 22716- 22727.

[186] Rupasinghe N, Yapıcı Y, Güvenç İ and Kakishima Y (2019) Non-Orthogonal Multiple Access for mmWave Drone Networks with Limited Feedback. *IEEE Transactions on Communications,* 67 (1): 762-777.

[187] Nguyen T M, Ajib W and Assi C (2018) A Novel Cooperative NOMA for Designing UAV-assisted Wireless Backhaul Networks. *IEEE Journal on Selected Areas in Communications,* 36 (11): 2497-2507.

CURRICULUM VITAE

Ferdi Kara was born in Zonguldak, Turkey in 1989. He graduated from Oktay-Olcay Yurtbay Anatolian High School at 2007. During his high school education, he was awarded by 2*nd* place within Zonguldak in Math Olympics by The Scientific and Technological Research Council of Turkey (TÜBİTAK). He received the B.S. degree (Honors) in Electronics and Communications Engineering from Süleyman Demirel University in 2011. He received MSc degree from Zonguldak Bülent Ecevit University in 2015. He has been with Department of Electrical-Electronics Engineering at Zonguldak Bülent Ecevit University since 2011 as Research/Teaching assistant at the Wireless Communication Technologies Laboratory (WCTLab). His research spans within wireless communications such as MIMO, cooperative communication, NOMA, spatial modulation and also machine learning paradigms in physical layer communication.

ADDRESS:

Address: Department of Electrical-Electronics Engineering at ZBEU, İncivez, Zonguldak, Turkey, 67100

Phone: +90 372 291 1910
E-mail: f.kara@beun.edu.tr